COMMISSIONING AND DOSIMETRIC VERIFICATION FOR AN ENHANCED DYNAMIC WEDGE IN ECLIPSE 8.0 TREATMENT PLANNING SYSTEM FOR 6 MV PHOTON BEAM

WARAPORN SANGSRIJAN

**A THESIS SUBMITTED IN PARTIAL FULFILLMENT
OF THE REQUIREMENTS FOR
THE DEGREE OF MASTER OF SCIENCE
(MEDICAL PHYSICS)
FACULTY OF GRADUATE STUDIES
MAHIDOL UNIVERSITY
2009**

Thesis
Entitled

COMMISSIONING AND DOSIMETRIC VERIFICATION FOR AN ENHANCED DYNAMIC WEDGE IN ECLIPSE 8.0 TREATMENT PLANNING SYSTEM FOR 6 MV PHOTON BEAM

……...
Miss Waraporn Sangsrijan
Candidate

……...
Assoc. Prof. Lalida Tuntipumiamorn,
M.Sc. (Radiation Science)
Major-Advisor

……...
Asst. Prof. Surat Vinijsorn,
M.Eng (Nuclear Technology)
Co-Advisor

……
Asst. Prof. Chumput Kakanaporn,
M.Sc. (Medical Physics)
Co-Advisor

……...
Asst. Prof. Auemphorn Mutchimwong,
Ph.D.
Acting Dean
Faculty of Graduate Studies

……
Assoc. Prof. Vipa Boonkitticharoen,
Ph.D. (Radiation Biology)
Chair
Master of Science Programme
In Medical Physics
Faculty of Medicine
Ramathibodi Hospital

Thesis
Entitled

COMMISSIONING AND DOSIMETRIC VERIFICATION FOR AN ENHANCED DYNAMIC WEDGE IN ECLIPSE 8.0 TREATMENT PLANNING SYSTEM FOR 6 MV PHOTON BEAM

was submitted to the Faculty of Graduate Studies, Mahidol University
for the degree of Master of Science (Medical Physics)
on
February 6, 2009

……...
Miss Waraporn Sangsrijan
Candidate

……...	……...
Assoc. Prof. Lalida Tuntipumiamorn, M.Sc. (Radiation Science) Member	Assoc. Prof. Sivalee Suriyapee, M.Eng. (Nuclear Technology) Chair
……...	……
Asst. Prof. Surat Vinijsorn, M.Eng (Nuclear Technology) Member	Asst. Prof. Chumput Kakanaporn, M.Sc. (Medical Physics) Member
…….....	……
Asst. Prof. Auemphorn Mutchimwong, Ph.D. Acting Dean Faculty of Graduate Studies, Mahidol University	Prof. Rajata Rajatanavin, M.D., F.A.C.E. Dean Faculty of Medicine Ramathibodi Hospital Mahidol University

ACKNOWLEDGEMENTS

I would like to express my sincere gratitude to Assoc. Prof. Lalida Tuntipumiamorn at Department of Radiology, Siriraj Hospital, my major advisor for her guidance, invaluable advice, supervision, constructive comments, stimulating and encouragement throughout. She was always nice and kindness. I am equally grateful to Assist.Prof. Chumpot Kakanaporn, Assist. Prof. Surat Vinijsorn, my co-advisor for their guidance, constructive comments, supervision and encouragement.

I thank the entire staff of the Department of radiology, Siriraj Hospital, who answered many questions pertaining to this thesis and lent an open ear in times of need. Special thanks to Archan Porntip Iampongpaiboon for her supporting on the use of the treatment planning system, helpful and valuable suggestion. I also would like to thank Mr.Wuttichai Bunrat and Miss.Piyanan Liammookda for their help in experiment during the period of my thesis. They were always nice and friendly.

I would like to thank Assoc. Prof. Dr. Vipa Boonkiticharoen, Director of School of Medical Physics and Assist. Prof. Chirapa Tannanonta for valuable advice and comment in the research proposal.

I am thankful to all friends in the school of Medical Physics, Faculty of Medicine, Ramathibodi Hospital, Mahidol University, for entirely care. Also my sincere thanks go to Miss Wassana Sangchang for helpfulness and being friend.

I am grateful to all lectures and all staffs and colleagues in the school of Medical Physics, Ramathibodi Hospital, Mahidol University, for supplying me academic knowledge on Medical physics.

Finally, I would like to thank my family for their financial support, entirely care and understanding during the entire course of study. I can not reach to this goal without them.

Waraporn Sangsrijan

COMMISSIONING AND DOSIMETRIC VERIFICATION FOR AN ENHANCED DYNAMIC WEDGE IN ECLIPSE 8.0 TREATMENT PLANNING SYSTEM FOR 6 MV PHOTON BEAM

WARAPORN SANGSRIJAN 4836296 RAMP/M

M.Sc. (MEDICAL PHYSICS)

THESIS ADVISORS : LALIDA TUNTIPUMIAMORN, M.Sc. (RADIATION SCIENCE), CHUMPUT KAKANAPORN, M.Sc. (MEDICAL PHYSICS), SURAT VINIJSORN, M.Eng (NUCLEAR TECHNOLOGY)

ABSTRACT

The objective of this study was to commission and verify the dosimetric parameters for an enhanced dynamic wedge (EDW) in Eclipse 8.0 treatment planning system (TPS) using pencil beam convolution algorithm. The accuracy of the 6 MV, 25^0 and 45^0 EDW beam characteristics on Clinac 23EX were investigated. Beam parameters including depth doses, profiles, wedge factors, wedge angles were examined for both the symmetric and asymmetric EDW fields. In order to verify the MU calculations, three different EDW plans were generated on the verification phantom for this purpose. Then the measured EDW dosimetric parameters were compared with those calculated from the Eclipse TPS. Results of the study revealed that, for the depth doses, agreements between the measured and calculated were within $\pm$1.5% in the depth beyond d_{max} (δ_1) and $\pm$4.35% in the build-up region region (δ_2). Moreover, the EDW beam depth doses also presented the same characteristics of dose as the open beam. On the EDW profiles, measured profiles with the CA24 chamber array were evaluated with the calculated profiles. It was found that the deviations in the penumbra region (δ_2) and the high dose-low dose gradient region (δ_3) in most cases, except for the largest asymmetric field size of 40 x 30 cm^2, were smaller than 1.5 mm and $\pm$2.0%, respectively. For the effective wedge factors, the comparative accuracy between the measurements and calculations was within $\pm$1.5% for both the symmetric and asymmetric EDW fields. EDW wedge factors were also found to be independent from depth of measurements. In most of the field sizes, the measured EDW angles differed from the TPS EDW angles within $\pm$1.8 degree, except in the field size of 20 x 5 cm^2 in which a maximum deviation of 4.7 degree was detected. For MUs verification, all three calculated EDW plans provided an accuracy of dose within $\pm$2% of the measured dose. The results of this study clearly show that the commissioning of 6 MV, 25^0 and 45^0 enhanced dynamic wedges meets the clinical accuracy requirements. The Eclipse 8.0 TPS with the pencil open beam calculation model and Golden STT for the other EDW angles are judgeed to be satisfactory for planning.

KEY WORDS : ENHANCED DYNAMIC WEDGE / COMMISSIONING / IMPLEMENTATION / VERIFICATION / CA24 CHAMBER ARRAY

169 pp.

การ COMMISSIONING และตรวจสอบความถูกต้องในการคำนวณปริมาณรังสีของ ENHANCED DYNAMIC WEDGE ในเครื่องวางแผนการรักษา ECLIPSE 8.0 สำหรับโฟตอนพลังงาน 6 เมกะโวลท์
(COMMISSIONING AND DOSIMETRIC VERIFICATION FOR AN ENHANCED DYNAMIC WEDGE IN ECLIPSE 8.0 TREATMENT PLANNING SYSTEM FOR 6 MV PHOTON BEAM)

วราภรณ์ แสงศรีจันทร์ 4836296 RAMP/M

วท.ม. (ฟิสิกส์การแพทย์)

คณะกรรมการควบคุมวิทยานิพนธ์ : ลลิดา ตันติภูมิอมร, M.Sc. (RADIATION SCIENCE),
จุมพฏ คัคนาพร, M.Sc. (MEDICAL PHYSICS), สุรัตน์ วินิจสร, M.Eng (NUCLEAR TECHNOLOGY)

บทคัดย่อ

งานวิจัยนี้มีวัตถุประสงค์เพื่อ Commissioning และตรวจสอบความถูกต้องในการคำนวณปริมาณรังสีของ enhanced dynamic wedge (EDW) ด้วยเครื่องคอมพิวเตอร์วางแผนการรักษา Eclipse 8.0 สำหรับโฟตอนพลังงาน 6 เมกะโวลท์ โดยทำการตรวจสอบใน EDW ขนาดมุม 25 และ 45 องศา ที่ได้จากเครื่องเร่งอนุภาคอิเลคตรอน Clinac 23EX ถึงคุณลักษณะของลำรังสีด้านต่างๆ ซึ่งได้แก่ ค่าปริมาณรังสีตามความลึก (depth dose) ค่าปริมาณรังสีตามแนวขวางจากจุดกึ่งกลางลำรังสี (dose profile), ค่าแก้ปริมาณรังสีเนื่องจากการใช้ wedge (wedge factor) และ มุม wedge (wedge angle) โดยทำการศึกษาในพื้นที่ลำรังสีแบบสมมาตรและไม่สมมาตร สำหรับความถูกต้องในการคำนวณปริมาณรังสีเป็นค่ามอนิเตอร์ยูนิท (monitor unit; MU) จะทำการตรวจสอบโดยการวัดปริมาณรังสีในหุ่นจำลองด้วยแผนการรักษาที่ใช้ EDW ที่แตกต่างกันสามแผนการรักษาที่ได้จากคำนวณด้วยเครื่องวางแผนการรักษา Eclipse 8.0 จากนั้นเปรียบเทียบข้อมูลที่ได้จากการวัดกับข้อมูลที่ได้จากการคำนวณด้วยเครื่องวางแผนการรักษา ผลการศึกษาพบว่าค่าปริมาณรังสีตามความลึกของ EDW ที่ได้จากการวัดและจากการคำนวณ มีค่าสอดคล้องกัน โดยที่ความลึกใดๆที่อยู่ลึกกว่าความลึกที่ให้ปริมาณรังสีสูงสุด (δ_1) จะพบความแตกต่างในช่วง $\pm$1.5% ของปริมาณรังสีที่วัดได้ และที่ความลึกในช่วง build-up region (δ_2) พบความแตกต่างในช่วง $\pm$4.35% โดยลำรังสีเมื่อมีและไม่มี EDW (open beam) ให้ค่าปริมาณรังสีตามความลึกที่ไม่แตกต่างกัน สำหรับค่าปริมาณรังสีตามแนวขวางจากจุดกึ่งกลางลำรังสี พบว่าในพื้นที่ลำรังสีขนาดต่าง ๆ ยกเว้นที่พื้นที่ลำรังสีสูงสุด 40 x 30 ตารางเซนติเมตร มีค่าแตกต่าง ของปริมาณรังสีที่บริเวณ penumbra (δ_2) และ high dose-low dose gradient region (δ_3) น้อยกว่า 1.5 มิลลิเมตร และ $\pm$2.0% ตามลำดับ การแก้ค่าปริมาณรังสีเนื่องจากการใช้ wedge ค่าแก้ที่ได้จากการวัดและจากการคำนวณมีความแตกต่างอยู่ภายในช่วง $\pm$1.5% การศึกษามุมของ EDW ที่ได้จากการวัดเมื่อเปรียบเทียบกับการคำนวณพบว่า โดยส่วนมากของข้อมูลมีความแตกต่างอยู่ภายในช่วง $\pm$1.8 องศา ยกเว้นที่พื้นที่ลำรังสี 20x5 ตารางเซนติเมตร ที่พบความแตกต่างของมุม wedge สูงสุด 4.7 องศา ในการตรวจสอบความถูกต้องของการคำนวณปริมาณรังสีของค่ามอนิเตอร์ยูนิท พบว่าในทุกแผนการรักษา ค่าปริมาณรังสีที่วัดได้มีความแตกต่างจากการคำนวณอยู่ภายใน $\pm$2% จากผลการศึกษาครั้งนี้สามารถสรุปได้ว่า EDW ที่มีขนาดมุม 25 และ 45 องศา สำหรับโฟตอนพลังงาน 6 เมกะโวลท์ ที่ได้ จากเครื่องเร่งอนุภาคอิเลคตรอน 23 EX และเครื่องวางแผนการรักษาคอมพิวเตอร์ Eclipse 8.0 มีความถูกต้องแม่นยำที่จะนำไปใช้ในงานทางการรักษาได้ ผลการศึกษาชี้แนะว่าการคำนวณปริมาณรังสี EDW ด้วย pencil beam algorithm โดยใช้ข้อมูลลำรังสีของ open beam กับ Golden STT น่าจะพบความถูกต้องแม่นยำสำหรับ EDW มุมอื่นๆที่ไม่ได้ครอบคลุมในการศึกษานี้ด้วย

169 หน้า

CONTENTS

LIST OF TABLES

LIST OF TABLES (cont.)

LIST OF TABLES (cont.)

LIST OF TABLES (cont.)

LIST OF TABLES (cont.)

LIST OF FIGURES

LIST OF FIGURES (cont.)

LIST OF FIGURES (cont.)

LIST OF FIGURES (cont)

LIST OF FIGURES (cont.)

LIST OF FIGURES (cont)

LIST OF FIGURES (cont.)

LIST OF FIGURES (cont)

LIST OF FIGURES (cont.)

LIST OF FIGURES (cont.)

LIST OF ABBREVIATIONS

Abbreviation	Term
3D	Three dimensional
3D-CRT	Three dimensional conformal radiation therapy
AAA	Analytical anisotropic algorithm
CAX	Central beam axis
cm	Centimeter
cm^2	Square centimeter
cm^3	Cubic centimeter
cmu	Centi-monitor unit
^{60}Co	Cobalt-60
DD	Depth dose
d_{max}	Depth of maximum dose
DW	Dynamic wedge
$D_{W,Q}$	Absorbed dose to water
EDW	Enhanced dynamic wedge
g / cm^3	Gram per cubic centimeter
IAEA	International Atomic Energy Agency
ICRU	International Commission on Radiation Units and Measurements
ID	Identification number
IEC	International Electrotechnical Commission
IMRT	Intensity modulated radiation therapy
Kb	Boundary kernel
Ks	Scatter kernel
kV	Kilovolt
MeV	Megaelectron volt
MLC	Multileaf collimator

LIST OF ABBREVIATIONS (cont.)

Abbreviation	Term
mm	Millimeter
MU	Monitor unit
MV	Megavolt
No.	Number
Pb	Boundary function
PBC	Pencil beam convolution
Pc	Envelope function
PDD	Percentage depth dose
PMMA	Polymethyl-methacrylate
PSF	Phantom scatter factor
PW	Physical wedge
RW_{50}	Radiological width
SAD	Source-axis distance
SSD	Source-surface distance
STT	Segmented treatment table
TPS	Treatment planning system
VW	Virtual wedge
X	The lower collimator
Y	The upper collimator
Z	Atomic number

CHAPTER I

INTRODUCTION

With the objective to obtain the high probability of tumor control and low probability of complication for the cancer patients, goal of radiotherapy treatment planning is to deliver the maximum dose to tumors and keep the minimum dose to normal tissues. In clinical applications, the use of mechanical or physical wedge (PW) filters is a well established method to compensate for the dose inhomogeneity in photon radiation therapy. The set of mechanical wedges, conventionally, are constructed into the certain wedge angles ; 15^0, 30^0, 45^0, and 60^0 and were mounted externally on the treatment head of the radiation treatment machines. However, a number of adverse attributes were encountered. For the physical aspects, the mechanical wedge filters were limited in size. They were constructed with the high density materials which were heavy and also blocked the light field during treatment setting-up. For dosimetry, a large variation in wedge factor for 60^0 may be found in PWs (1). The high atomic number (Z) material also as an additional source for the low-energy electron and photon scatter which increases the peripheral dose and surface dose (2-3). Moreover, the beam-hardening effect is another issue to be concerned for the physical wedges (4-5). Recently, with a capability of the computer-controlled linear accelerator, the wedge-isodosed distributions can be accomplished by controlling the collimation jaws motion under simultaneous adjustment of dose rate. This concept was referred as the dynamic wedge, and was first proposed by Kijewski et al, in 1978 (6). Then, Leavitt DD et al, in 1990 (7) reported the first implementation of the dynamic wedge. They used the looked up computer tables which the optimized segment weights are stored in a two-dimensional array of collimator setting and centi-monitor unit (cmu) setting, to generate the dynamic wedge distributions.

In 1991, Varian introduced the Dynamic Wedge (DW) as the first clinical implementation on Clinac C-series and provided the “Segmented treatment table” (STT) to specify the relationship between delivered dose rate and the position of the moving jaws. Later in 1996, they introduced the Enhanced Dynamic Wedge (EDW) and Golden STT which the capabilities of the dynamic wedge were significantly improved. Nowadays, it is widely acceptable that the nature of dynamic wedge functions offer great ease for photon beam treatment delivery. However, to implement the dynamic wedge into a clinic, it requires a sophisticated treatment planning system (TPS) that is able to model the photon fluence which actually generated by the dynamic delivery process accurately. In this study, with the ability of dynamic dose delivery of the 23 EX Varian linear accelerator using Golden STT and the Eclipse 8.0 TPS, the commissioning and verification the validity of the EDW calculations using the pencil beam convolution (PBC) algorithm for the clinical implementation at the Division of Radiation Oncology, Department of Radiology, Faculty of Medicine, Siriraj Hospital were the main purpose.

CHAPTER II
THEORY

2.1 Basic principle of wedge filters

2.1.1 Physical wedge (PW)

The physical wedge filter (Figure 1) is usually constructed from a high dense material, such as lead, steal or tungsten and is mounted on a transparent plastic tray which can be inserted in the beam at a specified distance from the source. The distance from the wedge tray and the patient surface is usually at least 15 cm or more to preserve the skin sparing effect (8).

Two basic types of the physical wedge are currently in clinical use, the external and internal wedges (Figure 2)(9). The external wedges normally be attached to the treatment head below the secondary collimator with a standard set of fixed angles ; 15^0, 30^0, 45^0, and 60^0. The desired angle wedge will be manually loaded to the tray on treatment head.

Another type of the physical wedge is the internal wedges or we called the motorized wedges. It is a single wedge with a wedge angle of approximately 60^0, mounted permanently in the treatment head on a motorized plate. This wedge is automatically inserted into the radiation beam for a number of monitor units that came from the treatment planning calculation. It will be a 60^0 wedge angle if it was inserted in the beam for the whole of the treatment field time. Smaller wedge angle can be achieved by mixing open and wedged beams in a suitable proportions.

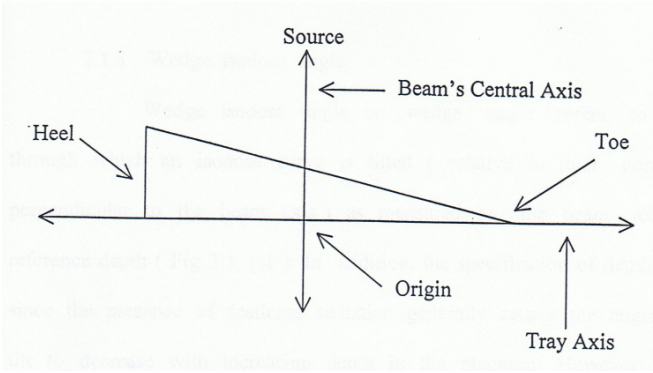

Figure 1. Schematic representation of a physical wedge.

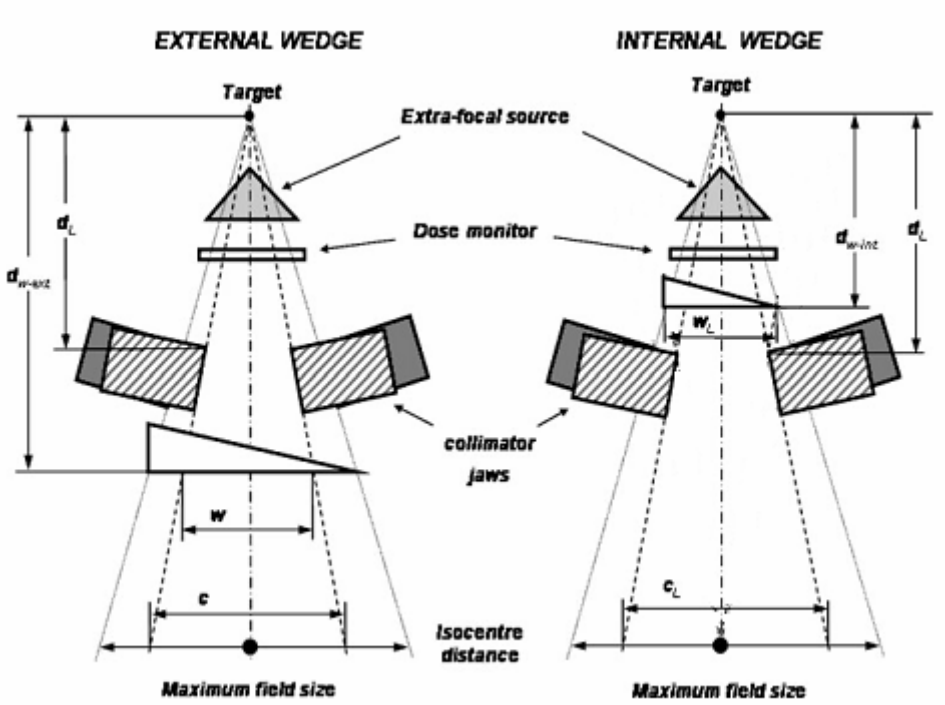

Figure 2. Schematic illustration of treatment head geometries for external and internal wedges (9). The external wedge will be positioned below the secondary collimator while the internal wedge between the flattening filter and secondary collimator

2.1.1.1 Dosimetric characteristics of the physical wedge

2.1.1.1.1 Wedge isodose distribution

A progressive decrease in the intensity across the beam with a presence of wedge filter was shown in Figure 3. Wedge-isodose curves are tilted toward the thin end and the degree of tilt depends on the design slope and the material of the wedge filter itself (8). The isodose curves for wedged beams may refer to a fixed source-surface distance (SSD) or to a fixed source-axis distance (SAD). In SSD method, one hundred percent of dose is at the depth of maximum absorbed dose along the central axis of beam while the SAD method, one hundred percent of dose will be at the axis of machine rotation.

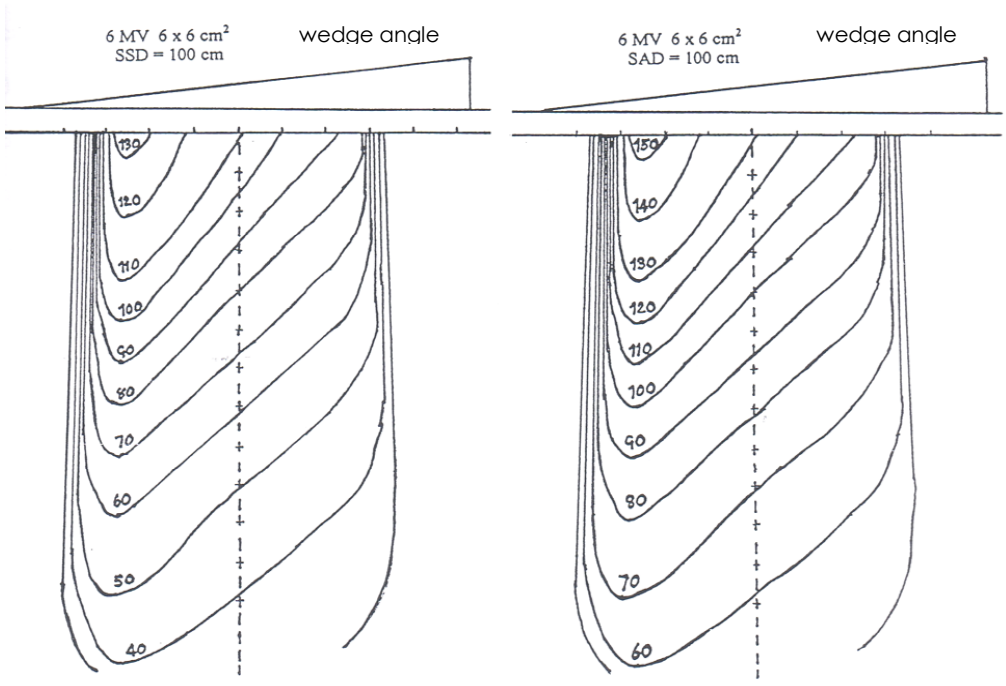

(a) (b)

Figure 3. Wedge-isodose distributions (10)

(a) refer to a fixed source surface distance (SSD)

(b) refer to a fixed source axis distance (SAD)

2.1.1.1.2 Wedge isodose angle

Wedge isodose angle refers to “the angle through which an isodose curve is tilted at the central ray of a beam at a specified depth” (8). The specification of depth is important due to the presence of scattered dose which the angle of isodose tilt will be affected. No general agreement was established for the reference depth. Therefore, wedge isodose angle may be specified as the angle between the 50% isodose curve and the normal to the central axis, which is shown in Figure 4(a) or selected the depth as a function of field size (e.g., 1/2 or 2/3 of the beam width) (8). However, because the wedge filters are mostly used for treating superficial tumors, in the high-energy beams such as 10 MV, the above specifications were impractical. The current recommendation is to use a single reference depth of 10 cm for wedge angle specification, which is shown in Figure 4(b).

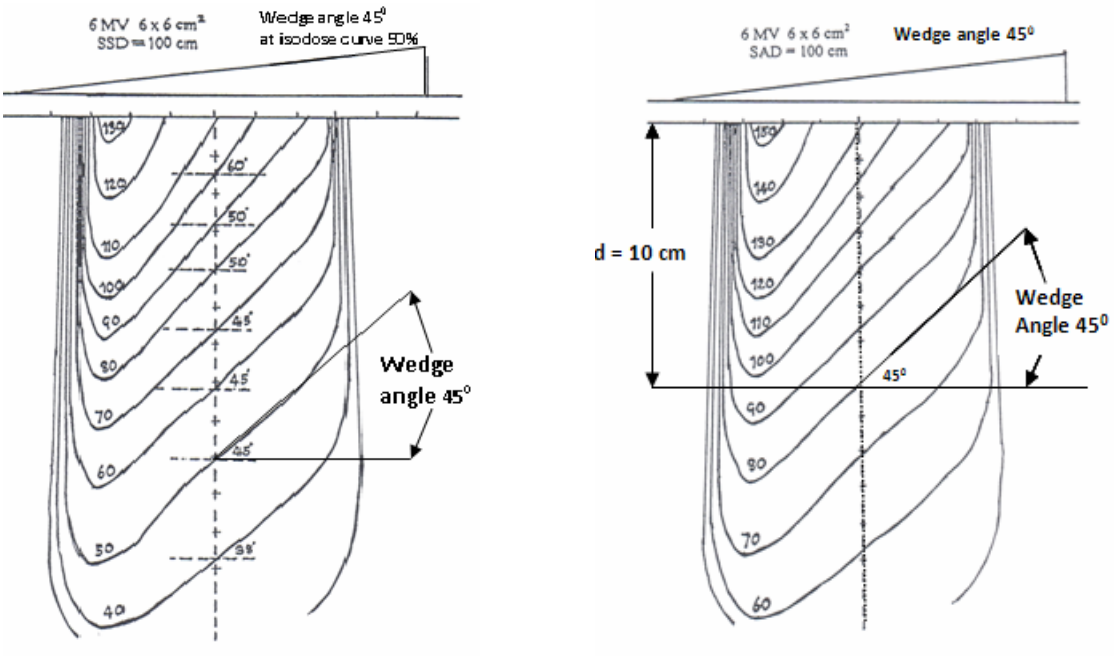

(a) (b)

Figure 4. Schematic illustrations of isodose wedge angle;

(a) The wedge angle determined at the 50% isodose line

(b) The wedge angle determined at depth 10 cm

2.1.1.1.3 Wedge transmission factor

The wedge transmission factor or wedge factor (WF), was defined as the ratio of the absorbed doses at a point in phantom along the central axis between the open beam and wedged beam. The measurements of WF were suggested to perform in the phantom at a suitable depth beyond the depth of maximum dose (8).

The wedge transmission factor, usually depends on the wedge angle, beam energy, field size, depth of measurement and components of the wedge filter (11).

2.1.1.1.4 Effect on beam quality (8)

Since, the physical wedge filter made of high density material so it can change the beam quality by attenuating the low energy photon and makes the beam harden. Occasionally, Compton scattering is occurred and energy is degraded which results in beam soften. For the ^{60}Co beam, the wedge filter does not significantly change the central axis percentage depth dose because the primary photon beam is monoenergetic. Another way, some beam hardening can be generated for X-ray beam and consequently, the depth dose distribution is altered, especially at the deep depth. Even though the wedge filters affect the beam quality, as mentioned above, the effect is not large enough to change other calculation parameters such as the backscatter factor or the equivalent square, which may be assumed to be similar to the corresponding open beams.

2.1.2 Non-physical wedge

2.1.2.1 Different modalities for non-physical wedge

Non-physical wedge is a term referred to the similar spatial dose distributions as those produced by the physical wedge. The idea of non-physical wedge was first proposed by Kijewski PK, and colleagues in 1978. They demonstrated the feasibility application of the computer-controlled linear accelerator Mevatron XII to produce the wedge-shaped dose distributions by moving the collimator jaws (6).

This idea was later supported by Leavitt DD et al (7) in 1990. They presented the fully integration of the collimator motion into the Varian 2100C linear accelerator. The clinical implementation of the dynamic wedge field technique then was introduced in 1991 by Varian Oncology Systems. Palo Alto. CA, the Dynamic Wedge (DW), on Clinac C-Series. The Siemens linear accelerator also provided this capability as the " Virtual Wedge (VW)" (12). Recently, Varian has introduced the Enhanced Dynamic Wedge (EDW) to add more functionality to this modality (13).

2.1.2.1.1 The Varian dynamic wedge (DW)

The dynamic wedge generates wedge isodose distribution by moving one of the collimator jaws under the computer control. One Y jaw and two X jaws are held stationary, while the other Y jaw moves dynamically during the irradiation. Driving the Varian DW, based on the controlled dataset called a Segmented Treatment Tables (STT). These tables define the fraction of total dose to be delivered during the collimator moves as a function of collimator position and four dynamic wedges angles (15^0, 30^0, 45^0 and 60^0) can be generated by this principle. However, for each wedge angle, 33 separate STTs were required to cover the field width in the range 4.0 to 20 cm (0.5 cm increment). The total of 132 STTs were required for the four wedge angles for each photon energy (14).

2.1.2.1.2 The Varian enhanced dynamic wedge (EDW)

The enhance dynamic wedge is the second generation of the DW which the underlying concept is using only one reference STT referred to as Golden STT, to generate seven wedge angles (10^0, 15^0, 20^0, 25^0, 30^0, 45^0, 60^0) for both symmetric and asymmetric field sizes. Any wedge angle less than 60^0 can be derived by means of weighted summation of the same size, an open beam and a 60^0 wedge beam (15). The Golden STT represents the full field width, 30 cm, along the wedge direction of a wedge angle of 60^0. By the upper Y1 or Y2 jaw can travel from full open position to 10 cm across the central axis, thus two wedge orientations, Y1-IN and Y2-OUT, are supported (as illustrated in Figure 5 and 6). Table 1 gives a brief overview of the general features of the EDW as compared to the first dynamic wedge system; DW.

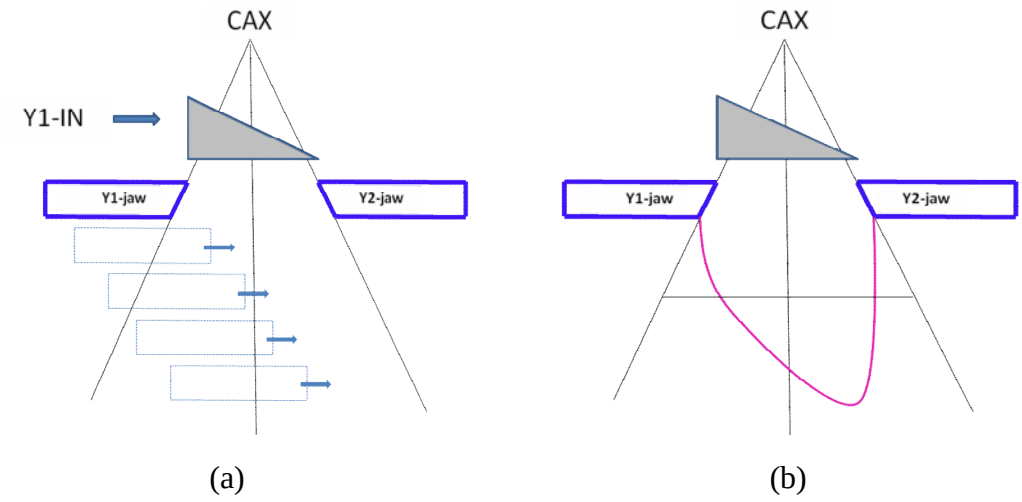

(a) (b)

Figure 5. Diagram illustrates for wedge orientation Y1-IN

(a) Y1-collimator jaw was set to move across the treatment beam

(b) Wedge isodose distribution will be created as the wedge orientation Y1-IN

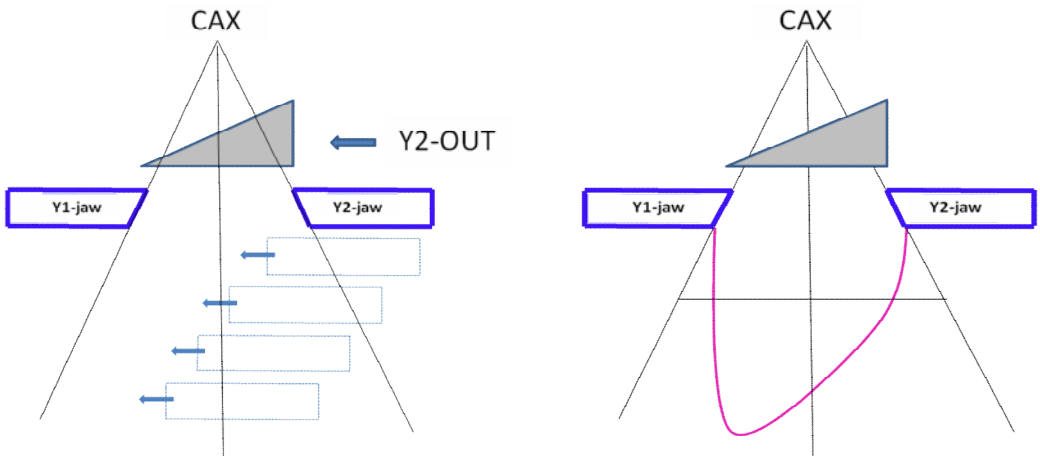

(a) (b)

Figure 6. Diagram illustrates for wedge orientation Y2-OUT

(a) Y2-collimator jaw was set to move across the treatment beam

(b) Wedge isodose distribution will be created as wedge orientation Y2-OUT

Table 1. General features compared between the dynamic wedge (DW) and the enhanced dynamic wedge (EDW) (15).

	Dynamic wedge	**Enhanced dynamic wedge**
Asymmetric field sizes	No	Yes
Wedge angles	15^0, 30^0, 45^0, 60^0	10^0, 15^0, 20^0, 25^0, 30^0, 45^0, 60^0
Field size width	4 to 20 cm in wedge direction	4 to 30 cm in wedge direction
Smooth wedge factor	No	Yes
Wedge orientation confirmation through pendant	Mandatory	User configurable through Physics mode.
STTs (Segmented Treatment Tables)	132 per photon energy	1 per photon energy
Portal imaging of wedged fields	No	Yes
Dynamic data logging (dynalog) capability	No	Yes
Real time beam's eye view graphic	No	Yes

Generally, all EDW treatments start with some portion of the dose being delivered as an open field. This means a portion of the total dose is delivered before the collimator starts moving. After the appropriate fraction of total dose has been delivered, the collimator starts sweeping the field from open to closed position. The exact fraction of dose that is delivered as an open field and wedge field is a function of the selected energy, field size, and wedge angle. The dose rate and collimator speed are also varied during the treatment. This allows for the treatment to be delivered in the shortest possible time (15).

2.1.2.1.3 The Siemens virtual wedge (VW)

Siemens virtual wedge (VW) also creates the wedge isodose distribution by controlling the motion of one of the collimator jaws across the field during irradiation. In contrast to the Varian EDW, the Siemens VW exposure commences with both jaws closed together (with a 1 cm gap) at the toe end of the wedge field. Then the jaw which defined the heel edge of the field is then driven open at a fixed speed while the dose rate is varied during the exposure to produce the desired fluence gradient (16).

The basic dosimetric principles of the Siemens VW are presented by Santvoort JV et al 1998 (17). The jaw motion in the wedge direction can be analytically described by an exponential function (18).

$$MU(Y) = MU(0)\exp(c\mu Y\tan\alpha) \quad \text{---------- (1)}$$

Where MU(Y) is the number of monitor units given while a point at position Y is within the field, MU(0) is the number of monitor units at the central axis (Y=0), α is the nominal wedge angle , c is the mean linear attenuation coefficient calibration factor and μ is the default mean linear attenuation coefficient. Equation (1) assumes that the wedge "toe" is in the positive side of the Y-axis and the wedge "heel" is in the negative side. The values of μ are derived from mean energies of energy spectra resulting from Monte Carlo calculations or measurements (17). For the radiation beam with the same nominal energy, the same value of μ is obtained. The value of the calibration factor, c, may be adjusted during the acceptance test such that the 60^0 VW field with the field of 20 x 20 cm^2 has the measured wedge angle equal to 60 ± 1^0 (18)(Siemens Medical Systems, "Virtual wedge option test procedures"). One of the important features of the Siemens VW is that the wedge factor is approximately unity. Unlike the Varian EDW, the Siemens VW gives the flexibility to create any wedge angle up to 60^0. The differences of the Varian EDW and the Siemens VW are presented in Table 2.

Table 2. General characteristics of the Varian EDW and Siemens VW (13).

Feature	Enhanced dynamic wedge	Virtual wedge
Jaw Position vs MU	Determined using segmented treatment table (STT)	Determined using analytic equation
Method of delivery	Variation of dose rate and moving jaw speed	Variation of dose rate only
Initial/Final Jaw Positions	Initially open; final position 0.5 cm from fixed jaw	Initially 1.0 cm from fixed jaw ; final position fully opened
Wedge direction option	EDW for Y (upper) jaws only. Treatment prohibited if fixed jaw > 0.5cm beyond moving jaw limits	VW for X or Y jaws. Treatment allowed if fixed jaw >1cm beyond moving jaw limits
Jaw travel limitations Gradient direction Non-gradient direction	 10 cm pass CAX. No limit.	 upper jaw: 2 cm pass CAX. lower jaw: 10 cm pass CAX. No limit.
Monitor Unit Input	MUs = Total MUs delivered during treatment	Programmed MUs = MUs delivered with CAX in the field. Total MUs termed MU_{max}.
Wedge Angle Selection	7 wedge angles (10^o, 15^o, 20^o, 25^o, 30^o, 45^o, 60^o)	Continuous to 60^o; Larger angles available with reduced field sizes.
Wedge Factors	Strong function of both wedge angle and field size; Weak function of off-axis distance	Approximately unity for symmetric fields; Strong function of off-axis distance.
Machine-independence	STTs same for all Varian machines	VW equation may vary with user-adjustable calibration factor c.

2.2 Basic principle of the Varian enhanced dynamic wedge

2.2.1 Golden STT and generation of the STT for the selected wedge angle and field size (15)

As previously mentioned, any resultant wedge angle less than 60^0 can be produced by a weighted summation of an open beam and a 60^0 wedge beam of the same size**.** In Varian EDW, the Golden STT of each photon energy are able to generate the dynamic wedge for any field size up to 30 cm with any wedge angle from 7 discrete wedge angles. In this section, the steps to generate STT for the selected field size and wedge angle will be followed as the process shown in Figure 7.

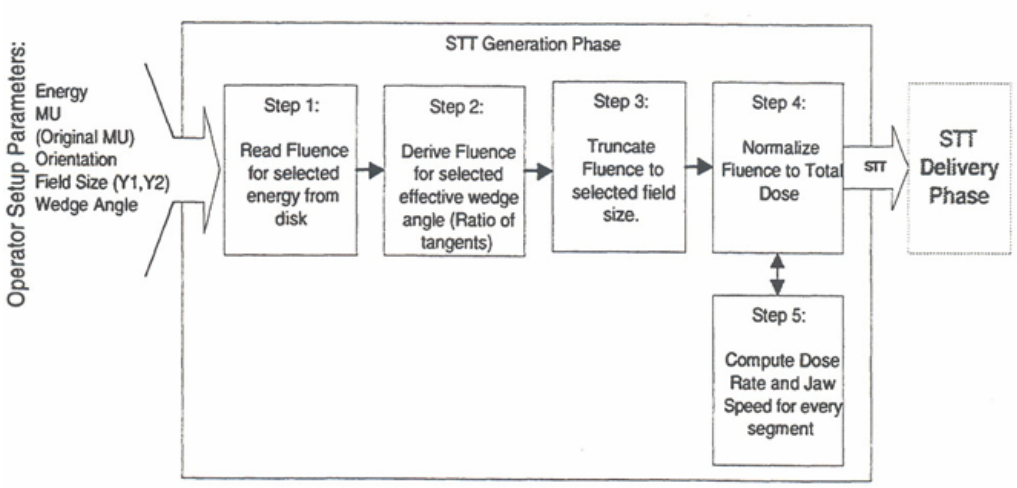

Figure 7. Process to generate STT for the selected field size and wedge angle (15)

Step 1. Read fluence for selected energy from the hard disk

After all the relevant planning parameters were designed for the treatment, to obtain the appropriate beam fluence profile, the process was first begun with reading the dataset from the Golden STT for the selected energy as shown in Table 3. The first column is the moving jaw position, and the second column express the fractional or normalization of total prescribed dose related to the collimator position.

Table 3. Golden STT for 6 MV photon, 60^0 EDW (15).

```
#-----------------------------------------#
#    CLINAC SEGMENTED TREATMENT TABLE (STT #
#              ENERGY: 6 MV               #
#         WEDGE ANGLE: 60 degrees         #
#-----------------------------------------#
      Dose     Position

    0.150691  -20.00 cm
    0.168051  -19.00 cm
    0.187220  -18.00 cm
    0.208376  -17.00 cm
    0.231707  -16.00 cm
    0.257422  -15.00 cm
    0.285748  -14.00 cm
    0.316933  -13.00 cm
    0.351245  -12.00 cm
    0.388978  -11.00 cm
    0.430453  -10.00 cm
    0.476017   -9.00 cm
    0.526050   -8.00 cm
    0.580964   -7.00 cm
    0.641210   -6.00 cm
    0.707274   -5.00 cm
    0.779690   -4.00 cm
    0.859035   -3.00 cm
    0.945937   -2.00 cm
    1.041080   -1.00 cm
    1.145206    0.00 cm
    1.259122    1.00 cm
    1.383704    2.00 cm
    1.519904    3.00 cm
    1.668756    4.00 cm
    1.831381    5.00 cm
    2.008999    6.00 cm
    2.202931    7.00 cm
    2.414611    8.00 cm
    2.645597    9.00 cm
    2.897577   10.00 cm
```

Step 2. Derive fluence for selected effective wedge angle

To derive the fluence profile that corresponds to any available effective wedge angle, the 60^0 Golden STT will be combined with the open field STT. Then, the effective wedge angle is computed by weighted averaging of the open field and 60^0 Golden STT using the ratio of tangents method (19).

Two weights, W_{0^0} (for open field) and W_{60^0} (for EDW field), are computed based on the any desired effective wedge angle : θ, as indicated in equation 2 and 3, respectively.

$$W_{0^0} = \frac{\tan 60^0 - \tan\theta}{\tan 60^0} \qquad \text{---------- (2)}$$

$$W_{60^0} = \frac{\tan\theta}{\tan 60^0} \qquad \text{---------- (3)}$$

The open and EDW filed fluence weights for any effective wedge angle are provided in Table 4.

Table 4. Open and 60^0 EDW fluence weights needed to create the desired effective wedge angle (15).

Wedge angle	**Open field fluence weight** W_{0^0}	**EDW field fluence weight** W_{60^0}
10^0	0.89820	0.10180
15^0	0.84530	0.15470
20^0	0.78986	0.21014
25^0	0.73078	0.26922
30^0	0.66667	0.33333
45^0	0.42265	0.57735
60^0	0.00000	1.00000

The fluence from the desired effective wedge angle, then is computed as the weighted average of the dose in the 0^0 and 60^0 fluences. The following linear combination formula as equation (4) is used.

$$\text{Dose}_\theta = (\text{Dose}_{\text{open}})W_{0^0} + (\text{Dose}_{60^0})W_{60^0} \qquad \text{---------- (4)}$$

where Dose_θ is the desired dose profile with the effective wedge angle θ, $\text{Dose}_{\text{open}}$ is the dose profile of the open field, diagram of the cumulative dose at any jaw position by the weighted averaging operation to derive the effective wedge angle fluence is shown in Figure 8.

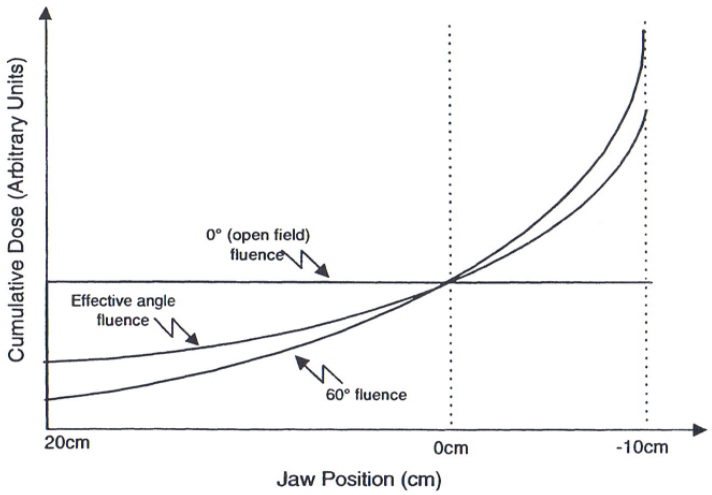

Figure 8. Illustrates the relationship between the cumulative doses vs. the jaw-positions in open field and 60^0 EDW fluences (15).

Example 1: To derive the Golden STT for the 45^0 effective wedge angle

From Table 3; data from Golden STT at Y1 position = -8 cm,

$Dose_{60^0} = 0.526050$ and $Dose_{open} = 1.145205$

(Because of the uniform intensity across the beam, the degenerate open field Golden STT or 0^0 angle STT at all Y1 position will composed the fractional dose value of 1.1425205. This is the same value for the 60^0 Golden STT at the at central axis which Y1 = 0.0 cm.)

From Table 4 , Fluence weights of the EDW 45^0 , $W_{0^0} = 0.42265$, $W_{60^0} = 0.57735$

That is, for Y1 = -8 cm, the fractional dose for the 45^0 effective wedge angle will be calculated as the following.

$$Dose_{45^0} = (1.145205 \times 0.42265) + (0.526050 \times 0.57735) = 0.787736$$

All other fractional doses at different Y1 position will be determined in the same way as the above example. Thus, the Golden STT for the selected 45^0 effective wedge was derived as shown in Table 5.

Table 5. Golden STT for the 45^0 effective wedge angle (15).

Dose	Position (cm)
0.732543	-10.00
0.787736	-8.00
0.819441	-7.00
1.282903	2.00
1.361538	3.00
1.447478	4.00
1.541369	5.00

Step 3. Truncate fluence to the selected field size

In this step, the effective wedge angle fluence of the maximum field size in the Golden STT will be truncated to the desired field size in the specific treatment planning. Figure 9 illustrates the truncation process, P1 and P2 correspond to the actual field size, as specified by the operator, Y1-jaw and the Y2-jaw EDW parameters. During the irradiation, the Y1-jaw sweeps the field from its starting position at P1 and closes to a final position of 0.5 cm from the stationary jaw P2.

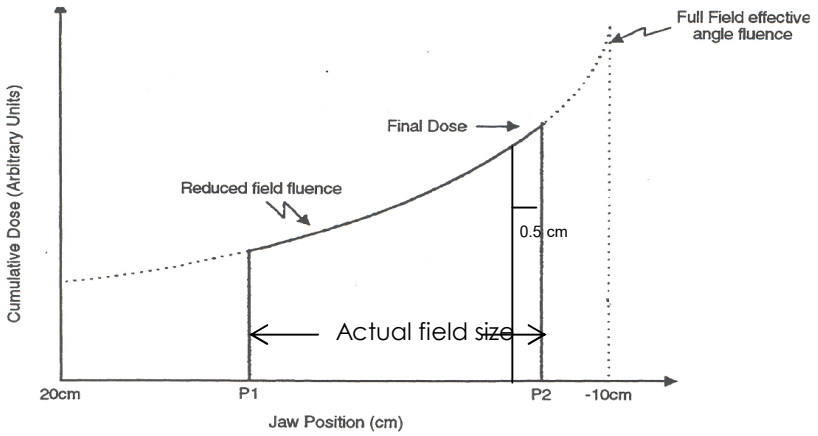

Figure 9. The truncation process to the selected field size and wedge angle (15).

Example 2: To derive the fluence profile for the asymmetric EDW field width of 15 cm (Total given dose 300 MU)

To create the asymmetric field width of 15 cm, EDW 45^0, the Y1-jaw at position = -10 cm will sweep across the central axis to the final position at Y2 = 4.5 cm , as illustrates in Figure 10.

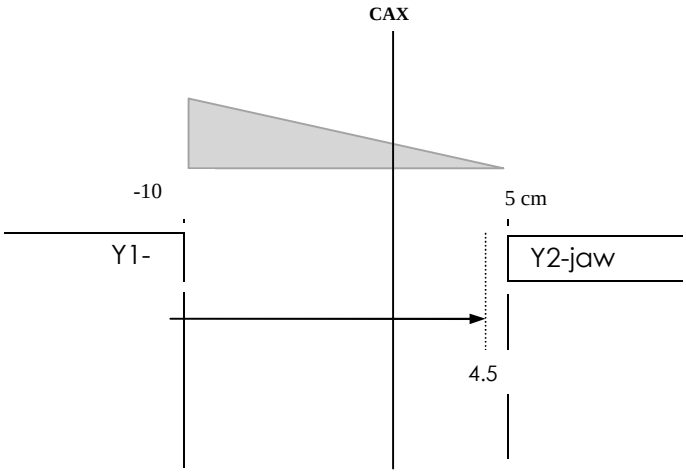

Figure 10. Diagram of the Y-jaw position in EDW asymmetric field width of 15 cm

In Table 5, The value of dose normalization were available only at the collimator position at 4 and 5 cm. Thus, at the collimator position 4.5 cm, dose normalization value must be interpolated.

From Table 5; dose value at Y1 = 4.0 cm and at Y1 = 5.0 cm are 1.447478 and 1.549369, respectively.

The dose value at Y1 = 4.5 cm is determined by,

$$1.447478 + (4.5\text{ cm} - 4.0\text{ cm}) \times \frac{(1.541369 - 1.447478)}{(5.0\text{ cm} - 4.0\text{ cm})} = 1.494424$$

At the other collimation positions, such as Y1 = 7.7 and -2.2 cm, the normalization dose were similarly determined from the above sample; Finally, STT for the 45^0 EDW, field size 15 x 15 cm^2 was obtained as shown in Table 6.

Table 6. STT for 45^0 EDW effective wedge angle, field size 15x15 cm^2 (15).

Y1	Dose
10.00 cm	0.732543
7.70 cm	0.797247
-2.20 cm	1.298630
-4.50 cm	1.494424

Step 4. Normalize fluence to total dose

To normalize fluence at each collimator position to the delivered dose, at the final collimator position of each dynamic wedge field, the value of dose normalization will be equal to the total prescribed MU. In this manner, we can calculate the given MU at each collimator position as the followings.

Example 3 : With the total prescribed dose, 300 MU, to determine the fractional of total dose to be given at the normalize fluence at Y1 = 7.7 cm

The truncated dose value at Y1 = -4.5 cm is 1.494424 and correspond to 300 MU
Thus, at collimator position = 7.7 cm, the given MU was determined by

$$\text{MU at collimator 7.7 cm} = \frac{300 \text{ MU} \times 0.797247}{1.494424} = 160.04 \text{ MU}$$

Similarly, the given MU at various Y1-positions for 45^0 EDW, asymmetric field width 15 cm, are calculated and presented in Table 7.

Table 7. The derived STT for the 45^0 EDW, asymmetric field width of 15 cm (Y1 = 10 cm, Y2 = 5 cm), wedge direction Y1-IN, 6 MV photon beam (15).

DYNAMIC BEAM STATISTICS

TOTAL DOSE DELIVERED	:	300 (MU)
DOSE STANDARD DEVIATON	:	0.03 (MU)
DOSE – POSITION STANDARD DEVIATION	;	0.01 (cm)
NUMBER OF SAMPLES	;	300

INSTANCE#	-- STT --		
	DOSE (MU)	**COLL Y1** (cm)	**COLL Y2** (cm)
1	0.00	10.00	5.00
2	**147.06**	**10.00**	**5.00**
3	151.15	9.23	5.00
4	155.38	8.48	5.00
5	**160.04**	**7.70**	**5.00**
6	164.85	6.95	5.00
7	170.26	6.18	5.00
8	175.88	5.43	5.00
9	182.08	4.65	5.00
10	188.45	3.90	5.00
11	195.58	3.13	5.00
12	203.02	2.38	5.00
13	211.21	1.60	5.00
14	219.64	0.85	5.00
15	228.99	0.08	5.00
16	238.81	-0.68	5.00
17	249.60	-1.45	5.00
18	**260.70**	**-2.20**	**5.00**
19	272.93	-2.98	5.00
20	285.83	-3.73	5.00
21	300.00	-4.50	5.00

Step 5. Compute dose rate and jaw speed for every segment

Once the STT has been correctly normalized, the dose rate and collimator speed to be used for each segment of the EDW treatment are calculated. Then the treatment with the desired dynamic wedge is performed successfully with the generated STT as presented above.

2.2.2 Dosimetric characteristics of enhanced dynamic wedges (EDW)

2.2.2.1 Central axis depth dose

Over past studies showed that the EDW depth doses are very similar to the open field depth doses. By Leavitt DD et al (20), depth doses for open and EDW fields were found to be within $\pm$2% for depths from D_{max} to 30 cm, with the maximum difference less than 2% for the 20 cm wide 60^0 EDW at 30 cm depth. Moreover, the study of Salk J et al (21) also shown that the EDW depth doses were close to those obtained for open fields. These data confirmed that depth doses measured for open fields can also be used for EDW field dose calculations.

2.2.2.2 Beam profile

The term off-axis ratio or dose is used to describe the dose at a point off the central axis of the beam relative to the dose on the central axis at the same depth. When wedge filters are used, they cause a progressive decrease the machine output and alter the open beam profile of the photon beam. Figure 11 illustrates the difference in beam profiles from the Clinac 2300 C/D in the 6 MV mode between the open, physical wedge and EDW fields. In the wedge direction, EDW profile is similar to the physical wedge profile. The beam profiles in the non-wedged direction produced from an open field, EDW field, and physical wedge filter also presented in Figure 12. A pretty match of the beam profiles from the open and EDW field was seen. However, the physical wedge filter demonstrates a decrease in dose at the field edges due to increasing beam hardening effect (22).

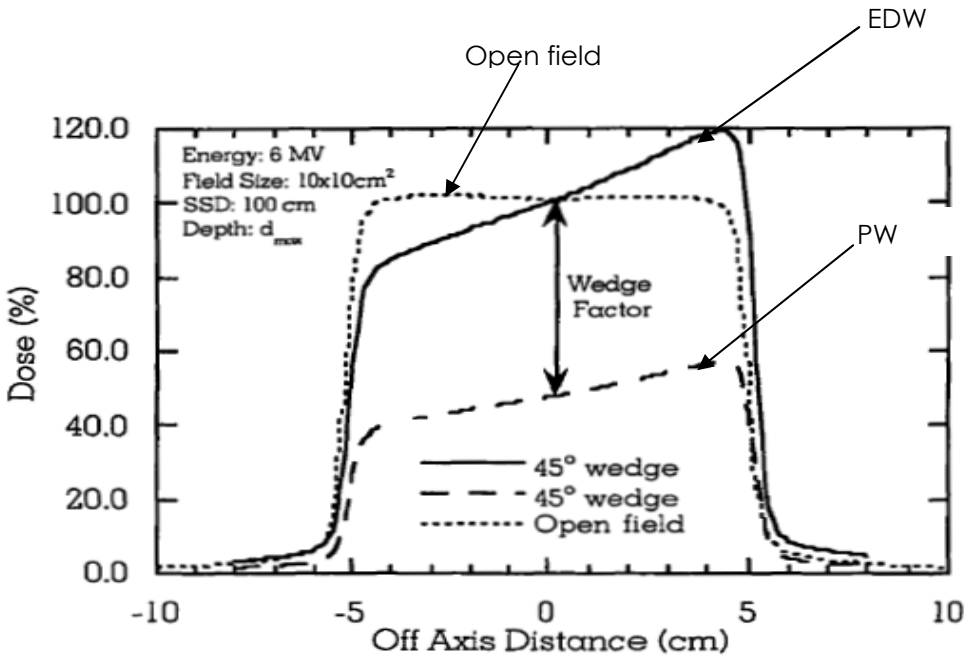

Figure 11. Comparison of the open field, 45^0 EDW and 45^0 PW beam profiles in the wedge direction for a 10 x 10 cm^2, 6 MV photon beam (22).

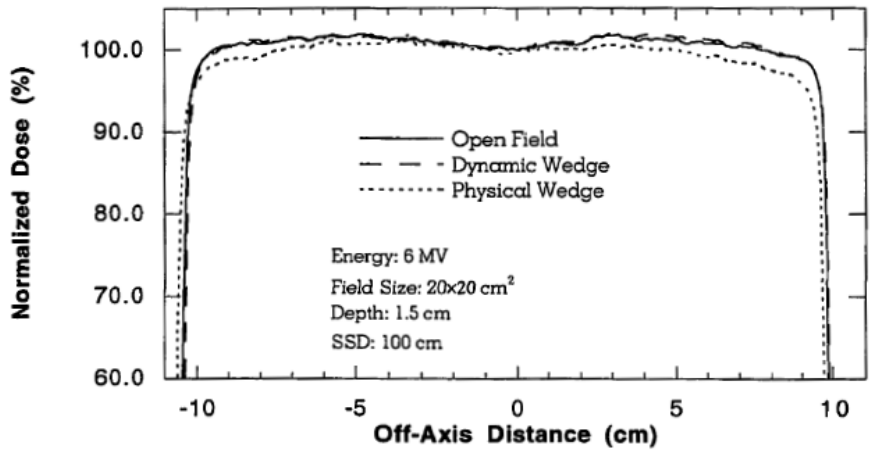

Figure 12. Comparison of open field, EDW, and PW beam profiles in the non-wedge direction for a 45^0 wedge angle with a field size of 20 x 20 cm^2 and a photon beam energy of 6 MV, 1.5 cm depth (22).

2.2.2.3 Effective wedge factor

For the dynamic wedge, the effective wedge factor is defined as the ratio of the integrated reading at a specified depth on the central axis to that of an open field for a fixed number of monitor units. (IEC 1989, ICRU 1976)

The effective wedge factor for dynamic wedges are greater (closer to unity) than physical wedge factors and depend on field dimension along the moving jaw, beam energy, and wedge angle (22). Thus, the effective wedge factor must be carefully considered in using the dynamic wedge. Unlike the dynamic wedge, where a strong non-monotonic field size dependence appears (23), hence the simple interpolation could not be used for clinical monitor unit calculation. The EDW effective wedge factors show a smooth and continuous decrease with increasing field size in wedge direction and appear to be independent of non-wedged dimension (X dimension) (13). For the asymmetric EDW, the effective wedge factor defined as the ratio of ion chamber readings in the beam center of the asymmetric fields to the symmetric open field, also depend on the off-axis distance in the wedged direction and the influence of the flattening filter and the variation from the hardening effect to the dose at an off-axis point will be included in the wedge factor (24). Figure 13(a) and 13(b) illustrates the effective wedge factor versus field size and wedge angle for fields to 20 cm wide for dynamic and EDW field, respectively.

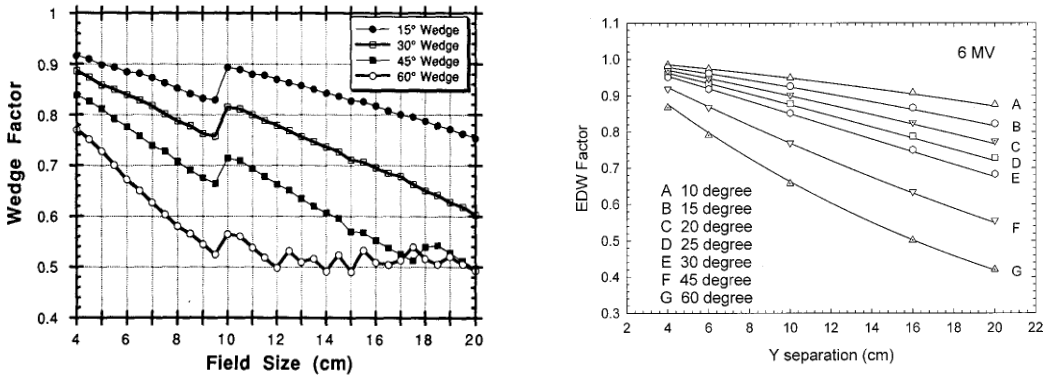

(a) (b)

Figure 13. The effective wedge factors as a function of field size (a) DW field and (b) EDW field (13).

2.2.2.4 Effective wedge angle

The definition of the effective wedge angle of EDW is different from the physical wedge, by it follows the wedge definition recommended by the IEC report 976 (25) and the ICRU report 24 (10) which defines the wedge angle to be the angle of line between the two points on the isodose curve at standard measurement depth that are equidistant a quarter of the field width away from the central axis. The standard measurement depth can be chosen to be either 5 cm or 10 cm. Figure 14(b) illustrates the effective wedge angle of EDW.

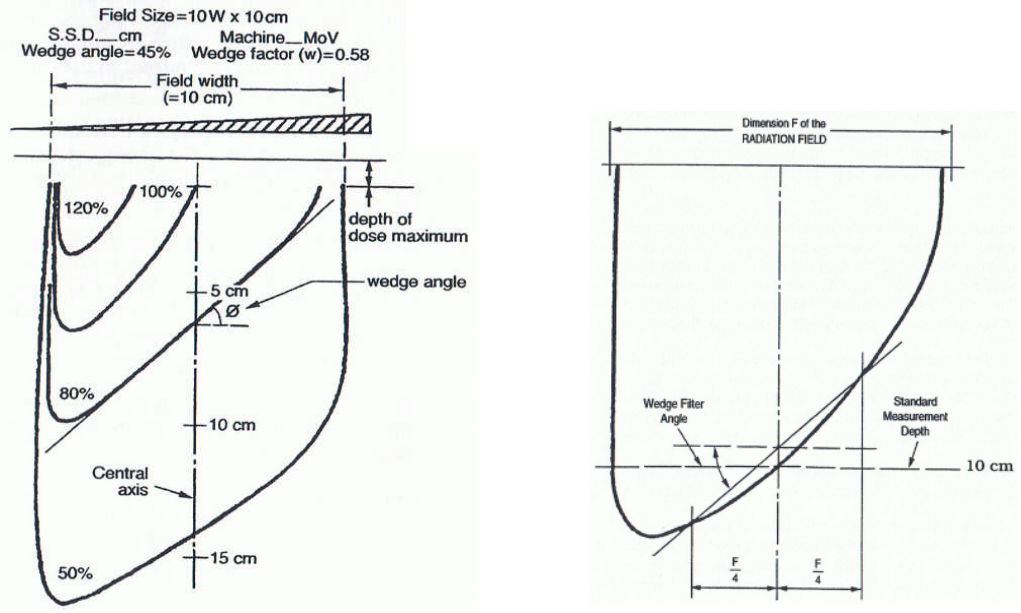

(a) (b)

Figure 14. Definition of the wedge angles

(a) For the physical wedge and (b) For the EDW.

2.2.2.5 Surface dose and peripheral dose

Due to the complication effect to the skin from the surface dose, and the radiation-induced carcinogenesis from the peripheral dose are clinically important in the treatment planning of breast, head and neck, thyroid, etc. The determination of surface and peripheral dose are essential to be considered.

Typically, the presence of absorber in the beam caused the unwanted scattered dose which increase the surface and peripheral dose as reported by some previous studies (2, 26-28). The studied on three different wedge systems including the lower wedge, the upper wedge and the DW by Li Z et al (3) found that in case of the physical wedge and the DW, since the difference in physical construction and relative positions to the linear accelerator source, the surface and peripheral dose of the lower wedge system was found to be higher than the open field and depend on the magnitude of field size. While the dynamic and upper wedge system delivered the similar of doses to those of the open fields. The peripheral dose produced by the physical wedge was also reported by Leavitt DD et al (20) to be nearly twice more than the EDW.

2.3 Advantages of the EDW over the physical wedge

2.3.1 The EDW can generate more available wedge angles than physical wedge.

2.3.2 The EDW has a capability of producing field size in wedge direction more than the physical wedge. (the maximum field up to 30 cm)

2.3.3 The use of EDW can eliminate the manual handling of the physical wedge during treatment so that, the setup time is reduced and also achieve the safety to the patient and user.

2.3.4 Compared to the physical wedge, there is no beam attenuation and thus no beam-hardening effect associated with the EDW (29).

2.3.5 Peripheral dose outside the geometric projection of EDW treatment field is reduced, compared to physical wedge field doses (3, 20).

2.3.6 EDW treatment produces the contralateral breast dose less than the physical wedge (30).

2.4 Commissioning of the enhanced dynamic wedge (EDW)

The process of acquiring the comprehensive set of beam data required for radiation therapy and entering it into a treatment planning system is called “commissioning”. To implement the EDW into a treatment planning system, typically, no additional measurements are required to configure the treatment planning. The calculation of EDW dose distribution will be based on the open beam model which included the central axis depth doses, beam profiles at selective depths, output factor and transmission factor. Then, using the transmission array such as the Golden STT to generate the desired wedge angle at selected energy and collimator jaw setting. The dose computation process will be combined with the open field model and transmission array. In this study, the EDW will be commissioned into Eclipse 8.0 TPS with the pencil beam convolution (PBC) model.

2.5 Pencil beam convolution (PBC) algorithm (31, 33)

Photon dose calculation with the pencil beam convolution (PBC) algorithm, generates the three dimensional (3D) dose distribution based on two different types of kernels, a scatter kernel and a boundary kernel, respectively. The scatter kernel is used for the convolution of the depth dose in the center of the field and is generally deconvolved from the measured depth doses and the peak scatter ratios. The boundary kernel using for the convolution of the off axis dose distribution is deconvolved from the five measured off axis dose profiles. The scatter and the boundary kernels are combined with a matrix representing the shape of the field for convoluting the dose distribution. In the dose computation process, the variation in the diagonal profile and the primary including the scattered photons from all parts of the irregularly shaped filed are taken into account.

For the DW and the EDW fields, the convolution of the depth dose and the off-axis dose distribution is undertaken using an intensity matrix representing the different subfields. The subfields are defined by the STTs from the accelerator.

2.5.1 Calculation of dose for EDW

The EDW calculation model is based on the Varian STT files and the open field beam data. The basic beam data required including the depth dose curves and profiles for square fields, output factors for rectangular fields and phantom scatter factors (PSF).

The relative absorbed dose value in an arbitrary point (x, y, z) in a water phantom is computed by using equation (5).

$$D(x, y, z; F) = Da(z; F) * Pb(x, y, z; F) * Pc(r, z) \quad \text{----------} \quad (5)$$

where Da (z; F) is the depth dose value at the field effective axis, Pb (x, y, z; F) is the boundary function and Pc (r, z) is the value of the envelope function at radial distance r = (x2 + y2) 1/2. Envelope profile describes the off-axis variation of an open, non-collimated beam. The formula is developed from rectangular beam model algorithm.

The boundary function Pb is computed by a convolution of the field intensity matrix Fw (x, y) with the boundary kernel Kb in equation (6). The field intensity function is defined as a two-dimensional matrix which is equal to one inside the open field part, the transmission factor under block or multileaf, and to zero under collimator jaw.

$$Pb(x, y, z; F) = Fw(x, y) * Kb(z) \quad \text{---------- (6)}$$

The depth dose value Da is computed by a convolution of the field intensity matrix Fw with the scatter kernel Ks on the beam axis.

$$Da(z; F) = Fw(x, y) * Ks(z) \quad \text{---------- (7)}$$

The STT is a two-entry table, which provides the position of the jaw (Xi) and the number of monitor units (M') for each field segment. The field intensity matrix Fw for the dynamic wedge field is computed using the STTs:

$$Fw(x, y) = \sum_{i=1}^{n} Wi * Fi(x, y) \quad \text{---------- (8)}$$

where Fi (x, y) is the field intensity matrix of the asymmetric field segment i. The intensity matrix value is equal to one in the open part of the beam and equal to the collimator jaw transmission factor under the jaw. Wi is the weight corresponding to the monitor unit value M'. For the dose calculation, the monitor unit values are converted to effective weight (in photon flux) by using the collimator factors:

$$Wi = \frac{Sc(Fi)}{Sc(Fo)} Mi \quad \text{---------- (9)}$$

where Sc (Fi) is the collimator factor of the ith field segment and Sc (Fo) relates the calculated dose to the dose of the open field. Therefore the open field output factors can be used in monitor unit calculations.

CHAPTER III
OBJECTIVES

The main objectives of this study are:

1. To commission the 6 MV EDW from Clinac 23EX into the Eclipse 8.0 treatment planning system (TPS) using pencil beam convolution (PBC) algorithm.
2. To verify the accuracy of the EDW dosimetric characteristics which include the central axis depth dose, beam profiles, effective wedge factors and effective wedge angles in the Eclipse 8.0 TPS.
3. To verify the accuracy of monitor units (MUs) calculation for the EDW treatment plans from the Eclipse 8.0 TPS.

The sub-objectives of this study are:

4. To understand the capabilities and limitation of the PBC algorithm in Eclipse 8.0 TPS for EDW.
5. To get the experience on the test procedures of the EDW dosimetric characteristics in order to develop the efficient methods.

CHAPTER IV
LITERATURE REVIEWS

The physical properties and the dosimetric parameter of Enhanced dynamic wedge (EDW) including the depth dose, the beam profile, the effective wedge factor, the surface and peripheral dose were subject of intensive studies in earlier works (20, 21, 32, 33, 34)

Leavitt DD et al (20) studied the dosimetric parameters include depth doses, surface doses, build up doses, peripheral doses, beam profiles, wedge angles and wedge factors for 6 MV and 18 MV photon beams from a Clinac 2100C. These parameters and their application to treatment planning are evaluated and compared with standard open field and metal wedge field dosimetric parameters. Depth doses were measured in water phantom using an ionization chamber sequentially positioned to depths of 30 cm. EDW field depth dose differ only marginally from open field depth doses, with the maximum difference less than 2% for the 20 cm wide 60^0 EDW at 30 cm depth. The measured EDW dose profiles were measured by using a linear detector array of 25 energy-compensated diodes in water phantom for depths from near-surface to 30 cm for the full range of field widths and wedge angles. And these EDW dose profiles were compared to those that calculated as the sum of asymmetric fields weighted by the STT. Excellent agreement was achieved between the measured and calculated profiles. Dose in the buildup region was measured using a parallel plate ionization chamber positioned on central axis. Build up dose of EDW was similar to open field, but differ from physical wedge. They also found that the EDW peripheral doses were nearly identical to the open field doses when the same dose to central axis is delivered. By comparison, the peripheral dose was nearly twice as high when the physical wedge is applied. The effective wedge factor was relatively insensitive to measurement depth. However, the effective wedge factor was dependent on beam energy and varied smoothly across the entire field range to 30 cm wide.

The dependence of EDW wedge angle on field width was compared with standard wedges, the EDW angle was greater than the standard metal wedge for all field widths, and converged toward the desired wedge angle for larger fields.

Salk J et al (21) investigated the dosimetric parameter of EDW including the depth dose, the beam profile and the effective wedge factor and also validated the EDW calculation obtained by a commercial treatment planning system. The measurements were performed for both 6 MV and 18 MV photons on a Clinac 2300 C/D accelerator. A linear ion chamber array has been used to measure dose profiles of both symmetric and asymmetric fields in water phantom. Depth doses were acquired by single point measurements using an ionization chamber. The measurements were performed for various field sizes at a fixed source-phantom-distance of 100 cm. The effective wedge factors for symmetric field were measured with an ionization chamber at a depth of 10 cm. For asymmetric field the measurement were performed at depths of 5, 10 and 20 cm. They reported that the TPS calculated and measured beam profiles for the symmetric EDW field differed by less than 1.5%, except for the hot spot and peripheral dose in the toe region of the EDW. The largest deviation of approximately 5% was found in the hot spot region of a 20 x 20 cm^2 field and a 60° EDW at the depth of the dose maximum. For asymmetric EDW fields, the computed and measured beam profiles were in good agreement. Inside the geometrical field edges the deviations between calculated and measured dose profiles are typically less than 1.5%. Measured and calculated EDW depth doses showed an excellent agreement. The differences were typically less than 0.5%. The EDW depth doses were found to be close to those obtained for open fields. The observed differences increased with increasing wedge angle, field size, depth and decreasing beam energy. The largest difference of 2% was found in the case of 6 MV photons, the 60° EDW and field size of 20 x 20 cm^2 at a depth of 40 cm.

There was a good agreement between measured and calculated effective wedge factors for both symmetric and asymmetric field. For symmetric fields, the deviations are typically $\leq$0.5% except for the 60° EDW where the effective wedge factor was systematically overestimated by approximately 1-2%. The largest difference of 2.3% was observed for 6 MV photons at a field size of 20 x 20 cm^2. The agreement between measured and calculated effective wedge factors for asymmetric fields at various depths was in most cases within 1%. The largest difference of 2.3% appeared for 18 MV photons for the 60° EDW with orientation Y2-OUT at an asymmetric field size of 5 x 20 cm^2 and a depth of 10 cm.

Liu HH et al (32) investigated the measuring dose distributions for EDW using a commercial multi-chamber detector array (CA24 chamber array). The technical aspects of using the chamber array, including chamber calibration, selection of measurement parameters, and use of the reference chamber, have been fully investigated. The measurement results from the chamber array were also confirmed by those from the single chamber and radiographic film measurements. The dose profiles including the penumbra dose measured by the chamber array agree with those measured by the single chamber. The new relative sensitivity factors for the 23 chambers were normally within 1%-2% of unity. For the static open fields also showed that the relative dose profiles including the penumbra dose at a particular depth measured by the films agreed with those from the single chamber and the chamber array measurements. For EDW field, the results showed that the absolute difference in the percent dose (dose relative to the D_{max}) was within 2.0% from the chamber array and the film measurements. Thus the chamber array is a reliable dosimetry system for the dose measurement in the static and the EDW fields.

Samuelsson A et al (33) investigated and verified the dose calculations in Cadplan treatment planning systems for 4 MV X-ray EDW from a Varian Clinac 600 and 6 and 15 MV X-ray from a Varian Clinac 2300 C/D. Profiles were measured in a water phantom with eleven diodes combined in a Linear Detector Array (LDA) and the Radiation Field Analyzer 300 (RFA300). Integrated measurements over 100 MU were performed at five different positions separated by 5 mm in the direction of the wedge.

Before performing the measurements some profiles measured with the LDA were compared with profiles measured with a single ionization chamber. The agreement between the two measuring methods was good.

The agreement between measured and calculated profiles were, in general, good. The deviations near the center of the fields were in most cases smaller than 2% , and near the high dose region (thin edge) of the field, the calculating curve underestimates the relative dose and the deviations could be somewhat larger. In the region of low dose and low gradient, the underestimation of calculating dose was found in all fields. The agreement between measured and calculated MU was good in fields including the collimator axis, always within 1.5%. The deviation in asymmetric fields excluding the collimator axis showed a somewhat larger deviation and the maximum deviation was 4.4%.

Picon C et al (34) verified the dose distribution and monitor unit calculations for EDW in Cadplan treatment planning systems on 6 MV photon of Varian Clinac 600 and 6 and 18 MV photons of a Varian Clinac 2100 C/D. Using diode array and a cylindrical ionization chamber for obtaining dose profiles and point absorbed dose respectively. For absorbed dose calculations in reference point, agreement within 1.5% was obtained for 6 MV and within 1% for 18 MV. For high dose and low dose gradient region calculations, agreement within 2% was obtained, in general, for all photon beams. Near the high dose region (thin edge of the equivalent hard wedge), the underestimation of the calculated curve was found and an agreement within 2.5%. For large dose gradient region (>30%/cm), agreement within 2 mm was found if appropriate grid size was used for all photon beams. For low dose and low dose gradient region (i.e. <7% of normalization dose), the underestimation of the calculated curve was found, agreement within 5% (of normalization dose) was obtained for large field (i.e. >10 x 10 cm^2); agreement within 3% was obtained for small fields. MU calculations agreement are within 1.5%.

CHAPTER V
MATERIALS AND METHODS

5.1 Materials

5.1.1 Clinac 23EX linear accelerator

The therapy unit used in this study is the Clinac 23EX linear accelerator which shown in Figure 15, manufactured by Varian Oncology System, Palo Alto, CA. It provides the dual photon beam energies of 6 MV and 10 MV, and six electron beam energies of 6, 9, 12, 15, 18, and 22 Mev. The photon field sizes are in range from 0.3 x 0.3 cm^2 to 40 x 40 cm^2 at isocenter. The distance from the target to isocenter is 100 cm. The dose rate are in ranges from 100 to 600 monitor unit per minute. It includes the dynamic MLC which composed of the maximum number of 120 tungsten MLC leaves, mounted below the secondary collimator in the same direction of X-jaws. The distance from the target to the block tray is 65.4 cm and the distance from the target to the bottom of the leaves is 53.8 cm.

Figure 15. The Clinac 23EX linear accelerator (Varian Oncology System, Palo Alto, CA)

5.1.2 Three-dimensional beam analyzing system (Blue phantom)

The Blue phantom (Scanditronix Wellhofer Dosimetric, Schwarzenbruck, Germany), with the scanning volume 48 x 48 x 41 cm^3, was made from acrylic plastic (perspex) as shown in Figure 16. For measuring the fast and accurate radiation fields commissioning, the phantom is prepared for external control by the OmniPro-Accept 6.1 Software. (IBA Advanced Radiotherapy, Scanditronix Wellhofer, Uppsala, Sweden). Measurement sequences can easily be set up and the measured data can be analyzed precisely. The central axis depth doses and beam profiles from the EDW fields were measured using this phantom.

Figure 16. Blue phantom (Scanditronix Wellhofer Dosimetric, Schwarzenbruck, Germany)

5.1.3 Water phantom

The water phantom with the dimensions of 38 x 38 x 38 cm^3 ; MT-150, for point dose measurement, as shown in Figure 17, is manufactured by MED-TECH company. This type of phantom allows the users to adjust the detector to be positioned at the selective depth with the increment of 0.01 mm. Measurements of the effective wedge factor will be performed with this phantom in this study.

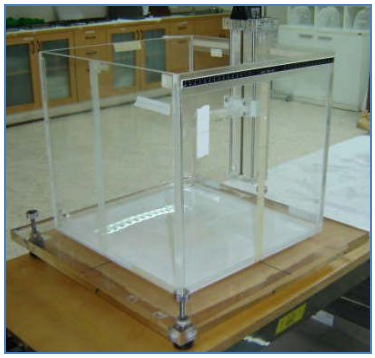

Figure 17. MT-150 water phantom

5.1.4 Cylindrical phantom

The in-house cylindrical phantom shown in Figure 18, is made of polymethyl-methacrylate (PMMA). It is approximately 35.5 cm in length, and 26 cm in diameter. There are five holes for inserting the ionization chamber to measure the absorbed dose at the selected point. The measurements to verify the accuracy of MU calculations were undertaken with this phantom.

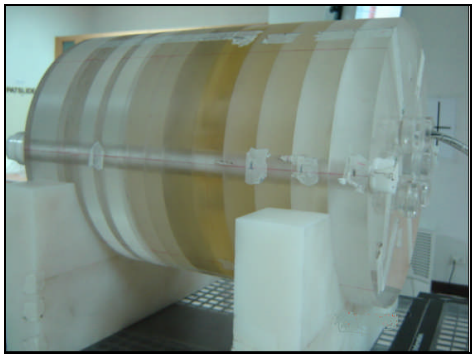

Figure 18. Cylindrical phantom

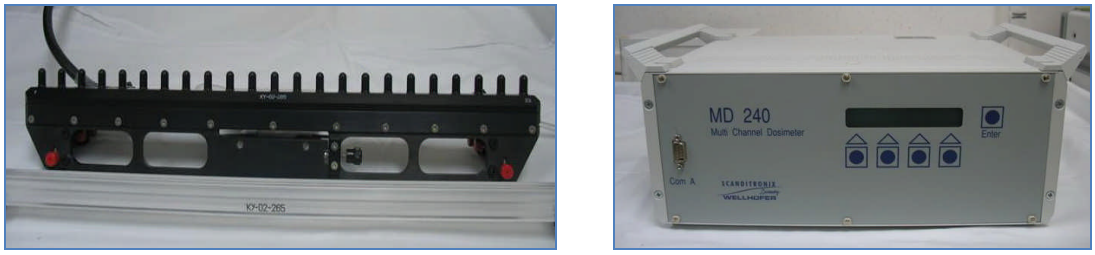

Figure 19. CA24 linear ion chamber array with MD240 24-channel-dosimeter, Wellhofer.

5.1.5 Linear ion chamber array (35)

A linear ion chamber array (CA24 with MD240 24-channel-dosimeter, Wellhofer) which is shown in Figure 19, has been used to measure the dose profiles for both symmetric and asymmetric EDW fields. This device allows the simultaneous of doses be collected in 23 measurement points. The spacing between adjacent chamber is 2.0 cm. Each ion chamber has an active volume of 0.147 cm^3, with a diameter of 0.6 cm, an active length of 0.33 cm and a chamber wall thickness of 0.4 mm. The chamber wall and the chamber electrode are made of polyoximethylene, conductive plastic. When performing the measurements, it was mounted on the scanning drive of the Blue phantom and the OmniPro-Accept 6.1 Software package was used for positioning and readout.

5.1.6 CC13 (0.13 cm^3) ionization chamber

The CC13 compact cylindrical ionization chamber of Scanditronix Wellhofer, Shcwazenbruck, Germany which is shown in Figure 20(a) was used for the absolute absorbed dose and percentage depth dose measurements in this study. The chamber is vented through a waterproof silicon sleeve, making it convenient for water measurements. It has a relatively small sensitive volume of 0.13 cm^3. It has an outer diameter of 6.8 mm, an inner wall thickness of 0.4 mm and a total active length of 5.8 mm. Both the outer wall and inner electrodes are composed of an air equivalent plastic called Shonka C552 (1.76 g/cm^3). The recommended polarizing voltage is $\pm$300 Volts. The leakage current is $< \pm 4 \times 10^{-15}$ A. Its sensitivity is 3.8×10^{-9} C/Gy.

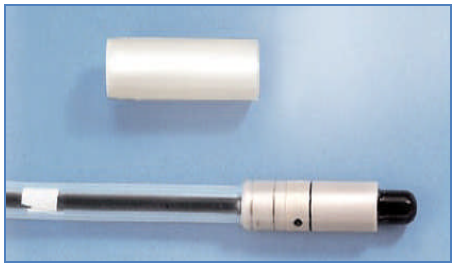

(a)

(b)

(c)

Figure 20. (a) CC13 ionization chamber
(b) NE 2571 Farmer 0.6 CC ionization chamber
(c) NE 2570/1 electrometer

Figure 21. CU500E electrometer

5.1.7 2571 Farmer (0.6 cm^3) ionization chamber and NE 2570/1 electrometer

The 0.6 cm^3 Farmer ionization chamber of Nuclear Enterprise limited (NE) type 2571 and NE 2570/1 electrometer, shown in Figure 20(b) and 20(c) are widely used for the dosimetry of photons and electrons at therapy level dose rates. The chamber can be calibrated to measure air kerma, surface absorbed dose or absorbed dose to water at photon energy range from 50 kV to 35 MV and the electron energy from 5 MeV to 35 MeV. It is constructed from a thin-walled, high purity graphite thimble and aluminum electrode, with detachable build-up cap. The sensitive volume is 0.69 cm^3 with the length volume and thickness of 24.1 mm and 0.36 mm, respectively. This chamber was used to measure the effective wedge factor for the EDW and the absorbed dose for MU verification.

5.1.8 CU500E electrometer

The CU500E control unit which is shown in Figure 21 has a built-in dual channel electrometer with reversible polarity and auto ranging for set-up that is controlled by Omnipro-Accept 6.1 software. This electrometer can be used with 0.13 cm^3 ionization chamber for both fields and reference detectors. Furthermore, it can be used with CA24 chamber array for beam profile measurement. It has full polarizing voltage from 0 to $\pm$ 480 Volts in steps of 1V.

5.1.9 Eclipse treatment planning system

The Eclipse treatment planning system version 8.0 (Varian Oncology systems, Palo Alto, CA, USA) is shown in Figure 22. The system provides for treatment planning capabilities for simple radiation treatment, for 3D conformal radiation therapy (3D-CRT), as well as the intensity modulated radiation therapy (IMRT). The hardware contains the electronics, central processing unit, graphic display systems, and the others devices. For the software component, two available dose calculation algorithms, a pencil beam convolution (PBC) and an analytical anisotropic algorithm (AAA) algorithm were used to calculate the radiation dose in the volume of interest. In this study, the PBC algorithm was used to calculate the dose distribution from the EDW.

Figure 22. Treatment planning system (Eclipse 8.0, Varian Oncology System)

5.1.10 Thermometer and barometer

Thermometer and barometer was used to measure the air pressure and water temperature to correct for the chamber readings as shown in Figure 23.

Figure 23. Thermometer and barometer

5.1.11 Spirit level

Spirit level which used in entire measurements is shown in Figure 24.

Figure 24. Spirit level

5.2 Methods

5.2.1 Commissioning of the enhanced dynamic wedge (EDW) into Eclipse 8.0 treatment planning system

To incoperate the EDW capabilities into the Eclipse 8.0 treatment planning system, the steps for commissioning the EDW were firstly started with the machine configuration in the selected machines and energy for seven wedge angles (10^0, 15^0, 20^0, 25^0, 30^0, 45^0 and 60^0), each EDW angle will be specified with the identification number (ID) and properties as shown in Figure 25(a-c). Then, these all enhanced dynamic wedges were assigned to be match with EDWs field model in the photon beam configuration task.

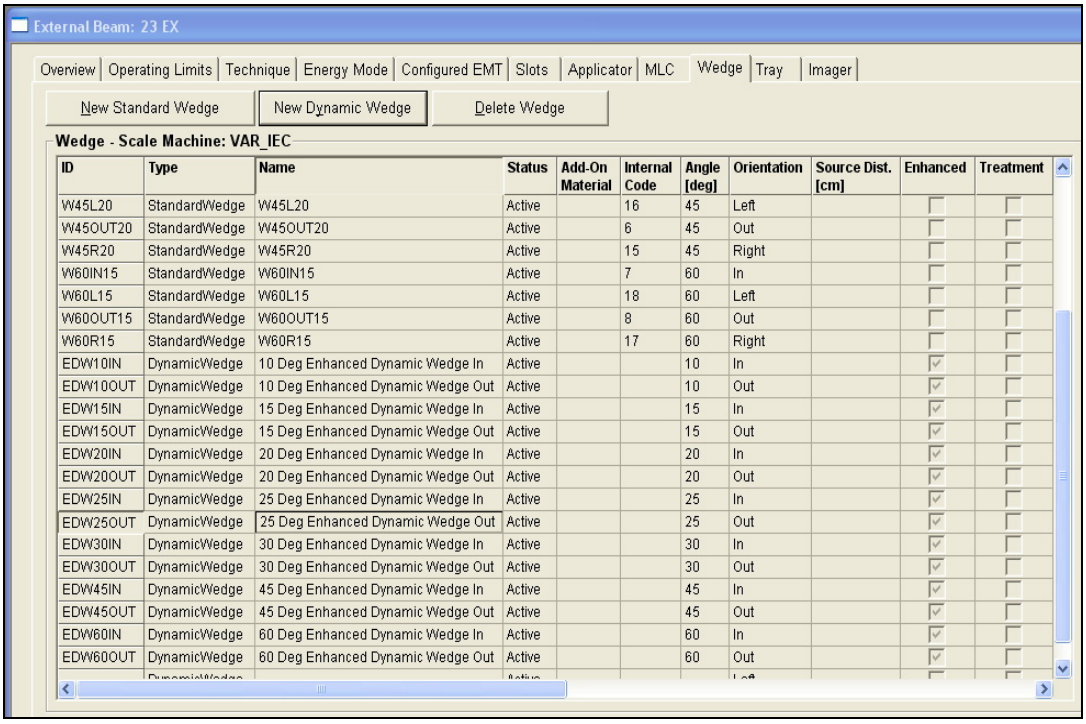

ID	Type	Name	Status	Add-On Material	Internal Code	Angle [deg]	Orientation	Source Dist. [cm]	Enhanced	Treatment
W45L20	StandardWedge	W45L20	Active		16	45	Left			
W45OUT20	StandardWedge	W45OUT20	Active		6	45	Out			
W45R20	StandardWedge	W45R20	Active		15	45	Right			
W60IN15	StandardWedge	W60IN15	Active		7	60	In			
W60L15	StandardWedge	W60L15	Active		18	60	Left			
W60OUT15	StandardWedge	W60OUT15	Active		8	60	Out			
W60R15	StandardWedge	W60R15	Active		17	60	Right			
EDW10IN	DynamicWedge	10 Deg Enhanced Dynamic Wedge In	Active			10	In			
EDW10OUT	DynamicWedge	10 Deg Enhanced Dynamic Wedge Out	Active			10	Out			
EDW15IN	DynamicWedge	15 Deg Enhanced Dynamic Wedge In	Active			15	In			
EDW15OUT	DynamicWedge	15 Deg Enhanced Dynamic Wedge Out	Active			15	Out			
EDW20IN	DynamicWedge	20 Deg Enhanced Dynamic Wedge In	Active			20	In			
EDW20OUT	DynamicWedge	20 Deg Enhanced Dynamic Wedge Out	Active			20	Out			
EDW25IN	DynamicWedge	25 Deg Enhanced Dynamic Wedge In	Active			25	In			
EDW25OUT	DynamicWedge	25 Deg Enhanced Dynamic Wedge Out	Active			25	Out			
EDW30IN	DynamicWedge	30 Deg Enhanced Dynamic Wedge In	Active			30	In			
EDW30OUT	DynamicWedge	30 Deg Enhanced Dynamic Wedge Out	Active			30	Out			
EDW45IN	DynamicWedge	45 Deg Enhanced Dynamic Wedge In	Active			45	In			
EDW45OUT	DynamicWedge	45 Deg Enhanced Dynamic Wedge Out	Active			45	Out			
EDW60IN	DynamicWedge	60 Deg Enhanced Dynamic Wedge In	Active			60	In			
EDW60OUT	DynamicWedge	60 Deg Enhanced Dynamic Wedge Out	Active			60	Out			

(a)

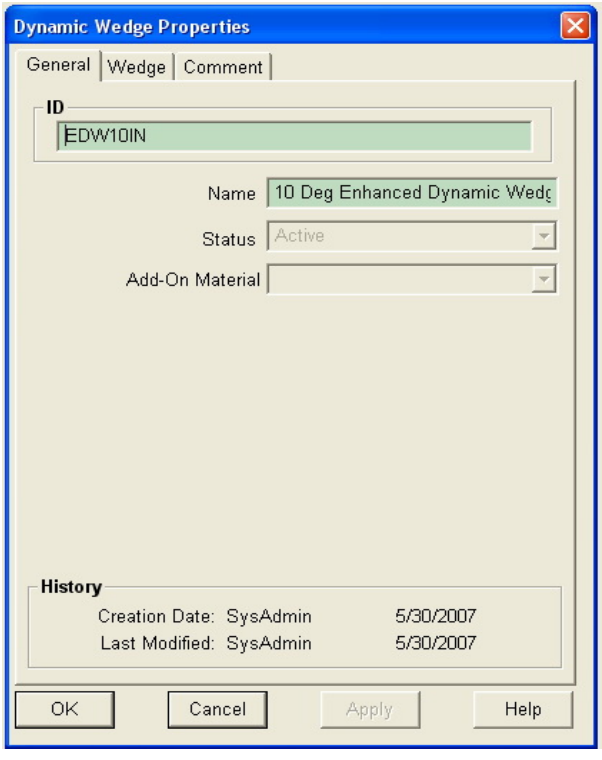

(b)

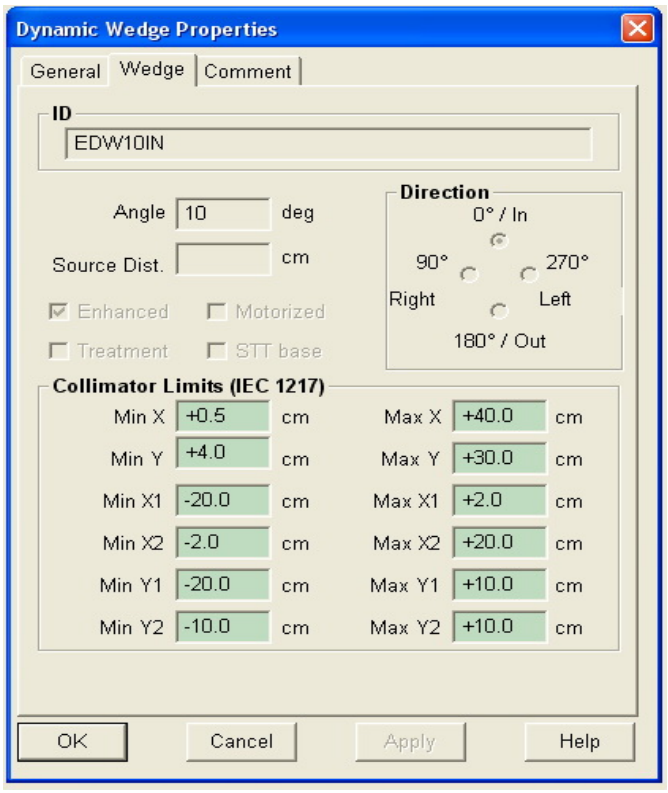

(c)

Figure 25. Illustrate the steps for commissioning of the EDW in the Eqlipse 8.0 TPS.

(a) The window for creating new EDW

(b) Specify ID for each EDW

(c) Specify the properties for each EDW

5.2.2 Verification the accuracy of EDW dosimetric parameters

5.2.2.1 Chamber array calibration

Dosimetric characteristics for EDW including the central axis depth doses, beam profiles, effective wedge factors and effective wedge angle were essential to be investigated before accurately implementing the EDW into the clinic.

Since the measurement of dose distributions for dynamic wedge requires integration of the dose during the entire exposure, hence the dosimeter for this purpose has to be static. For the beam profile measurements, using a regular single ion chamber is inefficient and more time consuming. Because the dose at each grid point has to be measured separately. Alternatively, beam profiles can be measured more efficiently by using radiographic films or a multiple diode array. In this study, the CA24 ion chamber array was used to measure the EDW beam profiles.

The CA24 chamber array contains 23 ion chambers. By default, the relative sensitivity factor for each chamber will be set at 1.0. However, response to the radiation dose of the 23 chambers can be different, thus the calibration of the CA24 chamber array before measurement is needed. The calibration was started by measuring the beam profile at 23 fixed point of 2.0 cm spacing, in step by step using a single Wellhofer CC13 ionization chamber with a maximum static open field 40 x 40 cm^2 (45^0 collimator angle) at the depth of 5 cm, irradiated by 6 MV photon beam. Then, doses measurement using the chamber array (CA24 with MD240 24-channel-dosemeter, Wellhofer) were performed at the same position as the measurements performed by using the single CC13 ionization chamber. The two measured dose profiles from CC13 and CA24 chamber are then compared, and the calibration factors are determined by the software as shown in Figure 26(a-c). These calibration factors will be automatically applied to the raw chamber readings for any subsequent measurements.

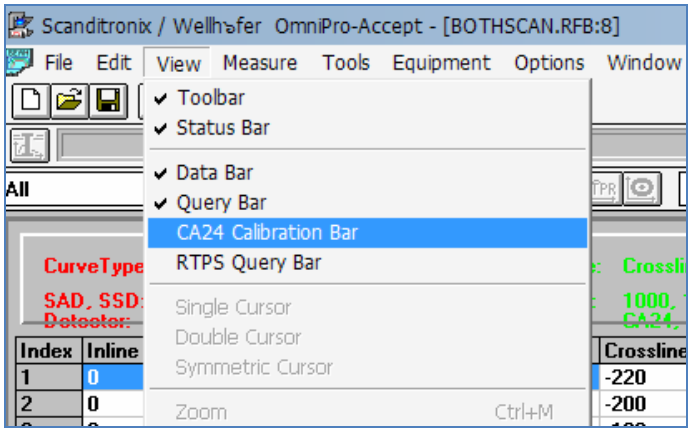
Scanditronix / Wellhöfer OmniPro-Accept - [BOTHSCAN.RFB:8]
File Edit View Measure Tools Equipment Options Window
Toolbar
Status Bar
Data Bar
Query Bar
CA24 Calibration Bar
RTPS Query Bar
Single Cursor
Double Cursor
Symmetric Cursor
Zoom Ctrl+M
All
CurveType
SAD, SSD:
Detector:
Index Inline Crossline
1 0 -220
2 0 -200

(a)

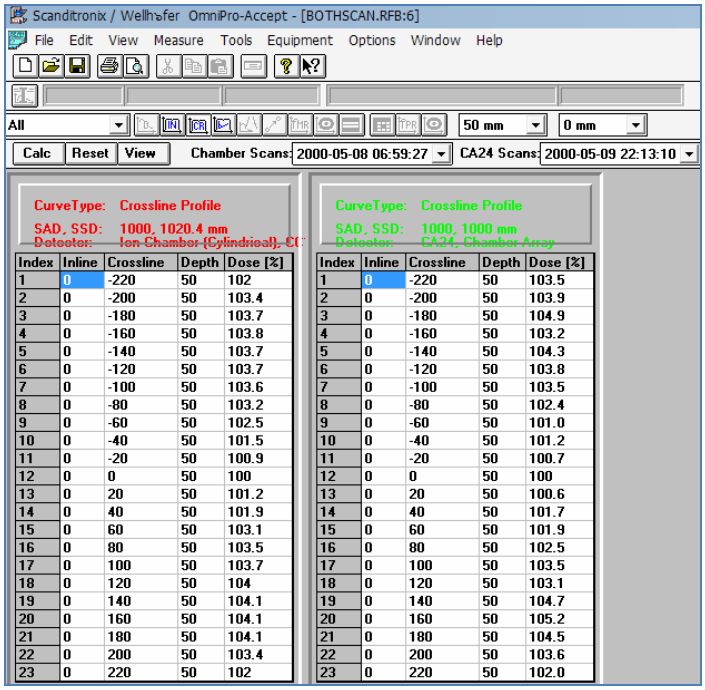
Scanditronix / Wellhöfer OmniPro-Accept - [BOTHSCAN.RFB:6]
File Edit View Measure Tools Equipment Options Window Help
All
50 mm
0 mm
Calc Reset View
Chamber Scans: 2000-05-08 06:59:27
CA24 Scans: 2000-05-09 22:13:10
CurveType: Crossline Profile
SAD, SSD: 1000, 1020.4 mm
Detector: Ion Chamber (Cylindrical), CC
Index Inline Crossline Depth Dose [%]
1 0 -220 50 102
2 0 -200 50 103.4
3 0 -180 50 103.7
4 0 -160 50 103.8
5 0 -140 50 103.7
6 0 -120 50 103.7
7 0 -100 50 103.6
8 0 -80 50 103.2
9 0 -60 50 102.5
10 0 -40 50 101.5
11 0 -20 50 100.9
12 0 0 50 100
13 0 20 50 101.2
14 0 40 50 101.9
15 0 60 50 103.1
16 0 80 50 103.5
17 0 100 50 103.7
18 0 120 50 104
19 0 140 50 104.1
20 0 160 50 104.1
21 0 180 50 104.1
22 0 200 50 103.4
23 0 220 50 102
CurveType: Crossline Profile
SAD, SSD: 1000, 1000 mm
Detector: CA24, Chamber Array
Index Inline Crossline Depth Dose [%]
1 0 -220 50 103.5
2 0 -200 50 103.9
3 0 -180 50 104.9
4 0 -160 50 103.2
5 0 -140 50 104.3
6 0 -120 50 103.8
7 0 -100 50 103.5
8 0 -80 50 102.4
9 0 -60 50 101.0
10 0 -40 50 101.2
11 0 -20 50 100.7
12 0 0 50 100
13 0 20 50 100.6
14 0 40 50 101.7
15 0 60 50 101.9
16 0 80 50 102.5
17 0 100 50 103.5
18 0 120 50 103.1
19 0 140 50 104.7
20 0 160 50 105.2
21 0 180 50 104.5
22 0 200 50 103.6
23 0 220 50 102.0

(b)

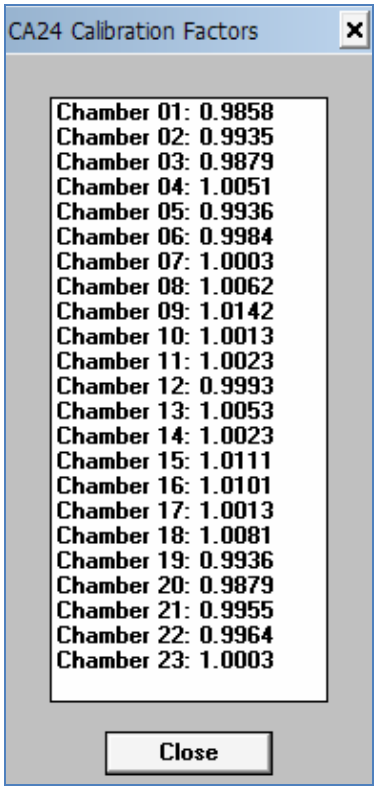

(c)

Figure 26. Illustrates the steps for CA24 calibration in dosimetry software

(a) The menu for starting CA24 calibration

(b) CA24 calibration bar

(c) Relative sensitivity or Calibration factors for CA24 ionizaion chamber

5.2.2.2 Measurements of the EDW dosimetric parameters

5.2.2.2.1 Central axis depth dose measurements

Since dose at the central axis at a given depth of the EDW field was a result of the integration of dose from the dynamic exposure. To acquire depth dose data for the EDW field, measurement of dose at each defined depth must be undertaken with the single point dose measurements. In this study, a single chamber (CC13 ionization chamber) connected to a CU500E electrometer, positioned at the central axis of the field at a selected depth from 0.0 to 30.0 cm was used to measure the EDW depth dose. From 0.0 to 5.0 cm depth, the increment of measurement was 0.2 cm and then every 2.5 cm from 5.0 to 30.0 cm depth were selected. All measurements were performed with 6 MV photon beam at a fixed source-surface-distance (SSD) of 100 cm for 25^0 and 45^0 EDW angle, for both wedge Y1-IN and Y2-OUT directions. Various symmetric square and rectangular EDW field sizes of 5 x 5 cm^2, 10 x 10 cm^2, 15 x 15 cm^2, 20 x 20 cm^2, 20 x 5 cm^2, 20 x 10 cm^2 and 20 x 15 cm^2, and the asymmetric field sizes of 20 x 5 cm^2, 20 x 10 cm^2, 20 x 15 cm^2, 40 x 30 cm^2 with the corresponding beam centers were 2.5, 5, and 7.5 cm off-axis, respectively were chosen for the measurements as shown in Figure 27(a-c). The open field depth doses were also measured with the same conditions as the EDW and compared to the EDW depth doses. Analysis will be performed by comparing the measured and calculated depth dose which obtained from the Eclipse 8.0 treatment planning system (TPS).

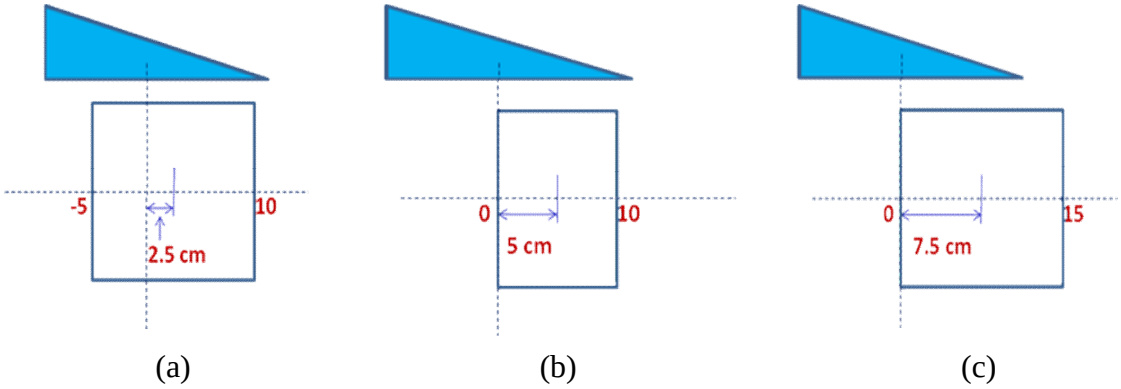

Figure 27. The diagram of off-axis distance for asymmetric field sizes.
(a) Off-axis distance 2.5 cm for 15 cm width
(b) Off-axis distance 5.0 cm for 10 cm width
(c) Off-axis distance 7.5 cm for 15 cm width

5.2.2.2.2 Profile measurement

From a limitation of the chamber spacing, 2 cm apart, was found on the CA24 chamber array. To achieve the EDW beam profile with 5 mm increments, four exposures had to be carried out. This process was performed by moving the CA24 in the wedge direction, 5 mm, between each of the multiple exposures as illustrated in Figure 28.

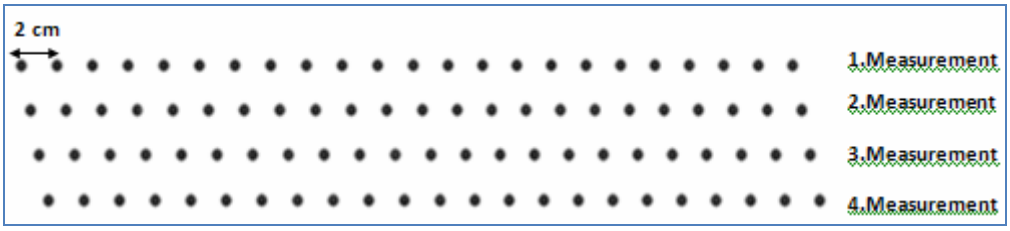

Figure 28. The diagram for four exposures on the CA24 chamber array, each chamber is shifted 5 mm for each measurement (35).

Measurements of profiles were taken at four depths, d_{max} (1.6 cm), 5, 10 and 20 cm for 25^0 and 45^0 EDW angle for both wedge directions, Y1-IN and Y2-OUT with the same energy, field sizes and geometry as used in the depth dose measurements. Each profile was normalized to the corresponding center of the beam for each wedge angle and then the measured profiles were compared with the calculated profiles by Eclipse 8.0 treatment planning system (TPS).

5.2.2.2.3 Effective wedge factor measurement

By definition, the effective wedge factor for a given symmetric field size is the ratio of integrated dose on the central axis, to that of an open field for a fixed number of monitor unit (21).

Measurement of the effective wedge factors for symmetric square field sizes of 5 x 5 cm^2, 10 x 10 cm^2, 15 x 15 cm^2, 20 x 20 cm^2, and rectangular field sizes of 20 x 5 cm^2, 20 x 10 cm^2 and 20 x 15 cm^2 were taken with the 0.6 CC ion chamber for 6 MV photon beam for the EDW angle 25^0 and 45^0 at 5, 10 and 20 cm depth with the SSD of 100 cm. To verify that the effective wedge factors do not depend on the collimator angle, comparison between the 0^0 and 90^0 collimator angle at field size 10 x 10 cm^2 and 20 x 10 cm^2 were performed. To account for the misalignment, every measurement was repeated with the opposed wedge orientation and averaged the chamber readings obtained from two wedge orientations.

About the wedge factor in asymmetric EDW fields, the ion chamber readings will change from the central axis to at the beam center of the asymmetric EDW field to the symmetric open field. With this definition the influence of the flattening filter and the variations in beam hardening to the dose at an off-axis point are included in the effective wedge factor (21). In this study, the measurements of the effective wedge factor for the asymmetric field sizes as indicated in the depth dose measurements were followed by the above definition at depth, 5, 10 and 20 cm.

5.2.2.2.4 Wedge angle measurement

The enhance dynamic wedge angle will be calculated according the IEC-976 definition (25), which defines the wedge angle to be the angle of a line between the two points on the isodose curve at standard measurement depth that are equidistance a quarter of the field width away from the central axis (see in Figure 14). The standard measurement depth was recommended at either 5 or 10 cm (OmniPro-Accept System Manual, P.121) In this research, the wedge angles were measured at 10 cm depth for the EDW isodose distributions that generated from the depth dose and beam profile data. Then the measured and calculated wedge angles were compared.

5.2.2.3 Monitor Units (MUs) verification

To verify the accuracy of monitor units (MUs) calculation by Eclipse TPS, three EDW treatment plans were generated. Detail of each plan was described as shown in Figure 29-31 and Table 8-10. All plans were transferred to the 23EX treatment machine via record and verify system (ARIA). Point absorbed dose at isocenter then be measured with the 0.6 cc Farmer ionization chamber and NE 2570/1 dosimeter in the PMMA cylindrical phantom. The IAEA TRS No. 398 is the protocol using for the absorbed dose determination (38). Comparison between the calculated dose from TPS and measured dose were undertaken.

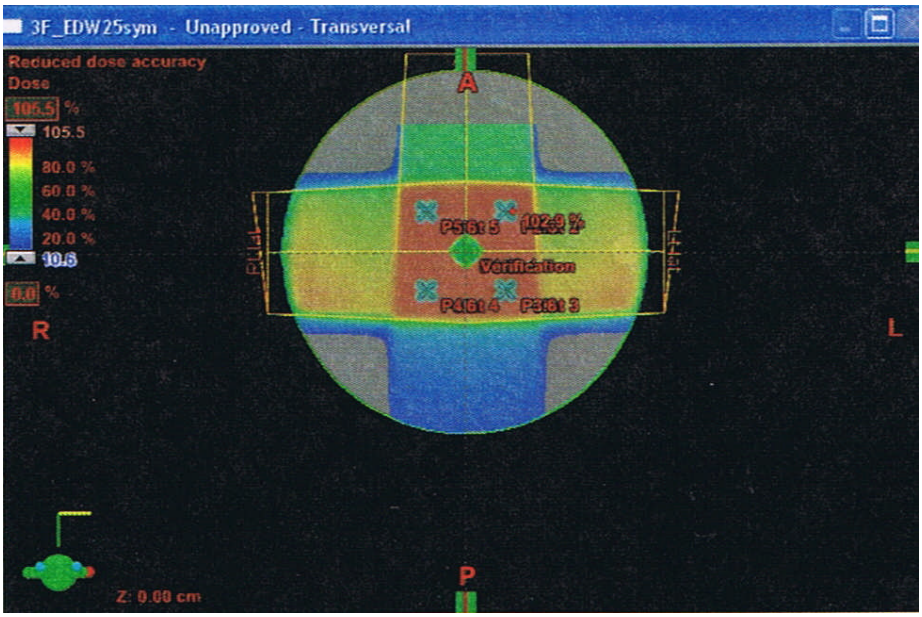

Figure 29. Plan 1**:** Three fields plan with 25^0 EDW symmetric field, SAD technique with the prescription dose, 2 Gy at isocenter.

Table 8. Treatment detail of Plan 1

Treatment Parameter	Field ID		
	AP	Right lateral	Left lateral
Gantry (degree)	0.0	270.0	90.0
Collimator (degree)	0.0	90.0	90.0
Wedge	None	25^0EDWY1IN	25^0EDWY2OUT
Field X (cm)	10.0	20.0	20.0
Field Y (cm)	20.0	10.0	10.0
SSD (cm)	87.0	86.9	87.1
MU	82	113	112

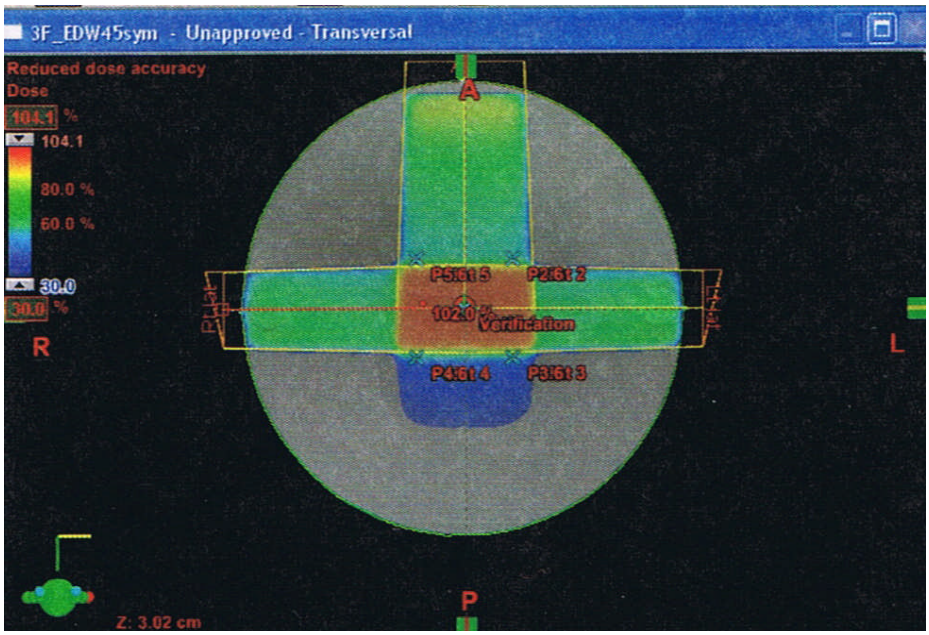

Figure 30. Plan 2**:** Three fields plan with 45^0 EDW symmetric field, SAD technique with the prescription dose, 2 Gy at isocenter.

Table 9. Treatment detail of Plan 2

Treatment Parameter	Field ID		
	AP	Right lateral	Left lateral
Gantry (degree)	0.0	270.0	90.0
Collimator (degree)	0.0	90.0	90.0
Wedge	None	45^0EDWY1IN	45^0EDWY2OUT
Field X (cm)	8.0	10.0	10.0
Field Y (cm)	10.0	5.0	5.0
SSD (cm)	87.0	86.9	87.1
MU	130	104	104

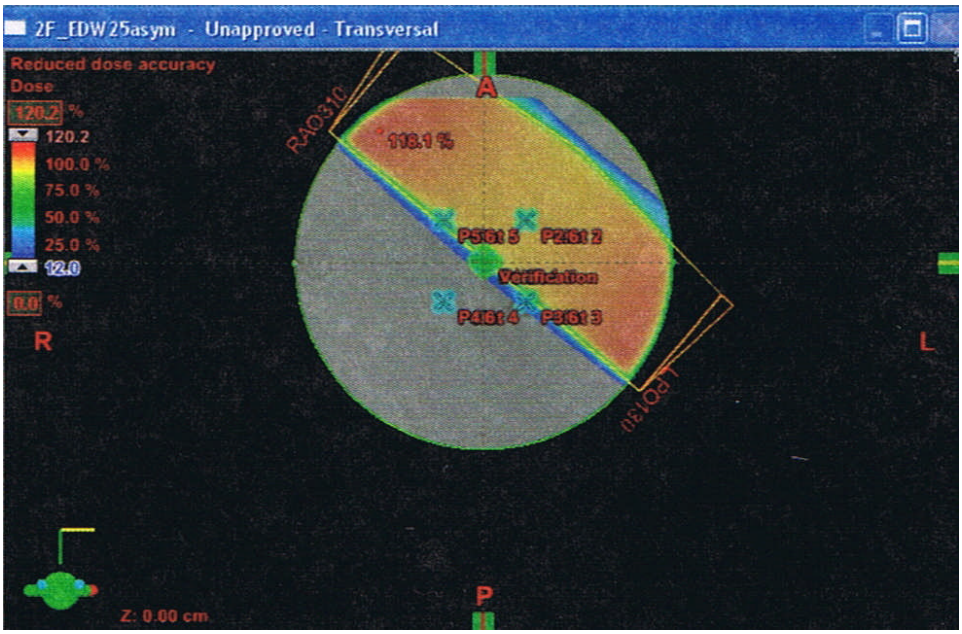

Figure 31. Plan 3**:** Two tangential fields with the 25^0 EDW asymmetric half- block field**,** SAD technique with the prescription dose, 2 Gy at isocenter.

Table 10. Treatment detail of Plan 3

Treatment Parameter	Field ID	
	RAO310	LPO130
Gantry (degree)	310.0	130.0
Collimator (degree)	90.0	90.0
Wedge	25^0EDWY1IN	25^0EDWY2OUT
Field X (cm)	20.0	20.0
Field Y (cm)	10.0	10.0
Y1 (cm)	10.0	0.0
Y2 (cm)	0.0	10.0
SSD (cm)	87.0	87.3
MU	147	144

5.2.3 Acceptance criteria

To investigate the accuracy of EDW beam characteristics, criteria for acceptability of dose comparison recommended by Dyk JV et al (37) and Venselaar J et al (38) were used in this study. For depth dose, dose at the location δ_1 and δ_2 as shown in Figure 32, are defined as percent of dose difference for data points on the central beam axis beyond the depth of d_{max} and in the build-up region were selected for the comparison. In this study, δ_1 was selected at depth 10 cm and at depth 90% of dose for δ_2. Similarly for the beam profile, δ_2, δ_3, δ_4 and RW_{50} as shown in Figure 33, will be the parameters to achieve the accuracy. The δ_2 presented the data points in the penumbra region and was selected at 30% of dose in this study. The δ_3 presented the data points in the high dose-low dose gradient region (about one quarter of the field size from the central axis of beam), δ_4 in the low dose-small dose gradient region (off the geometrical beam edges), and RW_{50} as the radiological width (the width of a profile measured at half its height compared to the value at the beam axis). The δ_4 and $\delta_{50\text{-}90}$ which defines as the distance between the 90% and the 50% dose will not be used in this investigation because the measurement resolution from the CA24 chamber array was not properly to be used in the analysis for EDW beam profile. Table 11 provides the acceptance criteria for these different parameters used in depth dose and beam profiles analysis.

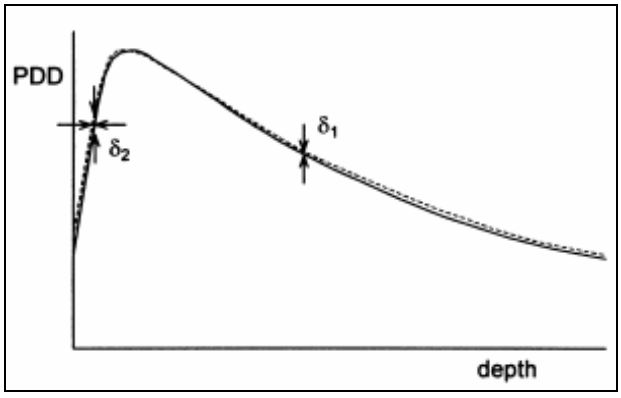

Figure 32. Regions of validity of the criteria δ_1 and δ_2 to compare calculated and measured depth dose (PDD) curves (38). δ_1 and δ_2 in this study, were selected at depth 10 cm and at depth 90% of dose, respectively.

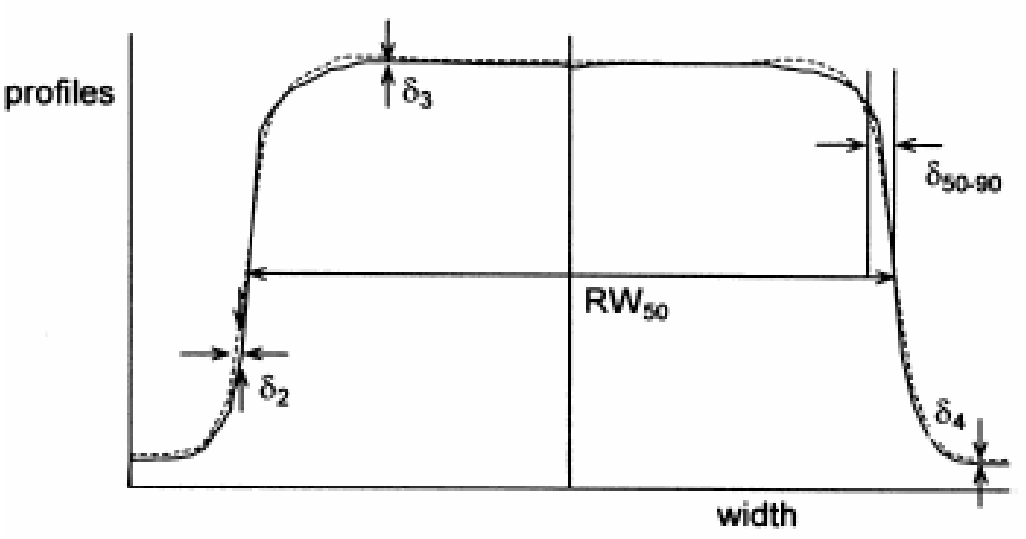

Figure 33. Regions of validity of the criteria δ_2, δ_3, δ_4, $\delta_{50\text{-}90}$ and RW_{50} to compare calculated and measured beam profiles (38). δ_2 and δ_3 in this study were selected at 30% of dose and at one quarter of the field size from the central axis of beam.

Table 11. Illustrates the deviations (δ) for different regions (38).

	Location	Type of region	1. Simple geometry (homogeneous)	2. Complex geometry (wedge, inhomogeneit, asymmetry)	More complex geometry (combinations of 1 and 2
δ_1	Central beam axis	High dose, small dose gradient	2%	3%	4%
δ_2 [a]	Buildup region of central axis and penumbra region of profiles	High dose, large dose gradient	2 mm or 10%	3 mm or 15%	3 mm or 15%
δ_3	Outside central beam axis region	High dose, small dose gradient	3%	3%	4%
δ_4	Outside beam edges	Low dose, small dose gradient	3% [b] (30%)	4% [b] (40%)	5% [b] (50%)
RW_{50} [a]	Radiological width		2 mm or 1%	2 mm or 1%	2 mm or 1%
$\delta_{50\text{-}90}$	Beam fringe		2 mm	3 mm	3 mm

[a] These values are preferably expressed in mm. A shift of 1 mm corresponding to a dose variation of 5% is assumed to be a realistic value in the high dose, large dose gradient region.

[b] This percentage is applicable to the following equation, $\delta_4 = 100\% \times (D_{calc} - D_{meas}) / D_{meas,cax}$ where $D_{meas,cax}$ is the dose on the central beam axis , since it is not always practicable with the local dose. The values in brackets are those determined from Eq. (6)

CHAPTER VI
RESULTS AND DISCUSSION

6.1 Results

6.1.1 The CA24 chamber array calibration factor

To calibrate the chamber array, profile measurements between the chamber array and single ion point were performed. The result presented the good agreement of the two beam profiles (Figure 34). The calibration factors of 23 ion chambers were also determined from the Wellhofer software and presented in Table 12. These factors are within 1% - 2% of unity. They are applied automatically by the software to the raw chamber readings for any subsequent measurements.

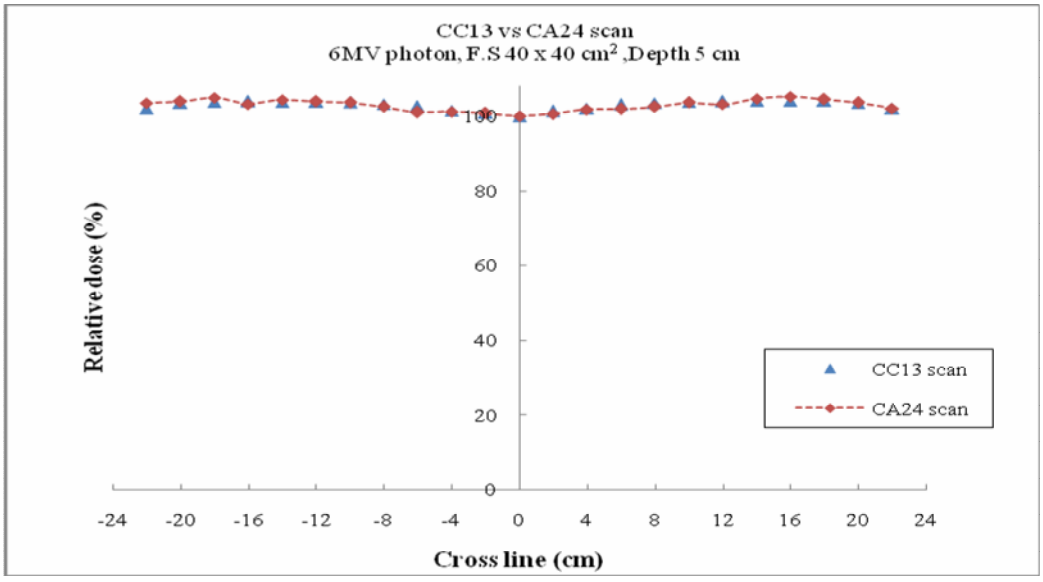

Figure 34. Comparison of the beam profiles between CA24 chamber array and CC13 single ion chamber measurements for a 6 MV photon beam, field size 40 x 40 cm^2 at depth of 5 cm.

Table 12. The calibration factors of the CA24 chamber array

Chamber No.	Cross line (cm)	Relative Dose (%)		Calibration factors	%Difference from unity
		CC13 scan	CA24 scan		
1	-22	102.03	103.47	0.9858	1.42
2	-20	103.39	103.92	0.9935	0.65
3	-18	103.73	104.91	0.9879	1.21
4	-16	103.84	103.25	1.0051	-0.51
5	-14	103.73	104.30	0.9936	0.64
6	-12	103.73	103.85	0.9984	0.16
7	-10	103.62	103.55	1.0003	-0.03
8	-8	103.16	102.42	1.0062	-0.62
9	-6	102.49	100.98	1.0142	-1.42
10	-4	101.47	101.21	1.0013	-0.13
11	-2	100.90	100.68	1.0023	-0.23
12	0	100.00	100.00	0.9993	0.07
13	2	101.24	100.60	1.0053	-0.53
14	4	101.92	101.66	1.0023	-0.23
15	6	103.05	101.89	1.0111	-1.11
16	8	103.50	102.49	1.0101	-1.01
17	10	103.73	103.55	1.0013	-0.13
18	12	103.95	103.09	1.0081	-0.81
19	14	104.07	104.68	0.9936	0.64
20	16	104.07	105.21	0.9879	1.21
21	18	104.07	104.45	0.9955	0.45
22	20	103.39	103.62	0.9964	0.36
23	22	102.03	101.96	1.0003	-0.03

6.1.2 Dosimetric parameter measurement for EDW

6.1.2.1 The accuracy of EDW depth doses

Results of the 6 MV depth doses from the measurements and TPS calculations in the symmetric open, 25^0 and 45^0EDW beam, for both wedge direction ,Y1-IN and Y2-OUT are presented in Fig 35 to 41 (a-d), respectively. For the asymmetric field, all the results also are presented in Fig 42 to 45 (a-d).

All TPS calculated EDW depth doses were verified the accuracy by comparing with the measurements using the criteria δ_1 and δ_2 which already described in the section 5.2.3. Table 13 and 14 presented the percentage of dose difference between the calculated and measured dose as well as the difference of dose between the measured open beam and EDW beam in the symmetric and asymmetric field for both wedge directions.

The results revealed that, for the symmetric EDW field, the percentage of dose difference between the calculated and measured EDW depth doses were in the range of $\pm$ 0.02-3.34%. The maximum percentage of dose difference -3.34% was found at the field size of 20 x 20 cm^2, 25^0EDW and Y2-OUT direction. For the asymmetric EDW depth doses, the percentage of dose difference between the calculated and measured EDW depth doses were in the range of $\pm$ 0.07-4.35%. The maximum percentage of dose difference about -4.35% was seen at the largest field size (40 x 30 cm^2), 25^0EDW and Y2-OUT direction. Using the acceptance criteria of Dyk JV et al (37) and Venselaar J et al (38), one hundred percent of the calculated EDW depth doses achieve the accuracy as shown in Table 15 to 17.

6.1.2.2 The open beam and EDW depth doses

Since the EDW depth dose, by principle, was created from the multiple open fields which the radiation transmission through the primary collimator jaw and the scattered radiation from the remainder of the irradiated field are included into the calculation model. Thus, the investigation clearly showed that, all EDW depth dose characteristics, in any field size of the symmetric and asymmetric field for both wedge directions, are similar to the open field depth doses. By the percentage of dose difference between the two depth doses were detected in the range of $\pm$ 0.01-4.42 %. However, the percentage of dose differences was found to be higher at the larger asymmetric field sizes at the depth deeper than 10 cm. Moreover, using $DD_{20/10}$ to define the beam quality, it was found that both the open and EDW beams for both wedge angles presented the same beam quality, as shown in Figure 46 (a-c) for the field size of 10 x 10 cm^2. Investigation of $DD_{20/10}$ for all field sizes of 25^0 and 45^0 EDW at both wedge directions were also summarized in Table 18 (a-b). For 25^0 EDW, the same beam quality as the open beam detected in all situations, but for the 45^0 EDW, a slightly difference of $DD_{20/10}$ was seen in the field size of 20 x 20 and 20 x 15 cm^2. This finding insisted that application of the EDW will not cause the beam hardening effect as found in the physical wedge.

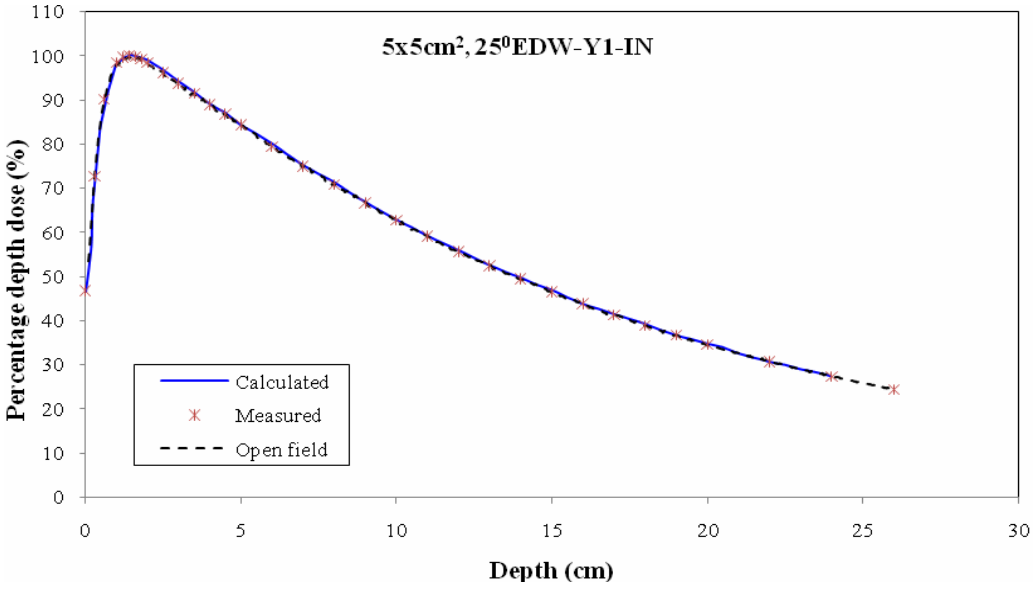
5x5cm², 25⁰EDW-Y1-IN
Percentage depth dose (%)
Depth (cm)
Calculated
Measured
Open field
0
10
20
30
40
50
60
70
80
90
100
110
0
5
10
15
20
25
30

(a)

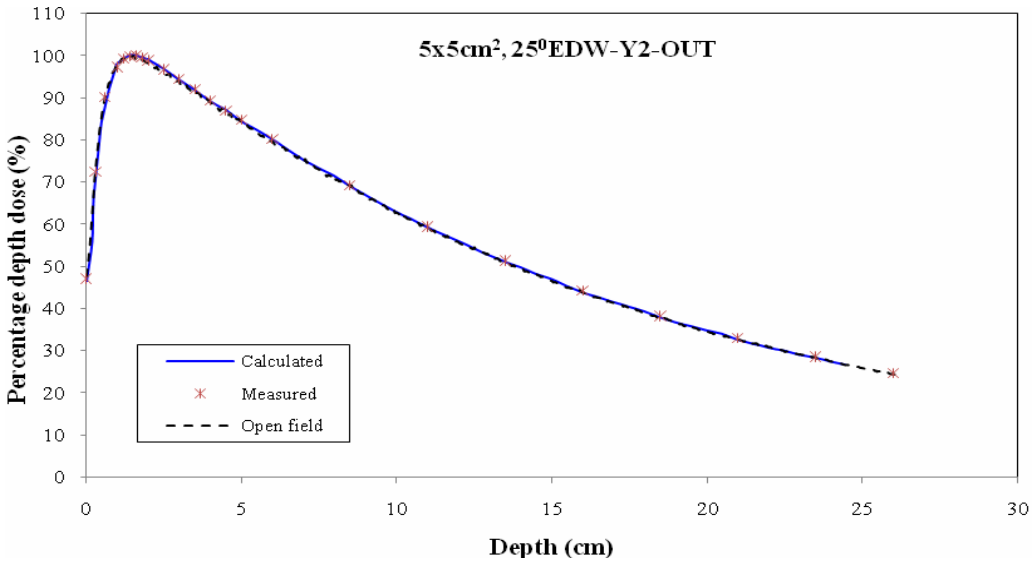
5x5cm², 25⁰EDW-Y2-OUT
Percentage depth dose (%)
Depth (cm)
Calculated
Measured
Open field
0
10
20
30
40
50
60
70
80
90
100
110
0
5
10
15
20
25
30

(b)

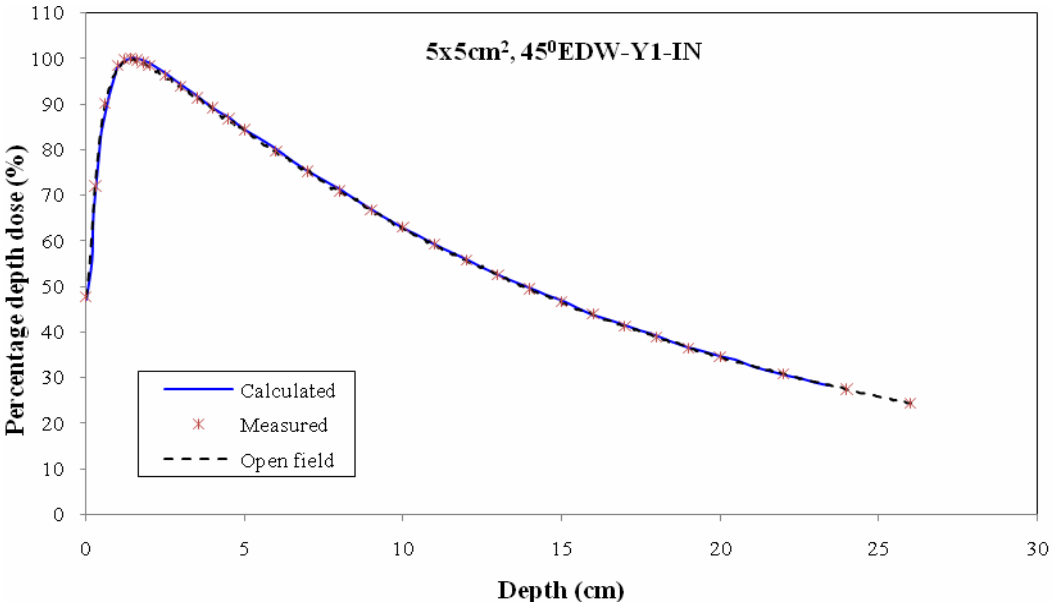

(c)

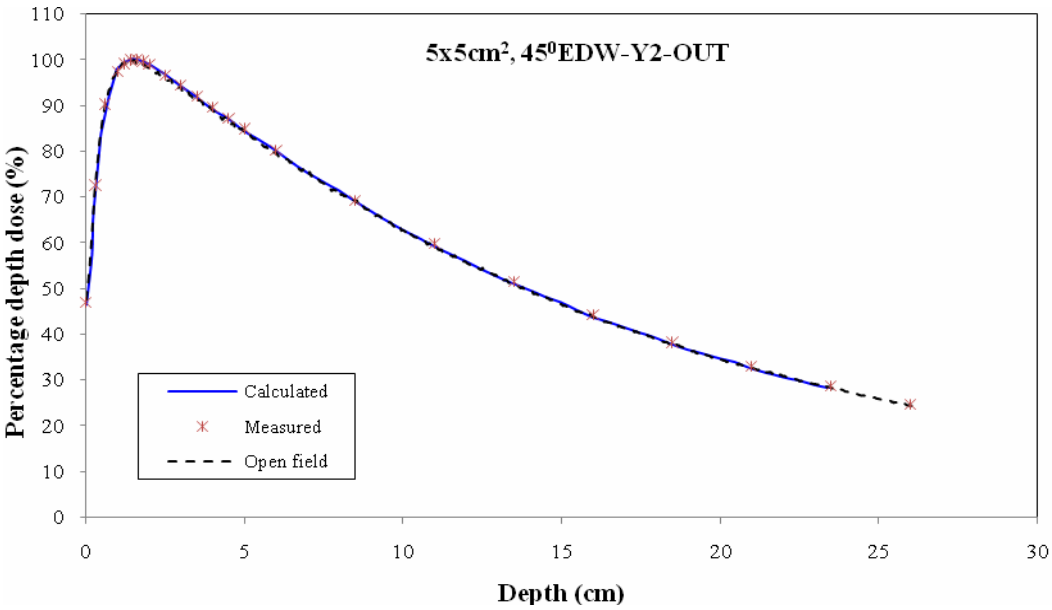

(d)

Figure 35. The comparison of open field (dash line), measured (symbols) and calculated (solid line) EDW depth doses for 6 MV photon beam at a symmetric field size of 5 x 5 cm^2 for (a) 25°EDW-Y1-IN (b) 25°EDW-Y2-OUT (c) 45°EDW-Y1-IN and (d) 45°EDW-Y2-OUT.

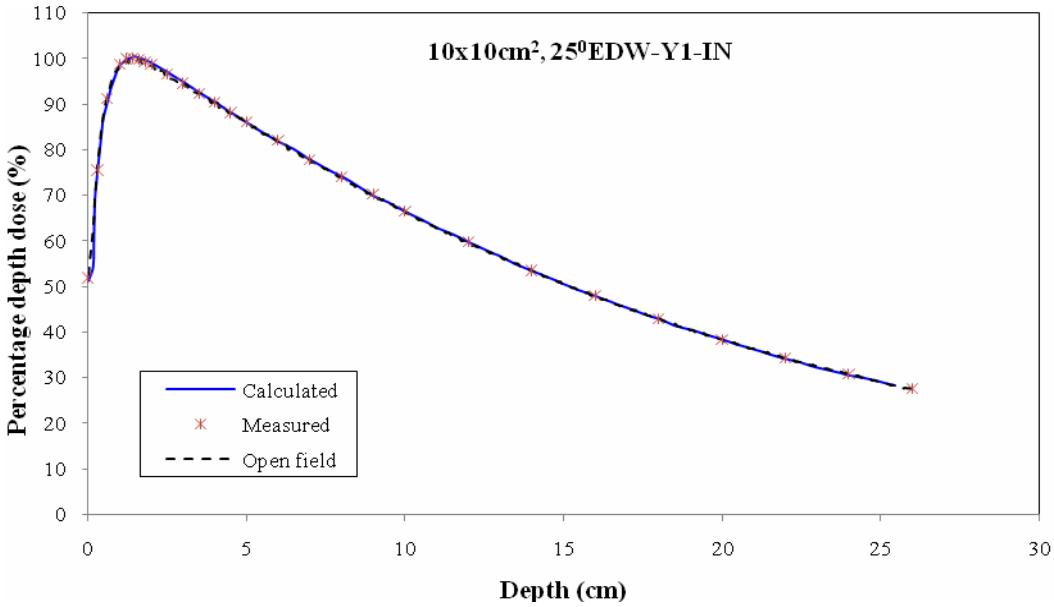
10x10cm², 25⁰EDW-Y1-IN
Percentage depth dose (%)
Depth (cm)
Calculated
Measured
Open field
0
10
20
30
40
50
60
70
80
90
100
110
0
5
10
15
20
25
30

(a)

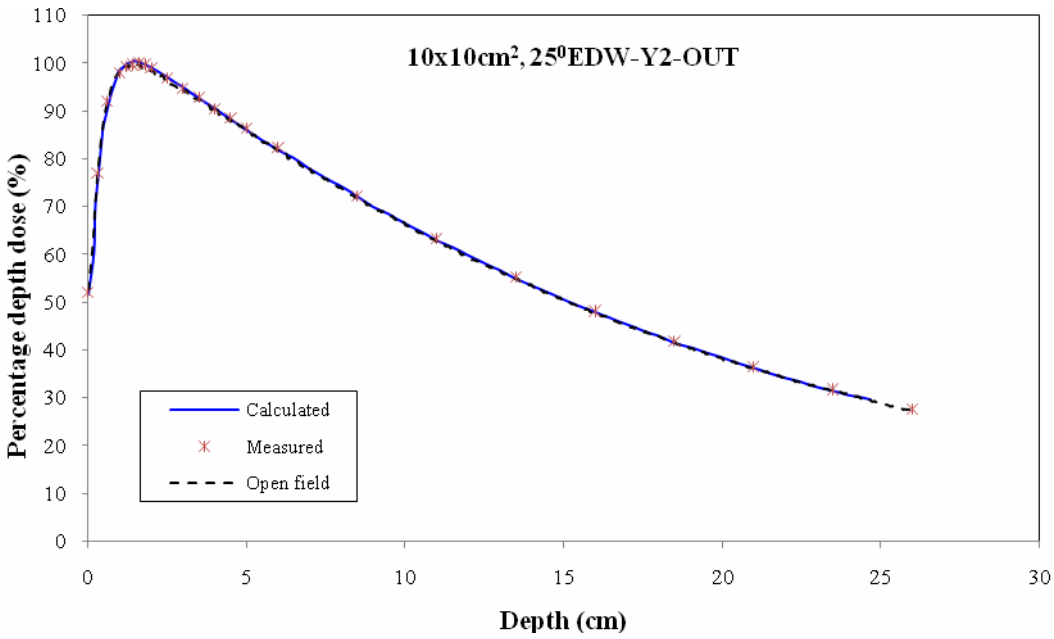
10x10cm², 25⁰EDW-Y2-OUT
Percentage depth dose (%)
Depth (cm)
Calculated
Measured
Open field
0
10
20
30
40
50
60
70
80
90
100
110
0
5
10
15
20
25
30

(b)

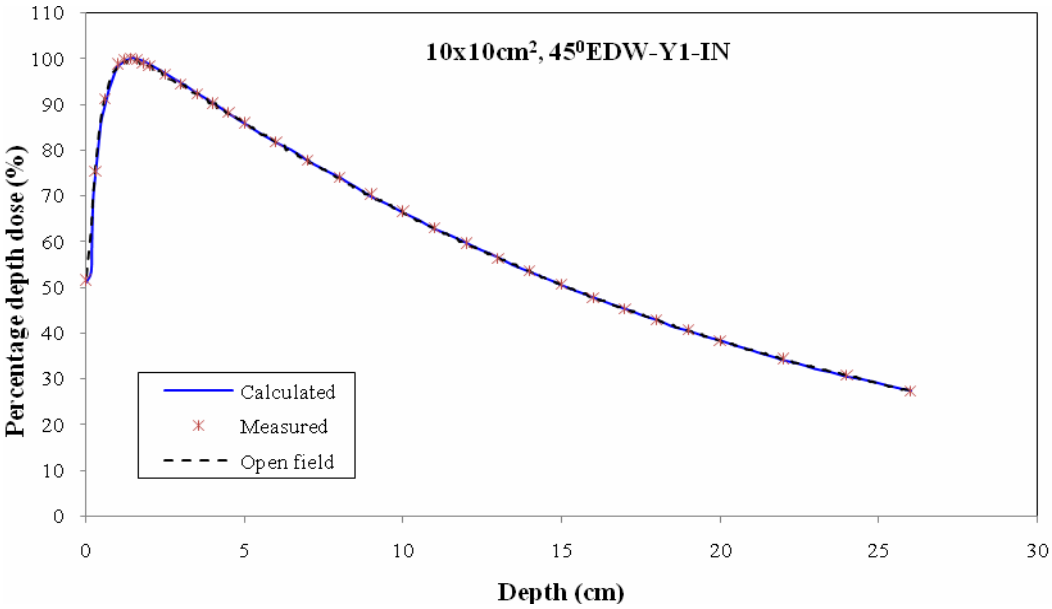

(c)

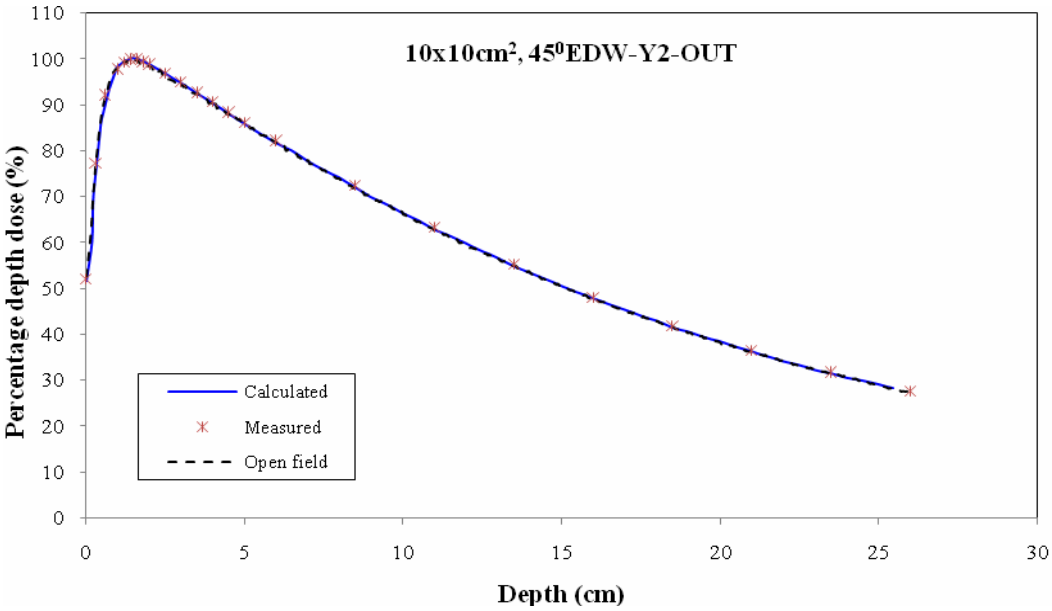

(d)

Figure 36. The comparison of open field (dash line), measured (symbols) and calculated (solid line) EDW depth doses for 6 MV photon beam at a symmetric field size of 10 x 10 cm^2 for (a) 25°EDW-Y1-IN (b) 25°EDW-Y2-OUT (c) 45°EDW-Y1-IN and (d) 45°EDW-Y2-OUT.

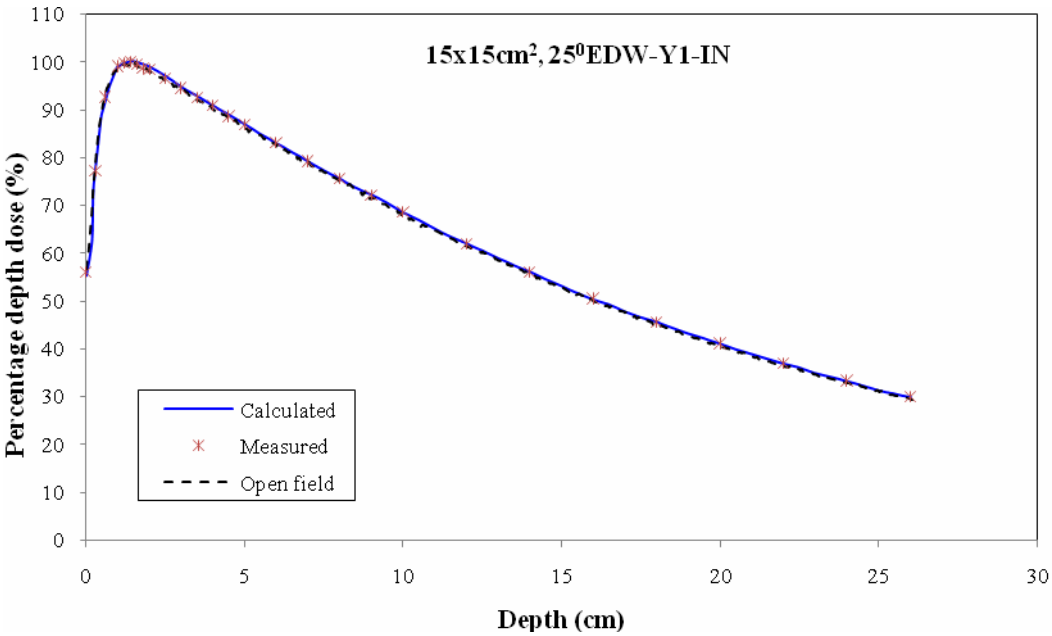
15x15cm², 25⁰EDW-Y1-IN
Percentage depth dose (%)
Depth (cm)
Calculated
Measured
Open field
0
10
20
30
40
50
60
70
80
90
100
110
0
5
10
15
20
25
30

(a)

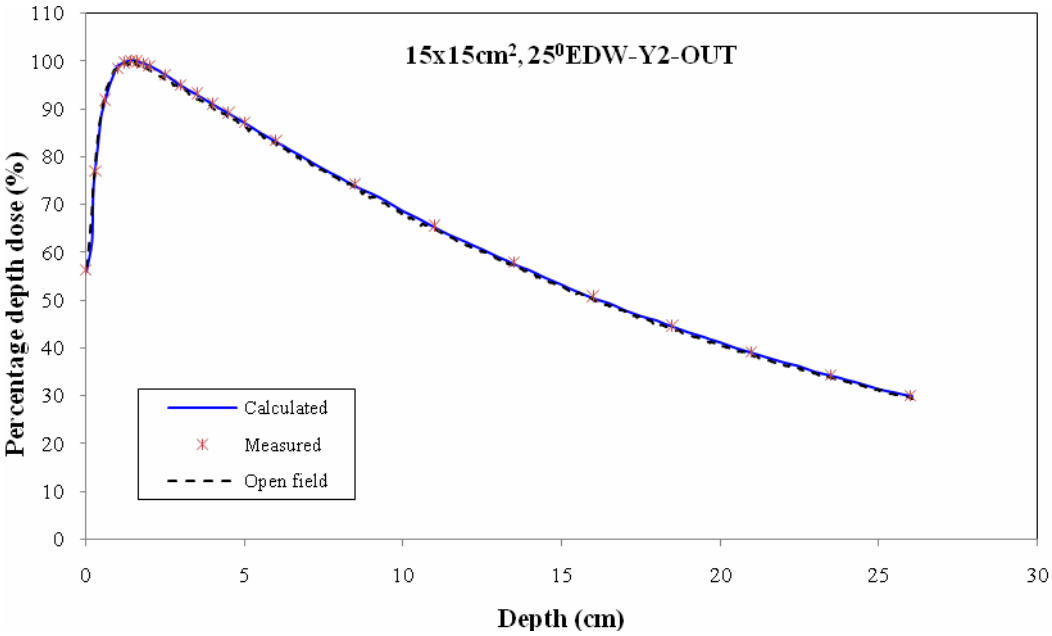
15x15cm², 25⁰EDW-Y2-OUT
Percentage depth dose (%)
Depth (cm)
Calculated
Measured
Open field
0
10
20
30
40
50
60
70
80
90
100
110
0
5
10
15
20
25
30

(b)

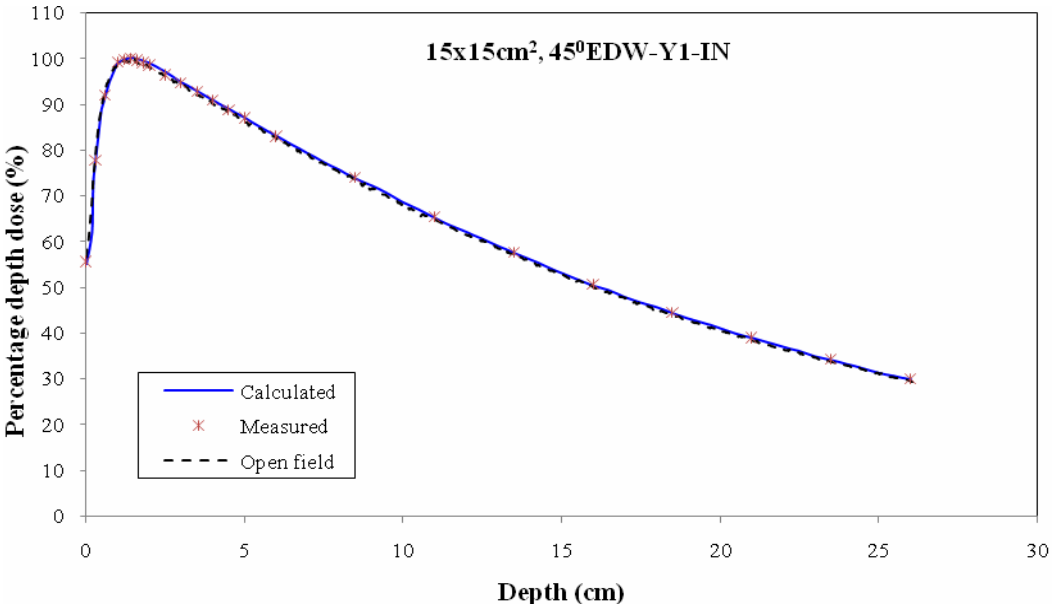

(c)

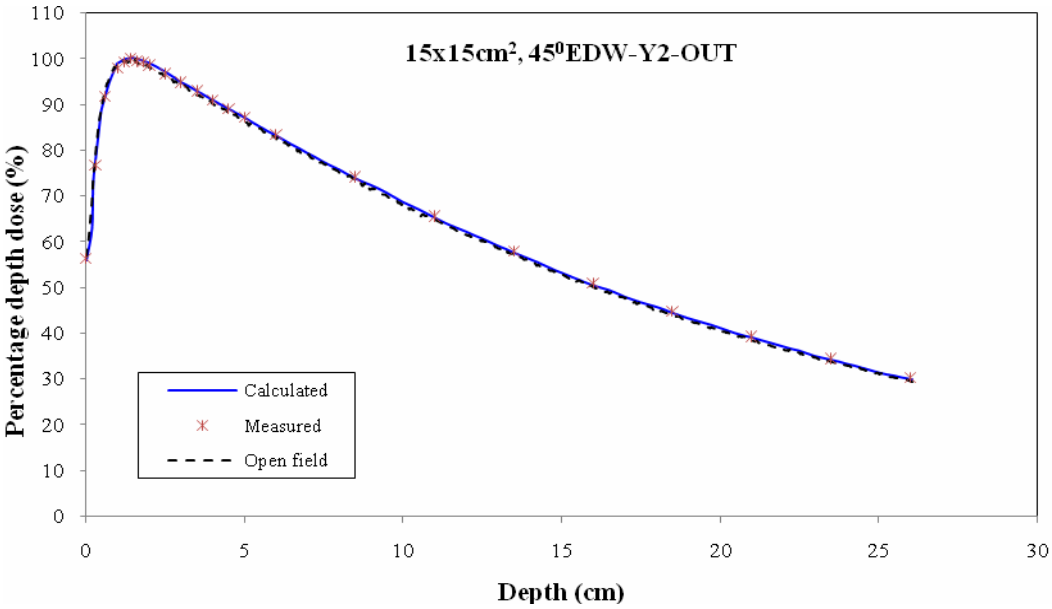

(d)

Figure 37. The comparison of open field (dash line), measured (symbols) and calculated (solid line) EDW depth doses for 6 MV photon beam at a symmetric field size of 15 x 15 cm^2 for (a) 25°EDW-Y1-IN (b) 25°EDW-Y2-OUT (c) 45°EDW-Y1-IN and (d) 45°EDW-Y2-OUT.

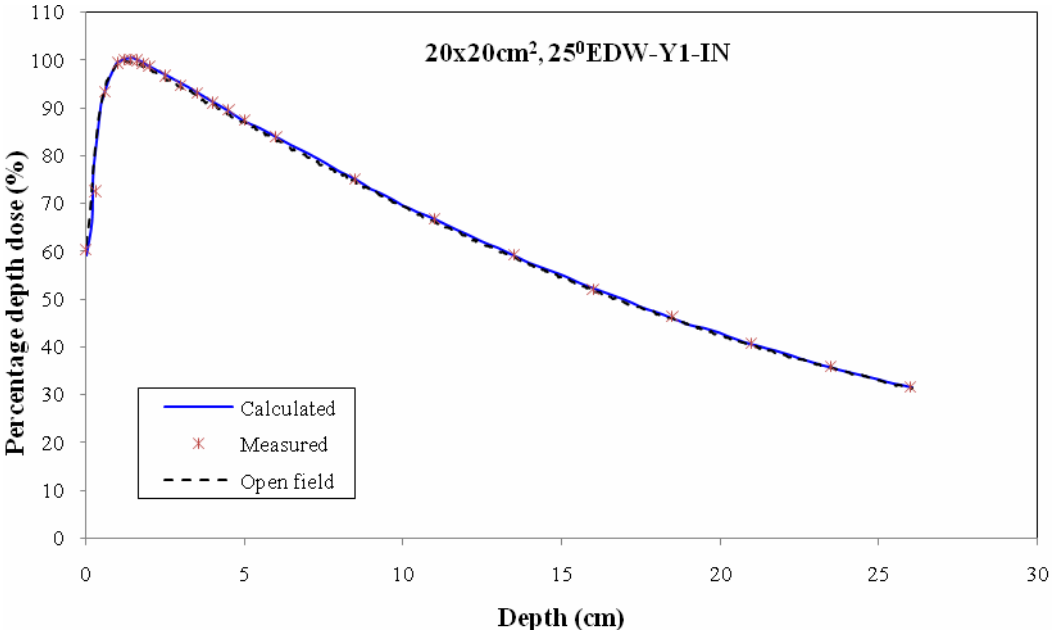
20x20cm², 25⁰EDW-Y1-IN
Percentage depth dose (%)
Depth (cm)
Calculated
Measured
Open field
0
10
20
30
40
50
60
70
80
90
100
110
0
5
10
15
20
25
30

(a)

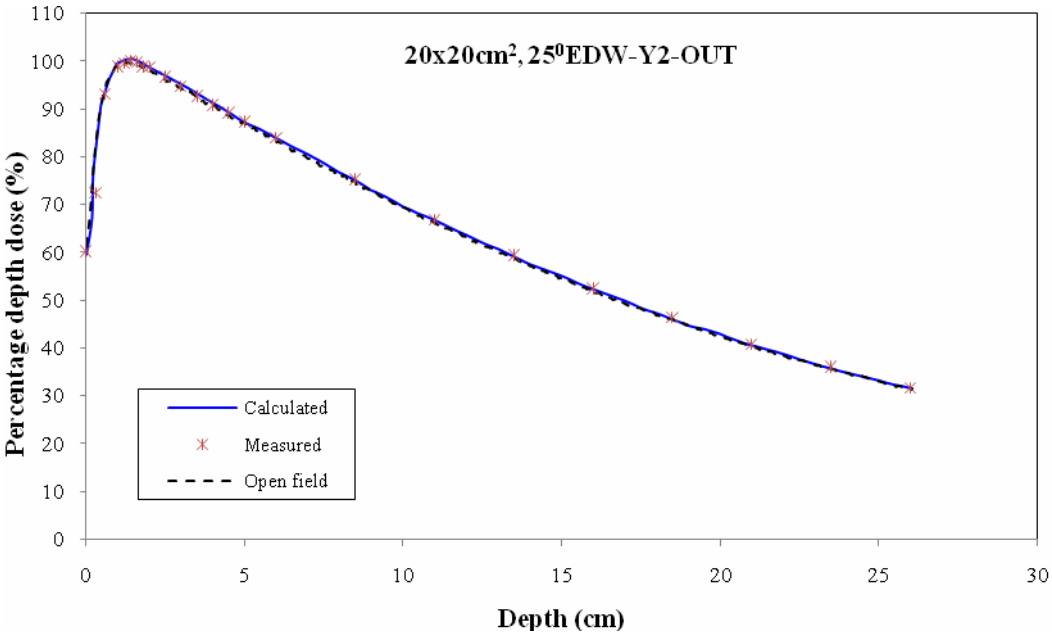
20x20cm², 25⁰EDW-Y2-OUT
Percentage depth dose (%)
Depth (cm)
Calculated
Measured
Open field
0
10
20
30
40
50
60
70
80
90
100
110
0
5
10
15
20
25
30

(b)

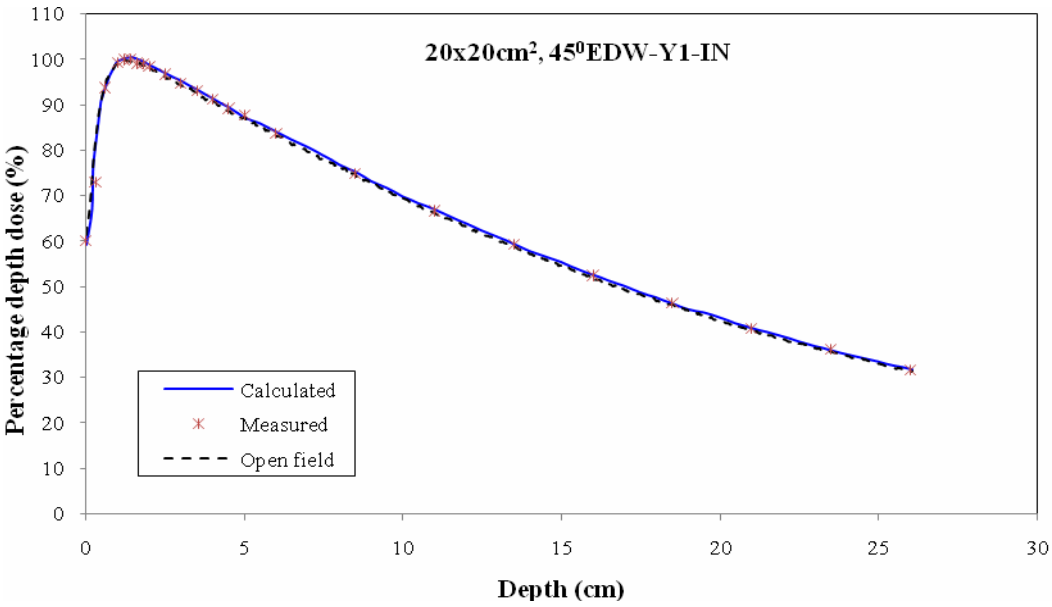

(c)

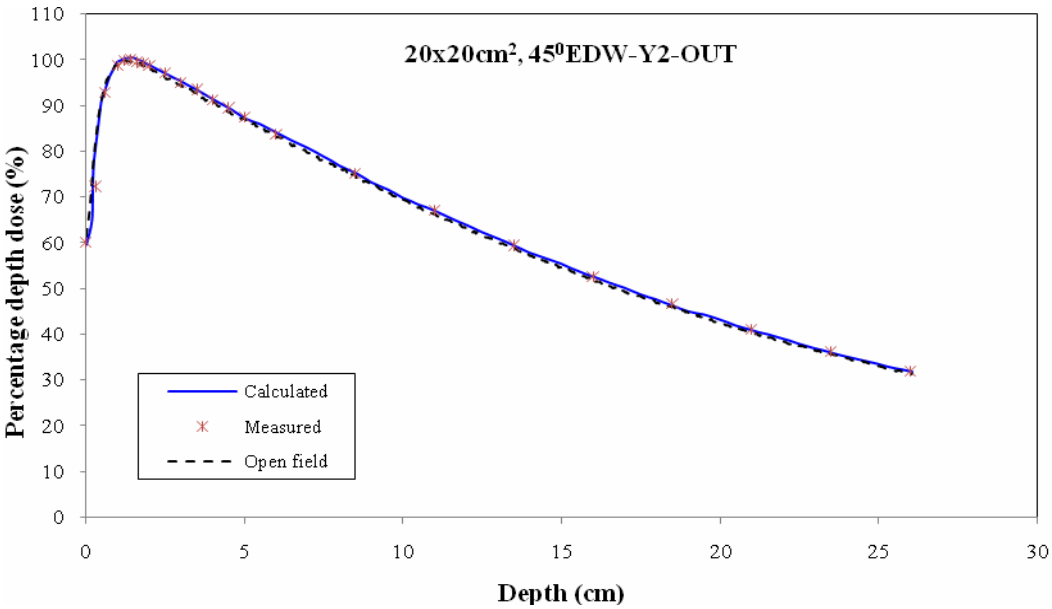

(d)

Figure 38. The comparison of open field (dash line), measured (symbols) and calculated (solid line) EDW depth doses for 6 MV photon beam at a symmetric field size of 20 x 20 cm^2 for (a) 25°EDW-Y1-IN (b) 25°EDW-Y2-OUT (c) 45°EDW-Y1-IN and (d) 45°EDW-Y2-OUT.

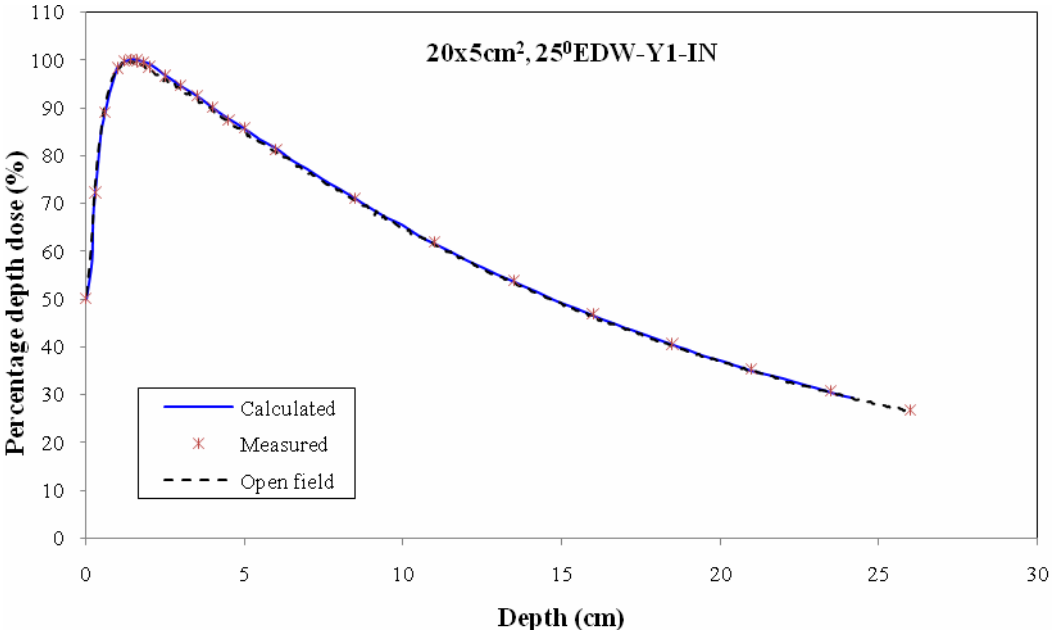
20x5cm², 25⁰EDW-Y1-IN
Percentage depth dose (%)
Depth (cm)
Calculated
Measured
Open field
0
10
20
30
40
50
60
70
80
90
100
110
0
5
10
15
20
25
30

(a)

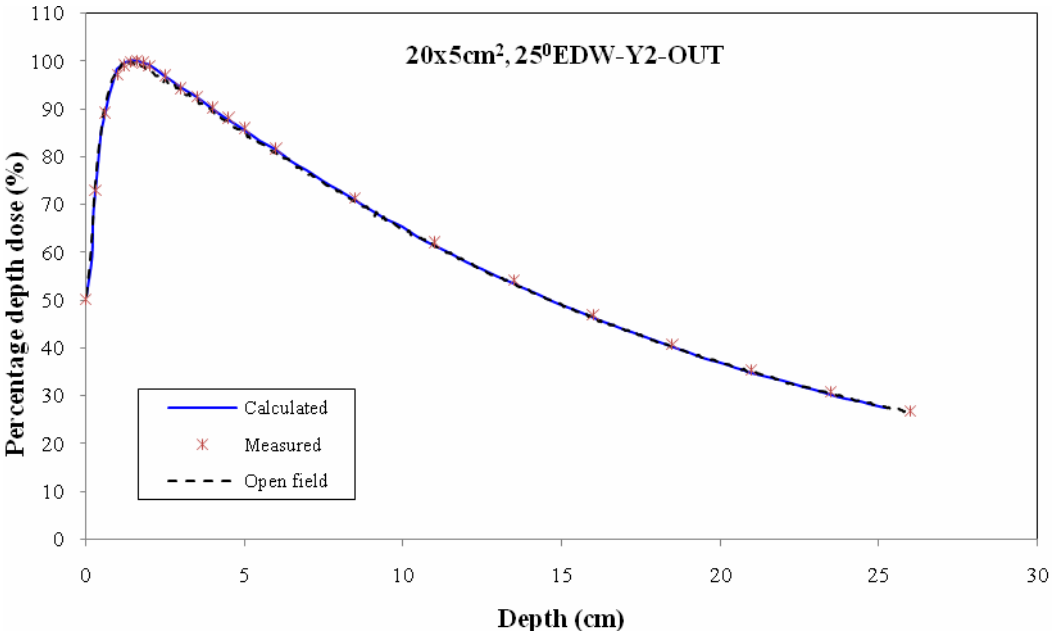
20x5cm², 25⁰EDW-Y2-OUT
Percentage depth dose (%)
Depth (cm)
Calculated
Measured
Open field
0
10
20
30
40
50
60
70
80
90
100
110
0
5
10
15
20
25
30

(b)

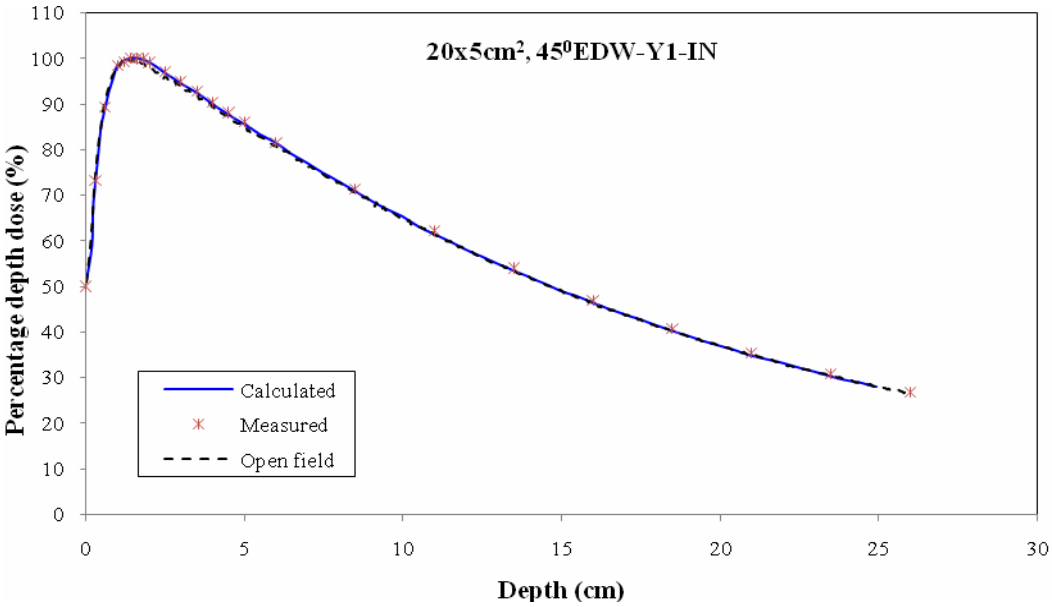

(c)

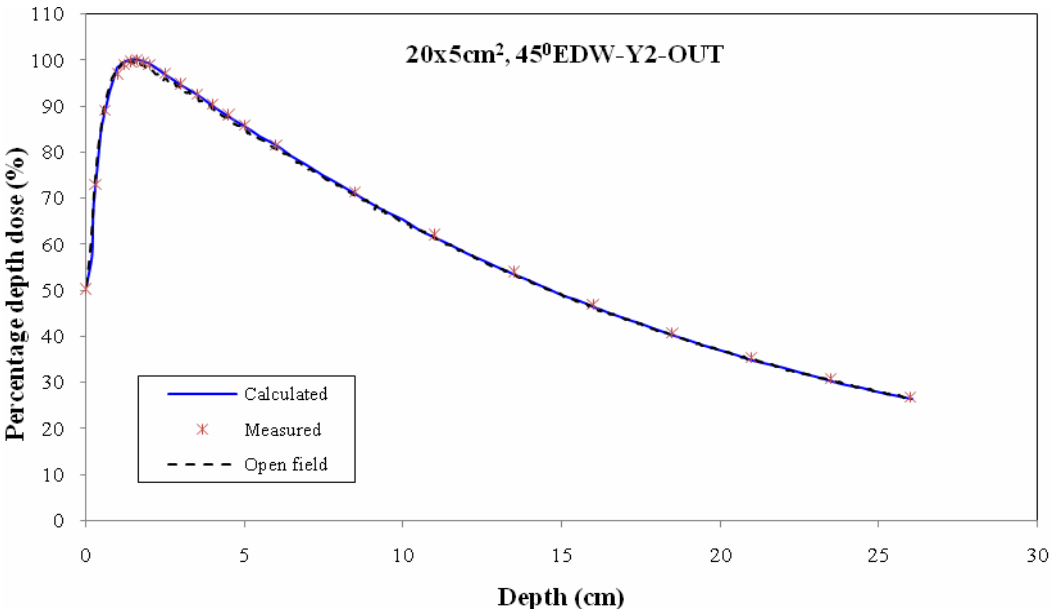

(d)

Figure 39. The comparison of open field (dash line), measured (symbols) and calculated (solid line) EDW depth doses for 6 MV photon beam at a symmetric field size of 20 x 5 cm^2 for (a) 25°EDW-Y1-IN (b) 25°EDW-Y2-OUT (c) 45°EDW-Y1-IN and (d) 45°EDW-Y2-OUT.

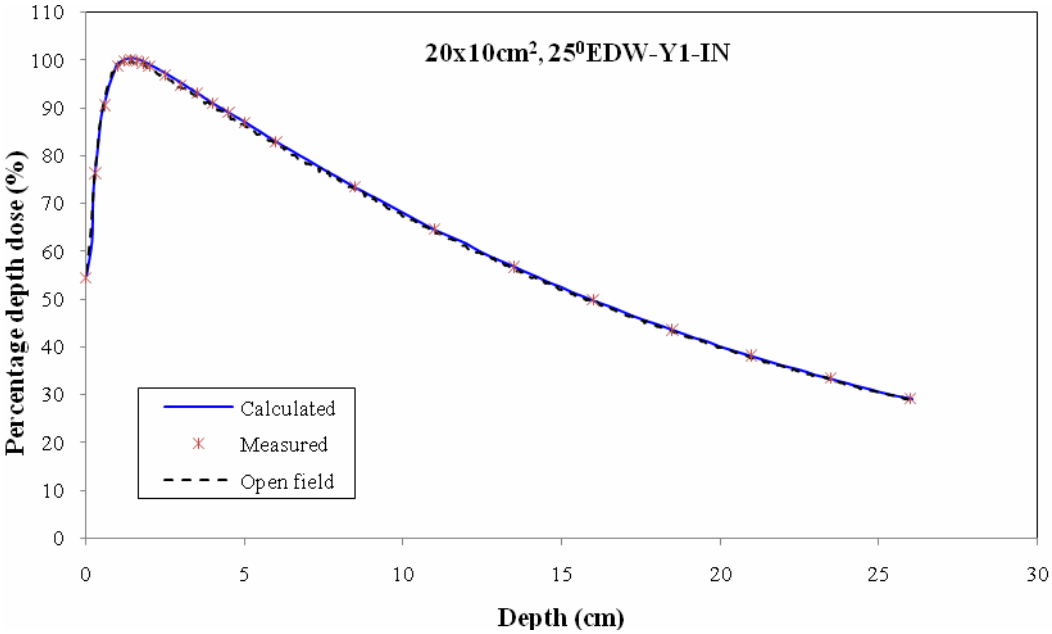
20x10cm², 25⁰EDW-Y1-IN
Percentage depth dose (%)
Depth (cm)
Calculated
Measured
Open field
0
10
20
30
40
50
60
70
80
90
100
110
0
5
10
15
20
25
30

(a)

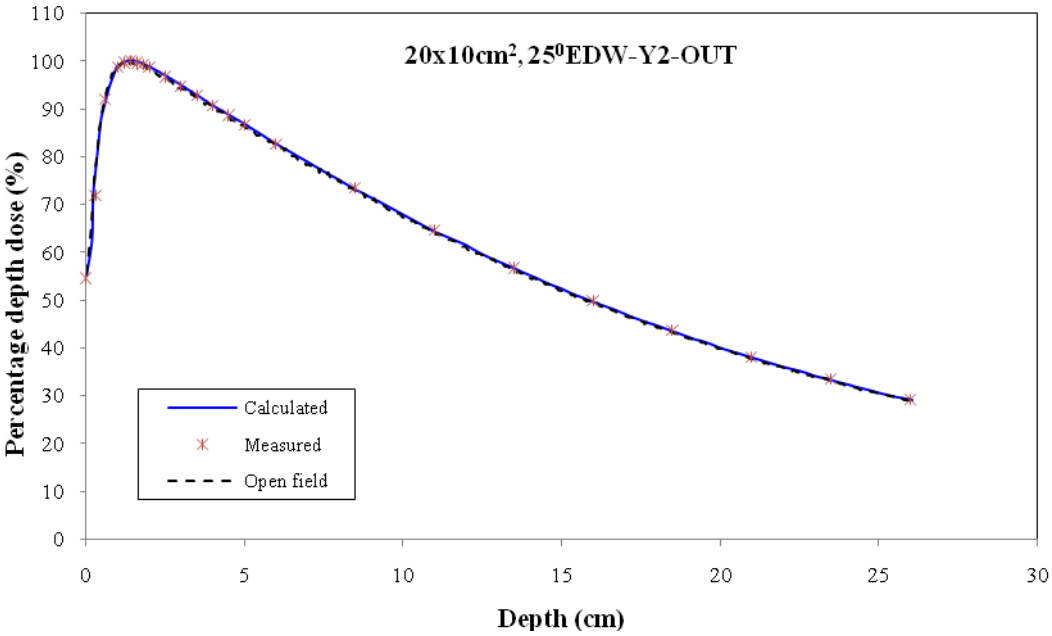
20x10cm², 25⁰EDW-Y2-OUT
Percentage depth dose (%)
Depth (cm)
Calculated
Measured
Open field
0
10
20
30
40
50
60
70
80
90
100
110
0
5
10
15
20
25
30

(b)

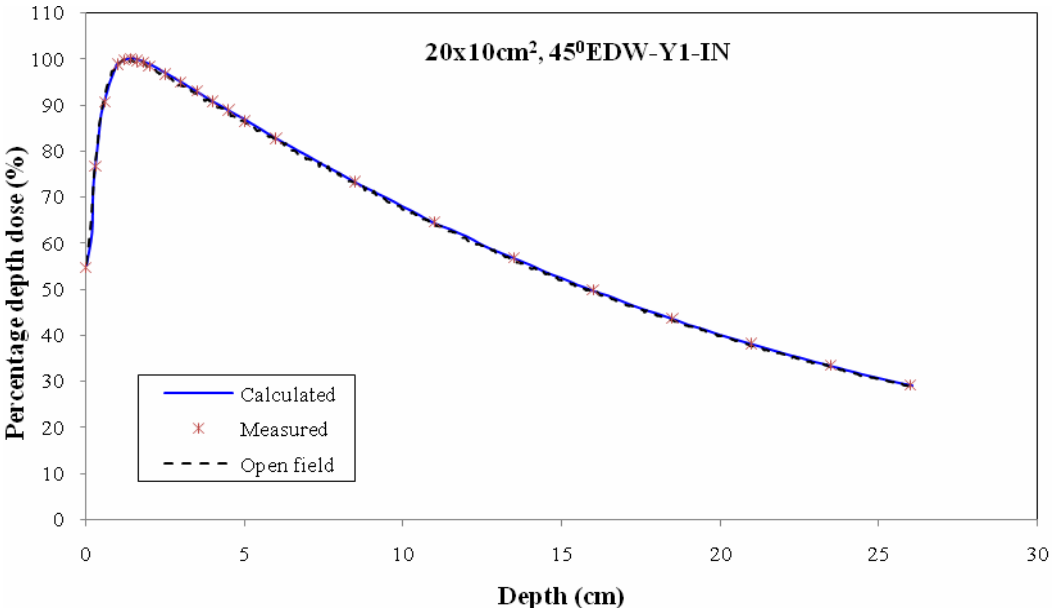

(c)

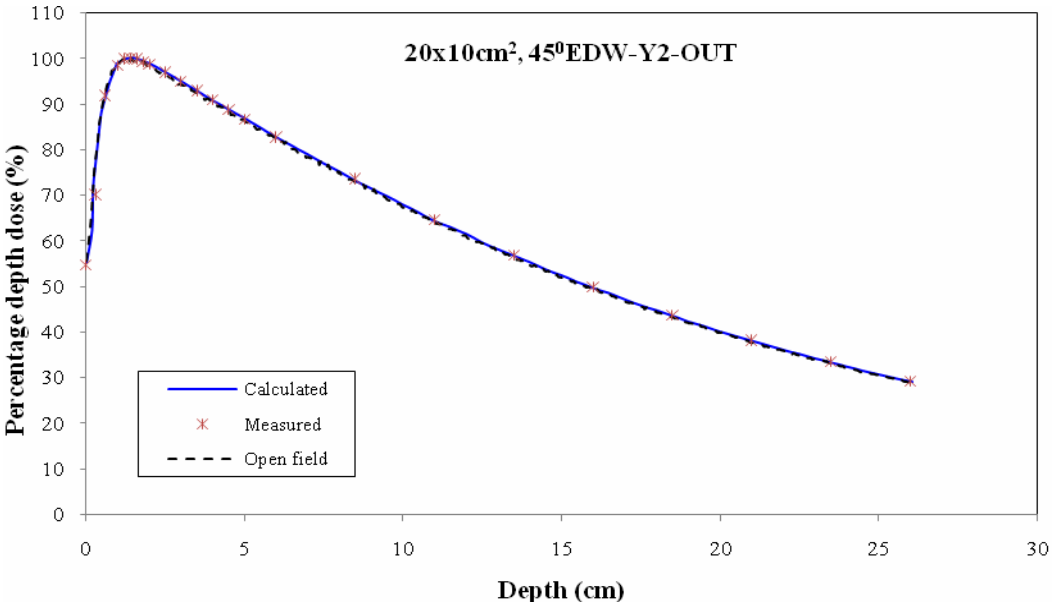

(d)

Figure 40. The comparison of open field (dash line), measured (symbols) and calculated (solid line) EDW depth doses for 6 MV photon beam at a symmetric field size of 20 x 10 cm^2 for (a) 25°EDW-Y1-IN (b) 25°EDW-Y2-OUT (c) 45°EDW-Y1-IN and (d) 45°EDW-Y2-OUT.

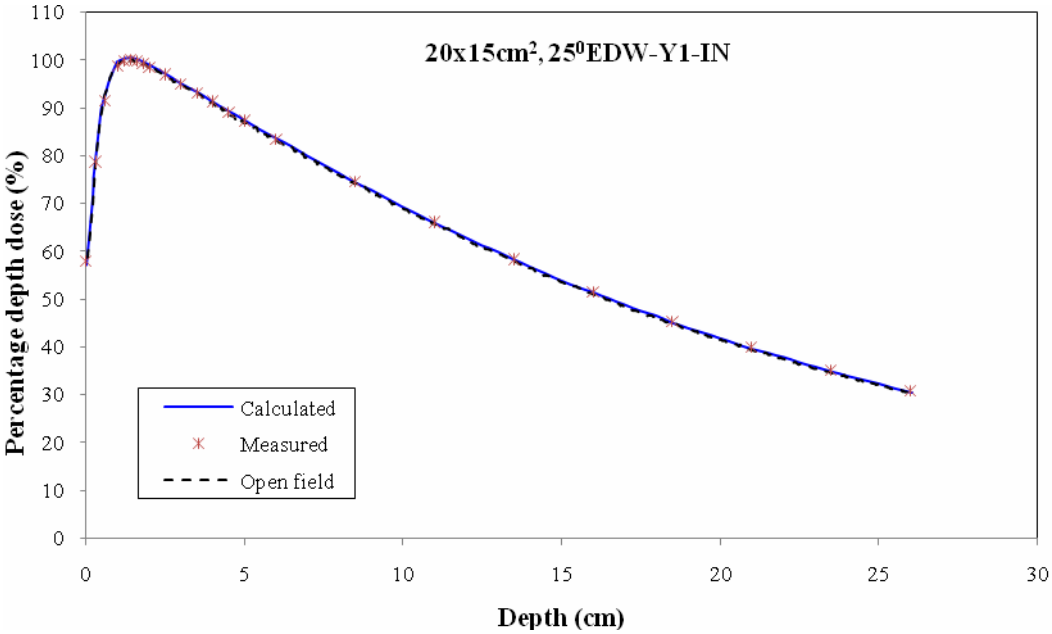
20x15cm², 25⁰EDW-Y1-IN
Percentage depth dose (%)
Depth (cm)
Calculated
Measured
Open field
0
10
20
30
40
50
60
70
80
90
100
110
0
5
10
15
20
25
30

(a)

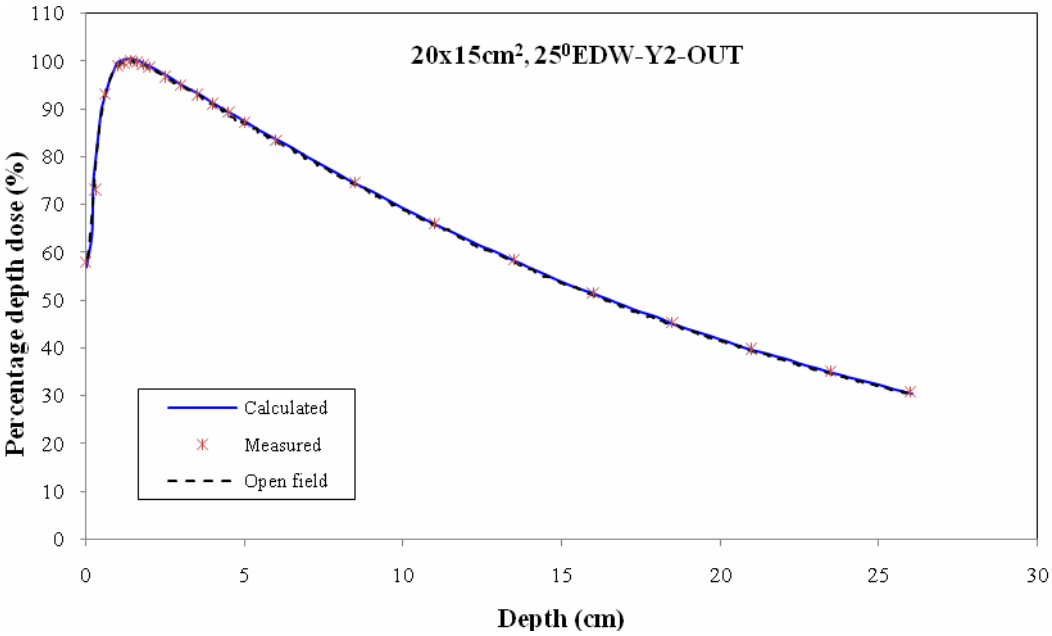
20x15cm², 25⁰EDW-Y2-OUT
Percentage depth dose (%)
Depth (cm)
Calculated
Measured
Open field
0
10
20
30
40
50
60
70
80
90
100
110
0
5
10
15
20
25
30

(b)

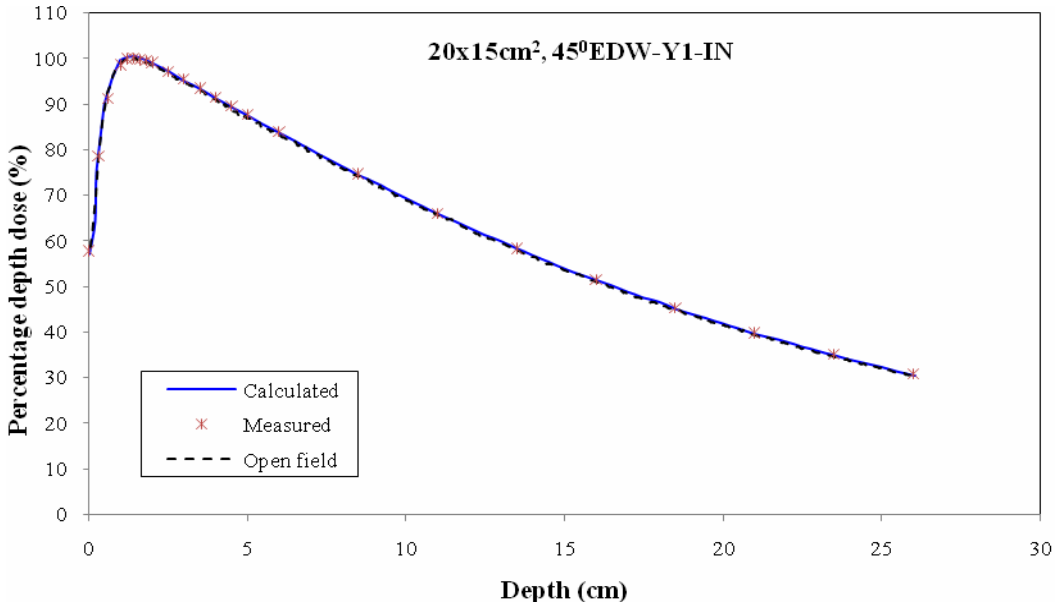

(c)

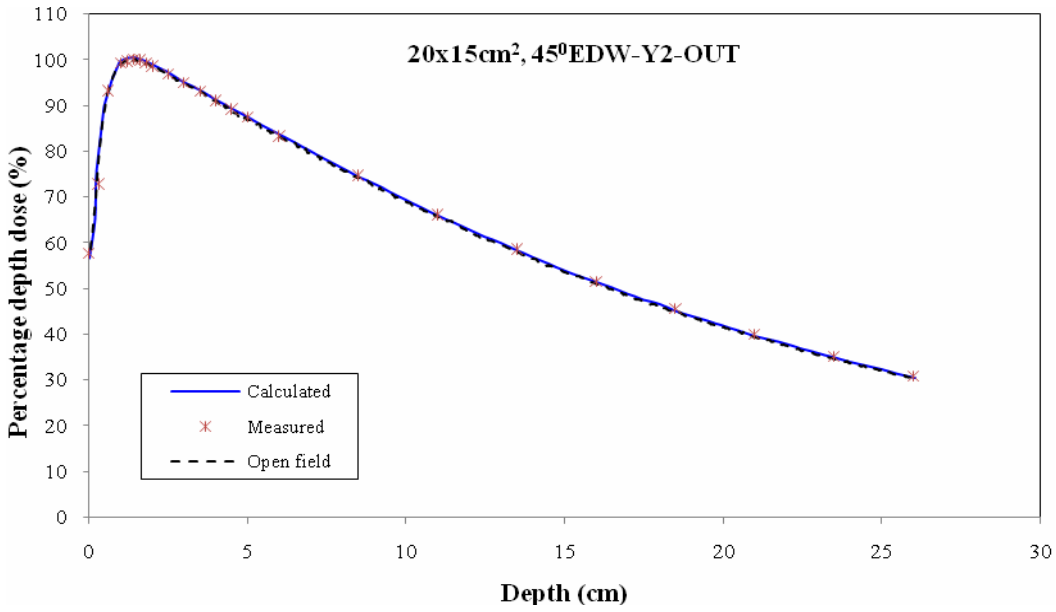

(d)

Figure 41. The comparison of open field (dash line), measured (symbols) and calculated (solid line) EDW depth doses for 6 MV photon beam at a symmetric field size of 20 x 15 cm^2 for (a) 25°EDW-Y1-IN (b) 25°EDW-Y2-OUT (c) 45°EDW-Y1-IN and (d) 45°EDW-Y2-OUT.

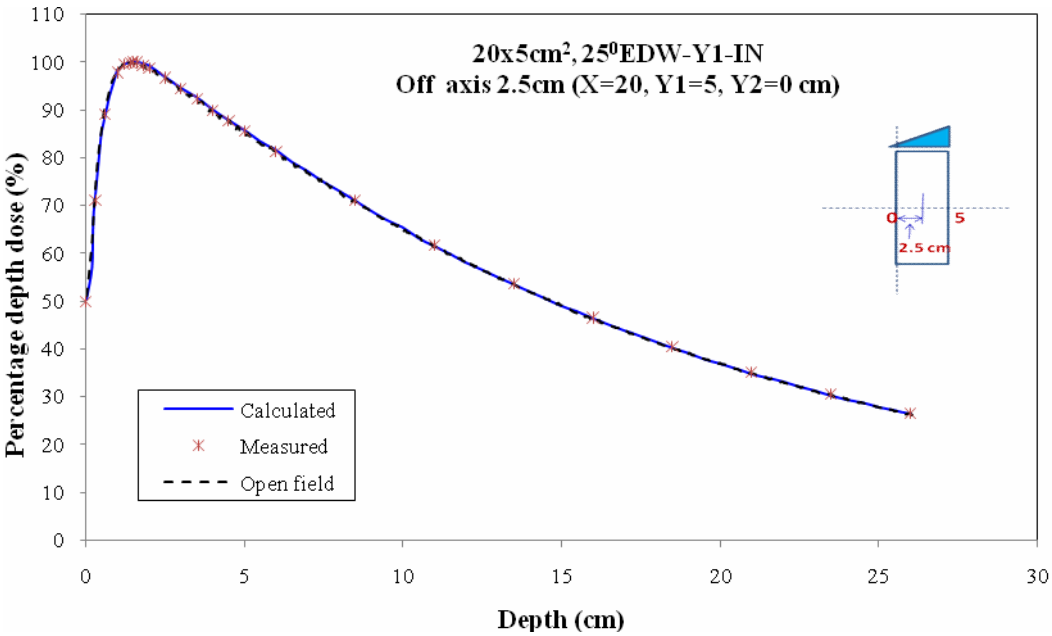
20x5cm², 25⁰EDW-Y1-IN
Off axis 2.5cm (X=20, Y1=5, Y2=0 cm)
Percentage depth dose (%)
Depth (cm)
Calculated
Measured
Open field
0
5
2.5 cm

(a)

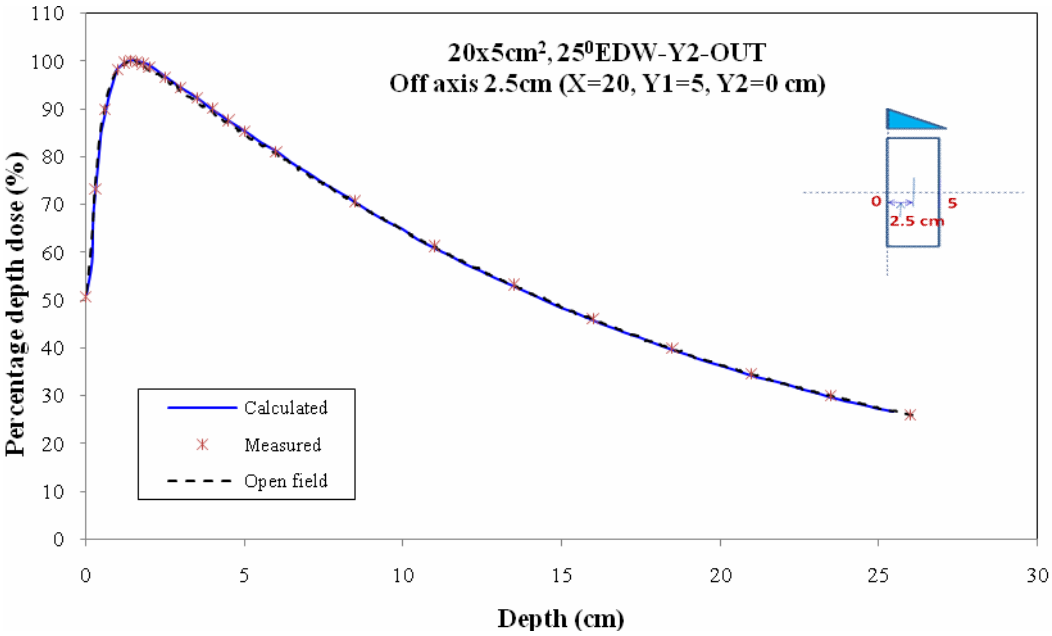
20x5cm², 25⁰EDW-Y2-OUT
Off axis 2.5cm (X=20, Y1=5, Y2=0 cm)
Percentage depth dose (%)
Depth (cm)
Calculated
Measured
Open field
0
5
2.5 cm

(b)

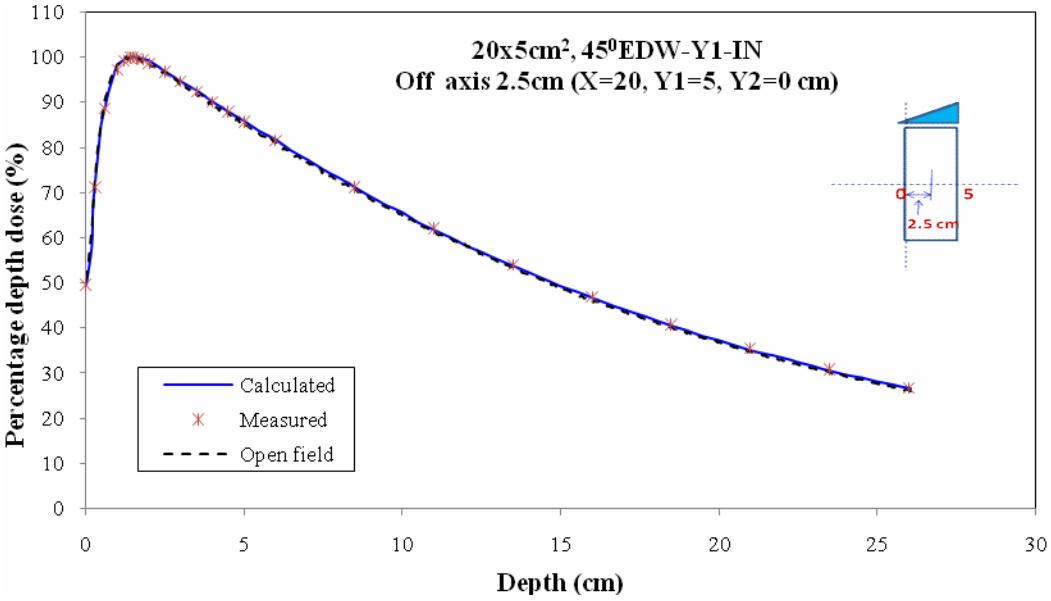

(c)

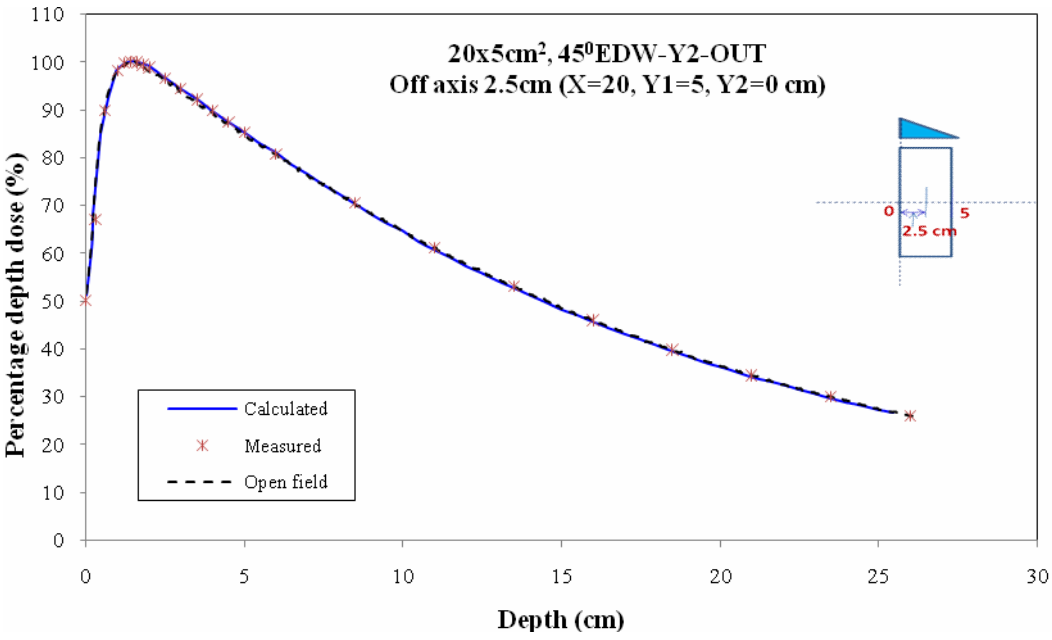

(d)

Figure 42. The comparison of open field (dash line), measured (symbols) and calculated (solid line) EDW depth doses for 6 MV photon beam at an asymmetric field size of 20 x 5 cm^2 for (a) 25°EDW-Y1-IN (b) 25°EDW-Y2-OUT (c) 45°EDW-Y1-IN and (d) 45°EDW-Y2-OUT.

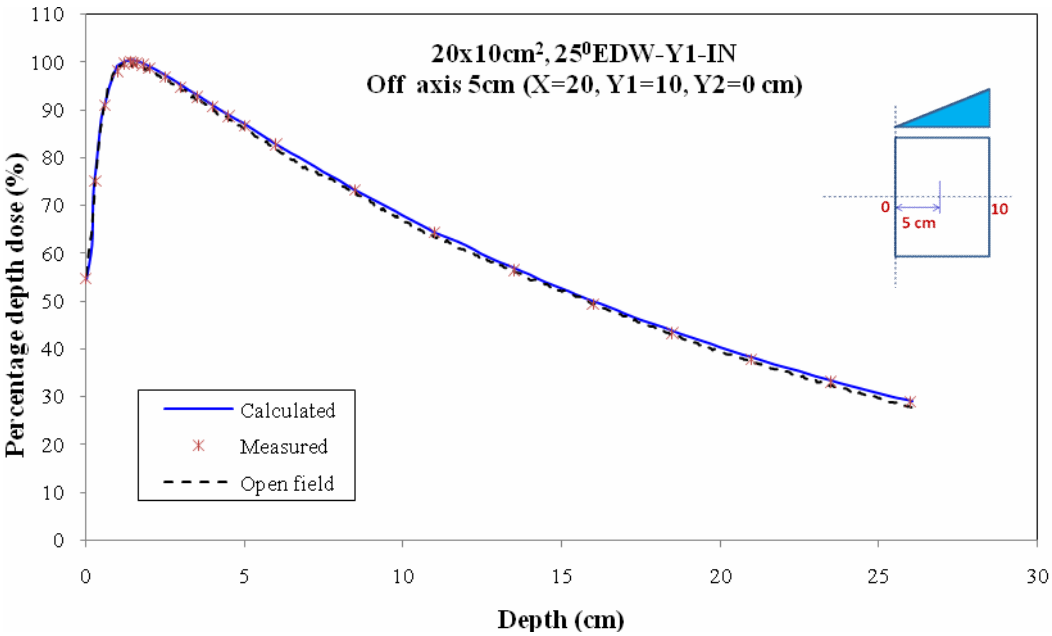
20x10cm², 25⁰EDW-Y1-IN
Off axis 5cm (X=20, Y1=10, Y2=0 cm)
Percentage depth dose (%)
Depth (cm)
Calculated
Measured
Open field
0
5 cm
10

(a)

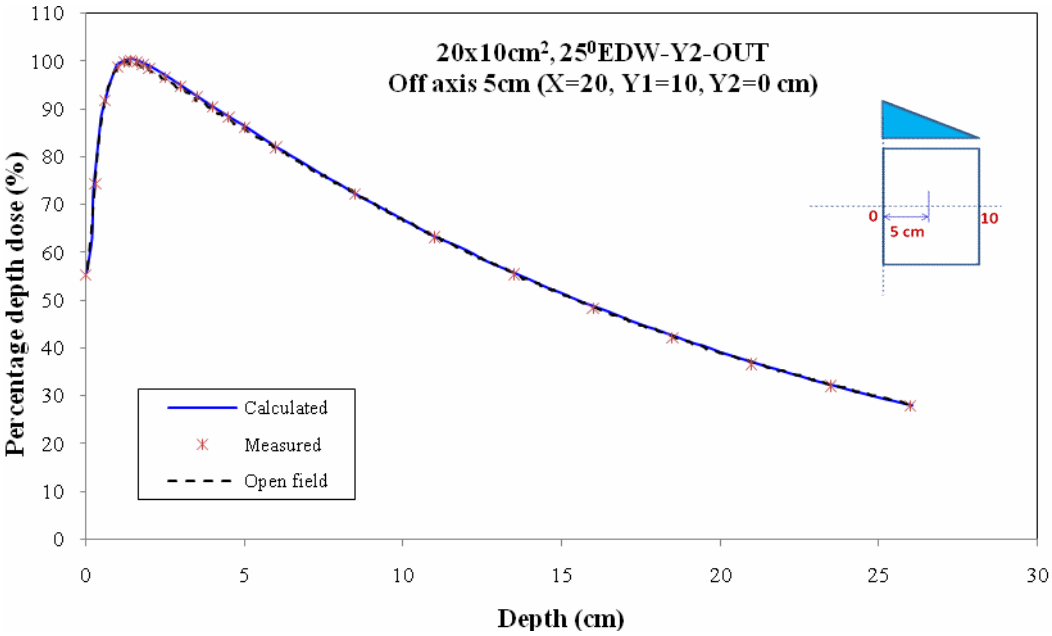
20x10cm², 25⁰EDW-Y2-OUT
Off axis 5cm (X=20, Y1=10, Y2=0 cm)
Percentage depth dose (%)
Depth (cm)
Calculated
Measured
Open field
0
5 cm
10

(b)

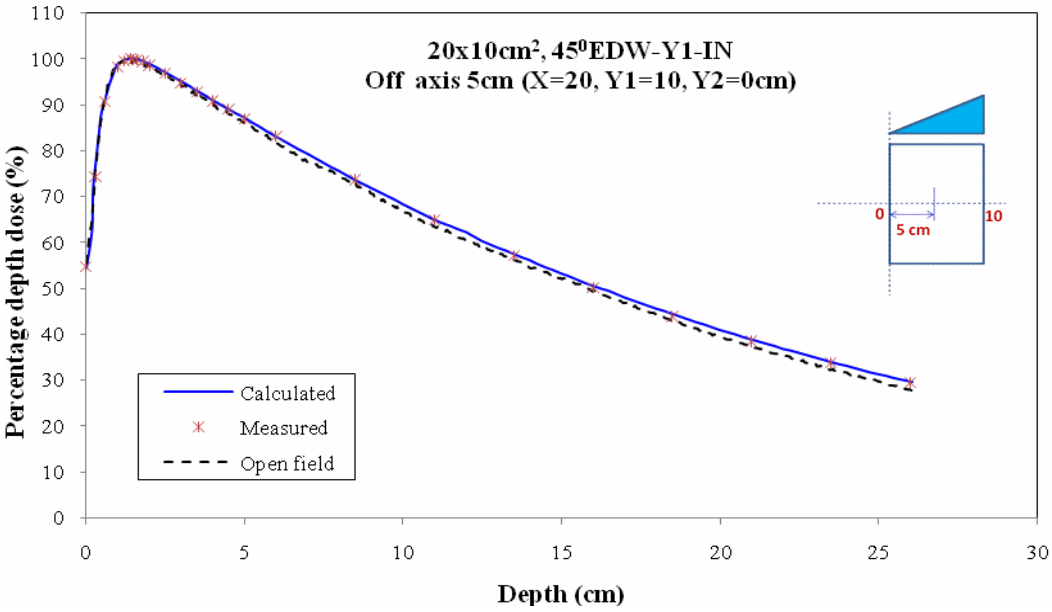

(c)

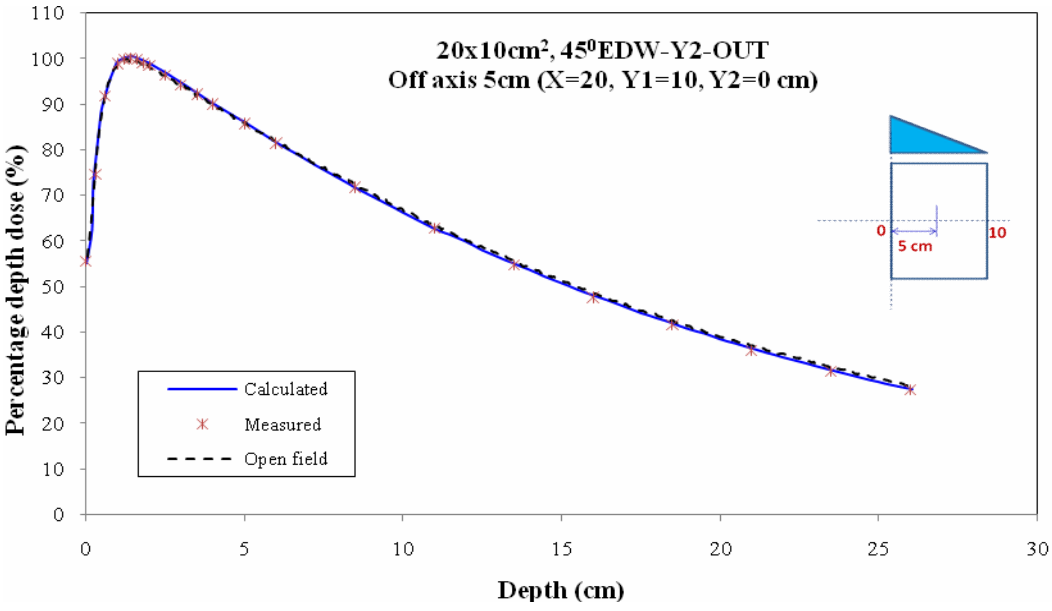

(d)

Figure 43. The comparison of open field (dash line), measured (symbols) and calculated (solid line) EDW depth doses for 6 MV photon beam at an asymmetric field size of 20 x 10 cm^2 for (a) 25°EDW-Y1-IN (b) 25°EDW-Y2-OUT (c) 45°EDW-Y1-IN and (d) 45°EDW-Y2-OUT.

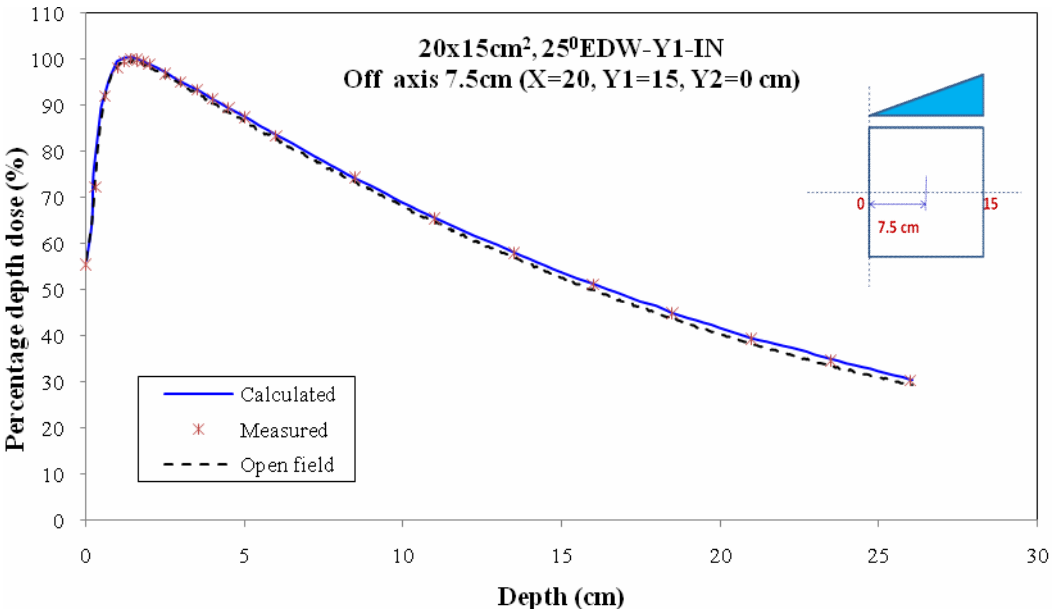
20x15cm², 25⁰EDW-Y1-IN
Off axis 7.5cm (X=20, Y1=15, Y2=0 cm)
Percentage depth dose (%)
Depth (cm)
Calculated
Measured
Open field
0
15
7.5 cm

(a)

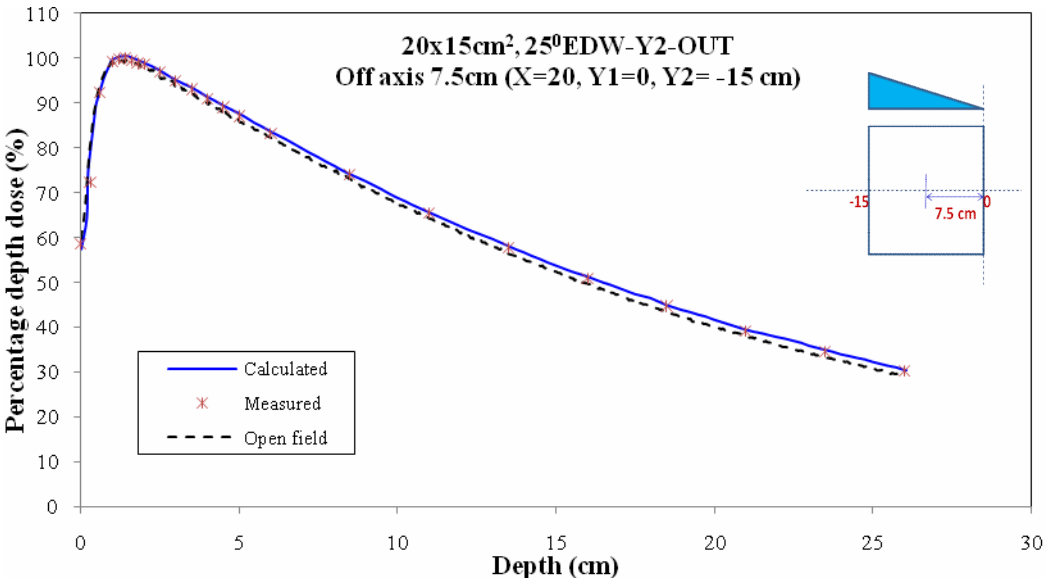
20x15cm², 25⁰EDW-Y2-OUT
Off axis 7.5cm (X=20, Y1=0, Y2= -15 cm)
Percentage depth dose (%)
Depth (cm)
Calculated
Measured
Open field
-15
0
7.5 cm

(b)

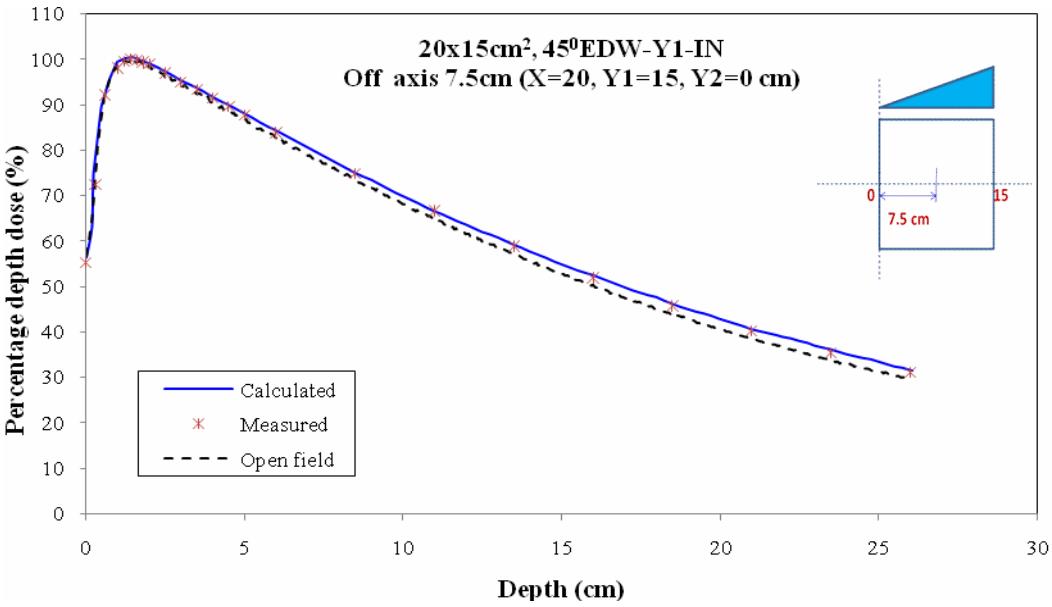

(c)

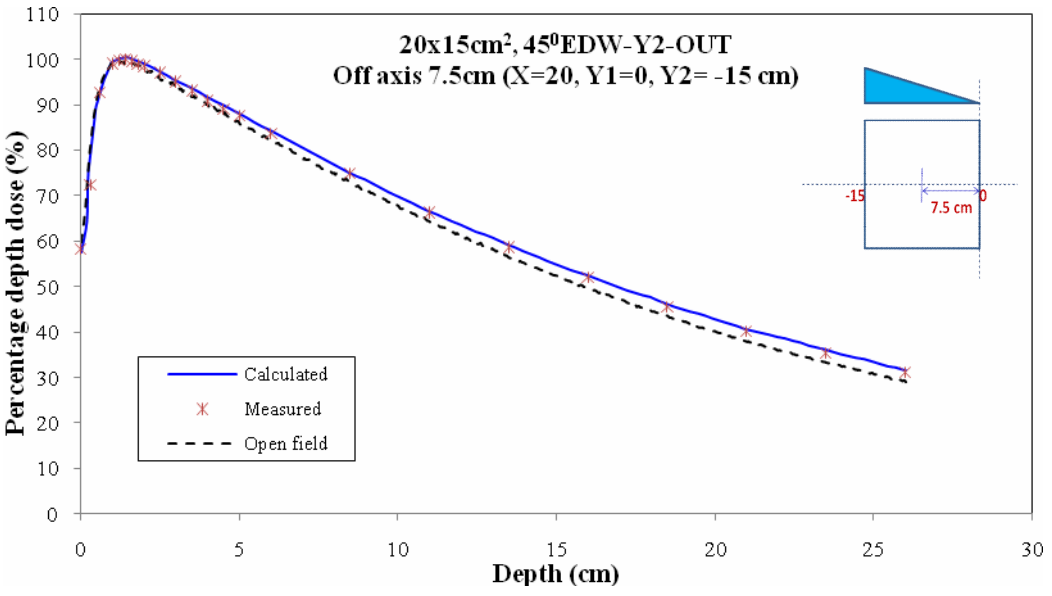

(d)

Figure 44. The comparison of open field (dash line), measured (symbols) and calculated (solid line) EDW depth doses for 6 MV photon beam at an asymmetric field size of 20 x 15 cm^2 for (a) 25°EDW-Y1-IN (b) 25°EDW-Y2-OUT (c) 45°EDW-Y1-IN and (d) 45°EDW-Y2-OUT.

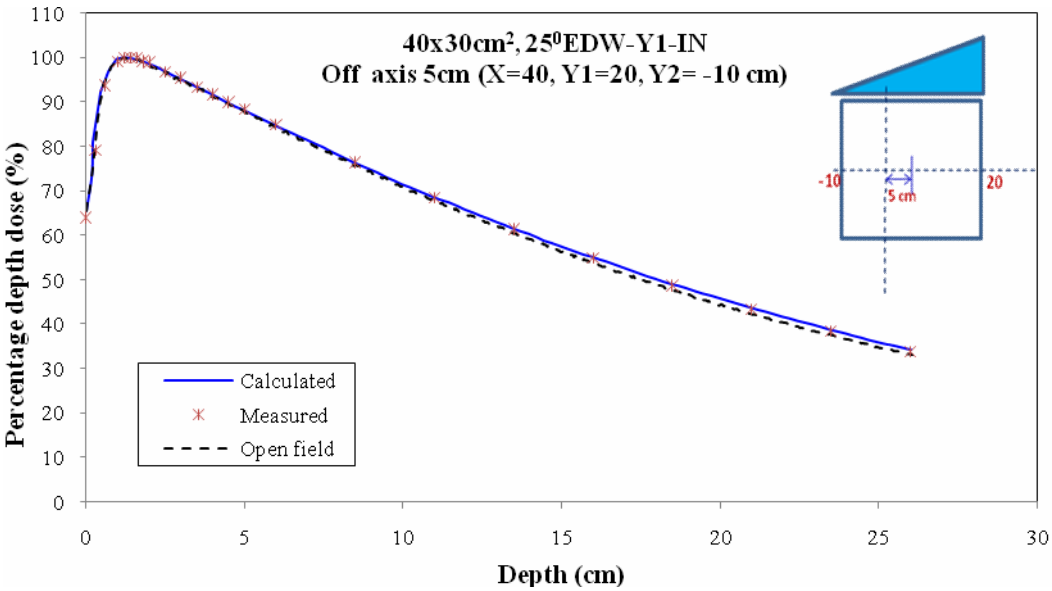
40x30cm², 25⁰EDW-Y1-IN
Off axis 5cm (X=40, Y1=20, Y2= -10 cm)
Percentage depth dose (%)
Depth (cm)
Calculated
Measured
Open field
-10
20
5 cm

(a)

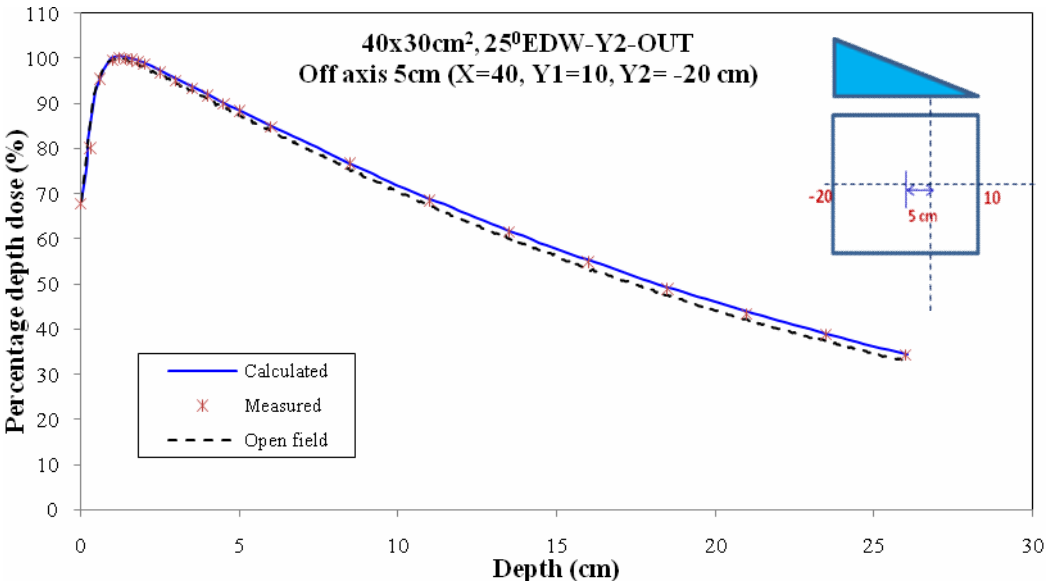
40x30cm², 25⁰EDW-Y2-OUT
Off axis 5cm (X=40, Y1=10, Y2= -20 cm)
Percentage depth dose (%)
Depth (cm)
Calculated
Measured
Open field
-20
10
5 cm

(b)

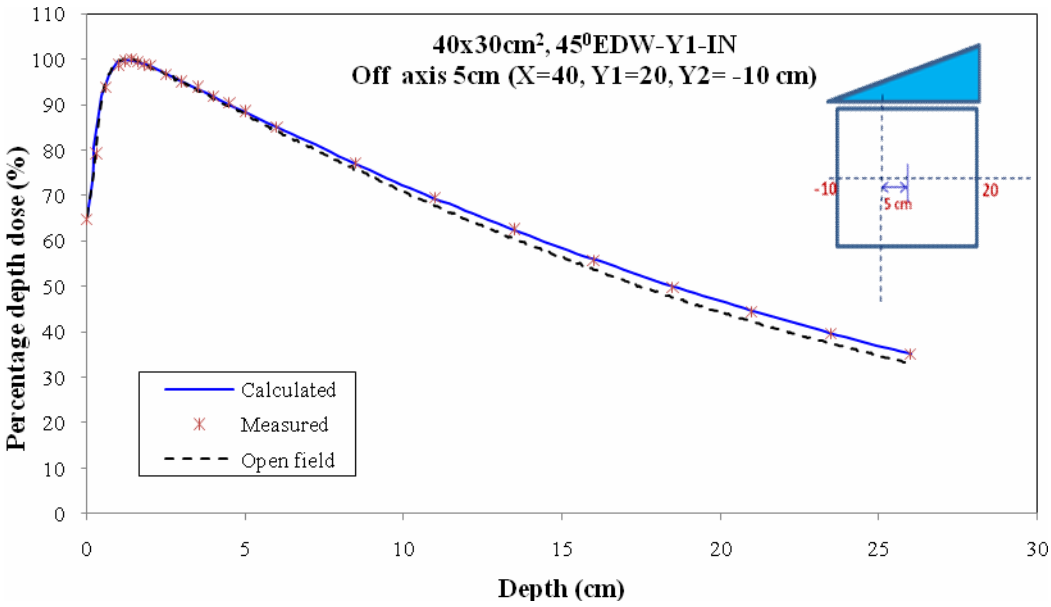

(c)

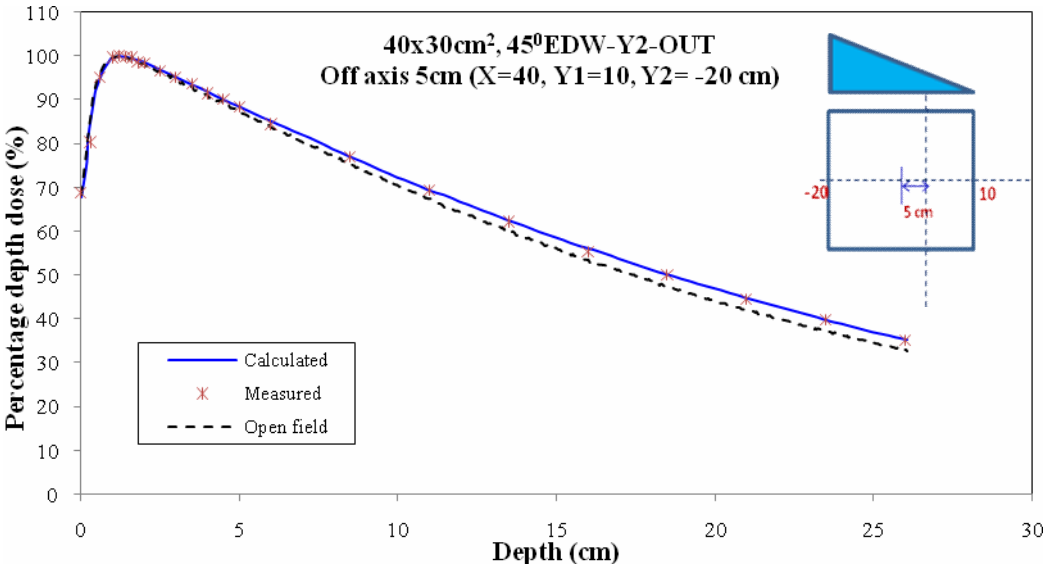

(d)

Figure 45. The comparison of open field (dash line), measured (symbols) and calculated (solid line) EDW depth doses for 6 MV photon beam at an asymmetric field size of 40 x 30 cm^2 for (a) 25°EDW-Y1-IN (b) 25°EDW-Y2-OUT (c) 45°EDW-Y1-IN and (d) 45°EDW-Y2-OUT.

Table 13. Percent dose difference for data points on the central beam axis beyond the depth of d_{max} (δ_1) and in the build-up region (δ_2) between open field, measured and calculated EDW depth doses for 6 MV photon beam with symmetric field sizes of 5 x 5 cm^2, 10 x 10 cm^2, 15 x 15 cm^2, 20 x 20 cm^2, 20 x 5 cm^2, 20 x 10 cm^2 and 20 x 15 cm^2 for 25^0 and 45^0 EDW both wedge directions (a) Y1-IN direction and (b) Y2-OUT direction.

(a) Symmetric field , Y1-IN direction

Field size (cm^2)	EDW angle	% Dose difference			
		Measured vs Calculated		Measured vs Open field	
		δ_1	δ_2	δ_1	δ_2
5 x 5	25^0	0.08	1.99	-0.52	-0.01
	45^0	0.47	2.10	-0.91	0.03
10 x 10	25^0	0.19	0.80	-0.52	-0.07
	45^0	0.45	1.03	-0.78	-0.14
15 x 15	25^0	0.02	0.61	-0.58	-0.49
	45^0	0.44	-1.60	-1.16	1.91
20 x 20	25^0	0.85	-3.07	-0.95	3.72
	45^0	0.41	-3.11	-0.81	3.72
20 x 5	25^0	0.51	-0.61	-0.75	-1.70
	45^0	1.00	-0.26	-1.21	1.02
20 x 10	25^0	0.54	-1.30	-1.47	1.40
	45^0	0.46	-1.17	-1.41	1.22
20 x 15	25^0	0.58	-2.64	-0.93	3.28
	45^0	0.38	-2.65	-0.96	3.28

(b) Symmetric field , Y2-OUT direction

Field size (cm^2)	EDW angle	% Dose difference (%)			
		Measured vs Calculated		Measured vs Open field	
		δ_1	δ_2	δ_1	δ_2
5 x 5	25^0	0.78	1.97	-0.86	-0.26
	45^0	1.13	1.75	-1.15	-0.26
10 x 10	25^0	0.82	0.86	-1.15	0.24
	45^0	0.86	0.95	-1.18	0.24
15 x 15	25^0	0.85	-1.16	-1.42	1.67
	45^0	0.53	-1.51	-1.22	1.91
20 x 20	25^0	0.98	***-3.34***	-1.07	3.72
	45^0	0.82	-3.14	-1.18	3.72
20 x 5	25^0	0.83	-0.76	-1.06	1.70
	45^0	0.89	-0.90	-1.12	2.04
20 x 10	25^0	0.42	-1.18	-1.32	1.26
	45^0	0.57	-1.19	-1.53	1.26
20 x 15	25^0	0.42	-1.97	-0.76	2.13
	45^0	0.51	-2.06	-1.05	2.13

Table 14. Percent dose difference for data points on the central beam axis beyond the depth of d_{max} (δ_1) and in the build-up region (δ_2) between open field, measured and calculated EDW depth doses for 6 MV photon beam with asymmetric field sizes of 20 x 5 cm^2, 20 x 10 cm^2, 20 x 15 cm^2 and 40 x 30 cm^2 for 25^0 and 45^0 EDW both wedge directions (a) Y1-IN direction and (b) Y2-OUT direction.

(a) Asymmetric field , Y1-IN direction

Field size (cm^2)	EDW angle	Off axis (cm)	%Difference (%)			
			Measured vs Calculated		Measured vs Open field	
			δ_1	δ_2	δ_1	δ_2
20 x 5	25^0	2.5 to Y1	0.28	-0.76	-1.58	1.65
	45^0	2.5 to Y1	0.30	-1.76	-1.99	2.07
20 x 10	25^0	5 to Y1	0.24	-0.71	-1.28	1.01
	45^0	5 to Y1	0.11	-1.08	-2.03	1.38
20 x 15	25^0	7.5 to Y1	0.26	-2.46	-1.28	1.07
	45^0	7.5 to Y1	0.29	-2.17	-2.78	1.07
40 x 30	25^0	5 to Y1	0.73	-4.00	-1.07	2.87
	45^0	5 to Y1	0.57	-3.91	-2.32	2.87

(b) Asymmetric field , Y2-OUT direction

Field size (cm^2)	EDW angle	Off axis (cm)	%Difference (%)			
			Measured vs Calculated		Measured vs Open field	
			δ_1	δ_2	δ_1	δ_2
20 x 5	25^0	2.5 to Y1	0.43	0.67	-0.79	1.05
	45^0	2.5 to Y1	0.46	0.07	-0.33	1.05
20 x 10	25^0	5 to Y1	0.18	-1.43	-0.41	1.71
	45^0	5 to Y1	0.35	-1.47	0.35	1.71
20 x 15	25^0	7.5 to Y2	0.08	-2.16	-1.36	3.11
	45^0	7.5 to Y2	-0.09	-1.73	-2.62	3.11
40 x 30	25^0	5 to Y2	-0.06	***-4.35***	-1.27	***4.42***
	45^0	5 to Y2	0.22	-3.59	-2.38	***4.42***

Table 15. The criteria acceptability for the comparison between measured and calculated EDW depth doses for 6 MV photon beam with symmetric field sizes of 5 x 5 cm^2, 10 x 10 cm^2, 15 x 15 cm^2, 20 x 20 cm^2, 20 x 5 cm^2, 20 x 10 cm^2 and 20 x 15 cm^2 for 25^0 and 45^0 EDW both wedge directions of (a) Y1-IN direction and (b) Y2-OUT direction.

(a) Symmetric field ,Y1-IN direction

Field size (cm^2)	EDW angle	Criteria acceptability	
		δ_1 = 3%	δ_2 = 15%
5 x 5	25^0	√	√
	45^0	√	√
10 x 10	25^0	√	√
	45^0	√	√
15 x 15	25^0	√	√
	45^0	√	√
20 x 20	25^0	√	√
	45^0	√	√
20 x 5	25^0	√	√
	45^0	√	√
20 x 10	25^0	√	√
	45^0	√	√
20 x 15	25^0	√	√
	45^0	√	√
√ define as pass × define as not pass			

(b) Symmetric field , Y2-OUT direction

Field size (cm^2)	EDW angle	Criteria acceptability	
		δ_1 = 3%	δ_2 = 15%
5 x 5	25^0	√	√
	45^0	√	√
10 x 10	25^0	√	√
	45^0	√	√
15 x 15	25^0	√	√
	45^0	√	√
20 x 20	25^0	√	√
	45^0	√	√
20 x 5	25^0	√	√
	45^0	√	√
20 x 10	25^0	√	√
	45^0	√	√
20 x 15	25^0	√	√
	45^0	√	√
√ define as pass × define as not pass			

Table 16. The criteria acceptability for the comparison between measured and calculated EDW depth doses for 6 MV photon beam with asymmetric field sizes of 20 x 5 cm^2, 20 x 10 cm^2, 20 x 15 cm^2 and 40 x 30 cm^2 for 25^0 and 45^0 EDW both wedge directions (a) Y1-IN direction (b) Y2-OUT direction.

(a) Asymmetric field ,Y1-IN direction

Field size (cm^2)	Off axis (cm)	EDW angle	Criteria acceptability	
			δ_1 = 3%	δ_2 = 15%
20 x 5	2.5 to Y1	25^0	√	√
	2.5 to Y1	45^0	√	√
20 x 10	5 to Y1	25^0	√	√
	5 to Y1	45^0	√	√
20 x 15	7.5 to Y1	25^0	√	√
	7.5 to Y1	45^0	√	√
40 x 30	5 to Y1	25^0	√	√
	5 to Y1	45^0	√	√
√ define as pass × define as not pass				

(b) Asymmetric field , Y2-OUT direction

Field size (cm^2)	Off axis (cm)	EDW angle	Criteria acceptability	
			δ_1 = 3%	δ_2 = 15%
20 x 5	2.5 to Y1	25^0	√	√
	2.5 to Y1	45^0	√	√
20 x 10	5 to Y1	25^0	√	√
	5 to Y1	45^0	√	√
20 x 15	7.5 to Y1	25^0	√	√
	7.5 to Y1	45^0	√	√
40 x 30	5 to Y1	25^0	√	√
	5 to Y1	45^0	√	√
√ define as pass × define as not pass				

Table 17. Percentage of the cases which pass or not pass the criteria acceptability of Dyk JV et al (37) and Venselaar J et al (38) for depth dose characteristic of all EDW fields.

Criteria acceptability	Percentage (%)	
	Pass	Not pass
δ_1	100	0
δ_2	100	0

Table 18. $DD_{20/10}$ between the open beam and 25^0 and 45^0 EDW at both wedge directions for 6 MV photon beam for (a) symmetric field and (b) asymmetric field.

(a) Symmetric field

Field size (cm^2)	$DD_{20/10}$				
	Open field	Y1-IN		Y2-OUT	
		25^0EDW	45^0EDW	25^0EDW	45^0EDW
5 x 5	0.55	0.55	0.55	0.55	0.55
10 x 10	0.58	0.58	0.58	0.58	0.58
15 x 15	0.60	0.60	0.60	0.60	0.60
20 x 20	0.61	0.61	0.62	0.61	0.62
20 x 5	0.57	0.57	0.57	0.57	0.57
20 x 10	0.59	0.59	0.59	0.59	0.59
20 x 15	0.60	0.60	0.60	0.60	0.61

(b) Asymmetric field

Field size (cm^2)	Off axis (cm)	$DD_{20/10}$				
		Open field	Y1-IN		Y2-OUT	
			25^0EDW	45^0EDW	25^0EDW	45^0EDW
20 x 5	2.5	0.57	0.57	0.57	0.57	0.56
20 x 10	5.0	0.59	0.59	0.59	0.58	0.58
20 x 15	7.5	0.60	0.60	0.61	0.60	0.61
40 x 30	5.0	0.63	0.63	0.64	0.64	0.64

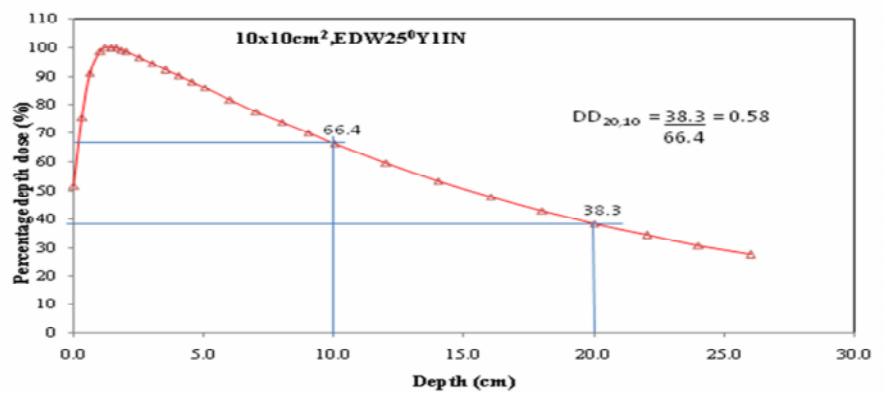

(a)

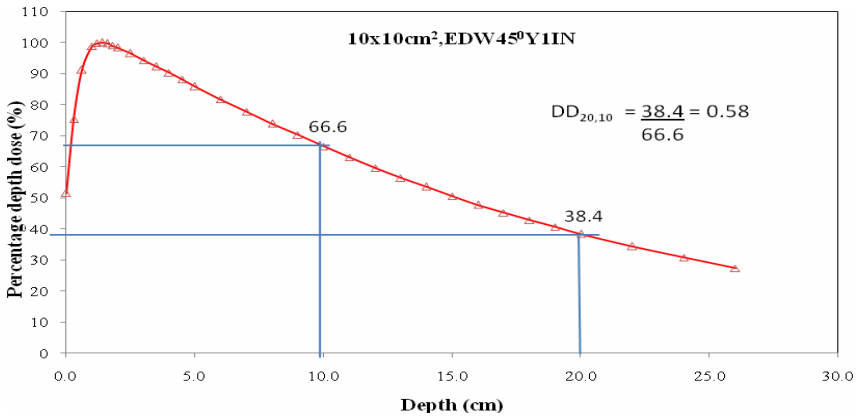

(b)

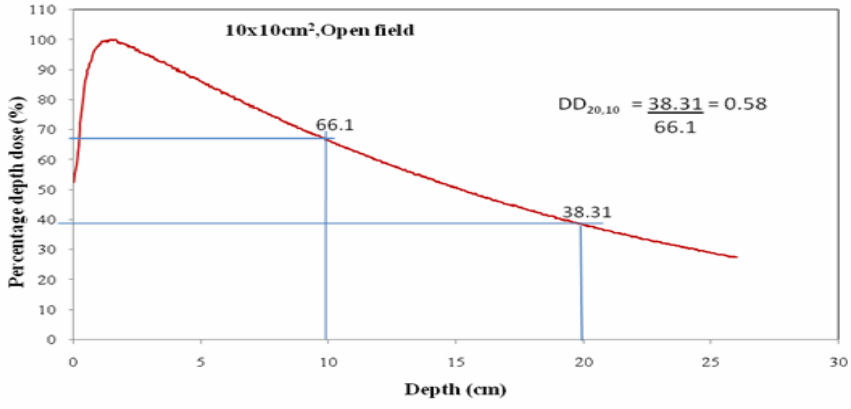

(c)

Figure 46. Ratio of relative dose at depth 20 cm to depth 10 cm ($DD_{20/10}$) at field size 10 x 10 cm^2 for (a) 25^0EDW-Y1-IN, (b) 45^0EDW-Y1-IN and (c) Open field depth doses

6.1.2.3 Beam profiles

To evaluate the EDW beam profiles, measurements of the 25^0 and 45^0EDW profiles at different depths using Wellhofer CA24 chamber array were performed. Dose is normalized to 100% at depth of d_{max} along the central axis of beam and the results were shown in Figures 47 to 53 (a-d). Acceptable match between the measured and calculated profiles for the symmetric field sizes for both wedge direction, Y1-IN and Y2-OUT of 6 MV were observed. Similarity between the EDW beam profiles for both wedge direction, Y1-IN and Y2-OUT was found. Except at the thin edge of beam profile, which the Y2-OUT showed the difference slightly larger than the Y1-IN profile. Using the acceptance criteria previously mentioned, it can be seen that the deviations in the penumbra region (δ_2) and the high dose-low dose gradient region (δ_3) were in most cases smaller than 1.5 mm and $\pm$2.0% respectively. The differences of measured and calculated RW_{50} were overall within 1.5 mm. All the deviations between the calculated and measured EDW profiles in the symmetric fields are summarized in Table 19 (a-g).

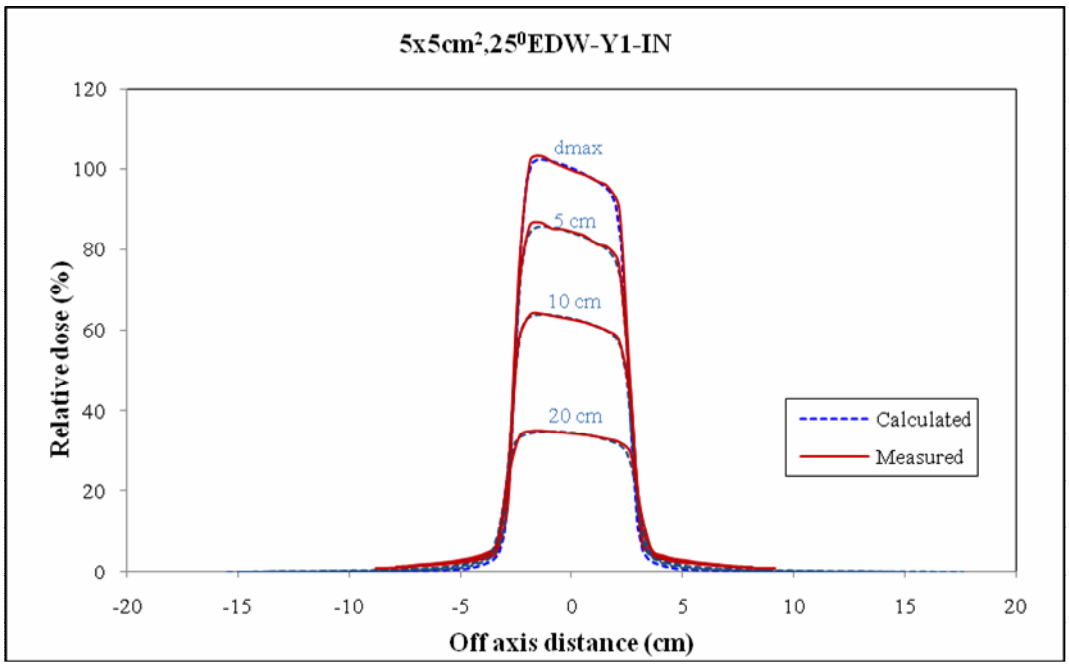

(a)

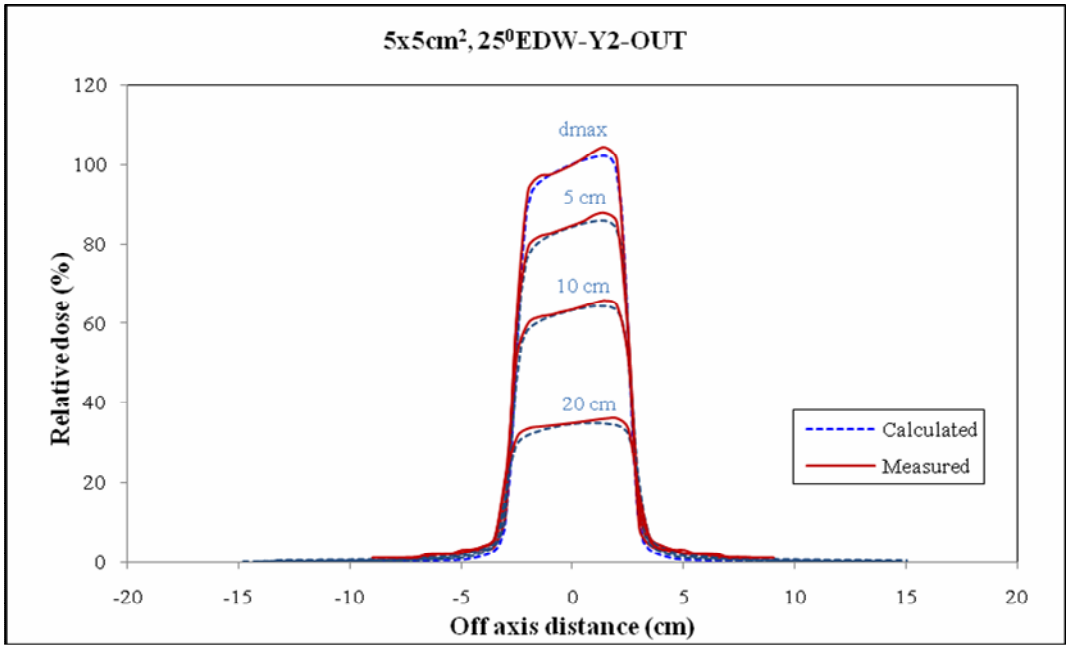
5x5cm², 25⁰EDW-Y2-OUT
Relative dose (%)
Off axis distance (cm)
dmax
5 cm
10 cm
20 cm
Calculated
Measured

(b)

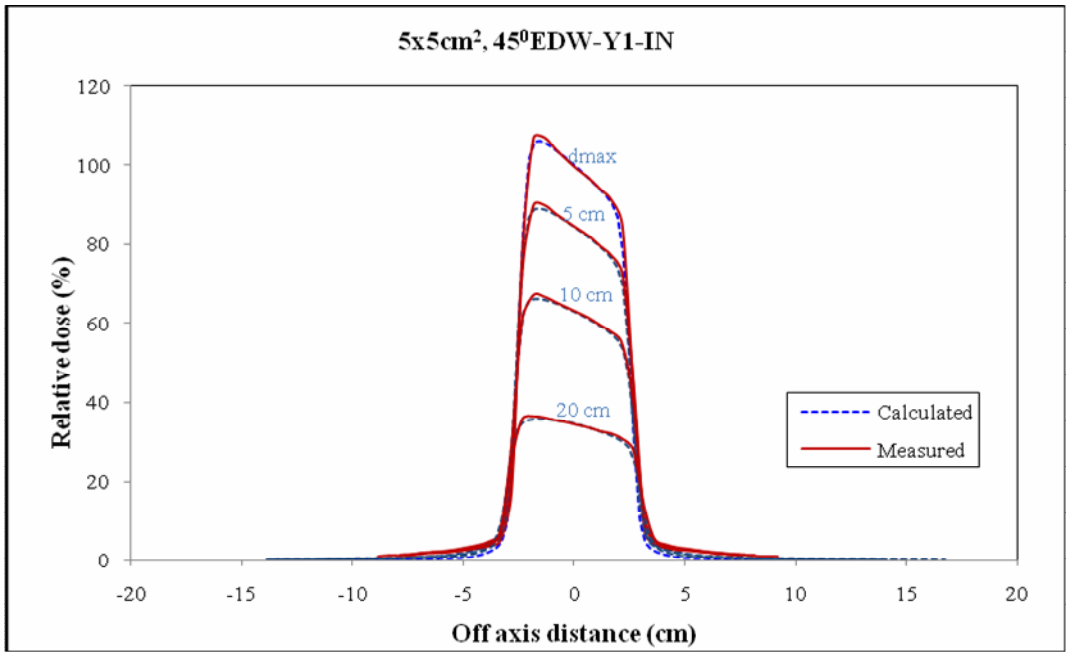
5x5cm², 45⁰EDW-Y1-IN
Relative dose (%)
Off axis distance (cm)
dmax
5 cm
10 cm
20 cm
Calculated
Measured

(c)

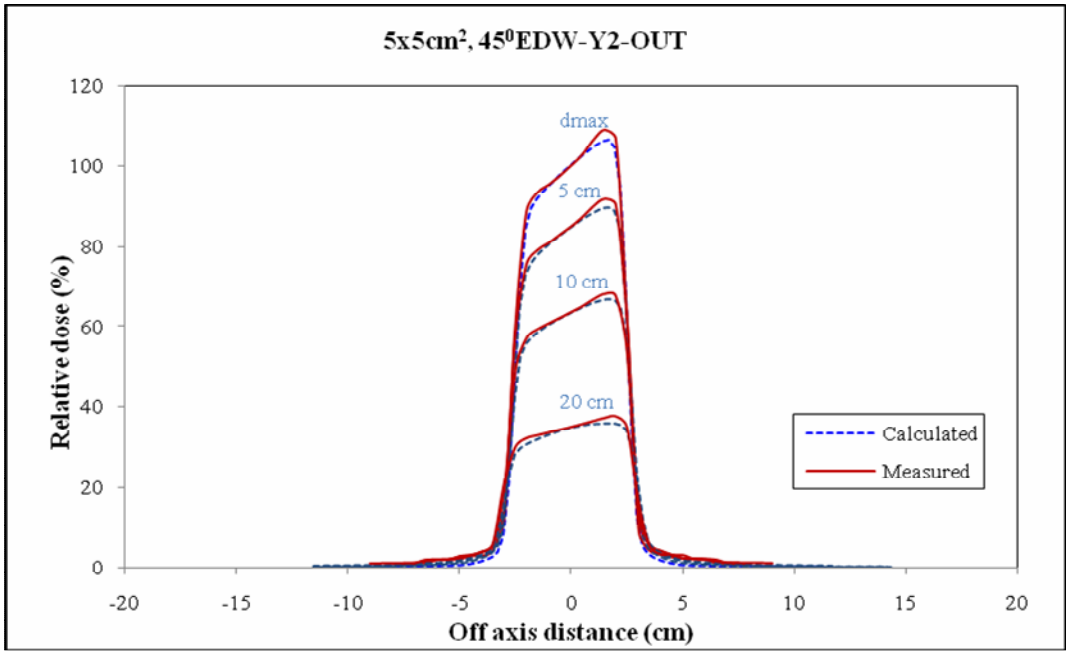

(d)

Figure 47. Calculated (dash lines) and measured (solid lines) dose profiles for 6 MV photons at a field size of 5 x 5 cm^2 and depths of d_{max} (=1.6 cm), 5 , 10 and 20 cm for (a) 25°EDW-Y1-IN (b) 25°EDW-Y2-OUT (c) 45°EDW-Y1-IN and (d) 45°EDW-Y2-OUT.

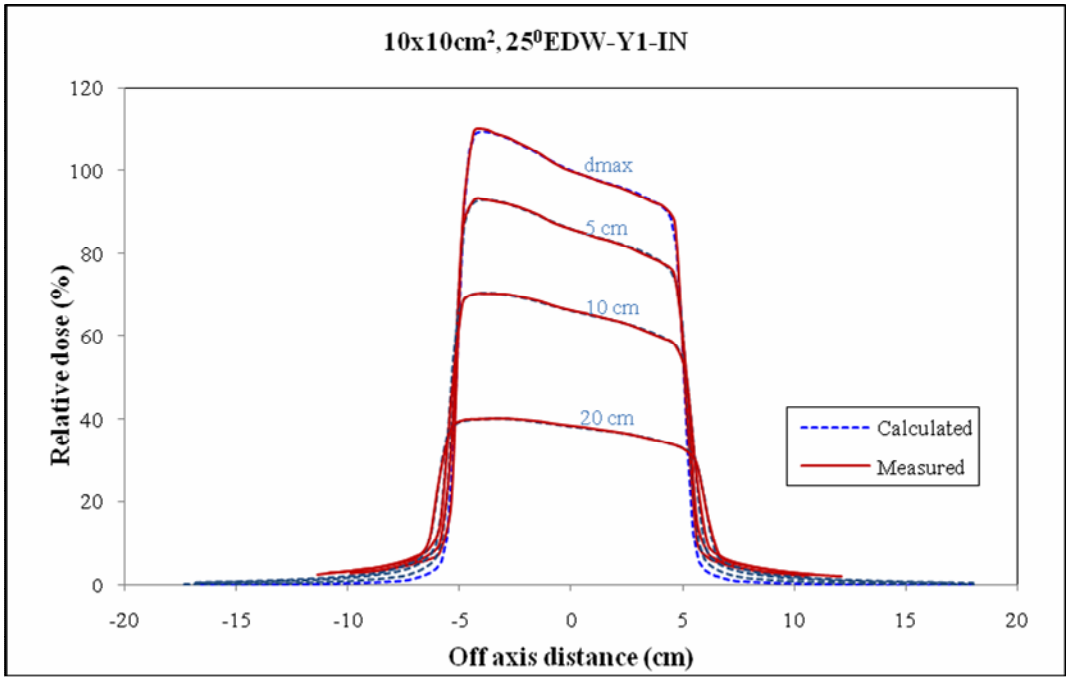
10x10cm², 25⁰EDW-Y1-IN
Relative dose (%)
Off axis distance (cm)
dmax
5 cm
10 cm
20 cm
Calculated
Measured

(a)

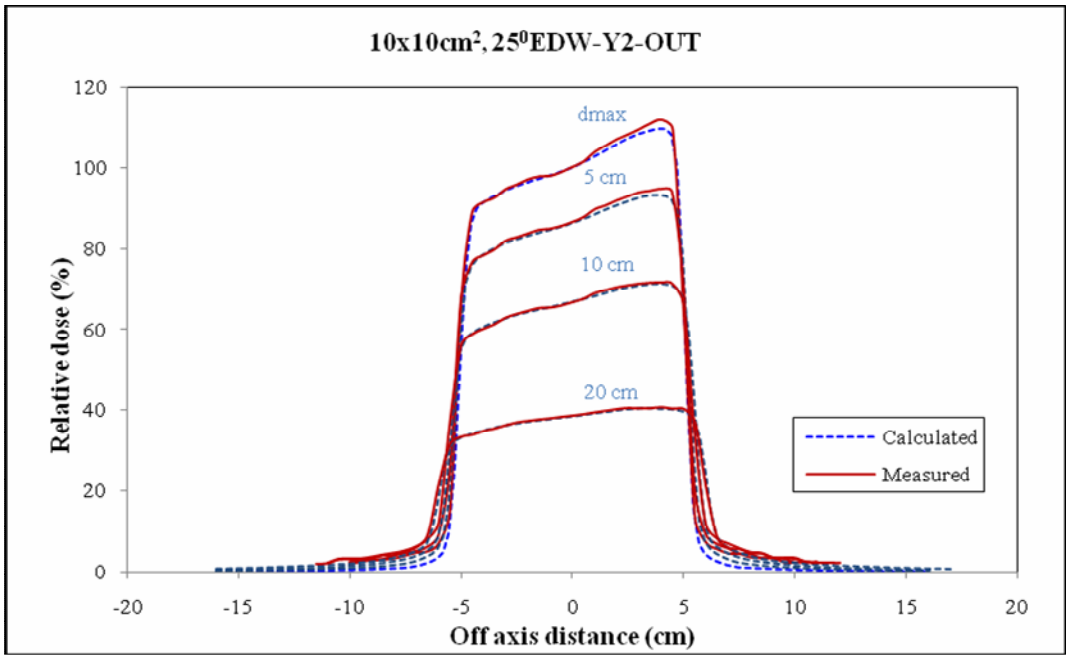
10x10cm², 25⁰EDW-Y2-OUT
Relative dose (%)
Off axis distance (cm)
dmax
5 cm
10 cm
20 cm
Calculated
Measured

(b)

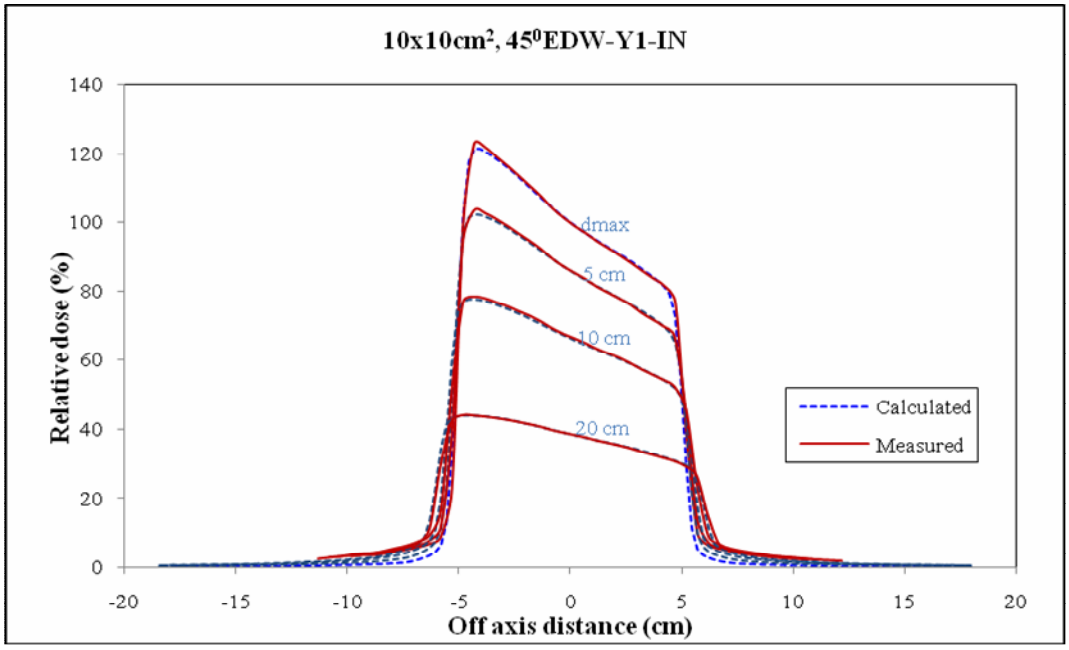

(c)

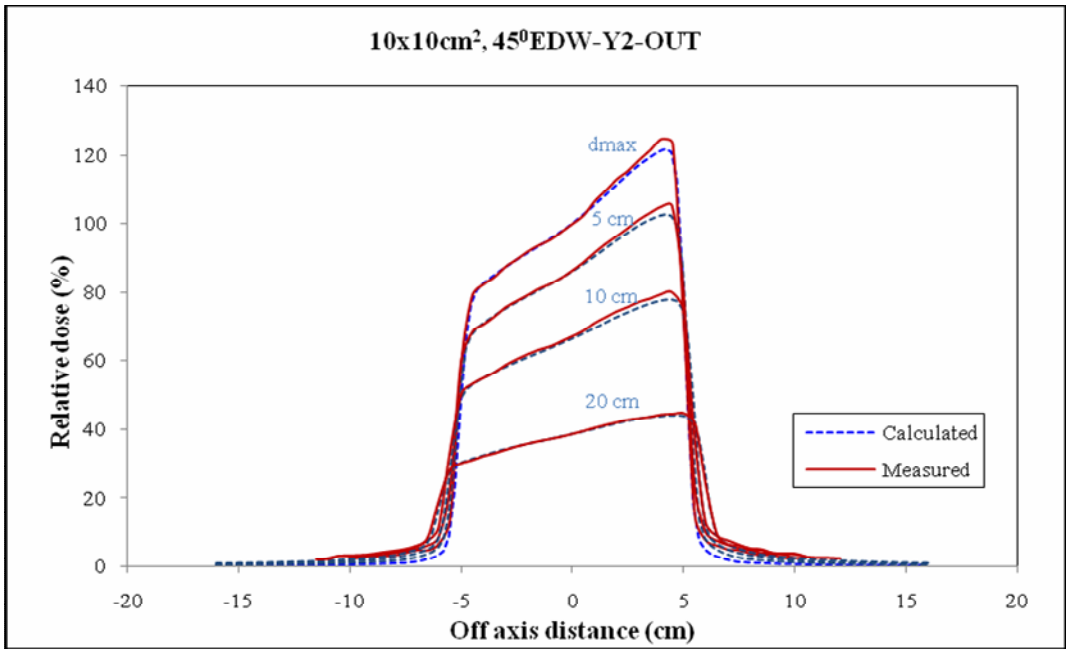

(d)

Figure 48. Calculated (dash lines) and measured (solid lines) dose profiles for 6 MV photons at a field size of 10 x 10 cm^2 and depths of d_{max} (=1.6 cm), 5, 10 and 20 cm for (a) 25°EDW-Y1-IN (b) 25°EDW-Y2-OUT (c) 45°EDW-Y1-IN and (d) 45°EDW-Y2-OUT.

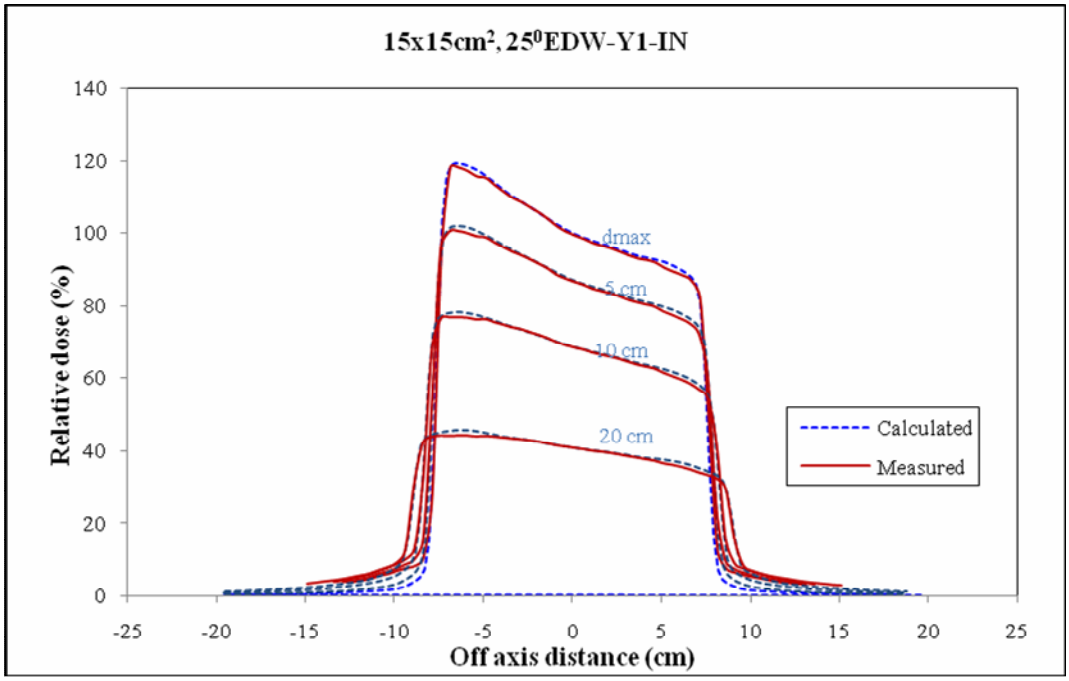
15x15cm², 25⁰EDW-Y1-IN
Relative dose (%)
Off axis distance (cm)
dmax
5 cm
10 cm
20 cm
Calculated
Measured

(a)

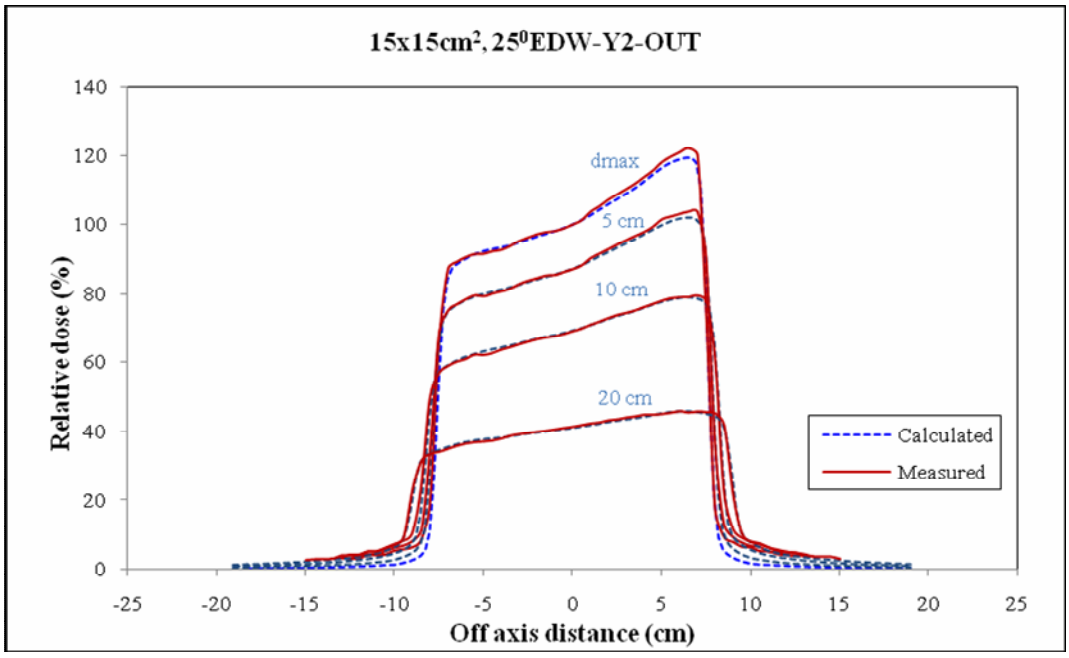
15x15cm², 25⁰EDW-Y2-OUT
Relative dose (%)
Off axis distance (cm)
dmax
5 cm
10 cm
20 cm
Calculated
Measured

(b)

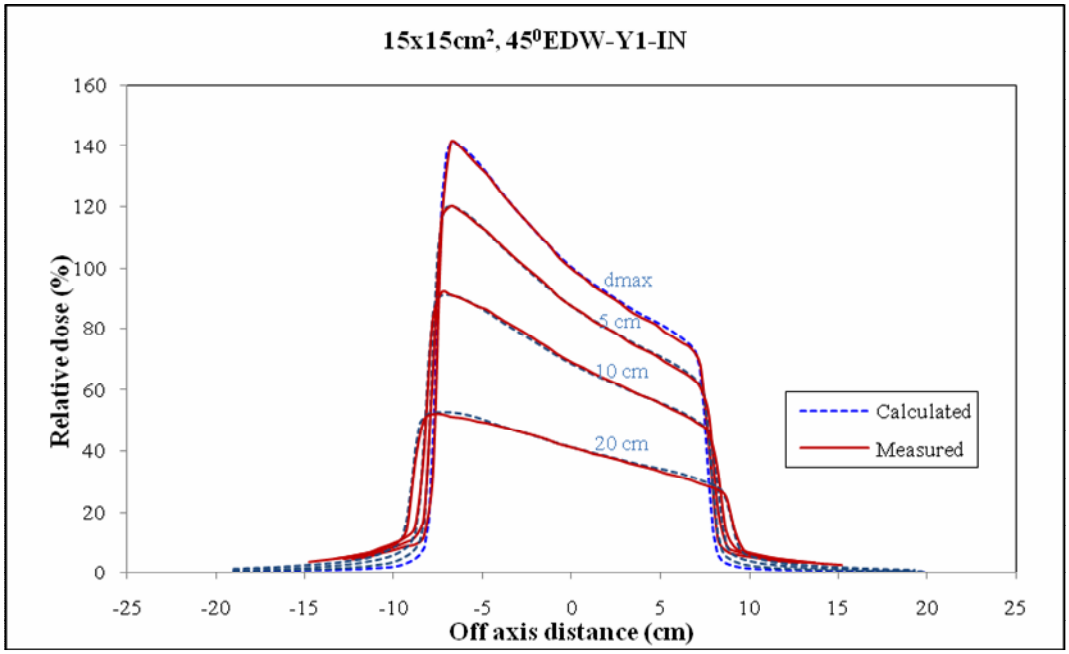

(c)

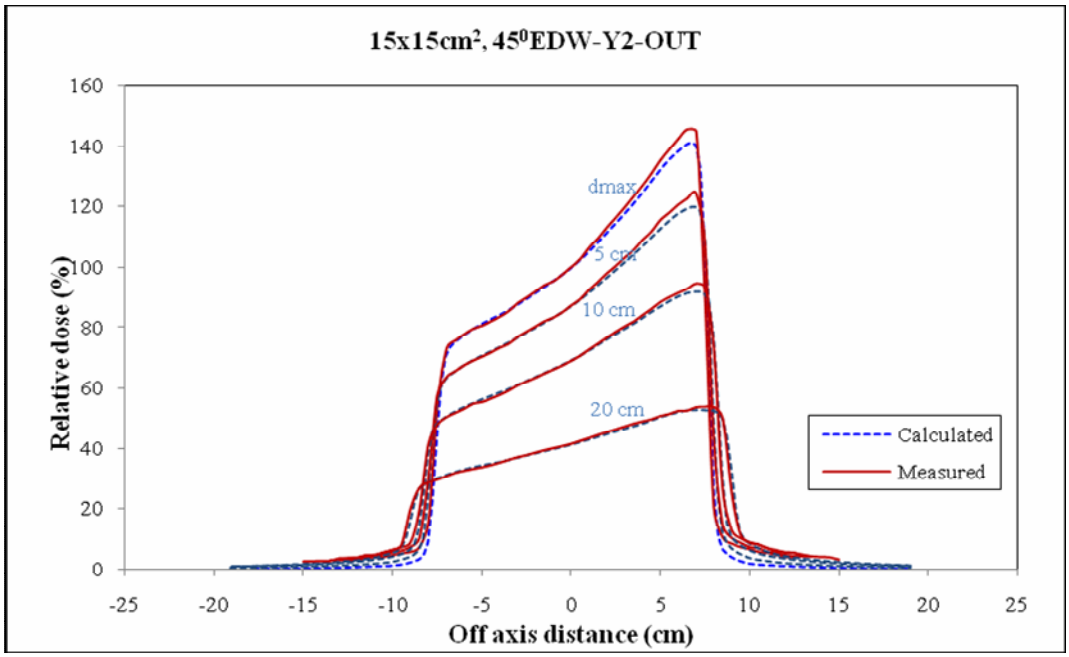

(d)

Figure 49. Calculated (dash lines) and measured (solid lines) dose profiles for 6 MV photons at a field size of 15 x 15 cm^2 and depths of d_{max} (=1.6 cm), 5, 10 and 20 cm for (a) 25°EDW-Y1-IN (b) 25°EDW-Y2-OUT (c) 45°EDW-Y1-IN and (d) 45°EDW-Y2-OUT.

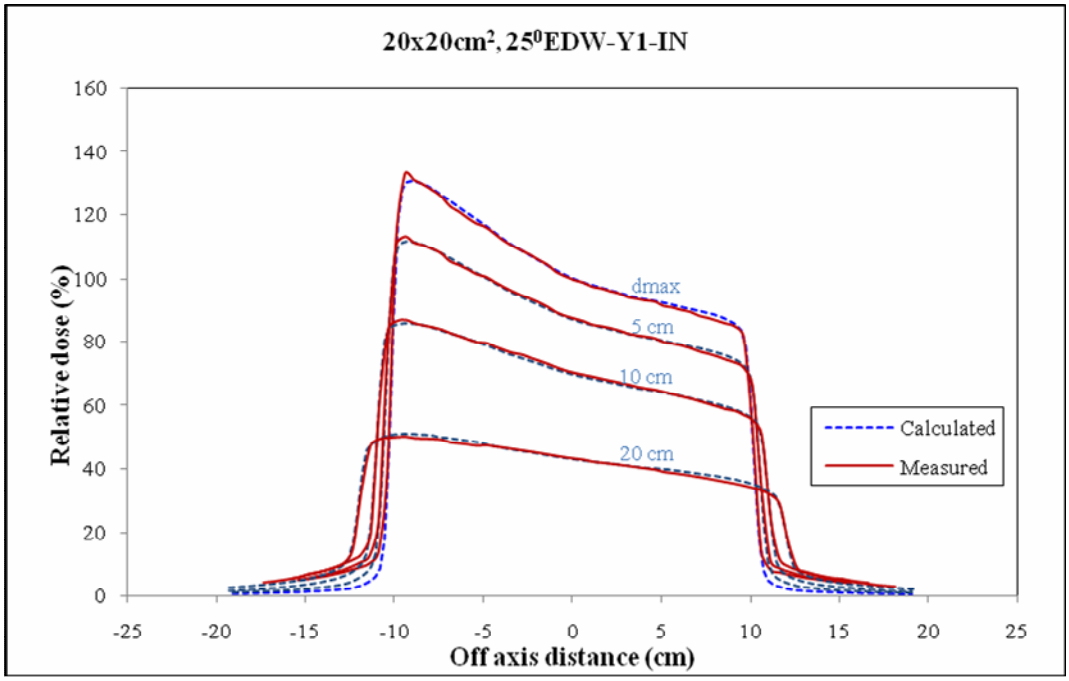
20x20cm², 25⁰EDW-Y1-IN
Relative dose (%)
Off axis distance (cm)
dmax
5 cm
10 cm
20 cm
Calculated
Measured

(a)

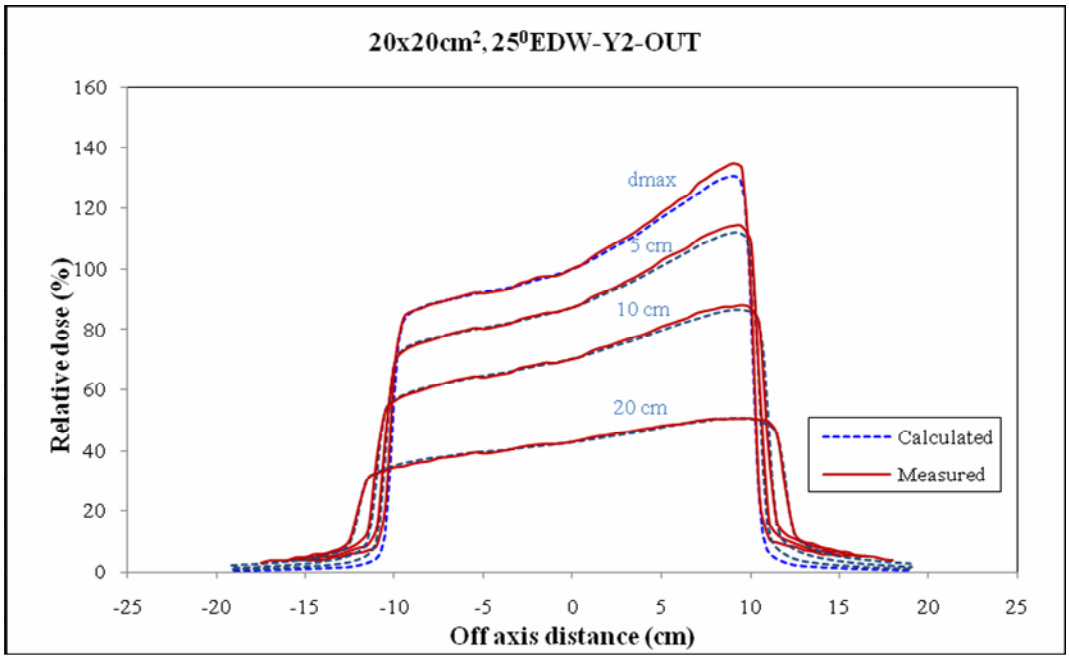
20x20cm², 25⁰EDW-Y2-OUT
Relative dose (%)
Off axis distance (cm)
dmax
5 cm
10 cm
20 cm
Calculated
Measured

(b)

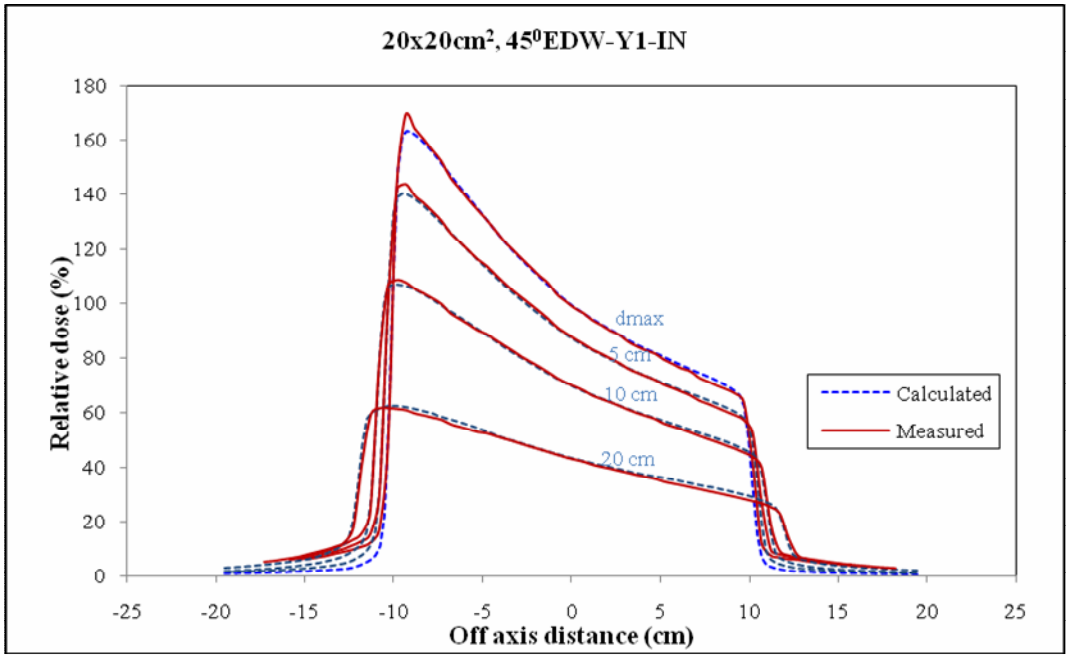

(c)

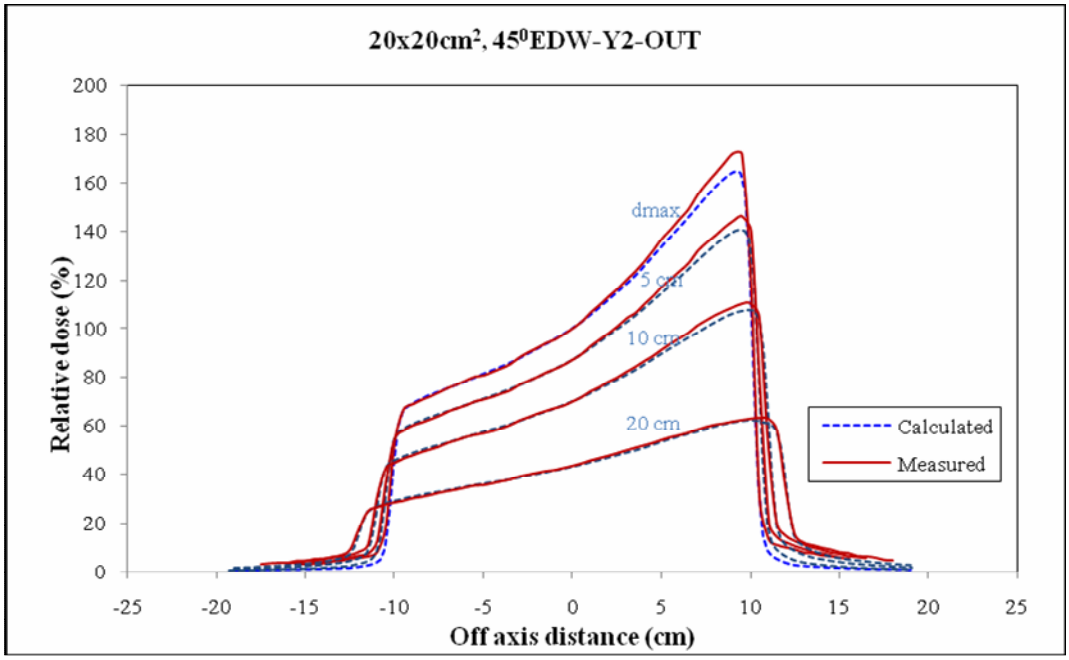

(d)

Figure 50. Calculated (dash lines) and measured (solid lines) dose profiles for 6 MV photons at a field size of 20 x 20 cm^2 and depths of d_{max} (=1.6 cm), 5, 10 and 20 cm for (a) 25°EDW-Y1-IN (b) 25°EDW-Y2-OUT (c) 45°EDW-Y1-IN and (d) 45°EDW-Y2-OUT.

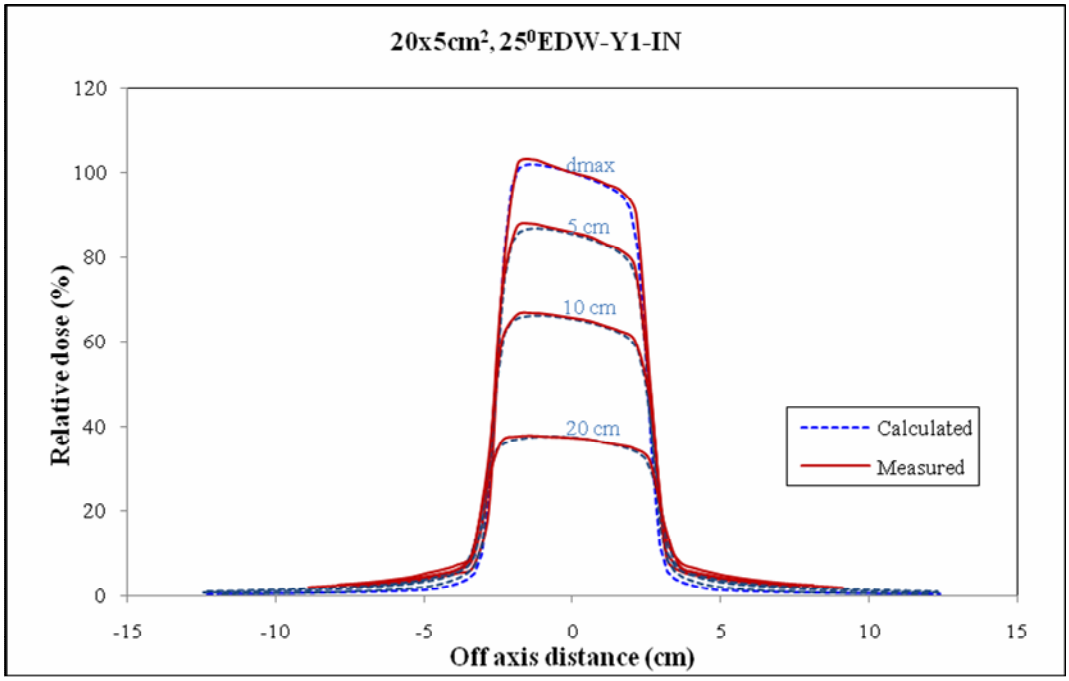
20x5cm², 25⁰EDW-Y1-IN
Relative dose (%)
Off axis distance (cm)
dmax
5 cm
10 cm
20 cm
Calculated
Measured

(a)

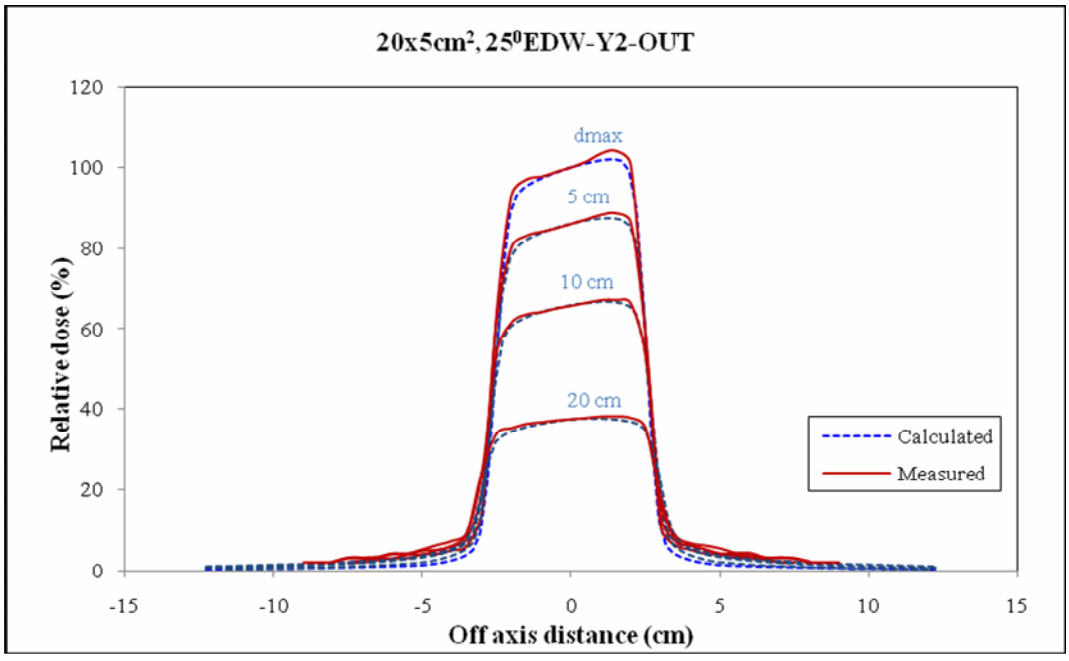
20x5cm², 25⁰EDW-Y2-OUT
Relative dose (%)
Off axis distance (cm)
dmax
5 cm
10 cm
20 cm
Calculated
Measured

(b)

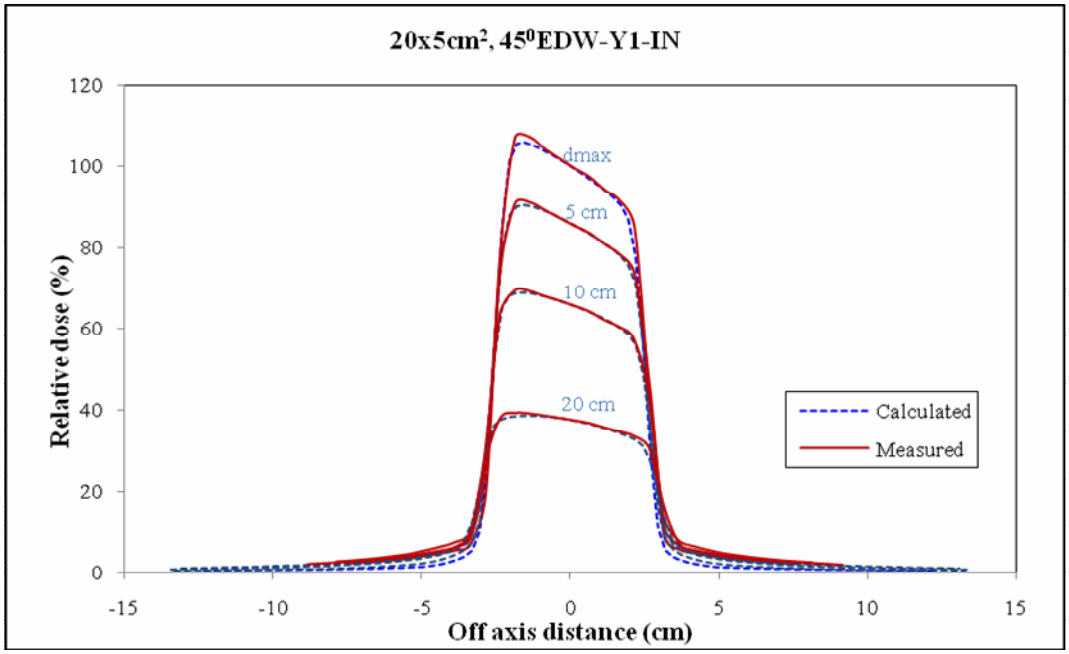

(c)

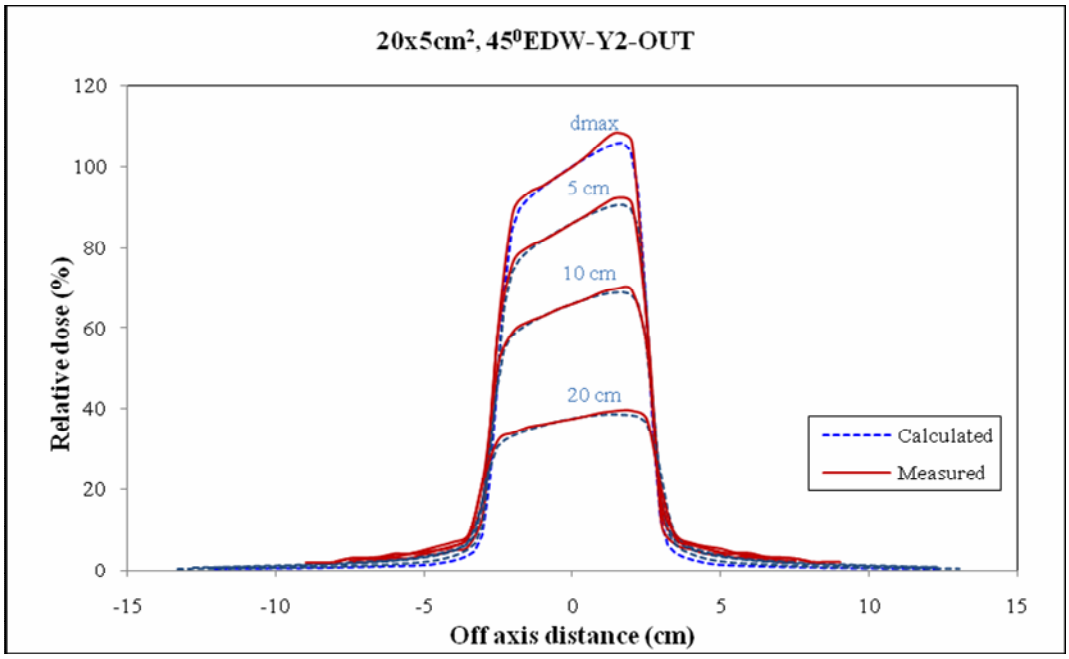

(d)

Figure 51. Calculated (dash lines) and measured (solid lines) dose profiles for 6 MV photons at a field size of 20 x 5 cm^2 and depths of d_{max} (=1.6 cm), 5, 10 and 20 cm for (a) 25°EDW-Y1-IN (b) 25°EDW-Y2-OUT (c) 45°EDW-Y1-IN and (d) 45°EDW-Y2-OUT.

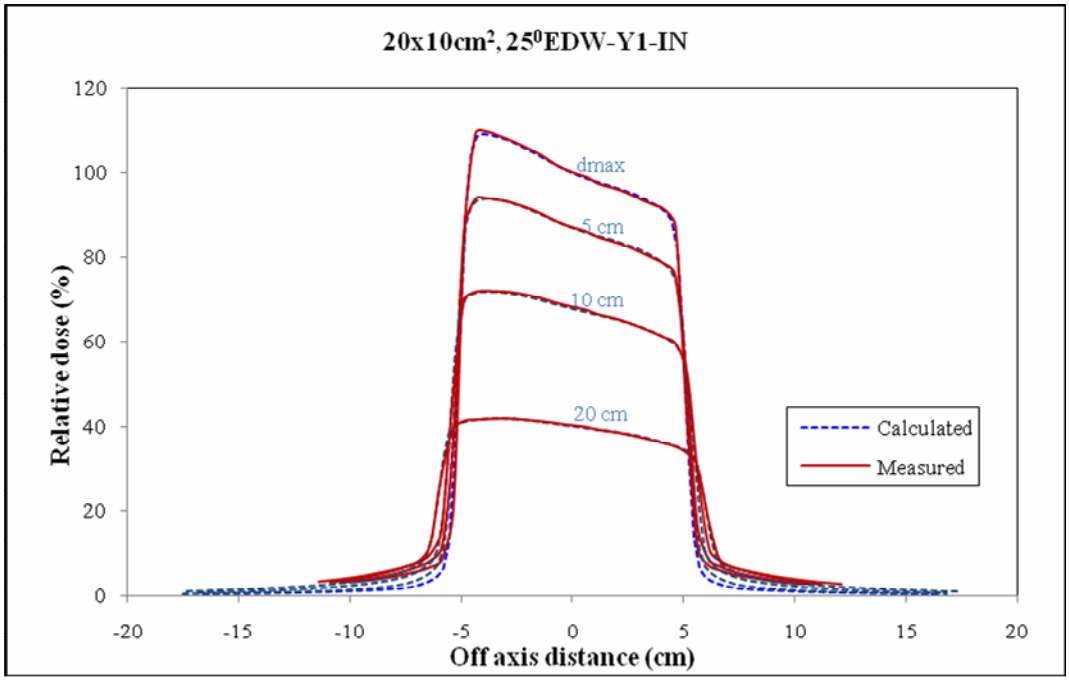
20x10cm², 25⁰EDW-Y1-IN
Relative dose (%)
Off axis distance (cm)
dmax
5 cm
10 cm
20 cm
Calculated
Measured

(a)

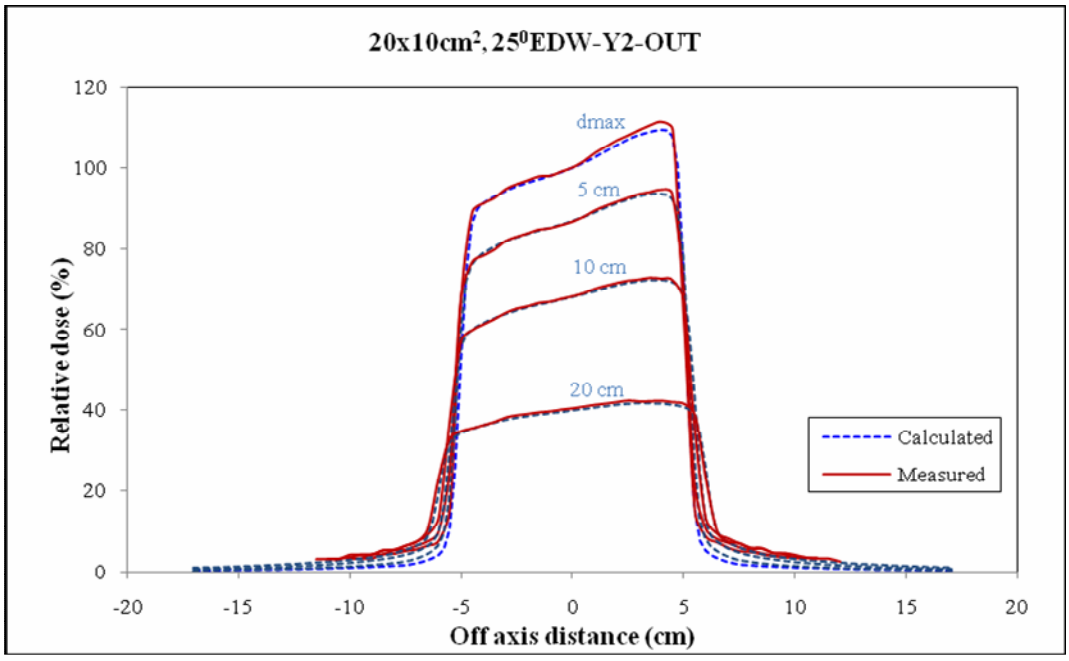
20x10cm², 25⁰EDW-Y2-OUT
Relative dose (%)
Off axis distance (cm)
dmax
5 cm
10 cm
20 cm
Calculated
Measured

(b)

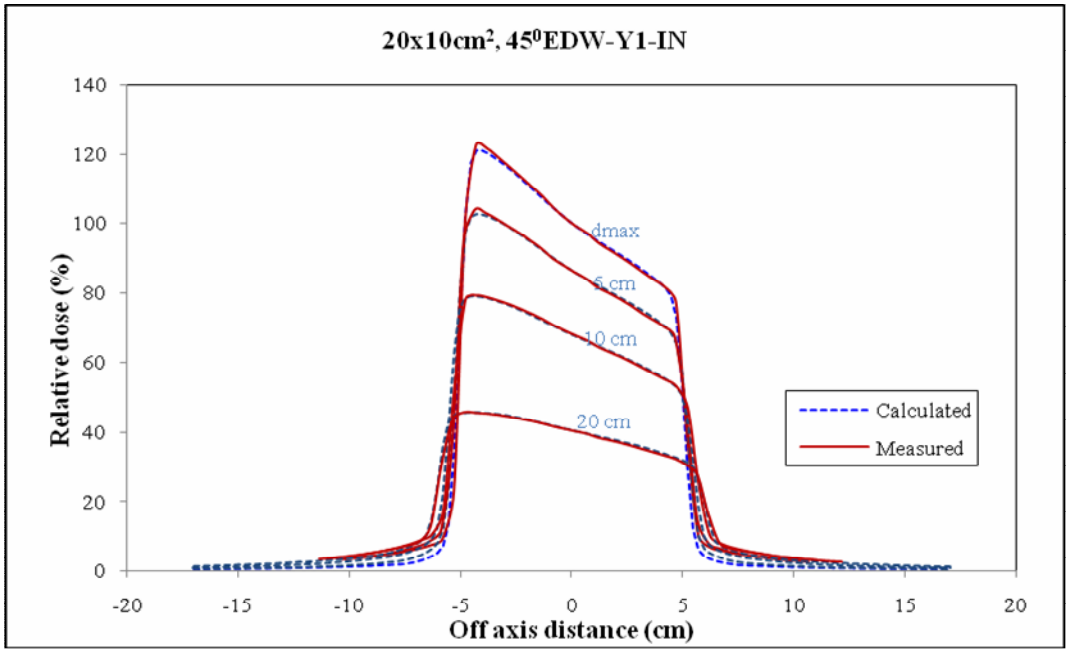

(c)

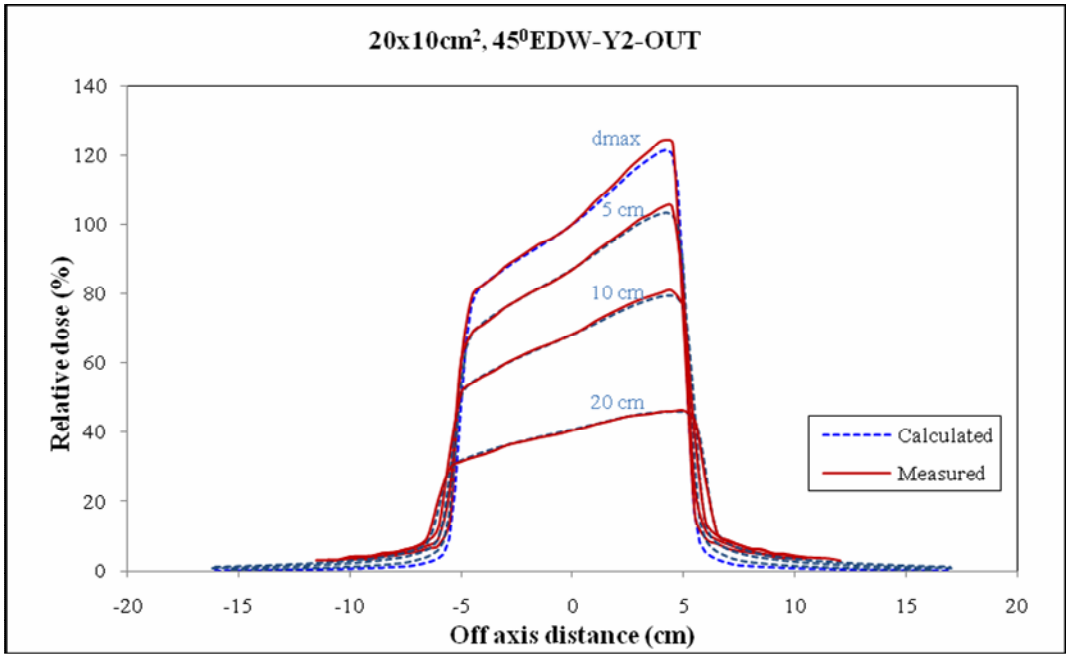

(d)

Figure 52. Calculated (dash lines) and measured (solid lines) dose profiles for 6 MV photons at a field size of 20 x 10 cm^2 and depths of d_{max} (=1.6 cm), 5, 10 and 20 cm for (a) 25°EDW-Y1-IN (b) 25°EDW-Y2-OUT (c) 45°EDW-Y1-IN and (d) 45°EDW-Y2-OUT.

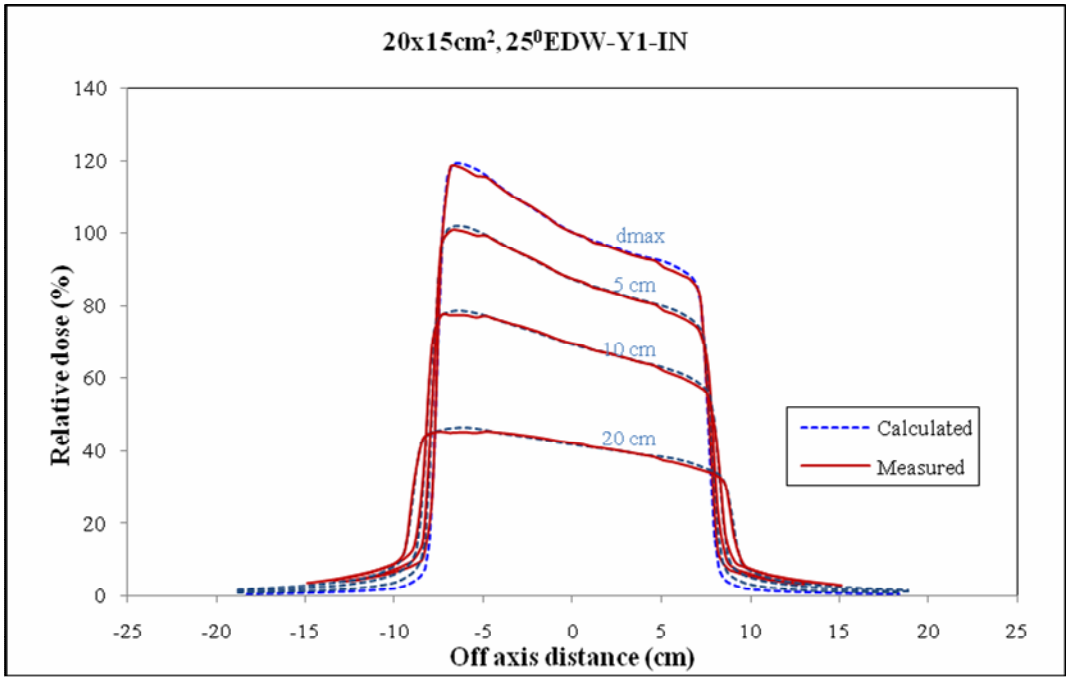
20x15cm², 25⁰EDW-Y1-IN
Relative dose (%)
Off axis distance (cm)
dmax
5 cm
10 cm
20 cm
Calculated
Measured

(a)

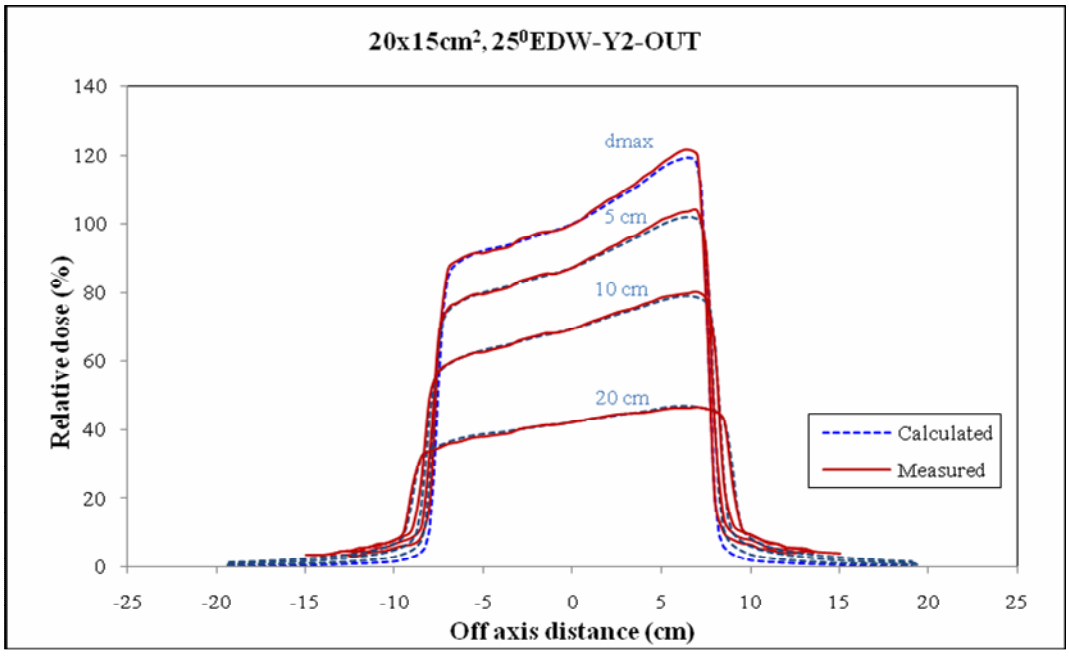
20x15cm², 25⁰EDW-Y2-OUT
Relative dose (%)
Off axis distance (cm)
dmax
5 cm
10 cm
20 cm
Calculated
Measured

(b)

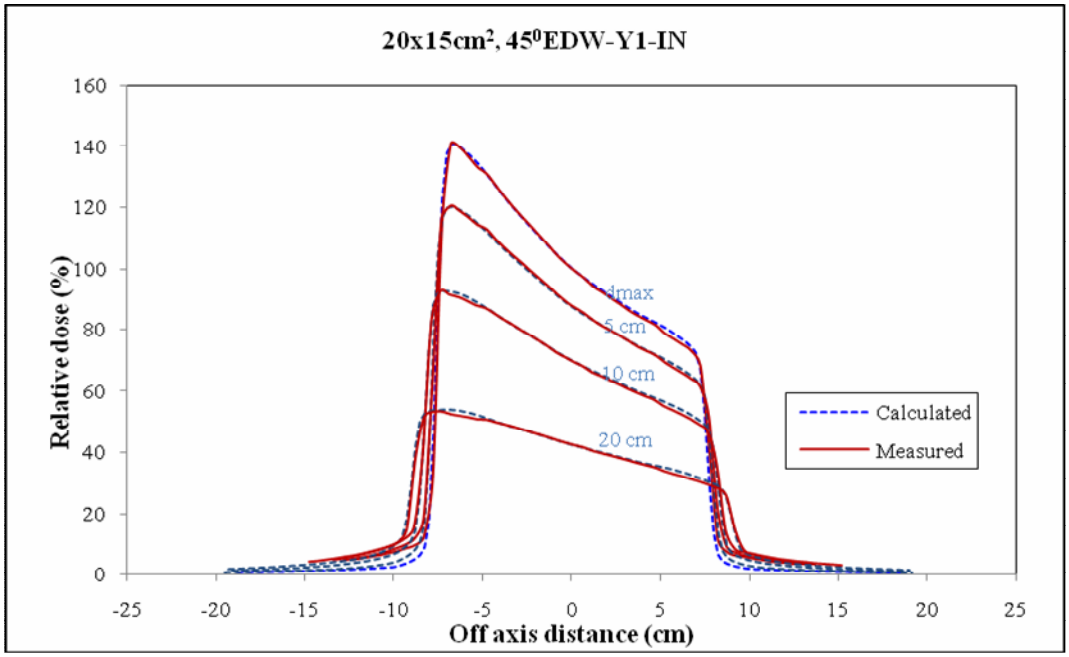

(c)

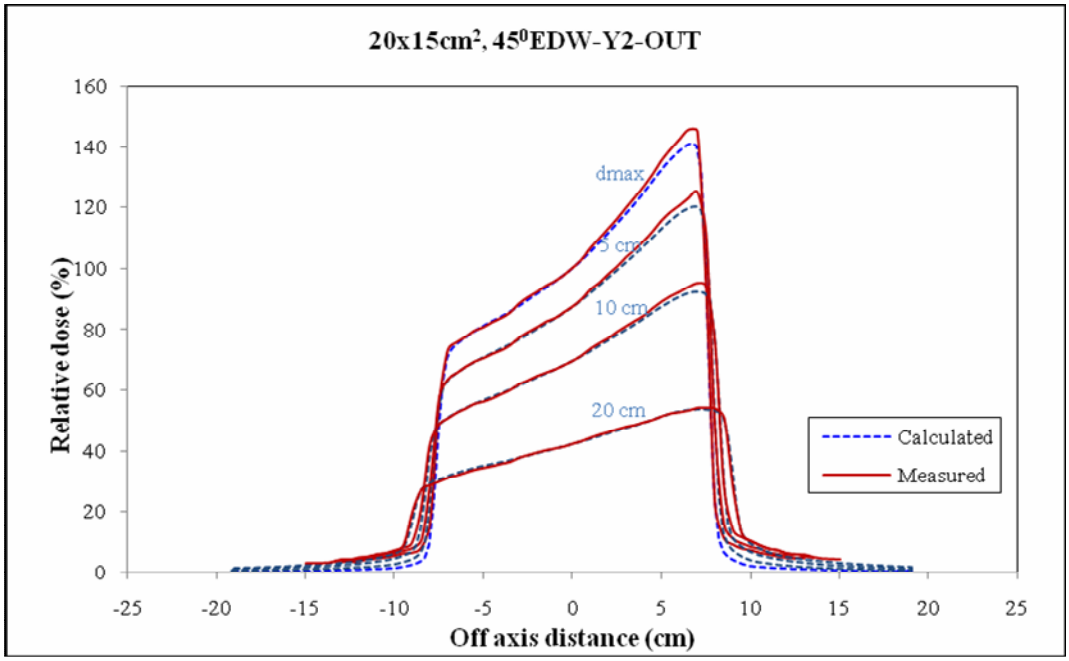

(d)

Figure 53. Calculated (dash lines) and measured (solid lines) dose profiles for 6 MV photons at a field size of 20 x 15 cm^2 and depths of d_{max} (=1.6 cm), 5, 10 and 20 cm for (a) 25°EDW-Y1-IN (b) 25°EDW-Y2-OUT (c) 45°EDW-Y1-IN and (d) 45°EDW-Y2-OUT.

Table 19. The deviations for data points in the penumbra region (δ_2), data points within the high dose-low dose gradient region (δ_3), and the radiological width (RW_{50}) between TPS calculation and measurement for 25^0 and 45^0 EDW both wedge directions Y1-IN and Y2-OUT, with 6 MV photon beam for symmetric field sizes of (a) 5 x 5 cm^2, (b) 10 x 10 cm^2, (c) 15 x 15 cm^2, (d) 20 x 20 cm^2, (e) 20 x 5 cm^2, (f) 20 x 10 cm^2 and (g) 20 x 15 cm^2.

(a) 5 x 5 cm^2

Wedge direction	EDW angle	Depth (cm)	Deviation		
			δ_2 (mm)	δ_3 (%)	RW_{50} (mm)
Y1-IN	25^0	1.6	1.5	1.02	0.7
		5.0	1.0	-0.42	1.0
		10.0	0.8	0.53	0.5
		20.0	1.3	1.31	0.3
	45^0	1.6	1.5	1.33	0.7
		5.0	1.3	0.93	0.9
		10.0	0.9	0.69	0.7
		20.0	1.5	1.38	0.4
Y2-OUT	25^0	1.6	1.0	1.83	1.2
		5.0	1.1	1.49	1.1
		10.0	1.4	1.54	0.7
		20.0	1.3	1.82	0.6
	45^0	1.6	1.1	2.19	1.3
		5.0	0.9	1.80	1.0
		10.0	1.2	1.5	0.6
		20.0	1.3	2.28	0.6

(b) 10 x 10 cm^2

Wedge direction	EDW angle	Depth (cm)	Deviation		
			δ_2 (mm)	δ_3 (%)	RW_{50} (mm)
Y1-IN	25^0	1.6	1.1	0.28	0.1
		5.0	0.6	-0.20	0.2
		10.0	1.3	-0.24	0.0
		20.0	1.2	-0.44	1.5
	45^0	1.6	1.4	0.49	0.1
		5.0	1.0	0.46	0.1
		10.0	2.0	0.30	0.1
		20.0	1.7	-0.55	0.1
Y2-OUT	25^0	1.6	1.1	0.78	0.9
		5.0	0.7	1.03	0.2
		10.0	1.4	0.92	0.4
		20.0	1.4	0.39	0.6
	45^0	1.6	1.1	0.96	0.9
		5.0	0.6	1.11	0.3
		10.0	1.4	1.08	0.5
		20.0	1.4	0.78	0.7

(c) 15 x 15 cm^2

Wedge direction	EDW angle	Depth (cm)	Deviation		
			δ_2 (mm)	δ_3 (%)	RW_{50} (mm)
Y1-IN	25^0	1.6	1.1	0.26	0.4
		5.0	1.4	-0.34	0.5
		10.0	1.4	-0.32	0.5
		20.0	0.6	-0.48	0.2
	45^0	1.6	1.7	-0.76	0.5
		5.0	1.3	-0.88	0.9
		10.0	1.1	-0.88	0.8
		20.0	1.2	-1.06	0.9
Y2-OUT	25^0	1.6	1.1	1.22	1.0
		5.0	1.7	0.96	0.1
		10.0	1.5	-0.58	0.5
		20.0	1.2	0.89	0.3
	45^0	1.6	1.0	1.67	0.9
		5.0	1.2	1.40	0.1
		10.0	1.1	1.20	0.5
		20.0	1.3	1.07	0.5

(d) 20 x 20 cm^2

Wedge direction	EDW angle	Depth (cm)	Deviation		
			δ_2 (mm)	δ_3 (%)	RW_{50} (mm)
Y1-IN	25^0	1.6	1.3	-0.61	1.0
		5.0	1.3	-0.80	0.6
		10.0	0.7	-0.43	0.1
		20.0	1.0	-2.53	0.3
	45^0	1.6	1.7	-0.62	0.1
		5.0	1.4	-1.08	0.4
		10.0	0.3	-1.83	0.0
		20.0	1.2	-2.87	0.3
Y2-OUT	25^0	1.6	1.2	1.39	1.0
		5.0	1.5	2.00	1.5
		10.0	1.6	1.66	1.1
		20.0	1.5	-1.93	0.9
	45^0	1.6	1.1	2.46	1.0
		5.0	1.5	2.30	1.0
		10.0	1.5	1.81	0.6
		20.0	1.7	-2.73	0.1

(e) 20 x 5 cm^2

Wedge direction	EDW angle	Depth (cm)	Deviation		
			δ_2 (mm)	δ_3 (%)	RW_{50} (mm)
Y1-IN	25^0	1.6	1.7	0.94	0.9
		5.0	0.9	0.53	1.0
		10.0	1.4	0.41	0.9
		20.0	1.0	0.85	0.4
	45^0	1.6	1.6	1.27	0.7
		5.0	1.4	0.83	1.0
		10.0	1.1	0.53	0.9
		20.0	1.7	1.12	0.6
Y2-OUT	25^0	1.6	1.2	1.69	1.3
		5.0	1.2	1.21	1.3
		10.0	1.8	0.90	0.8
		20.0	1.4	1.50	0.8
	45^0	1.6	1.2	2.06	1.4
		5.0	1.1	1.48	1.1
		10.0	1.7	1.10	0.8
		20.0	1.4	2.04	0.7

(f) 20 x 10 cm^2

Wedge direction	EDW angle	Depth (cm)	Deviation		
			δ_2 (mm)	δ_3 (%)	RW_{50} (mm)
Y1-IN	25^0	1.6	1.0	0.53	0.1
		5.0	0.8	-0.61	0.0
		10.0	1.4	-0.58	0.1
		20.0	1.1	-0.81	0.3
	45^0	1.6	1.4	-0.61	0.2
		5.0	0.7	-0.68	0.2
		10.0	1.7	-0.78	0.0
		20.0	1.6	-0.88	0.0
Y2-OUT	25^0	1.6	1.1	0.83	1.0
		5.0	0.6	0.70	0.3
		10.0	1.4	0.51	0.5
		20.0	1.5	0.63	0.9
	45^0	1.6	1.1	1.39	1.2
		5.0	0.7	0.96	0.3
		10.0	1.4	0.94	0.5
		20.0	1.4	0.56	0.9

(g) 20 x 15 cm^2

Wedge direction	EDW angle	Depth (cm)	Deviation		
			δ_2 (mm)	δ_3 (%)	RW_{50} (mm)
Y1-IN	25^0	1.6	1.1	-0.36	0.7
		5.0	1.0	-0.41	0.6
		10.0	1.5	-0.46	0.5
		20.0	0.6	-0.72	0.4
	45^0	1.6	1.7	-0.60	0.3
		5.0	1.3	-0.56	0.8
		10.0	1.0	-0.67	0.8
		20.0	1.4	-0.26	0.1
Y2-OUT	25^0	1.6	1.1	1.13	1.2
		5.0	1.7	0.99	0.4
		10.0	1.7	0.90	0.8
		20.0	1.3	1.70	0.6
	45^0	1.6	1.0	1.56	1.1
		5.0	1.3	1.44	0.4
		10.0	1.3	1.22	0.7
		20.0	0.8	1.68	0.7

For the asymmetric EDW profiles, result of the comparisons for the field sizes of 20 x 5, 20 x 10, 20 x 15 and 40 x 30 cm^2 with the corresponding beam centers were 2.5, 5, and 7.5 cm off-axis, respectively, at several depths were shown in Figure 54 to 57 (a-d). Similar results with the symmetric fields were also observed in the asymmetric EDW profiles which illustrated in Table 20 (a-d). Almost one hundred percent of the tests pass the acceptance criteria at the penumbra region (δ_2), the high dose-low dose gradient (δ_3) and RW_{50} as presented in Table 23. Except for the largest asymmetric field size of 40 x 30 cm^2, at deeper depth (20 cm) which the larger deviations of 3.2 mm, 3.53% and 2.9 mm were found in the penumbra region (δ_2), the high dose-low dose gradient (δ_3) and RW_{50}, respectively.

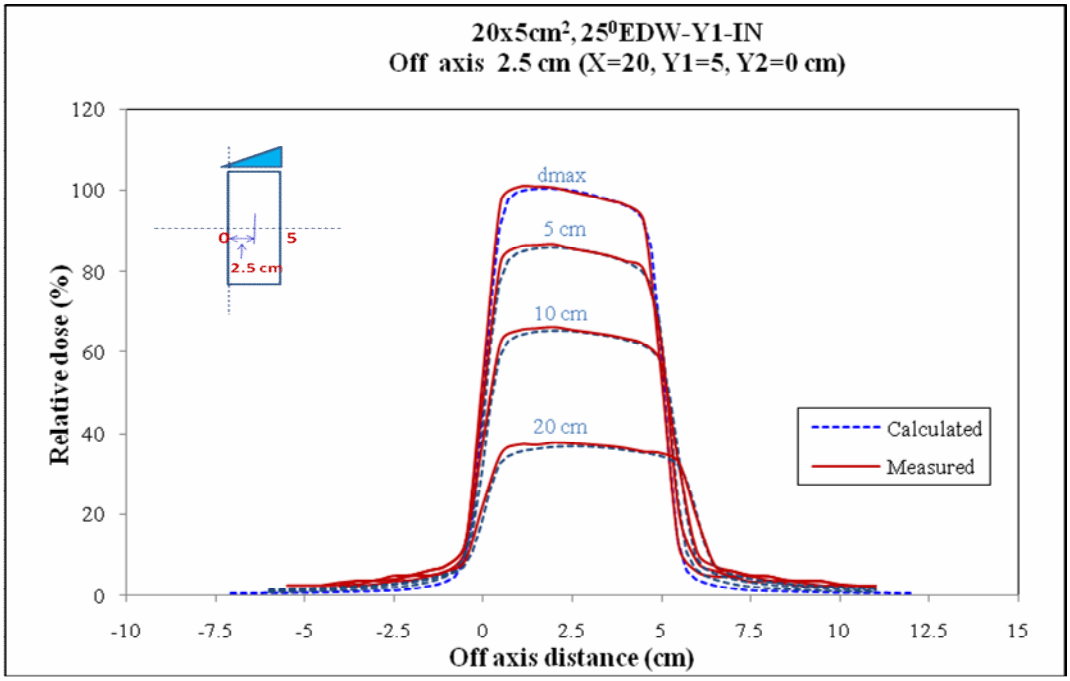
20x5cm², 25⁰EDW-Y1-IN
Off axis 2.5 cm (X=20, Y1=5, Y2=0 cm)
Relative dose (%)
Off axis distance (cm)
dmax
5 cm
10 cm
20 cm
Calculated
Measured
0
5
2.5 cm

(a)

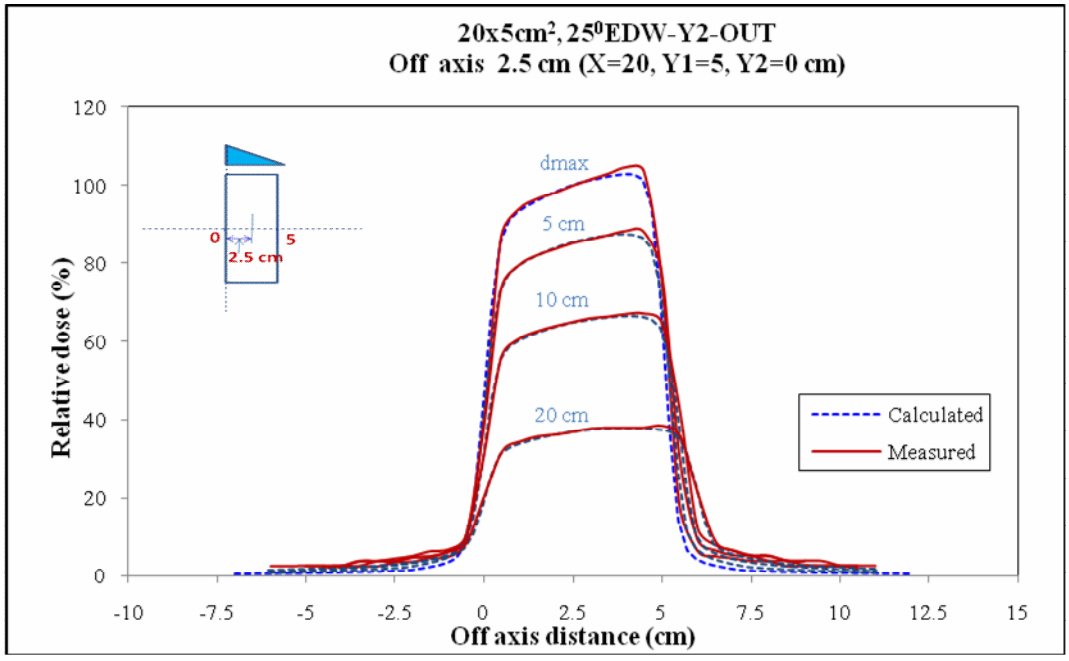
20x5cm², 25⁰EDW-Y2-OUT
Off axis 2.5 cm (X=20, Y1=5, Y2=0 cm)
Relative dose (%)
Off axis distance (cm)
dmax
5 cm
10 cm
20 cm
Calculated
Measured
0
5
2.5 cm

(b)

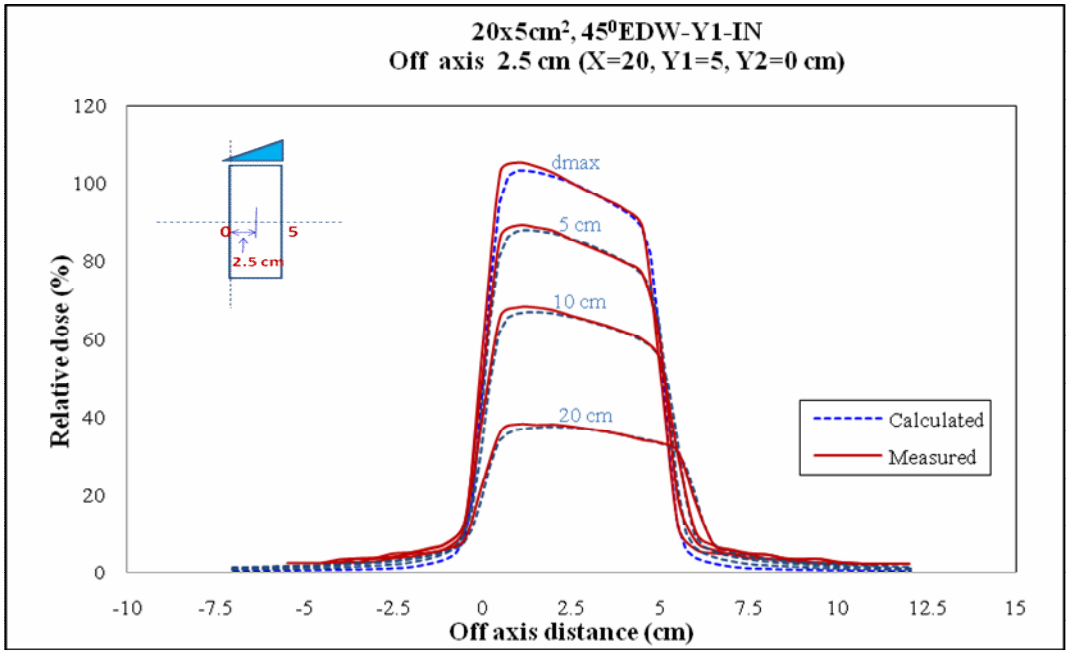

(c)

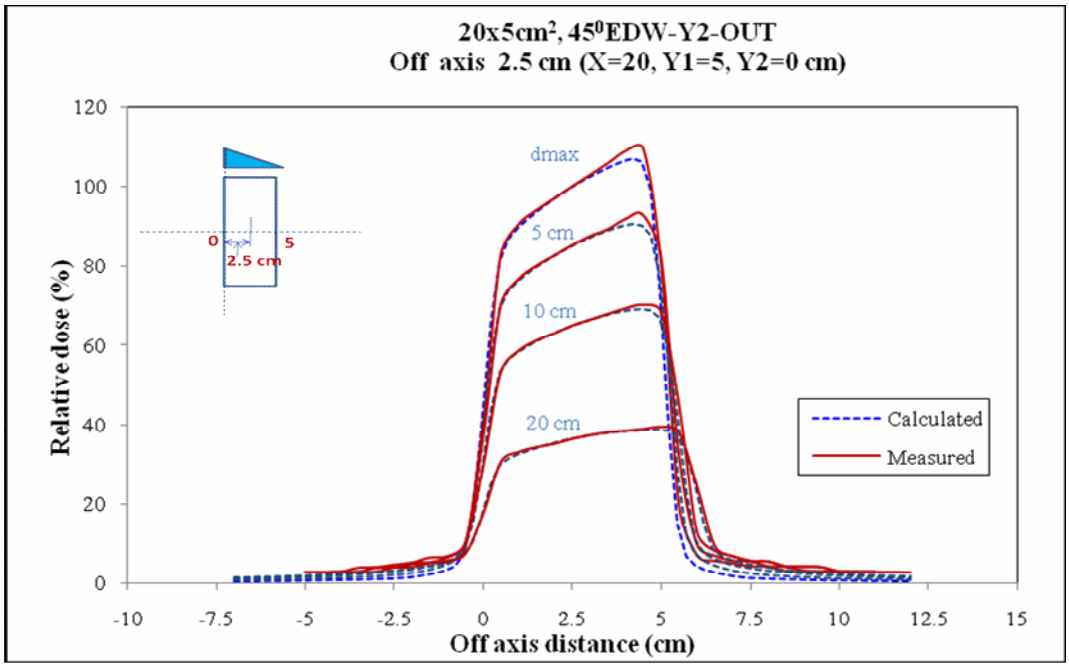

(d)

Figure 54. Calculated (dash lines) and measured (solid lines) dose profiles for 6 MV photons at an asymmetric field size of 20 x 5 cm^2, off central-axis distance 2.5 cm and depths of d_{max} (=1.6 cm), 5, 10 and 20 cm for (a) 25°EDW-Y1-IN (b) 25°EDW-Y2-OUT (c) 45°EDW-Y1-IN and (d) 45°EDW-Y2-OUT.

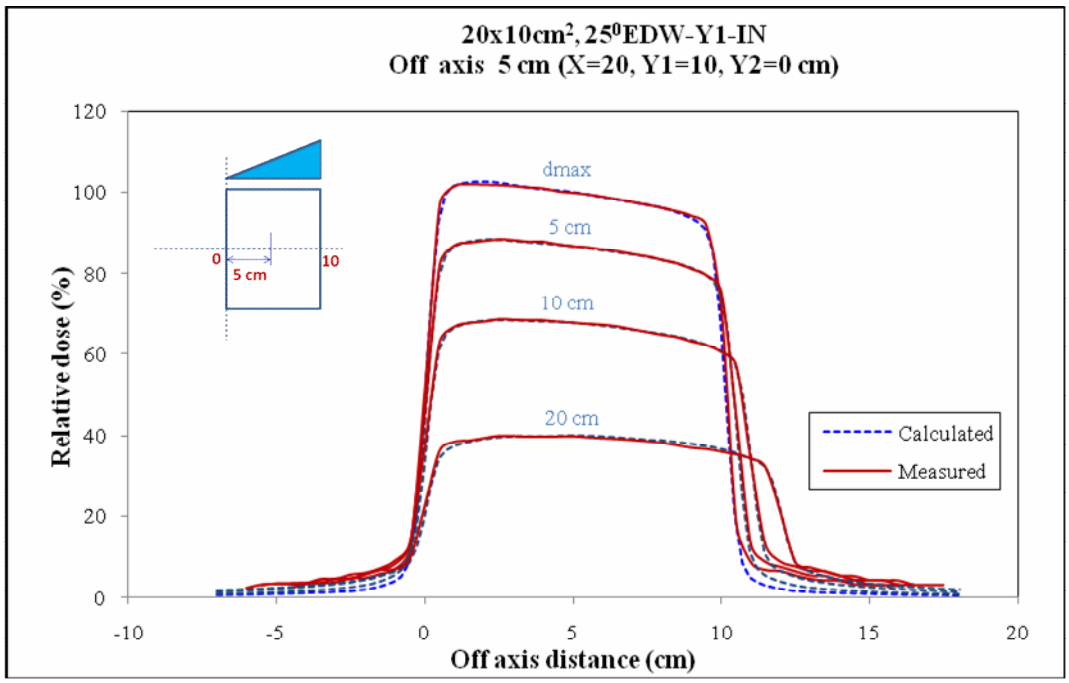
20x10cm², 25⁰EDW-Y1-IN
Off axis 5 cm (X=20, Y1=10, Y2=0 cm)
Relative dose (%)
Off axis distance (cm)
dmax
5 cm
10 cm
20 cm
Calculated
Measured
0
10
5 cm

(a)

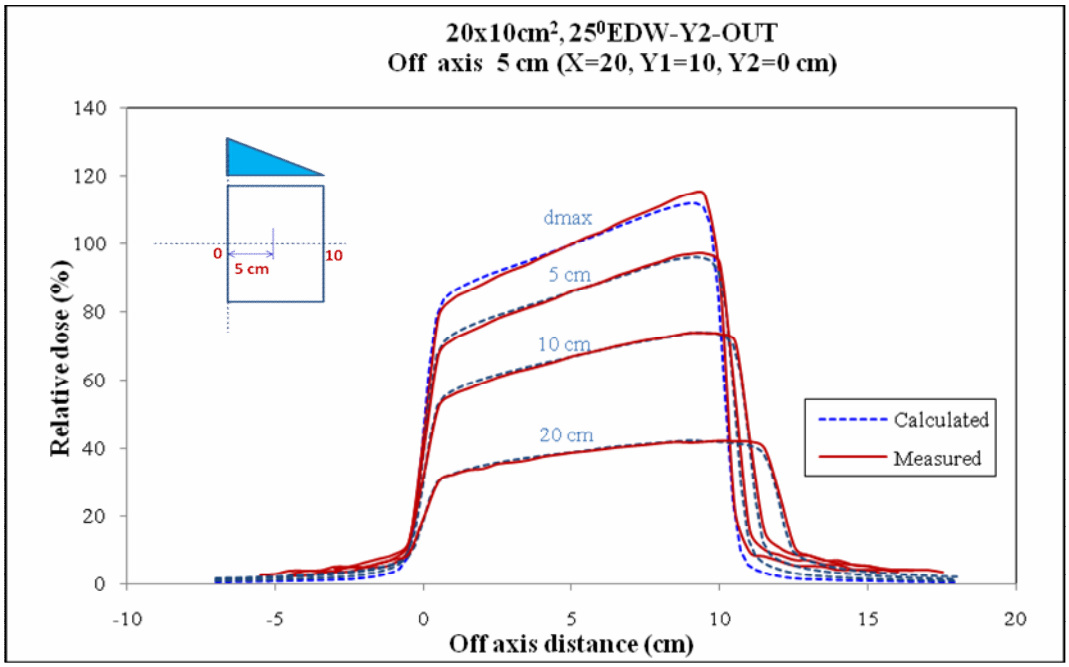
20x10cm², 25⁰EDW-Y2-OUT
Off axis 5 cm (X=20, Y1=10, Y2=0 cm)
Relative dose (%)
Off axis distance (cm)
dmax
5 cm
10 cm
20 cm
Calculated
Measured
0
10
5 cm

(b)

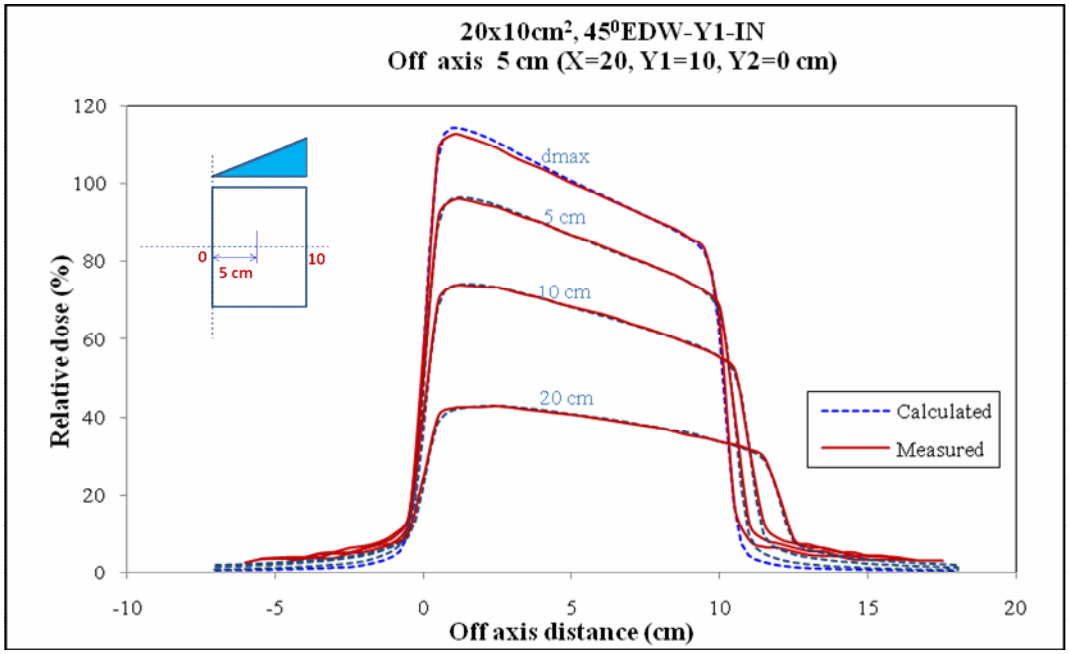

(c)

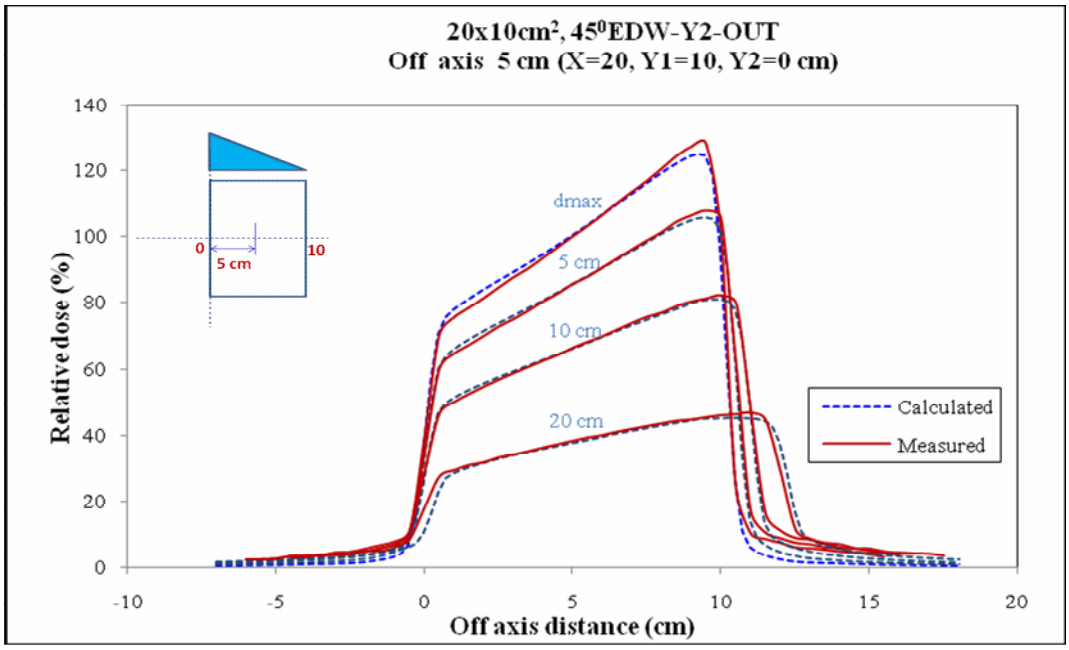

(d)

Figure 55. Calculated (dash lines) and measured (solid lines) dose profiles for 6 MV photons at an asymmetric field size of 20 x 10 cm^2, off central-axis distance 5 cm and depths of d_{max} (=1.6 cm), 5, 10 and 20 cm for (a) 25°EDW-Y1-IN (b) 25°EDW-Y2-OUT (c) 45°EDW-Y1-IN and (d) 45°EDW-Y2-OUT.

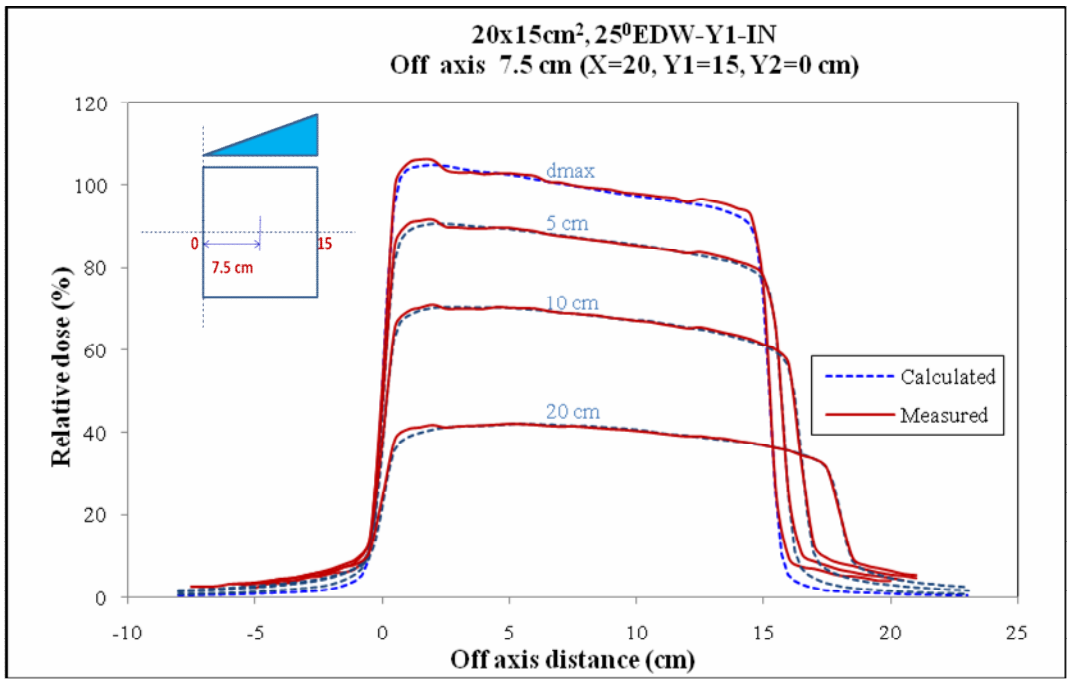
20x15cm², 25⁰EDW-Y1-IN
Off axis 7.5 cm (X=20, Y1=15, Y2=0 cm)
Relative dose (%)
Off axis distance (cm)
dmax
5 cm
10 cm
20 cm
Calculated
Measured
0
15
7.5 cm

(a)

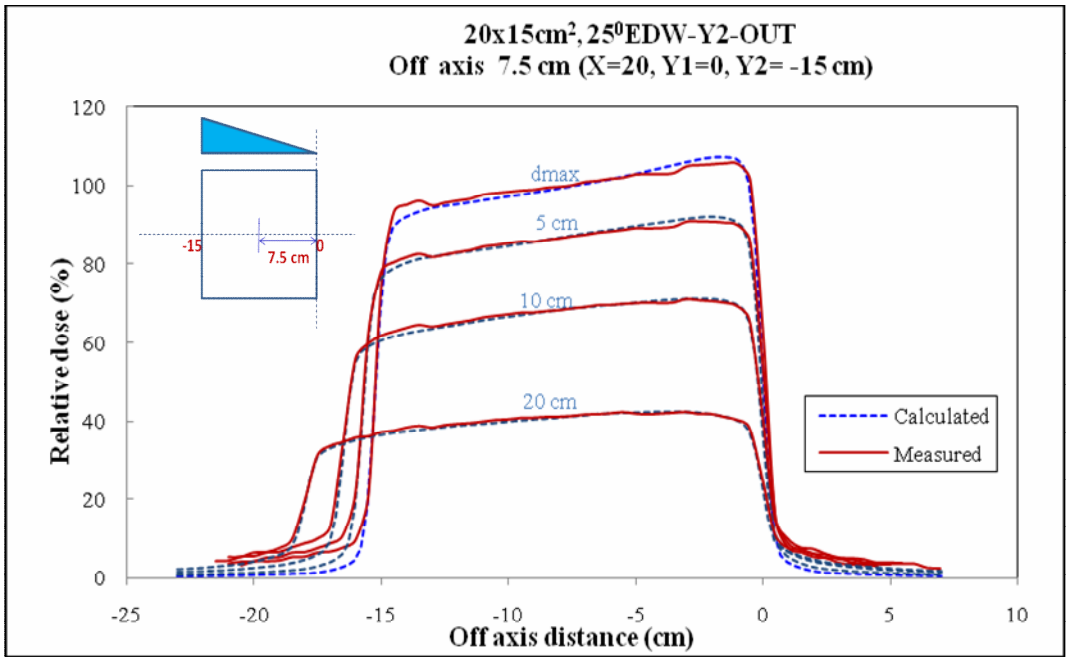
20x15cm², 25⁰EDW-Y2-OUT
Off axis 7.5 cm (X=20, Y1=0, Y2= -15 cm)
Relative dose (%)
Off axis distance (cm)
dmax
5 cm
10 cm
20 cm
Calculated
Measured
-15
0
7.5 cm

(b)

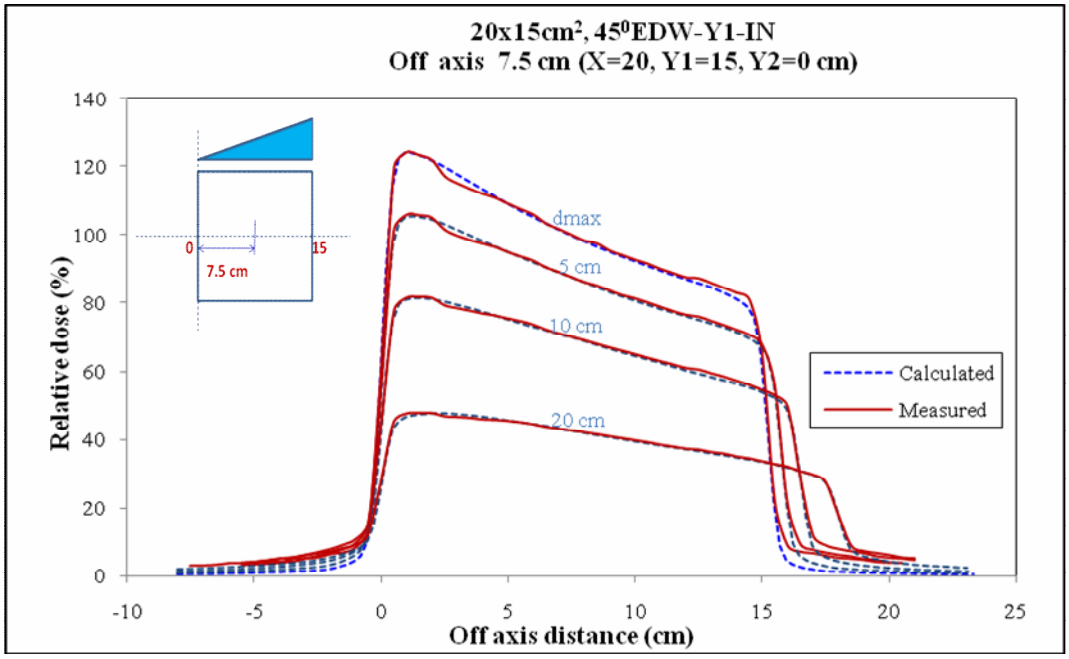

(c)

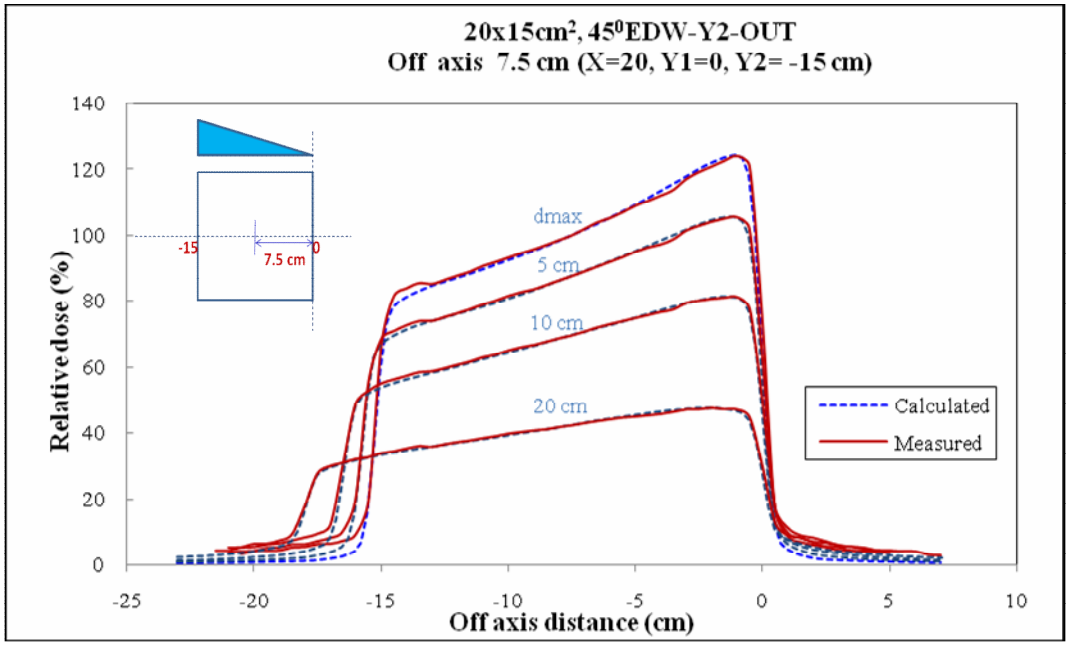

(d)

Figure 56. Calculated (dash lines) and measured (solid lines) dose profiles for 6 MV photons at asymmetric field size of 20 x 15 cm^2, off central-axis distance 7.5 cm and depths of d_{max} (=1.6 cm), 5, 10 and 20 cm for (a) 25°EDW-Y1-IN (b) 25°EDW-Y2-OUT (c) 45°EDW-Y1-IN and (d) 45°EDW-Y2-OUT.

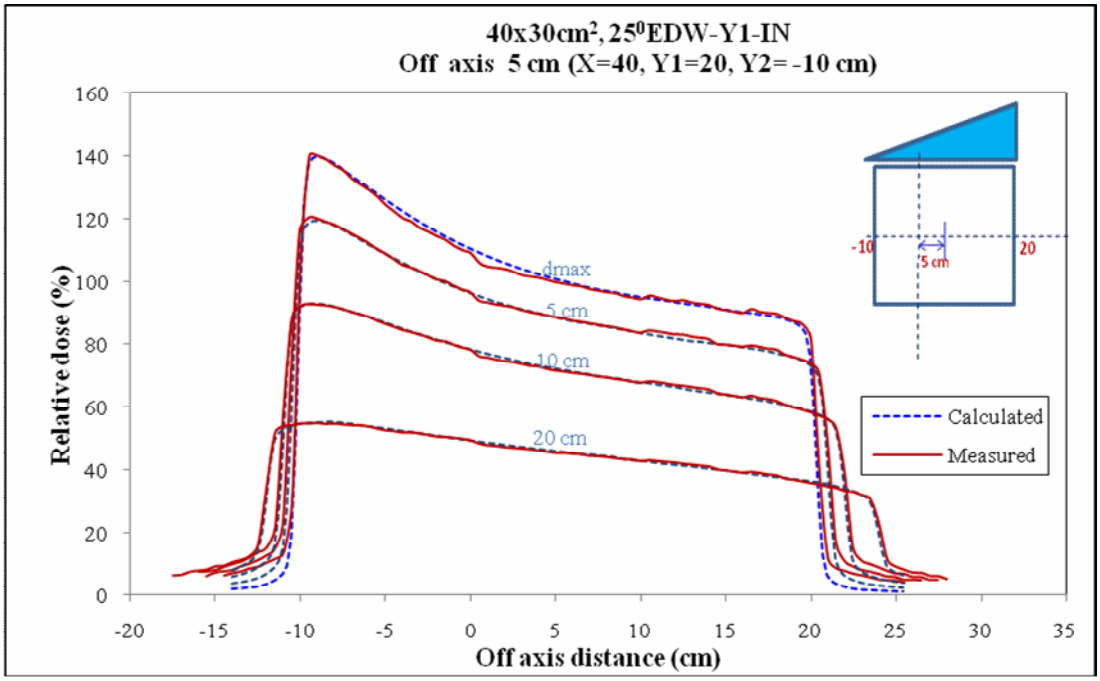
40x30cm², 25⁰EDW-Y1-IN
Off axis 5 cm (X=40, Y1=20, Y2= -10 cm)
Relative dose (%)
Off axis distance (cm)
dmax
5 cm
10 cm
20 cm
-10
20
5 cm
Calculated
Measured

(a)

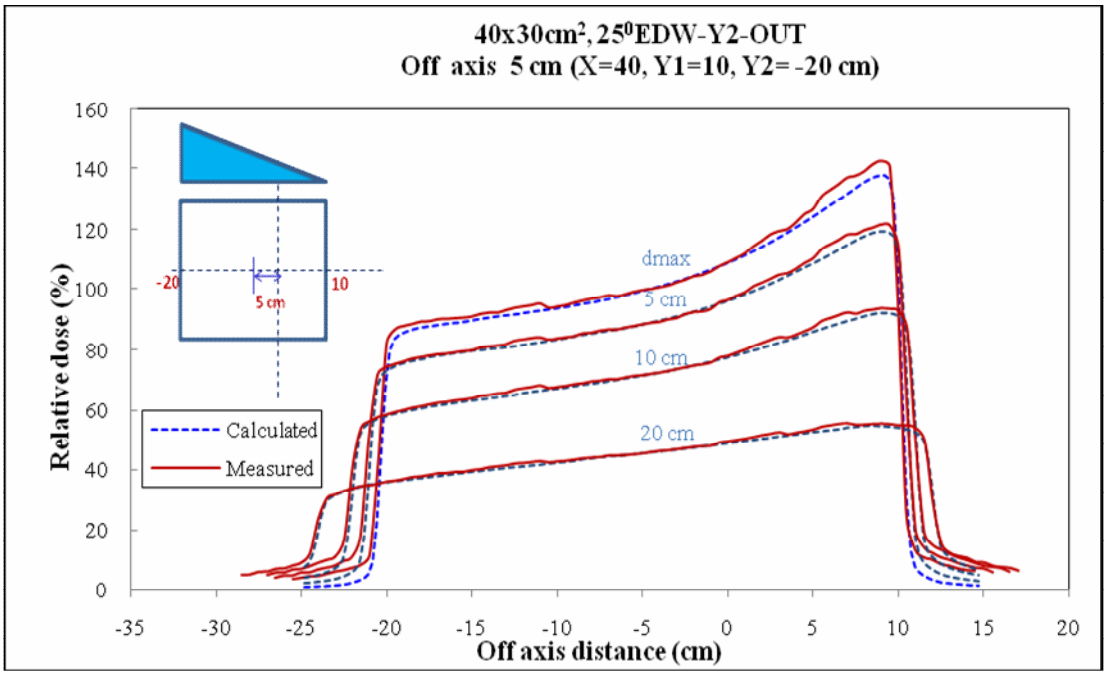
40x30cm², 25⁰EDW-Y2-OUT
Off axis 5 cm (X=40, Y1=10, Y2= -20 cm)
Relative dose (%)
Off axis distance (cm)
dmax
5 cm
10 cm
20 cm
-20
10
5 cm
Calculated
Measured

(b)

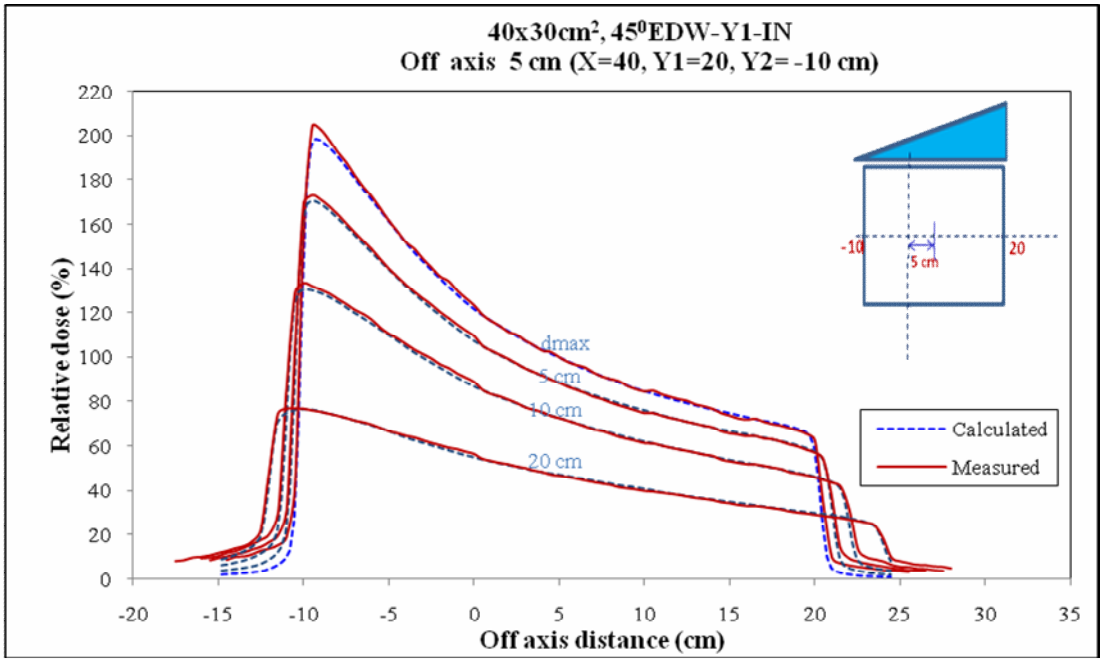

(c)

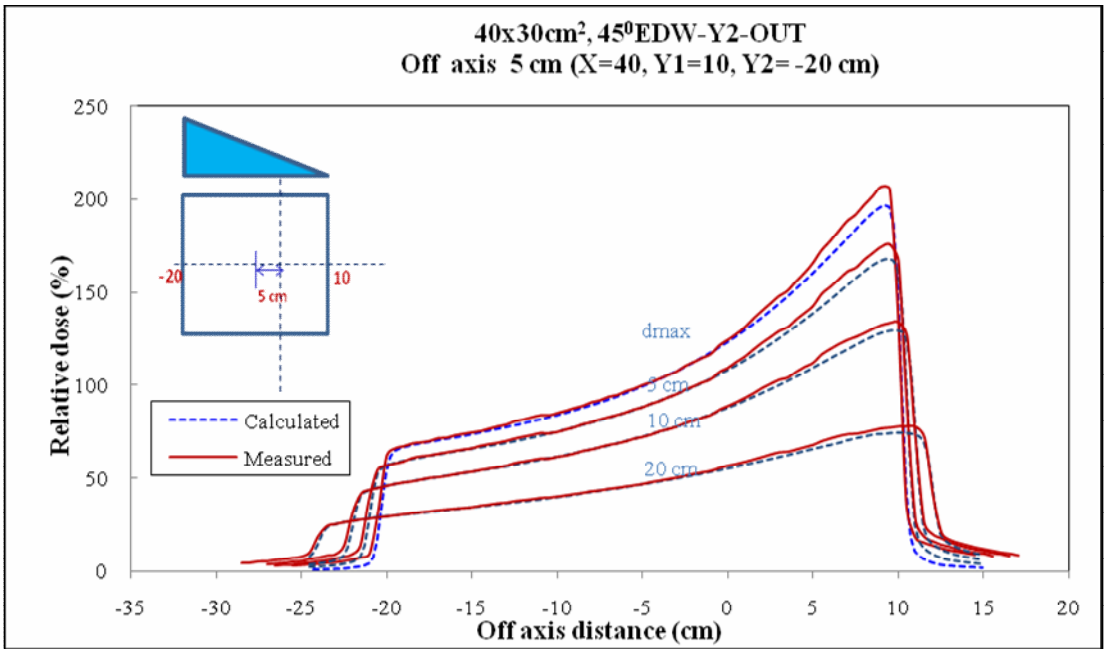

(d)

Figure 57. Calculated (dash lines) and measured (solid lines) dose profiles for 6 MV photons at asymmetric field size of 40 x 30 cm^2, off central-axis distance 5 cm and depths of d_{max} (=1.6 cm), 5, 10 and 20 cm for (a) 25°EDW-Y1-IN (b) 25°EDW-Y2-OUT (c) 45°EDW-Y1-IN and (d) 45°EDW-Y2-OUT.

Table 20. The deviations for data points in the penumbra region (δ_2), data points within the high dose-low dose gradient region (δ_3) and the radiological width (RW_{50}) between TPS calculation and measurement for 25^0 and 45^0 EDW both wedge directions Y1-IN and Y2-OUT, with 6 MV photon beam for asymmetric field sizes of (a) 20 x 5 cm^2, (b) 20 x 10 cm^2, (c) 20 x 15 cm^2 and (d) 40 x 30 cm^2 with the corresponding off-axis distances of 2.5, 5 and 7.5 cm, respectively.

(a) 20 x 5 cm^2 ; Off axis distance = 2.5 cm

Wedge direction	EDW angle	Depth (cm)	Deviation		
			δ_2 (mm)	δ_3 (%)	RW_{50} (mm)
Y1-IN	25^0	1.6	1.0	0.66	0.1
		5.0	1.2	1.11	0.0
		10.0	1.3	0.96	0.6
		20.0	1.2	2.19	0.7
	45^0	1.6	1.0	1.45	0.4
		5.0	1.2	1.26	0.6
		10.0	1.4	1.37	0.5
		20.0	1.1	1.92	0.6
Y2-OUT	25^0	1.6	1.1	1.22	1.9
		5.0	1.5	0.69	1.3
		10.0	1.3	0.29	1.4
		20.0	1.1	1.43	0.7
	45^0	1.6	1.1	1.54	0.4
		5.0	1.5	0.75	1.3
		10.0	1.2	0.41	1.5
		20.0	0.9	1.22	1.0

(b) 20 x 10 cm^2 ; Off axis distance = 5 cm

Wedge direction	EDW angle	Depth (cm)	Deviation		
			δ_2 (mm)	δ_3 (%)	RW_{50} (mm)
Y1-IN	25^0	1.6	0.9	-0.43	0.7
		5.0	1.0	0.14	0.6
		10.0	1.3	0.32	0.7
		20.0	1.0	1.58	1.0
	45^0	1.6	0.9	-1.33	1.0
		5.0	1.1	0.40	0.6
		10.0	1.3	-0.21	0.7
		20.0	1.1	0.18	0.9
Y2-OUT	25^0	1.6	0.5	-1.38	1.0
		5.0	1.0	-1.45	0.8
		10.0	1.0	-1.55	0.7
		20.0	1.0	-0.84	0.8
	45^0	1.6	0.4	-2.54	1.0
		5.0	0.9	-1.52	1.4
		10.0	0.9	-1.72	1.0
		20.0	1.0	-1.14	1.0

(c) 20 x 15 cm^2 ; Off axis distance = 7.5 cm

Wedge direction	EDW angle	Depth (cm)	Deviation		
			δ_2 (mm)	δ_3 (%)	RW_{50} (mm)
Y1-IN	25^0	1.6	0.8	0.70	0.5
		5.0	1.0	-0.22	0.7
		10.0	1.1	0.49	0.3
		20.0	1.1	0.35	0.9
	45^0	1.6	0.8	-1.27	0.8
		5.0	1.0	-0.87	0.9
		10.0	1.3	-0.81	0.5
		20.0	1.0	-1.91	0.5
Y2-OUT	25^0	1.6	1.4	1.68	1.3
		5.0	1.5	-1.38	1.3
		10.0	1.6	-1.03	1.6
		20.0	1.3	-1.10	1.2
	45^0	1.6	1.2	-1.32	1.6
		5.0	1.3	-1.12	1.3
		10.0	1.4	0.89	1.4
		20.0	1.1	-1.14	1.1

(d) 40 x 30 cm^2 ; Off axis distance = 5 cm

Wedge direction	EDW angle	Depth (cm)	Deviation		
			δ_2 (mm)	δ_3 (%)	RW_{50} (mm)
Y1-IN	25^0	1.6	1.9	2.17	1.8
		5.0	1.8	1.92	2.5
		10.0	1.9	2.20	***2.9***
		20.0	2.9	2.57	2.5
	45^0	1.6	2.3	1.20	1.6
		5.0	2.3	1.50	1.7
		10.0	2.8	1.90	1.8
		20.0	2.9	2.79	1.6
Y2-OUT	25^0	1.6	2.4	2.37	1.6
		5.0	1.9	2.10	2.1
		10.0	2.1	2.48	2.4
		20.0	1.9	2.94	2.0
	45^0	1.6	1.7	2.36	1.1
		5.0	1.8	2.99	1.2
		10.0	2.0	3.00	1.6
		20.0	***3.2***	***3.53***	1.1

Table 21. The criteria acceptability for the comparison between measured and calculated beam profiles for 25^0 and 45^0 EDW both wedge directions Y1-IN and Y2-OUT, with 6 MV photon beam for symmetric field sizes of (a) 5 x 5 cm^2, (b) 10 x 10 cm^2, (c) 15 x 15 cm^2, (d) 20 x 20 cm^2, (e) 20 x 5 cm^2, (f) 20 x 10 cm^2 and (g) 20 x 15 cm^2.

(a) 5 x 5 cm^2

Wedge direction	EDW angle	Depth (cm)	Criteria acceptability		
			δ_2 (3 mm)	δ_3 (3%)	RW_{50} (2 mm)
Y1-IN	25^0	1.6	√	√	√
		5.0	√	√	√
		10.0	√	√	√
		20.0	√	√	√
	45^0	1.6	√	√	√
		5.0	√	√	√
		10.0	√	√	√
		20.0	√	√	√
Y2-OUT	25^0	1.6	√	√	√
		5.0	√	√	√
		10.0	√	√	√
		20.0	√	√	√
	45^0	1.6	√	√	√
		5.0	√	√	√
		10.0	√	√	√
		20.0	√	√	√
√ define as pass × define as not pass					

(b) 10 x 10 cm^2

Wedge direction	EDW angle	Depth (cm)	Criteria acceptability		
			δ_2 (3 mm)	δ_3 (3%)	RW_{50} (2 mm)
Y1-IN	25^0	1.6	√	√	√
		5.0	√	√	√
		10.0	√	√	√
		20.0	√	√	√
	45^0	1.6	√	√	√
		5.0	√	√	√
		10.0	√	√	√
		20.0	√	√	√
Y2-OUT	25^0	1.6	√	√	√
		5.0	√	√	√
		10.0	√	√	√
		20.0	√	√	√
	45^0	1.6	√	√	√
		5.0	√	√	√
		10.0	√	√	√
		20.0	√	√	√

√ define as pass

× define as not pass

(c) 15 x 15 cm^2

Wedge direction	EDW angle	Depth (cm)	Criteria acceptability		
			δ_2 (3 mm)	δ_3 (3%)	RW_{50} (2 mm)
Y1-IN	25^0	1.6	√	√	√
		5.0	√	√	√
		10.0	√	√	√
		20.0	√	√	√
	45^0	1.6	√	√	√
		5.0	√	√	√
		10.0	√	√	√
		20.0	√	√	√
Y2-OUT	25^0	1.6	√	√	√
		5.0	√	√	√
		10.0	√	√	√
		20.0	√	√	√
	45^0	1.6	√	√	√
		5.0	√	√	√
		10.0	√	√	√
		20.0	√	√	√

√ define as pass

× define as not pass

(d) 20 x 20 cm^2

Wedge direction	EDW angle	Depth (cm)	Criteria acceptability		
			δ_2 (3 mm)	δ_3 (3%)	RW_{50} (2 mm)
Y1-IN	25^0	1.6	√	√	√
		5.0	√	√	√
		10.0	√	√	√
		20.0	√	√	√
	45^0	1.6	√	√	√
		5.0	√	√	√
		10.0	√	√	√
		20.0	√	√	√
Y2-OUT	25^0	1.6	√	√	√
		5.0	√	√	√
		10.0	√	√	√
		20.0	√	√	√
	45^0	1.6	√	√	√
		5.0	√	√	√
		10.0	√	√	√
		20.0	√	√	√

√ define as pass

× define as not pass

(e) 20 x 5 cm^2

Wedge direction	EDW angle	Depth (cm)	Criteria acceptability		
			δ_2 (3 mm)	δ_3 (3%)	RW_{50} (2 mm)
Y1-IN	25^0	1.6	√	√	√
		5.0	√	√	√
		10.0	√	√	√
		20.0	√	√	√
	45^0	1.6	√	√	√
		5.0	√	√	√
		10.0	√	√	√
		20.0	√	√	√
Y2-OUT	25^0	1.6	√	√	√
		5.0	√	√	√
		10.0	√	√	√
		20.0	√	√	√
	45^0	1.6	√	√	√
		5.0	√	√	√
		10.0	√	√	√
		20.0	√	√	√

√ define as pass

× define as not pass

(f) 20 x 10 cm^2

Wedge direction	EDW angle	Depth (cm)	Criteria acceptability		
			δ_2 (3 mm)	δ_3 (3%)	RW_{50} (2 mm)
Y1-IN	25^0	1.6	√	√	√
		5.0	√	√	√
		10.0	√	√	√
		20.0	√	√	√
	45^0	1.6	√	√	√
		5.0	√	√	√
		10.0	√	√	√
		20.0	√	√	√
Y2-OUT	25^0	1.6	√	√	√
		5.0	√	√	√
		10.0	√	√	√
		20.0	√	√	√
	45^0	1.6	√	√	√
		5.0	√	√	√
		10.0	√	√	√
		20.0	√	√	√

√ define as pass

× define as not pass

(g) 20 x 15 cm^2

Wedge direction	EDW angle	Depth (cm)	Criteria acceptability		
			δ_2 (3 mm)	δ_3 (3%)	RW_{50} (2 mm)
Y1-IN	25^0	1.6	√	√	√
		5.0	√	√	√
		10.0	√	√	√
		20.0	√	√	√
	45^0	1.6	√	√	√
		5.0	√	√	√
		10.0	√	√	√
		20.0	√	√	√
Y2-OUT	25^0	1.6	√	√	√
		5.0	√	√	√
		10.0	√	√	√
		20.0	√	√	√
	45^0	1.6	√	√	√
		5.0	√	√	√
		10.0	√	√	√
		20.0	√	√	√

√ define as pass

× define as not pass

Table 22. The criteria acceptability for the comparison between measured and calculated beam profiles for 25^0 and 45^0 EDW both wedge directions Y1-IN and Y2-OUT, with 6 MV photon beam for asymmetric field sizes of (a) 20 x 5 cm^2, (b) 20 x 10 cm^2, (c) 20 x 15 cm^2 and (d) 40 x 30 cm^2

(a) 20 x 5 cm^2 ; Off axis distance = 2.5 cm

Wedge direction	EDW angle	Depth (cm)	Criteria acceptability		
			δ_2 (3 mm)	δ_3 (3%)	RW_{50} (2 mm)
Y1-IN	25^0	1.6	√	√	√
		5.0	√	√	√
		10.0	√	√	√
		20.0	√	√	√
	45^0	1.6	√	√	√
		5.0	√	√	√
		10.0	√	√	√
		20.0	√	√	√
Y2-OUT	25^0	1.6	√	√	√
		5.0	√	√	√
		10.0	√	√	√
		20.0	√	√	√
	45^0	1.6	√	√	√
		5.0	√	√	√
		10.0	√	√	√
		20.0	√	√	√
√ define as pass × define as not pass					

(b) 20 x 10 cm^2 ; Off axis distance = 5 cm

Wedge direction	EDW angle	Depth (cm)	Criteria acceptability		
			δ_2 (3 mm)	δ_3 (3%)	RW_{50} (2 mm)
Y1-IN	25^0	1.6	√	√	√
		5.0	√	√	√
		10.0	√	√	√
		20.0	√	√	√
	45^0	1.6	√	√	√
		5.0	√	√	√
		10.0	√	√	√
		20.0	√	√	√
Y2-OUT	25^0	1.6	√	√	√
		5.0	√	√	√
		10.0	√	√	√
		20.0	√	√	√
	45^0	1.6	√	√	√
		5.0	√	√	√
		10.0	√	√	√
		20.0	√	√	√
√ define as pass × define as not pass					

(c) 20 x 15 cm^2 ; Off axis distance = 7.5 cm

Wedge direction	EDW angle	Depth (cm)	Criteria acceptability		
			δ_2 (3 mm)	δ_3 (3%)	RW_{50} (2 mm)
Y1-IN	25^0	1.6	√	√	√
		5.0	√	√	√
		10.0	√	√	√
		20.0	√	√	√
	45^0	1.6	√	√	√
		5.0	√	√	√
		10.0	√	√	√
		20.0	√	√	√
Y2-OUT	25^0	1.6	√	√	√
		5.0	√	√	√
		10.0	√	√	√
		20.0	√	√	√
	45^0	1.6	√	√	√
		5.0	√	√	√
		10.0	√	√	√
		20.0	√	√	√

√ define as pass

× define as not pass

(d) 40 x 30 cm^2 ; Off axis distance = 5 cm

Wedge direction	EDW angle	Depth (cm)	Criteria acceptability		
			δ_2 (3 mm)	δ_3 (3%)	RW_{50} (2 mm)
Y1-IN	25^0	1.6	√	√	√
		5.0	√	√	×
		10.0	√	√	×
		20.0	√	√	×
	45^0	1.6	√	√	√
		5.0	√	√	√
		10.0	√	√	√
		20.0	√	√	√
Y2-OUT	25^0	1.6	√	√	√
		5.0	√	√	×
		10.0	√	√	×
		20.0	√	√	√
	45^0	1.6	√	√	√
		5.0	√	√	√
		10.0	√	√	√
		20.0	×	×	√

√ define as pass

× define as not pass

Table 23. Percentage of the cases which pass or not pass the criteria acceptability of Dyk JV et al (37) and Venselaar J et al (38) for beam profile of all EDW fields

Criteria acceptability	Percentage (%)	
	Pass	Not pass
δ_2	99.43	0.57
δ_3	99.43	0.57
RW_{50}	99.97	0.03

Figure 58 showed the high dose region (thin edge) on the EDW profile which the underestimation of the calculated profiles by pencil beam (PBC) algorithm at this region both for the symmetric and asymmetric EDW profiles were found. All the deviations between measured and calculated EDW profile at this region were summarized in Table 24 to 25.

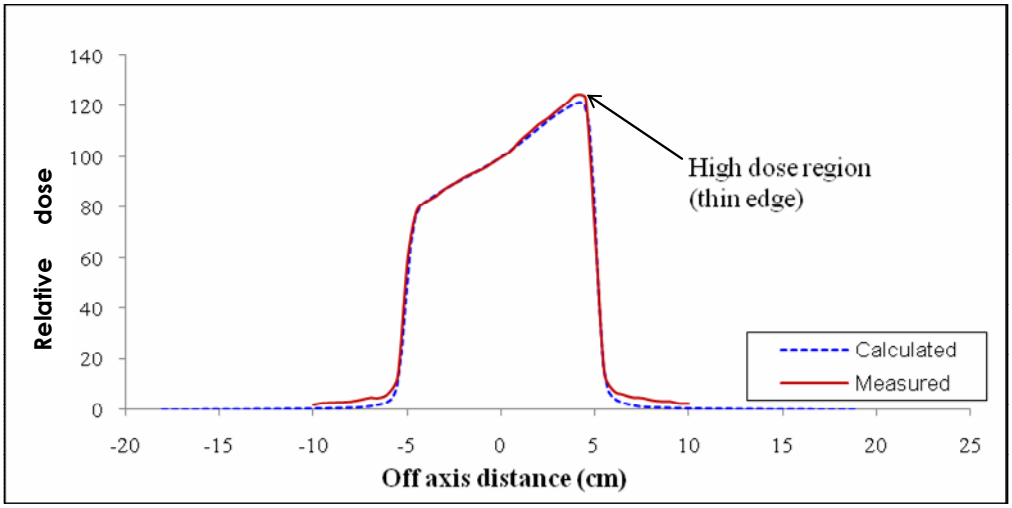

Figure 58. The high dose region (thin edge) on the EDW profile

Table 24. The deviations for data points in the high dose region (thin edge) between TPS calculation and measurement for 25^0 and 45^0 EDW both wedge directions Y1-IN and Y2-OUT, with 6 MV photon beam for symmetric field sizes of (a) 5 x 5 cm^2, (b) 10 x 10 cm^2, (c) 15 x 15 cm^2, (d) 20 x 20 cm^2, (e) 20 x 5 cm^2, (f) 20 x 10 cm^2 and (g) 20 x 15 cm^2.

(a) 5 x 5 cm^2

Wedge direction	EDW angle	Depth (cm)	Deviation (%)
Y1-IN	25^0	1.6	2.78
		5.0	1.95
		10.0	1.11
		20.0	2.46
	45^0	1.6	2.97
		5.0	2.11
		10.0	1.30
		20.0	2.52
Y2-OUT	25^0	1.6	3.77
		5.0	2.01
		10.0	1.98
		20.0	3.90
	45^0	1.6	4.10
		5.0	2.40
		10.0	2.19
		20.0	4.40

(b) 10 x 10 cm^2

Wedge direction	EDW angle	Depth (cm)	Deviation (%)
Y1-IN	25^0	1.6	1.91
		5.0	0.80
		10.0	-0.27
		20.0	-0.22
	45^0	1.6	1.54
		5.0	-1.93
		10.0	-0.41
		20.0	0.43
Y2-OUT	25^0	1.6	2.46
		5.0	2.27
		10.0	1.05
		20.0	1.15
	45^0	1.6	3.50
		5.0	3.20
		10.0	1.85
		20.0	0.96

(c) 15 x 15 cm^2

Wedge direction	EDW angle	Depth (cm)	Deviation (%)
Y1-IN	25^0	1.6	-0.23
		5.0	-1.01
		10.0	-1.54
		20.0	-3.03
	45^0	1.6	0.70
		5.0	-0.50
		10.0	-0.51
		20.0	-2.80
Y2-OUT	25^0	1.6	2.99
		5.0	2.43
		10.0	1.61
		20.0	0.72
	45^0	1.6	4.13
		5.0	3.63
		10.0	3.00
		20.0	2.06

(d) 20 x 20 cm^2

Wedge direction	EDW angle	Depth (cm)	Deviation (%)
Y1-IN	25^0	1.6	2.94
		5.0	-1.97
		10.0	-2.26
		20.0	-3.22
	45^0	1.6	3.43
		5.0	1.76
		10.0	-3.17
		20.0	-4.97
Y2-OUT	25^0	1.6	3.66
		5.0	2.06
		10.0	1.91
		20.0	-1.83
	45^0	1.6	5.49
		5.0	4.76
		10.0	3.40
		20.0	2.71

(e) 20 x 5 cm^2

Wedge direction	EDW angle	Depth (cm)	Deviation (%)
Y1-IN	25^0	1.6	2.61
		5.0	4.90
		10.0	3.44
		20.0	3.43
	45^0	1.6	3.03
		5.0	4.85
		10.0	4.33
		20.0	2.06
Y2-OUT	25^0	1.6	3.49
		5.0	2.01
		10.0	2.03
		20.0	2.50
	45^0	1.6	4.02
		5.0	2.46
		10.0	2.00
		20.0	4.11

(f) 20 x 10 cm^2

Wedge direction	EDW angle	Depth (cm)	Deviation (%)
Y1-IN	25^0	1.6	1.84
		5.0	0.72
		10.0	0.43
		20.0	-1.99
	45^0	1.6	1.30
		5.0	1.44
		10.0	-0.35
		20.0	-1.79
Y2-OUT	25^0	1.6	2.78
		5.0	2.27
		10.0	0.74
		20.0	0.31
	45^0	1.6	3.73
		5.0	2.95
		10.0	1.70
		20.0	1.53

(g) 20 x 15 cm^2

Wedge direction	EDW angle	Depth (cm)	Deviation (%)
Y1-IN	25^0	1.6	-1.83
		5.0	-1.67
		10.0	-2.05
		20.0	-3.78
	45^0	1.6	-2.37
		5.0	-1.91
		10.0	-2.74
		20.0	-3.45
Y2-OUT	25^0	1.6	2.88
		5.0	2.27
		10.0	2.18
		20.0	-2.14
	45^0	1.6	4.48
		5.0	3.74
		10.0	3.00
		20.0	-2.01

Table 25. The deviations for data points in the high dose region (thin edge) between TPS calculation and measurement for 25^0 and 45^0 EDW both wedge directions Y1-IN and Y2-OUT, with 6 MV photon beam for asymmetric field sizes of (a) 20 x 5 cm^2, (b) 20 x 10 cm^2, (c) 20 x 15 cm^2 and (d) 40 x 30 cm^2 with the corresponding off-axis distances of 2.5, 5 and 7.5 cm, respectively.

(a) 20 x 5 cm^2 ; Off axis distance = 2.5 cm

Wedge direction	EDW angle	Depth (cm)	Deviation (%)
Y1-IN	25^0	1.6	5.21
		5.0	4.96
		10.0	4.50
		20.0	5.16
	45^0	1.6	5.30
		5.0	5.38
		10.0	5.03
		20.0	5.23
Y2-OUT	25^0	1.6	3.29
		5.0	2.38
		10.0	1.26
		20.0	2.78
	45^0	1.6	4.16
		5.0	2.96
		10.0	4.15
		20.0	2.19

(b) 20 x 10 cm^2 ; Off axis distance = 5 cm

Wedge direction	EDW angle	Depth (cm)	Deviation (%)
Y1-IN	25^0	1.6	1.78
		5.0	2.17
		10.0	-0.36
		20.0	2.91
	45^0	1.6	-1.48
		5.0	2.81
		10.0	-0.84
		20.0	3.78
Y2-OUT	25^0	1.6	3.91
		5.0	4.12
		10.0	3.55
		20.0	4.52
	45^0	1.6	3.84
		5.0	4.92
		10.0	1.25
		20.0	5.09

(c) 20 x 15 cm^2 ; Off axis distance = 7.5 cm

Wedge direction	EDW angle	Depth (cm)	Deviation (%)
Y1-IN	25^0	1.6	2.83
		5.0	4.49
		10.0	3.69
		20.0	6.05
	45^0	1.6	3.56
		5.0	-1.83
		10.0	-1.43
		20.0	-2.61
Y2-OUT	25^0	1.6	3.90
		5.0	2.44
		10.0	2.40
		20.0	2.45
	45^0	1.6	3.89
		5.0	2.40
		10.0	2.02
		20.0	1.54

(d) 40 x 30 cm^2 ; Off axis distance = 5 cm

Wedge direction	EDW angle	Depth (cm)	Deviation (%)
Y1-IN	25^0	1.6	2.95
		5.0	3.35
		10.0	2.35
		20.0	2.60
	45^0	1.6	4.07
		5.0	4.20
		10.0	3.60
		20.0	5.68
Y2-OUT	25^0	1.6	4.11
		5.0	2.15
		10.0	3.00
		20.0	2.86
	45^0	1.6	5.56
		5.0	4.47
		10.0	4.99
		20.0	5.19

6.1.2.4 Effective wedge factor

Tables 26 (a-b) show the comparison between the effective wedge factors at collimator angle 0^0 and 90^0 of 25^0 EDW and 45^0 EDW for symmetric field sizes of 10 x 10 cm^2 and 20 x 10 cm^2, 6 MV photon, at various depth of 5, 10 and 20 cm. The excellent agreement between the effective wedge factors at both collimator angles was found and the difference were in the range of $\pm$ 0.00-0.78%.

Table 26. Comparison between the effective wedge factors at collimator angle 0^0 and 90^0 for (a) 25^0 EDW and (b) 45^0 EDW with symmetric field sizes of 10 x 10 cm^2 and 20 x 10 cm^2 for 6 MV photon beam.

(a) 25^0 EDW

Field size (cm^2)	Depth (cm)	Effective wedge factor		%Difference
		Collimator angle 0^0	Collimator angle 90^0	
10x10	5	0.877	0.879	-0.23
	10	0.880	0.879	0.11
	20	0.880	0.880	0.00
20x10	5	0.878	0.878	0.00
	10	0.878	0.878	0.00
	20	0.881	0.881	0.00

(b) 45^0 EDW

Field size (cm^2)	Depth (cm)	Effective wedge factor		%Difference
		Collimator angle 0^0	Collimator angle 90^0	
10x10	5	0.769	0.769	0.00
	10	0.774	0.772	0.26
	20	0.769	0.769	0.00
20x10	5	0.769	0.770	-0.13
	10	0.773	0.770	0.39
	20	0.771	0.777	-0.78

Tables 27 to 28 (a-b) show the comparison between measured and calculated effective wedge factors at collimator angle 0^0 of 25^0 EDW and 45^0 EDW for symmetric and asymmetric field sizes, 6 MV photon, at various depth of 5, 10 and 20 cm. The deviations between measured and calculated effective wedge factors are typically less than $\pm$0.5% in the symmetric fields and $\pm$1.5% for the asymmetric fields. The largest difference of 2.67% was found at 45^0 EDW, Y1-IN direction, asymmetric field size of 40 x 30 cm^2 (X = 40, Y1 = 20, Y2 = 10 cm) at depth of 20 cm. Effective wedge factors of the 25° and 45^0 EDW angle as a function on field width were shown in Figure 59 to 61. It was clearly shown that the EDW effective wedge factors decreased while the field width and wedge angle increased. Moreover, this relationship was found to be smoother in the symmetric field than in asymmetric field. Figure 62 to 64 also presented the effective wedge factors for 25^0 EDW and 45^0 EDW in the symmetric and asymmetric field sizes as a function of depth. The results suggest that the effective wedge factor is relatively insensitive to measurement depth.

Table 27. Measured and calculated effective wedge factors at collimator angle 0^0 for (a) 25^0 EDW and (b) 45^0 EDW with symmetric field sizes and 6 MV photon beam.

(a) 25^0 EDW

Field size (cm^2)	Depth (cm)	Effective wedge factor		%Difference
		Measured	Calculated	
5x5	5	0.948	0.947	0.11
	10	0.952	0.949	0.32
	20	0.951	0.953	-0.21
10x10	5	0.877	0.878	-0.11
	10	0.880	0.878	0.23
	20	0.880	0.879	0.11
15x15	5	0.804	0.804	0.00
	10	0.805	0.807	-0.25
	20	0.809	0.808	0.12
20x20	5	0.728	0.730	-0.27
	10	0.731	0.732	-0.14
	20	0.731	0.731	0.00
20x5	5	0.948	0.946	0.21
	10	0.951	0.949	0.21
	20	0.949	0.949	0.00
20x10	5	0.878	0.877	0.11
	10	0.877	0.878	-0.11
	20	0.881	0.881	0.00
20x15	5	0.806	0.806	0.00
	10	0.805	0.807	-0.25
	20	0.807	0.806	0.12

(b) 45^0 EDW

Field size (cm^2)	Depth (cm)	Effective wedge factor		%Difference
		Measured	Calculated	
5x5	5	0.894	0.894	0.00
	10	0.897	0.895	0.22
	20	0.898	0.896	0.22
10x10	5	0.769	0.770	-0.13
	10	0.774	0.769	0.65
	20	0.769	0.772	-0.39
15x15	5	0.657	0.659	-0.30
	10	0.660	0.660	0.00
	20	0.664	0.663	0.15
20x20	5	0.558	0.560	-0.36
	10	0.558	0.563	-0.90
	20	0.562	0.563	-0.18
20x5	5	0.896	0.892	0.45
	10	0.898	0.894	0.45
	20	0.895	0.892	0.34
20x10	5	0.769	0.770	-0.13
	10	0.773	0.770	0.39
	20	0.771	0.772	-0.13
20x15	5	0.657	0.660	-0.46
	10	0.661	0.662	-0.15
	20	0.662	0.662	0.00

Table 28. Measured and calculated effective wedge factors at collimator angle 0^0 for (a) 25^0 EDW and (b) 45^0 EDW with asymmetric field sizes and 6 MV photon beam.

(a) 25^0 EDW

EDW orientation	Field size (cm^2)	Depth (cm)	Off axis (cm)	Effective wedge factor		%Difference
				Measured	Calculated	
Y1-IN	20x5	5	2.5	0.968	0.963	0.52
		10	2.5	0.967	0.961	0.62
		20	2.5	0.968	0.966	0.21
	20x10	5	5	0.938	0.932	0.64
		10	5	0.933	0.927	0.64
		20	5	0.926	0.936	-1.08
	20x15	5	2.5	0.838	0.839	-0.12
		10	2.5	0.835	0.838	-0.36
		20	2.5	0.840	0.838	0.24
	40x30	5	5	0.676	0.673	0.53
		10	5	0.671	0.672	-0.15
		20	5	0.668	0.677	-1.35
Y2-OUT	20x5	5	2.5	0.961	0.946	1.56
		10	2.5	0.960	0.945	1.56
		20	2.5	0.955	0.949	0.63
	20x10	5	5	0.873	0.864	1.03
		10	5	0.872	0.860	1.38
		20	5	0.864	0.866	-0.23
	20x15	5	2.5	0.792	0.788	0.51
		10	2.5	0.794	0.788	0.76
		20	2.5	0.791	0.787	0.51
	40x30	5	5	0.669	0.673	-0.60
		10	5	0.668	0.672	-0.60
		20	5	0.665	0.677	-1.80

(b) 45^0 EDW

EDW orientation	Field size (cm^2)	Depth (cm)	Off axis (cm)	Effective wedge factor		%Difference
				Measured	Calculated	
Y1-IN	20x5	5	2.5	0.910	0.907	0.33
		10	2.5	0.908	0.907	0.11
		20	2.5	0.910	0.909	0.11
	20x10	5	5	0.823	0.823	0.00
		10	5	0.822	0.820	0.27
		20	5	0.818	0.827	-1.10
	20x15	5	2.5	0.682	0.687	-0.73
		10	2.5	0.684	0.687	-0.44
		20	2.5	0.684	0.685	-0.15
	40x30	5	5	0.450	0.454	-0.89
		10	5	0.449	0.454	-1.11
		20	5	0.449	0.461	***-2.67***
Y2-OUT	20x5	5	2.5	0.910	0.892	1.98
		10	2.5	0.908	0.891	1.87
		20	2.5	0.904	0.892	1.33
	20x10	5	5	0.773	0.764	1.16
		10	5	0.774	0.759	1.94
		20	5	0.767	0.767	0.00
	20x15	5	2.5	0.654	0.649	0.76
		10	2.5	0.655	0.651	0.61
		20	2.5	0.658	0.648	1.52
	40x30	5	5	0.448	0.454	-1.34
		10	5	0.449	0.454	-1.11
		20	5	0.451	0.461	-2.22

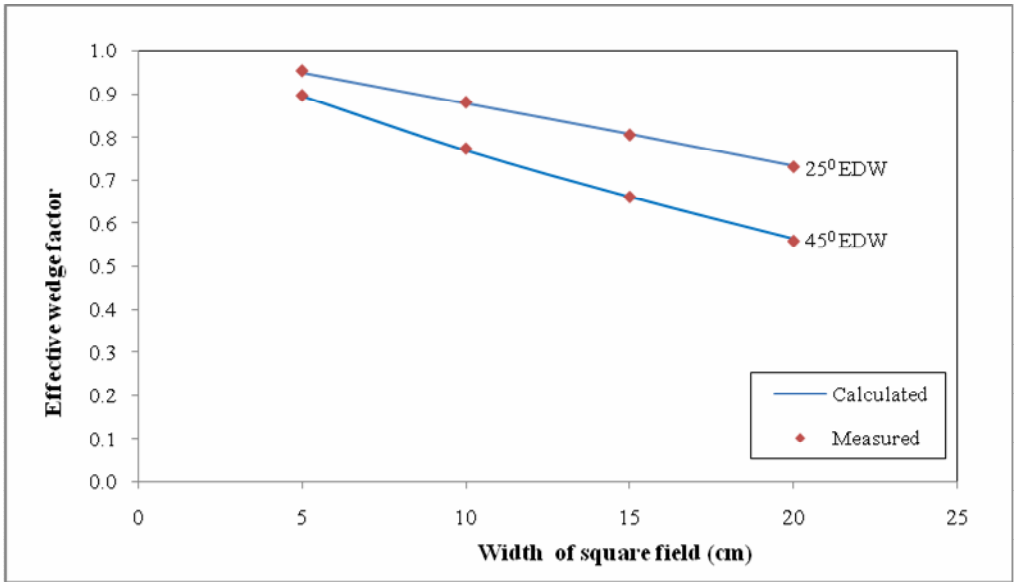

Figure 59. Calculated (solid lines) and measured (symbols) effective wedge factors versus square field size for 25^0 and 45^0 EDW, with 6 MV photon at depth of 10 cm.

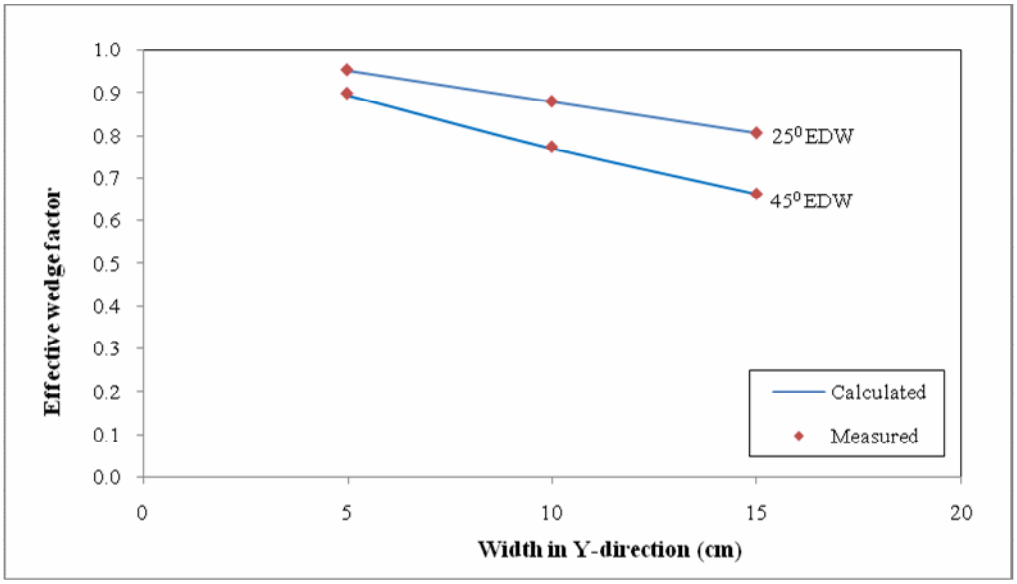

Figure 60. Calculated (solid lines) and measured (symbols) effective wedge factors versus width in Y-direction of rectangular field sizes (X= 20 cm) for 25^0 and 45^0 EDW, with 6 MV photon at depth of 10 cm.

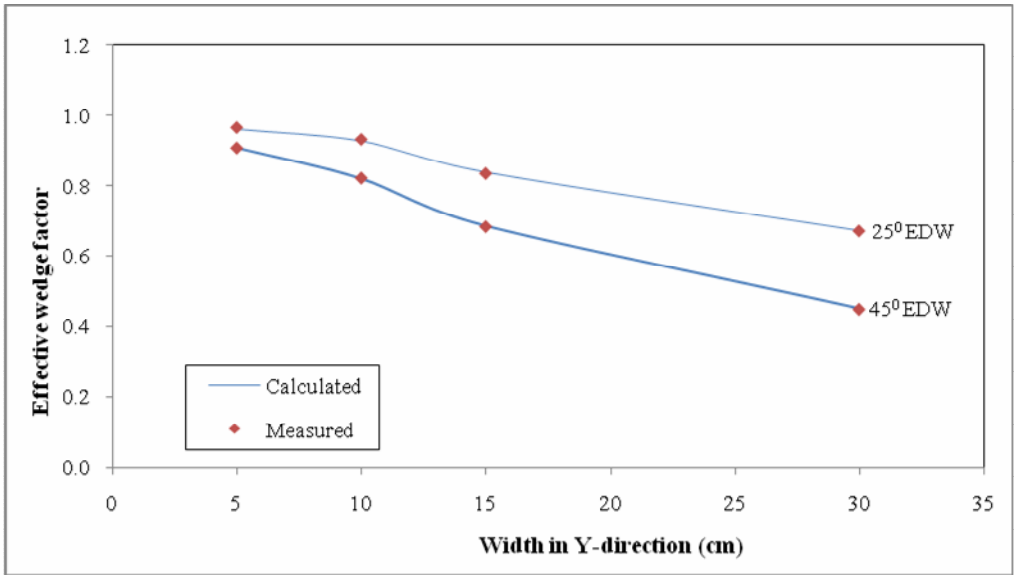

(a)

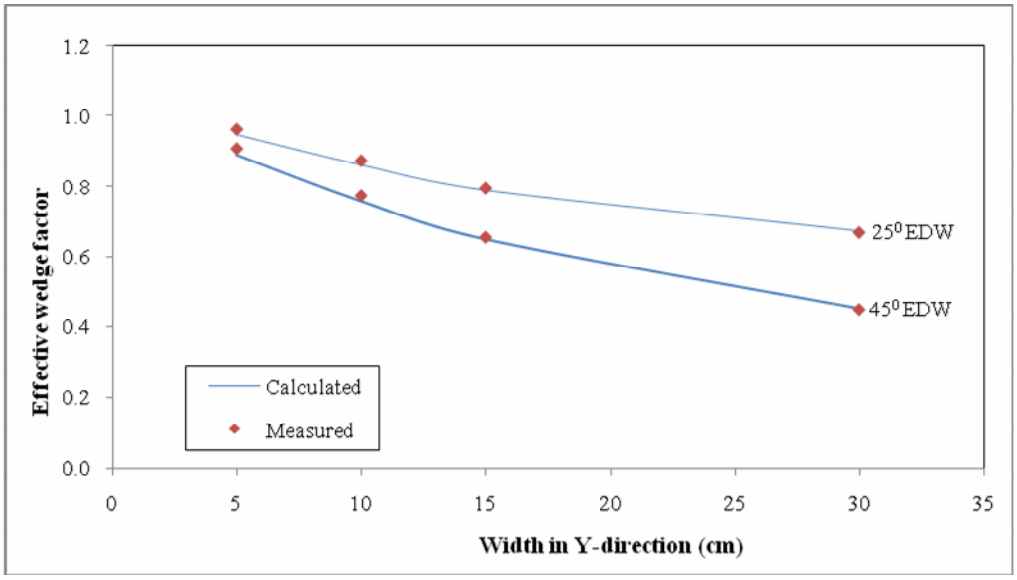

(b)

Figure 61. Calculated (solid lines) and measured (symbols) effective wedge factors versus width in Y-direction of asymmetric field sizes of 20 x 5 cm^2, 20 x 10 cm^2, 20 x 15 cm^2 and 40 x 30 cm^2, with 6 MV photon at depth of 10 cm for 25^0 and 45^0 EDW both wedge orientation of (a) Y1-IN and (b) Y2-OUT.

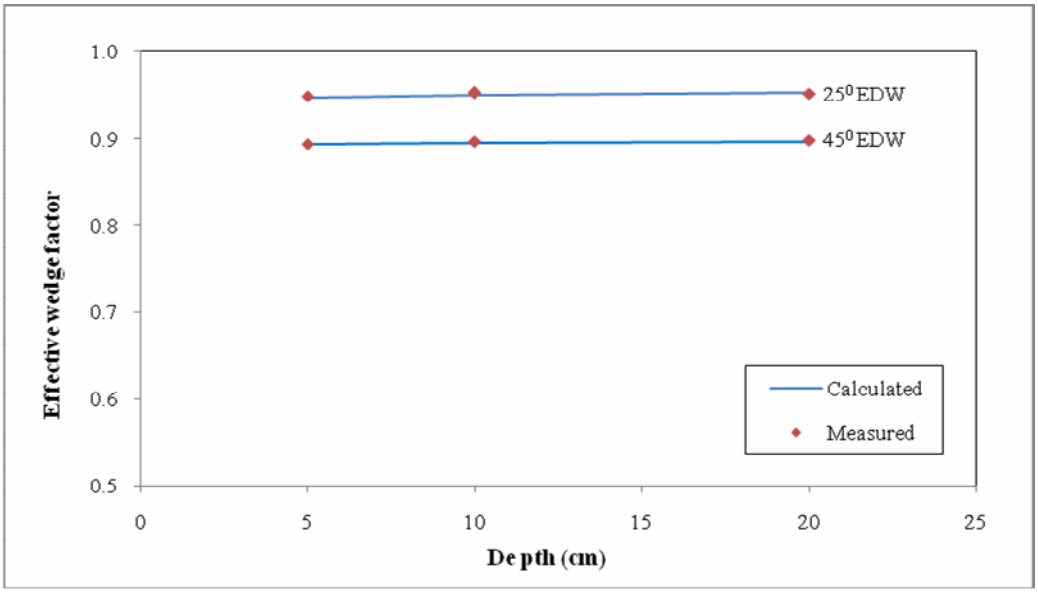
1.0
0.9
0.8
0.7
0.6
0.5
Effective wedge factor
0
5
10
15
20
25
De pth (cm)
25⁰EDW
45⁰EDW
Calculated
Measured

(a)

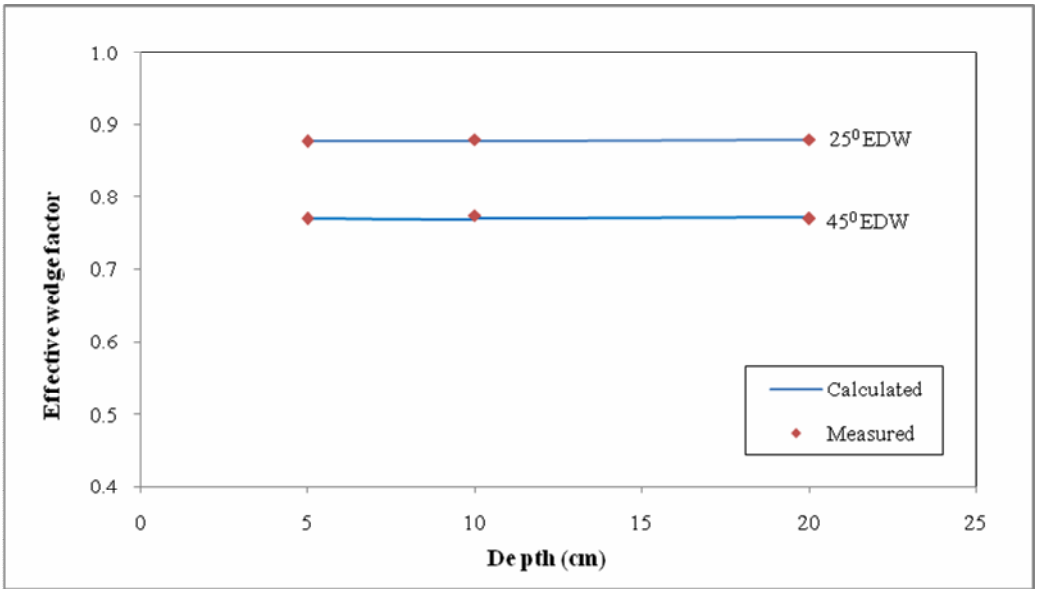
1.0
0.9
0.8
0.7
0.6
0.5
0.4
Effective wedge factor
0
5
10
15
20
25
De pth (cm)
25⁰EDW
45⁰EDW
Calculated
Measured

(b)

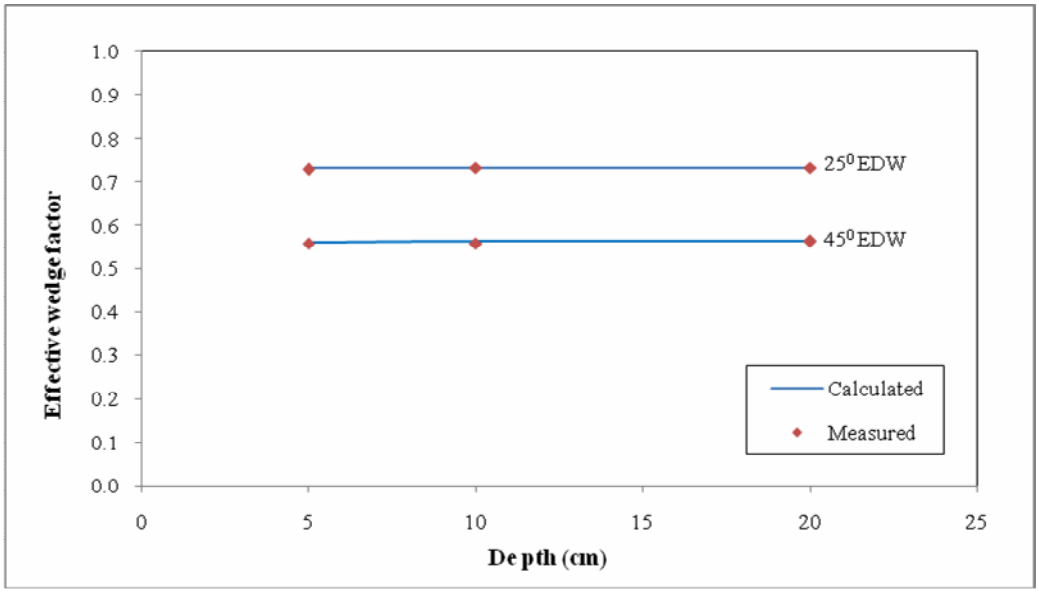

(c)

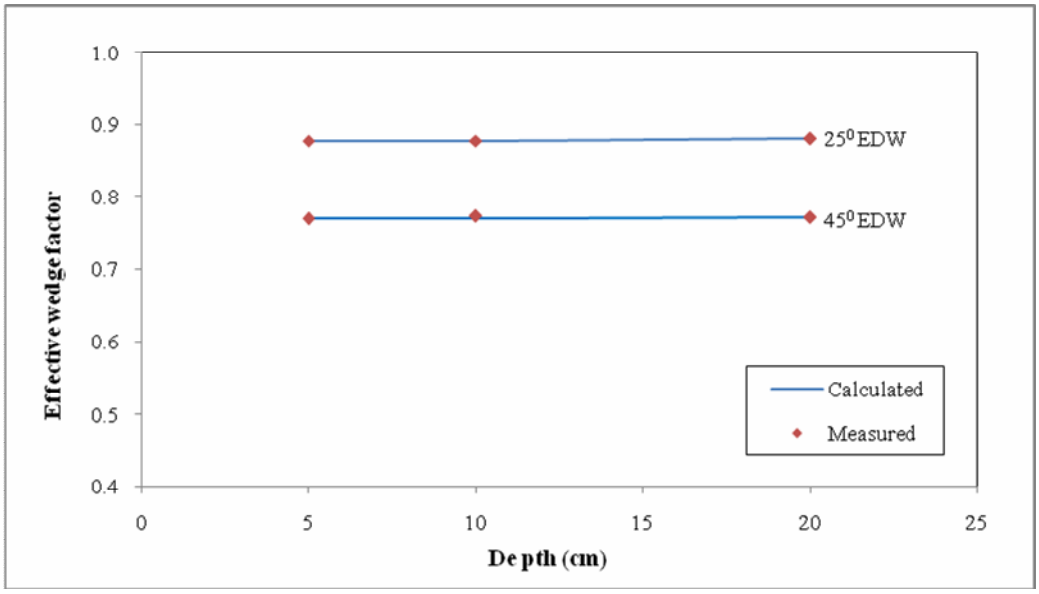

(d)

Figure 62. Calculated (solid lines) and measured (symbols) effective wedge factors versus depths for 25^0 and 45^0 EDW, with 6 MV photon for symmetric field sizes of (a) 5 x 5 cm^2, (b) 10 x 10 cm^2, (c) 20 x 20 cm^2 and (d) 20 x 10 cm^2.

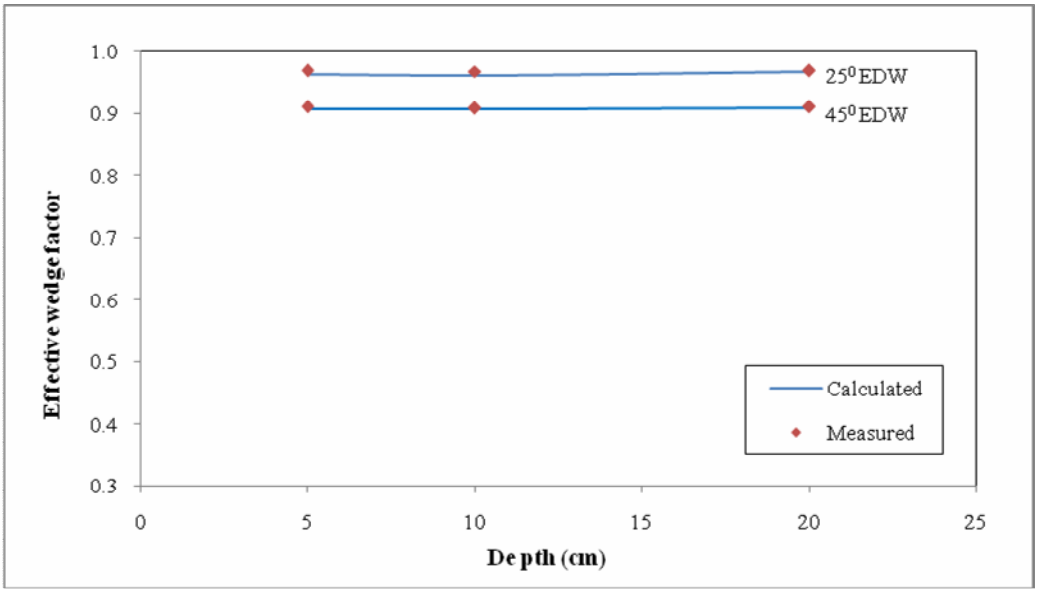
1.0
0.9
0.8
0.7
0.6
0.5
0.4
0.3
Effective wedge factor
0
5
10
15
20
25
De pth (cm)
25⁰EDW
45⁰EDW
Calculated
Measured

(a)

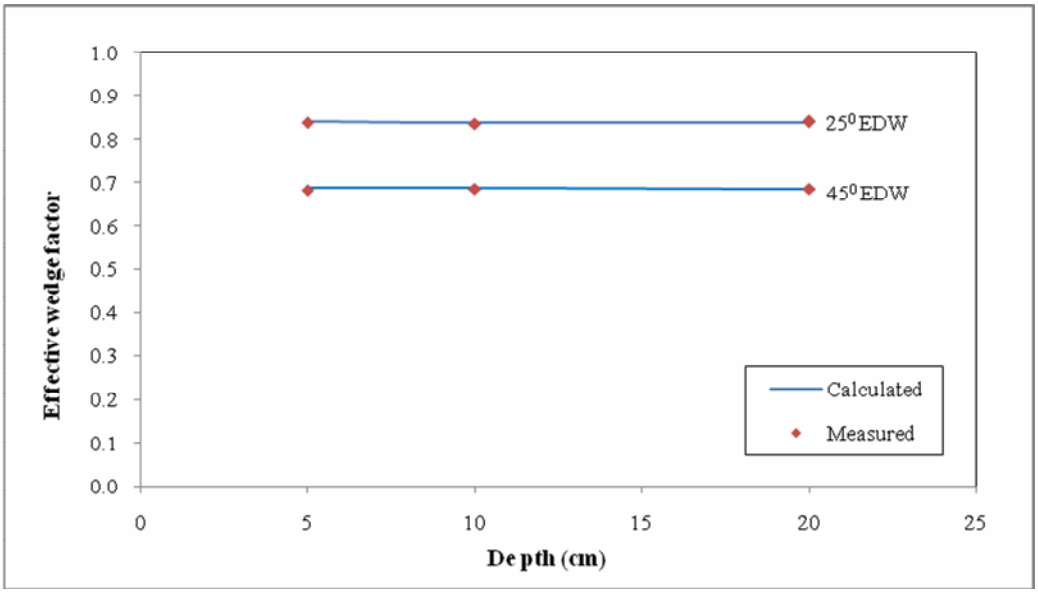
1.0
0.9
0.8
0.7
0.6
0.5
0.4
0.3
0.2
0.1
0.0
Effective wedge factor
0
5
10
15
20
25
De pth (cm)
25⁰EDW
45⁰EDW
Calculated
Measured

(b)

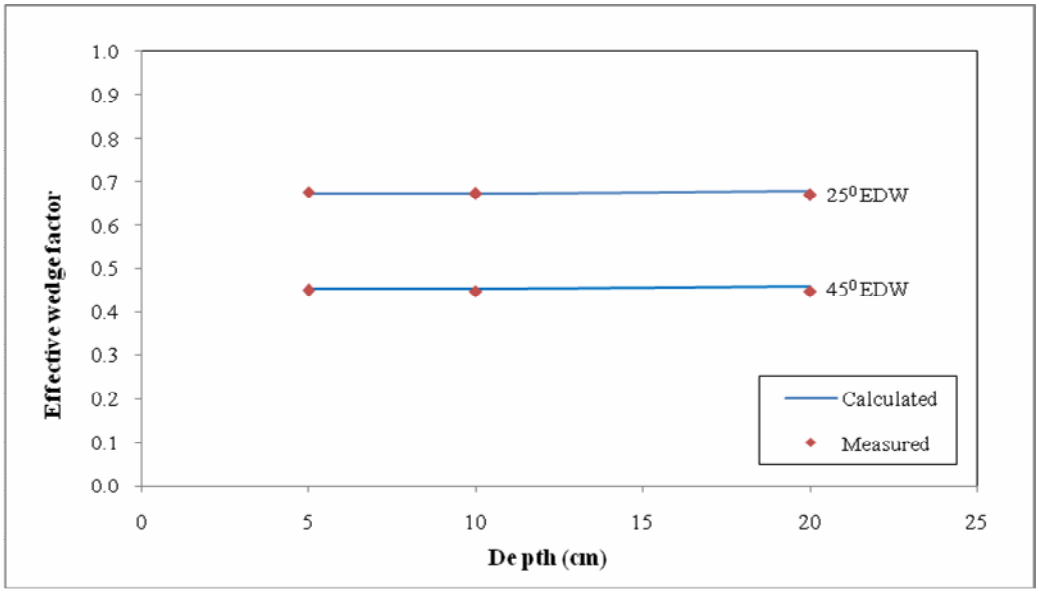

(c)

Figure 63. Calculated (solid lines) and measured (symbols) effective wedge factors versus depths for 25^0 and 45^0 EDW-Y1-IN, with 6 MV photon for asymmetric field sizes of (a) 20 x 5 cm^2, (b) 20 x 15 cm^2 and (c) 40 x 30 cm^2.

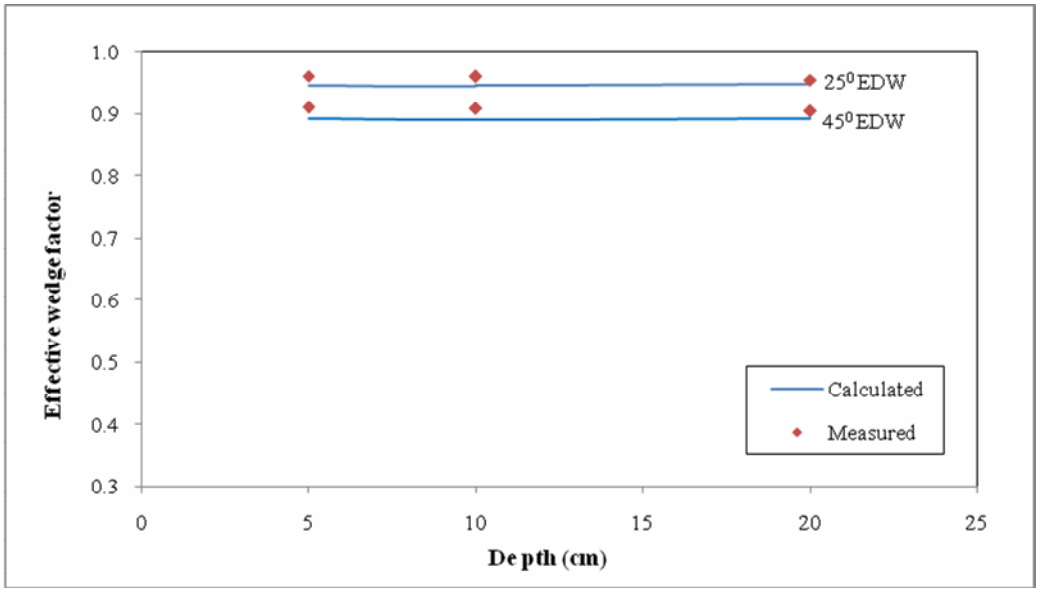

(a)

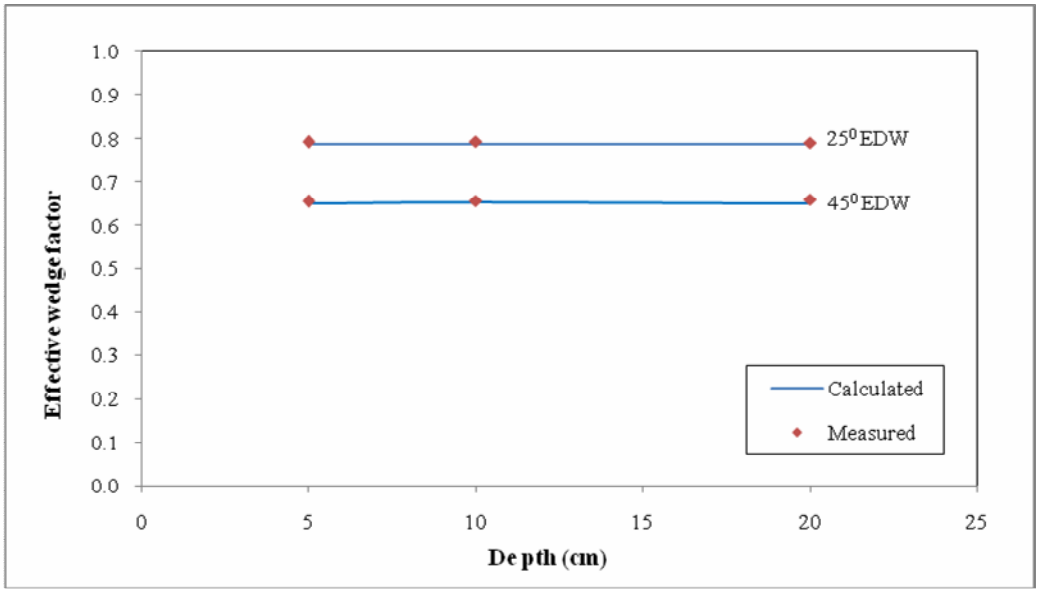

(b)

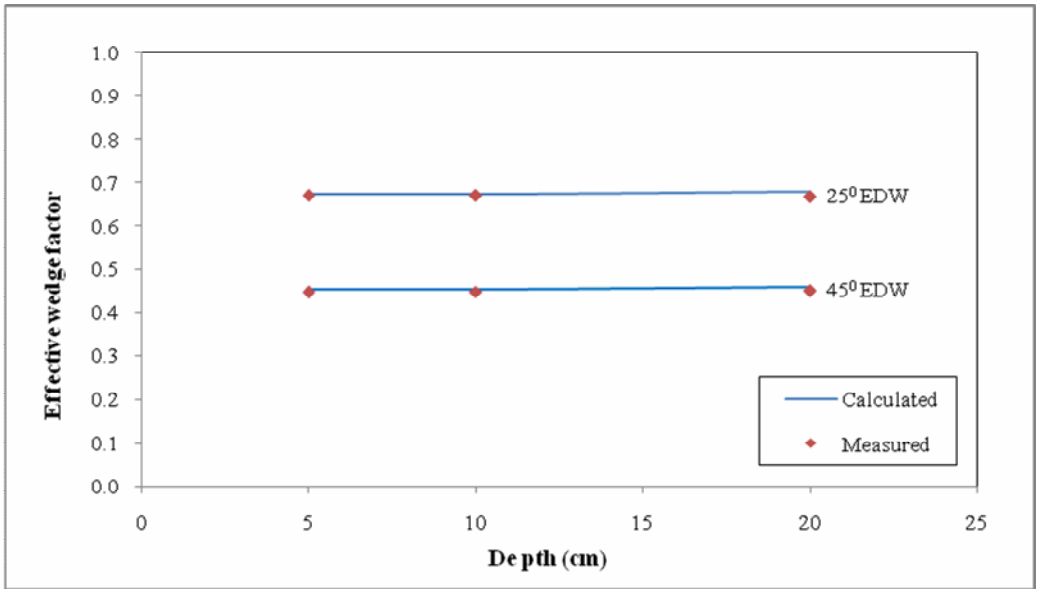

(c)

Figure 64 Calculated (solid lines) and measured (symbols) effective wedge factors versus depths for 25^0 and 45^0 EDW-Y2-OUT, with 6 MV photon for asymmetric field sizes of (a) 20 x 5 cm^2, (b) 20 x 15 cm^2 and (c) 40 x 30 cm^2.

6.1.2.5 Effective wedge angle

Comparison of the measured and calculated 25^0 and 45^0 EDW angles for the symmetric and asymmetric field sizes, in most cases, showed the measured EDW angles are higher than the calculated angles about 2 degree as shown in Table 29 to 30 (a-b). However, it can be observed that the deviation about 4-5 degree were found in the elongated 20 x 5 cm^2 EDW field.

Table 29. Comparison of measured and calculated EDW angles for 25^0 EDW and 45^0 EDW, with 6MV photon beam and symmetric field sizes of 5 x 5 cm^2, 10 x 10 cm^2, 15 x 15 cm^2, 20 x 20 cm^2, 20 x 5 cm^2, 20 x 10 cm^2 and 20 x 15 cm^2 for both wedge orientations of (a) Y1-IN and (b) Y2-OUT

(a) Y1-IN

Field size (cm^2)	25^0EDW-Y1-IN		Difference (degree)	45^0 EDW-Y1-IN		Difference (degree)
	Measured (degree)	Calculated (degree)		Measured (degree)	Calculated (degree)	
5 x 5	20.2	18.4	1.8	37.7	35.3	2.4
10 x 10	20.8	20.6	0.2	39.5	37.6	1.9
15 x 15	23.0	22.1	0.9	42.3	39.0	3.3
20 x 20	23.7	24.0	0.3	43.2	43.0	0.2
20 x 5	20.8	19.2	1.6	38.7	34.0	4.7
20 x 10	22.0	20.6	1.4	41.1	40.1	1.0
20 x 15	23.3	23.0	0.3	42.7	41.6	1.1

(b) Y2-OUT

Field size (cm^2)	25^0EDW-Y1-IN		Difference (degree)	45^0EDW-Y1-IN		Difference (degree)
	Measured (degree)	Calculated (degree)		Measured (degree)	Calculated (degree)	
5 x 5	19.8	18.1	1.7	37.4	35.2	2.2
10 x 10	21.4	20.9	0.5	40.0	37.7	2.3
15 x 15	23.7	22.1	1.6	42.9	41.4	1.5
20 x 20	25.3	23.6	1.7	44.4	43.0	1.4
20 x 5	19.6	18.9	0.7	37.9	34.2	3.7
20 x 10	21.0	21.3	0.3	40.8	40.1	0.7
20 x 15	24.0	22.8	1.2	43.6	41.7	1.9

Table 30. Comparison of measured and calculated EDW angles for 25^0 EDW and 45^0 EDW, with 6MV photon beam and asymmetric field sizes of, 20 x 5 cm^2, 20 x 10 cm^2, 20 x 15 cm^2 and 40 x 30 cm^2 for both wedge orientations of (a) Y1-IN and (b) Y2-OUT

(a) Y1-IN

Field size (cm^2)	Off axis (cm)	25^0EDW-Y1-IN		Difference (degree)	45^0EDW-Y1-IN		Difference (degree)
		Measured (degree)	Calculated (degree)		Measured (degree)	Calculated (degree)	
20 x 5	2.5	11.7	7.0	4.7	32.1	28	4.1
20 x 10	5.0	10.3	7.3	3.0	31.3	30.0	1.3
20 x 15	2.5	16.0	16.7	0.7	37.8	37.3	0.5
40 x 30	5.0	17.0	16.7	0.3	39.0	37.6	1.4

(b) Y2-OUT

Field size (cm^2)	Off axis (cm)	25^0 EDW-Y1-IN		Difference (degree)	45^0EDW-Y1-IN		Difference (degree)
		Measured (degree)	Calculated (degree)		Measured (degree)	Calculated (degree)	
20 x 5	2.5	28.50	28.80	0.3	43.4	41.6	1.8
20 x 10	5.0	32.20	30.90	1.3	47.3	46.4	0.9
20 x 15	2.5	29.80	29.00	0.8	47.3	45.8	1.5
40 x 30	5.0	17.80	16.50	1.3	39.4	37.6	1.8

6.1.3 Monitor units (MUs) verification

Verification the MU calculations in Eclipse 8.0 TPS, for three different EDW plans performed on homogeneous phantom, showed the acceptable accuracy of all plans within $\pm$2% as presented in Table 31.

Table 31. Comparison of measured and calculated absorbed dose ($D_{W,Q}$) for three EDW treatment plans, irradiated with 6MV photon beam.

Plan	$D_{W,Q}$ (Gy)		%Difference
	Measured	Calculated	
1	1.981	2.00	-0.96
2	2.011	2.00	0.54
3	1.962	2.00	-1.94

6.2 Discussion

In this study, the CA24 chamber array was found to be an effective dosimetry system to accurately measure the dose distributions for the EDW fields. Comparison with the single ion chamber, good agreement between the two detectors was obtained.

The measured dynamic wedge central axis depth dose data is excellent agreement with the open field depth dose data. Only at the large asymmetric field size and depth deeper than 10 cm which the EDW depth doses were slightly higher than the open field depth doses. This observation came from the addition of the scattered radiation dose from the collimator and phantom of the EDW field. This finding insisted the pros of dynamic wedge over the physical wedge in the subject of beam hardening effect.

About the accuracy of EDW dosimetry from the Eclipse TPS, most of experiments on the depth doses and profiles showed the acceptable results within $\pm$ 2% of the calculated data. However the deviation higher than $\pm$ 2% can be detected from the large EDW asymmetric field with Y2-OUT direction. It was also interesting that similar findings in this current study with the previous studies on underestimation of the calculated profiles by pencil beam (PBC) algorithm at the high dose region (thin edge) both for the symmetric and asymmetric EDW profiles were seen. Generally, with the PBC algorithm, the agreement within $\pm$ 2.0% was reported to be found only at the small dose gradient (near the center of the field) and can be detected up to 5% at the small dose gradient in low dose region (< 7% of normalization dose) in large fields (33-34). Several studies had compared the dose calculation between the PBC and anisotropic analytic algorithm (AAA) algorithm in the Eclipse TPS. They concluded that the extra-focal source in AAA algorithm which accounts for the secondary photons scattered in the head of the machine resulted in more accurate dose calculation in the high dose region and the penumbra than PBC.

EDW wedge factors in this investigation showed similar results with the previous studies (13, 20-22). A smooth and continuous decrease of the EDW effective wedge factor with increasing field dimension along the moving collimator and wedge angle, but independent of the measurement depth can be observed. Unlike the DW, where a strong non-monotonic field size dependence appeared (23) and the effective wedge factor showed a discontinuity between 9.5 and 10 cm width due to change in STT step size (13).

Good agreement between the measured and calculated EDW angles for both symmetric and asymmetric field size was undertaken. Except the deviation about 4- 5 degree was found on the elongated 20 x 5 cm^2 EDW field. This can be explained from the underestimation of dose at the thin edge (high dose region) and from the uncertainty in elongated field calculation of the PBC algorithm which not only in case of EDW but also can be found in the hard wedge or open field (34). However, this deviation was not clinically significant because only less than 2 mm between the measured and calculated EDW isodose distribution was detected.

For MU verifications, all treatment plans in homogeneous phantom yielded the acceptable accuracy in $\pm$2% of the calculation. Measurements with the inhomogeneous phantom is also suggested for the better accuracy approve.

CHAPTER VII
CONCLUSIONS

Wedged isodose distributions play an important role in many clinical situations for the external beam radiation therapy. Up to date, with the computer controlled linear accelerator capability, implementation the new dynamic wedge to replace the physical wedge in the clinic is enable and advantageous.

Generally, to commission the dynamic wedge into the treatment planning is a simple and fast procedure because no additional beam data are required. The dynamic dose distributions are calculated based on the open beam modeling and the information of transmission array only.

In this study, with the objective to implement the dynamic wedge into a clinic, the commissioning of the enhanced dynamic wedge (EDW) into the Eclipse 8.0 treatment planning was undertaken. Two EDW angles, 25^0 and 45^0, were selected to be verified for the accuracy of the PBC algorithm dose calculation. Extensive measurements of EDW beam characteristics provided by the operating in 6 MV x-ray mode on the Clinac 23 EX linear accelerator were performed and compared with the calculation from Eclipse TPS.

Using the acceptance criteria recommended by Dyk JV et al (37) and Venselaar J et al (38), results of the investigation clearly showed that the EDW dosimetry, central axis depth doses and beam profiles, for both symmetric and asymmetric fields, between the measured and calculated beam are in good agreement.

It is manifested from the study that, the EDW depth doses were found to be close to those obtained for open fields and no beam hardening effect was found in the EDW application. This result implies the use of open beam depth dose data is appropriate for the dose distribution calculation by Eclipse TPS.

Study of the EDW effective wedge factors, it was found that the good agreement between measured and calculated effective wedge factors in the symmetric and asymmetric fields, respectively. Moreover, the results show that the effective wedge factor of the EDW is a smooth function of the field dimension along the moving jaw and is independent of the depth.

Majority of the tests presented a well match between the measured and calculated EDW angles for both symmetric and asymmetric field size. Except the narrow and elongated field size of 20 x 5 cm^2 which a larger difference, 4-5 degree, in wedge angle can be observed in both wedge direction of 25^0 and 45^0 EDW. PBC algorithm was reported to provide the underestimation of dose at the toe edge and may be a source of the deviation found between the measured and calculated wedge angle.

Measurements of absolute absorbed dose in the homogeneous phantom in three different EDW plans showed the MUs calculation can be performed accurately by the PBC algorithm with the accuracy in $\pm$2% of measurement.

It can be concluded from the study that dose calculation model for the dynamic wedges in the Eclipse 8.0 TPS by PBC algorithm meet the clinical accuracy requirements. Accurate results of 6 MV, 25^0 and 45^0 EDW, suggested the other five EDW which not included in this examination would also have the same satisfactorily beam parameters. Quality assurance of the enhanced dynamic wedge program will enhance the quality of the radiation treatment for the cancer patients.

REFERENCES

1. Desanti S Muller-Runkel R. Using different sets of wedges: Clinical applications, dosimetry and safety interlocks. Med. Dosim 1989; 14: 137-243.
2. Fraass BA, Van de Geijn J . Peripheral dose from mega-voltage beams. Med. Phys 1983; 10: 809-818.
3. Li Z, Klein EE. Surface and Peripheral doses of dynamic and physical wedges. Int J Radiation Oncol Biol Phys 1997; 37: 921-5.
4. Kalend AM, Wu A, Yoder V, Mantz A. Seperation of dose-gradient effect from beam-haredening effect on wedge factors in photon fields. Med. Phys 1990; 17: 701-4.
5. Wu A, Zwicker R, Krasin F, Sternick E. Dosimetry characteristics of large wedges for 4 and 6 MV X-rays. Med. Phys 1984; 11: 186-8.
6. Kijewski PK, Chin LM, and Bjarngard BE. Wedge-shaped dose distributions by computer-controlled collimator motion. Med. Phys 1978; 5: 426-9.
7. Leavitt DD, Martin M, Moeller JH and Lee WL. Dynamic wedge field techniques through computer controlled collimator motion and dose delivery. Med. Phys 1990; 17: 87-91
8. Faiz M. Khan.The Physics of radiation therapy.3rd edition; 2003: 206, 219.
9. Georg D, Olofsson J, Kunzle T, Aiginger H and Karlsson M. A practical method to calculate head scatter factors in wedged rectangular and irregular MLC shaped beams for external and internal wedges. Phys Med Biol 2004; 49: 4689-700.
10. International Commission on Radiation Units and Measurement. Radiation dosimetry determination of absorbed dose in a patient irradiated by beams of x or gamma rays in radiotherapy procedures. ICRU report 24; 1976 Sep 15: p. 5-16.

11. Niroomand-Rad A, Haleem M, Rodgers J and Obecmea C. Wedge factor dependence on depth and field size for various beam energies using symmetric and half-collimated asymmetric jaw settings. Med Phys 1992; 19 (6 suppl): 1445-50.
12. Mcghee P, Chu T, Leszczynski K and Dunscombe P. The Siemens Virtual Wedge. Med. Dosim 1997; 22: 39-41.
13. Chang SX and Gibbons JP. Clinical Implementation of Non-Physical wedges. AAPM Refresher Course 1999.
14. Rubi A. Investigation quallity assurance monitor for dynamic wedge field in radiation therapy. Ontario Canada: Queen's university Kingston; 2000.
15. Varian Oncology Systems. Enhanced Dynamic Wedge^{TM} Implementation Guide. January 1996.
16. Walker CP, Richmonnd ND and Lambert GD. Optimal Clinical Implementation of the Siemens Virtual Wedge. Med Dosim 2003; 28 (3) : 149-54.
17. Santvoort JV. Dosimetric evaluation of the Siemens virtual wedge. Phys Med Biol 1998; 43: 2651-63.
18. Zhu XR, Gillin MT, Jursinic PA, Lopez F, Grimm DF and Rownd JJ. Comparison of dosimetric characteristics of Siemens virtual and physical wedges. Med Phys 2000; 27: 2267-77.
19. Paula LP and Robert LS. Effective Wedge Angles with a Universal Wedge. Phys Med Biol 1985; 30: 985-91.
20. Leavitt DD, Lee WL, Gaffney DK, Moeller JH and O'Rear JH. Dosimetric parameters of enhanced dynamic wedge for treatment planning and verification. Med. Dosim 1997; 20: 177-83.
21. Salk J, Blank P, Machold U, Rau E, Schneider E and Rottinger EM. Physical aspects in the clinical implementation of the Enhanced Dynamic Wedge (EDW). Proceedings of the 8th Varian European Users Meeting; 1997 Apr 27 - 30; Vilamoura, Algarve-Portugal.
22. Devin PB. Dynamic wedge dosimetry on a dual energy linear accelerator. Department of Medical Physics. Montreal: McGill Univ.; 1996: 38-59,108.

23. Liu C, Zhu TC and Palta JR. Characterizing Output for Dynamic Wedges. Med Phys 1996; 23 (7): 1213-8.

24. Liu C, Li Z, and Palta JR. Characterizing output for the Varian enhanced dynamic wedge field. Med Phys 1998; 25: 64-70.

25. International Electrotechnical Commission Medical Electron Accelerators - Functional Performance Characteristics IEC Performance Standard 976, Geneva; 1989 Oct.

26. Sherazi S and Kase KR. Measurements of dose from secondary radiation outside a treatment field: effects of wedges and blocks. Int.J.Radiat.Oncol.Biol.Phys 1985; 11: 2171-6.

27. Ochran TG, Boyer AL, Nyerick CB and Otte VA. Dosimetric characteristics of wedges mounted beyond the blocking tray. Med Phys 1992; 19: 187-94.

28. Klein EE and Purdy JA. Entrance and exit dose regions for a Clinac-2100C. Int.J.Radiat.Oncol.Biol.Phys 1993; 27: 429-35.

29. Shih R, Li XA and Chu JCH. Dynamic wedge versus physical wedge: A Monte Carlo study. Med Phys 1996; 28 (4): 612-9.

30. Warlick WB, O'Rear JH, Earley L, Moeller JH, Gaffney DK and Leavitt DD. Dose to the contralateral breast: A Comparison of two techniques using the enhanced dynamic wedge versus a standard wedge. Med dosim 1997; 22: 185-91.

31. Radiation oncology System. Eclipse Algorithm Reference Guide, Varian Medical System, USA, 2007.

32. Liu HH, Lief EP and McCullough EC. Measuring dose distributions of Enhanced dynamic wedges using a multichamber detector array. Med.Phys 1997; 24: 1515-19.

33. Samuelsson A, Johansson KA, Mattsson O, Palm A, Puurunen H and Sernbo G. Practical implementation of Enhanced dynamic wedge in the Cadplan treatment planning system. Med dosim 1997; 22: 207-11.

34. Picon C, Linero D, Gracia A, Saldafia O and Lizuain MC. Performance evaluation of Enhancement Dynamic Wedge Implementaton in a radiotherapy treatment planning system. Proceedings of the 22nd Annual EMBS International Conference; 2000 July 23-28; Chicago IL.

35. Degener R. MD240 / CA24 Linear Chamber Array User's Guide. Wellhofer dosimetrie: Germany; 1998 April.

36. International Atomic Energy Agency. Absorbed dose determination in external beam therapy. IAEA TRS 398, 2000: 66-83.

37. Dyk JV, Barnett RB, Cygler JE, Ghragge PC. Commissioning and quality assurance of treatment planning computers. Int J Radiant Oncol Biol Phys 1993; 26: 261-273.

38. Venselaar J, Welleweerd H and Mijnheer B. Tolerances for the accuracy of Phonton beam dose calculations of treatment planning systems. Radiotherapy and Oncology 2001; 60: 191-201.

39. Storchi P, Woudstra E, Verlinde P, Johansson KA and Samuelsson A. Calculation of absorbed dose distributions from dynamic wedges. Phys Med Biol 1998; 43: 1497-1506.

40. Liu HH and McCullough EC. Calculating dose distributions and wedge factors for photon treatment fields with dynamic wedges based on a convolution/superposition method. Med Phys 1998; 25: 56-63.

41. Caprile P, Venencia CD and Besa P. Comparison between measured and calculated dynamic wedge dose distributions using the anisotropic analytic algorithm and pencil-beam convolution. Applied Clinical Med Phys 2007; 8(1).

BIOGRAPHY

NAME	Miss Waraporn Sangsrijan
DATE OF BIRTH	11 June 1983
PLACE OF BIRTH	Phayao, Thailand
INSTITUTIONS ATTENDED	Mahidol University, 2005: Bachelor of Science (Radiological Technology) Mahidol University, 2007: Master of Science (Medical Physics)
HOME ADDRESS	605/112 Prachauthid road Samseannok, Huay Khwang, Bangkok, Thailand 10310 Tel. 0-2121-1303 E-mail: teww_wara@hotmail.com